

**THE ROLE OF CD137^{POS} T REGULATORY CELLS AND
SOLUBLE CD137 IN TYPE ONE DIABETES.**

BY
Kritika Kachapati

B.S. Biology, Hood College, 2005

Submitted to the Graduate Faculty of the
School of Medicine in partial fulfillment
of the requirements for the degree of
Doctor of Philosophy

University of Pittsburgh

2012

UNIVERSITY OF PITTSBURGH

School of Medicine

This thesis was presented

by

Kritika Kachapati

It was defended on

December 11th 2012

and approved by

Dr. Anuradha Ray, Ph.D.

Professor, Departments of Medicine and Immunology

Dr. Binfeng Lu, Ph.D.

Associate professor, Department of Immunology

Dr. John Piganelli, Ph.D.

Associate professor, Departments of Pediatrics, Pathology and Immunology

Dr. Massimo Trucco, M.D.

Professor, Departments of Pathology, Pediatrics and Human Genetics

Dr. Donald K Scott, Ph.D.

Professor, Departments of Endocrinology, Diabetes and Bone Disease

Dissertation Advisor: Dr. William M Ridgway, M.D.

Associate Professor, Department of Immunology

Copyright © by Kritika Kachapati

2012

The role of CD137^{pos} T regulatory cells and soluble CD137 in Type one diabetes.

Kritika Kachapati, Ph.D.

University of Pittsburgh, 2012

CD137 is an inducible T cell costimulatory molecule, and a subset of CD4+CD25+ T regulatory cells constitutively express CD137 (CD137^{pos} Tregs). The nonobese diabetic (NOD) mouse spontaneously develops Type one diabetes (T1D), and genetic mapping studies have implicated CD137 as a candidate gene in the chromosome four *Idd9.3* interval. We show that anti-CD137 treatment protects NOD mice from diabetes. Anti-CD137 antibody specifically binds to CD137^{pos} Tregs cells *in vivo*. Antibody treatment increases the percentage of Tregs and these cells prevent diabetes in transfer studies. Depleting CD4+CD25+ T cells eliminated anti-CD137 mediated diabetes protection. These studies demonstrate the importance of the CD137^{pos} Treg subset, which express the same amount of Foxp3 as CD137^{neg} Tregs but are functionally superior in contact dependent and independent suppression assays *in vitro*. Congenic NOD.B10 *Idd9.3* mice (that have a 40% decreased incidence of diabetes compared to NOD), have significantly increased numbers of peripheral CD137^{pos} Tregs compared to NOD. Mixed bone marrow chimeras using the two allotypically marked strains showed an intrinsic cellular basis for the accumulation of B10 *Idd9.3* CD137^{pos} Tregs. While CD137^{pos} Tregs from NOD and NOD.B10 *Idd9.3* showed no suppressive differences, the accumulation of the functionally superior Treg subset enables enhanced immunosuppression in the congenic mice. We show that CD137^{pos} Tregs are the major T cell source for the alternatively spliced CD137 isoform, soluble CD137, which causes reduced T cell proliferation. Increased serum soluble CD137 in NOD.B10 *Idd9.3* versus NOD mice associates soluble CD137 with diabetes protection. Anti-CD137 treatment increases serum soluble CD137. Soluble CD137-Fc directly

reduces CD4^{pos} T cells proliferation in a CD137 ligand dependent manner. We used a lentiviral approach to produce recombinant soluble CD137 *in vitro*. The purified soluble CD137 is predominantly a dimer, and directly suppresses CD4 T cell proliferation. Soluble CD137 protein prevents diabetes and significantly reduces insulinitis in NOD. Our data shows that diabetes protection by both anti-CD137 treatment and in NOD.B10 *Idd9.3* mice is associated with expansion of suppressive CD137^{pos} Tregs and subsequent accumulation of immunosuppressive soluble CD137. These studies establish the importance of the CD137^{pos} Treg subset and soluble CD137 in T1D and immunobiology.

TABLE OF CONTENTS

ACKNOWLEDGEMENTS	xiv
1.0 INTRODUCTION	1
1.1 TYPE 1 DIABETES (T1D)	1
1.2 IMMUNITY IN NOD MICE.....	4
1.2.1 T cells in NOD diabetes.....	4
1.2.2 Autoantigens in diabetes	5
1.2.3 Role of innate immunity and B cells in diabetes	5
1.2.4 T regulatory cells in diabetes.....	7
1.3 ENVIRONMENTAL FACTORS IN DIABETES.....	9
1.4 NOD CONGENICS	10
1.4.1 NOD genetics and linkage analysis.....	10
1.4.2 Limitations in congenic mapping	11
1.5 MAPPING <i>Idd9</i> AND ITS SMALLER INTERVALS.....	12
1.5.1 Mapping <i>Idd9</i>	12
1.5.2 Mapping <i>Idd9</i> subcongenic strains	13
1.5.3 NOD.B10 <i>Idd9.3</i> congenic strain	13
1.6 CD137 IN DIABTES.....	16
1.6.1 CD137 (4-1BB) costimulatory molecule.....	16
1.6.2 CD137 polymorphism.....	16
1.6.3 CD137 stimulation of T cells.....	19
1.6.4 Agonist anti-CD137 treatment	20
1.6.5 CD137 and human diabetes.....	20
1.6.6 CD137 and T regulatory cells.....	21
1.6.7 Soluble form of CD137	22

1.7 CD137L and its signaling.....	23
1.7.1 CD137 ligand (CD137L)	23
1.7.2 CD137L signaling on T cells.....	23
1.8 OUTLINE OF THE THESIS	25
2.0 CD137 MODULATES PROTECTIVE CD4 ^{pos} CD25 ^{pos} T CELLS AND PATHOGENIC CD4 T CELLS IN NOD TYPE 1 DIABETES	28
2.1 INTRODUCTION	28
2.2 METHODS.....	30
2.2.1 Mice and reagents:	30
2.2.2 Histology:.....	31
2.2.3 Cell purification and culture:	31
2.2.4 Suppression Assay:.....	31
2.2.5 Treg Transwell Suppression Assay:	32
2.2.6 Flow cytometry:	32
2.2.7 RT-PCR:.....	33
2.2.8 ELISA:	33
2.2.9 Adoptive transfer:	34
2.3 RESULTS	34
2.3.1 Anti-CD137 prevents diabetes but not insulinitis.....	34
2.3.2 CD4 T cells from anti-CD137 treated mice prevent adoptive transfer of diabetes.	36
2.3.3 Anti-CD137 treatment alters the cytokine phenotype of CD4 T cells.....	38
2.3.4 Naive CD4 ^{pos} CD25 ^{pos} T cells express CD137 and continue expressing Foxp3 after treatment.	40
2.3.5 Anti-CD137 antibody specifically binds to CD4 ^{pos} CD25 ^{pos} cells <i>in vivo</i>	41
2.3.6 Anti-CD137 treated CD4 ^{pos} CD25 ^{pos} T cells prevent adoptive transfer of diabetes.....	43
2.3.7 CD137 expressing CD4 ^{pos} CD25 ^{pos} T cells express high levels of IL-10 and ICOS.....	45
2.3.8 CD137 ^{pos} Tregs express high levels of CD69 and ICOS.	46
2.3.9 CD137 expressing CD4 ^{pos} CD25 ^{pos} T cells are highly suppressive <i>in vitro</i>	48
2.3.10 IL-10 and TGF- β block do not abrogate CD137 ^{pos} Treg suppression.	49

2.3.11 CD137 ^{pos} Tregs are functionally superior to CD137 ^{neg} Tregs in contact-independent suppression.....	52
2.4 DISCUSSION	55
3.0 THE B10 <i>Idd9.3</i> LOCUS MEDIATES ACCUMULATION OF FUNCTIONALLY SUPERIOR CD137 ^{pos} T REGULATORY CELLS IN TYPE 1 DIABETES MODEL.....	60
3.1 INTRODUCTION	60
3.2 METHODS.....	62
3.2.1 Mice and reagents:.....	62
3.2.2 Re-sequencing the <i>Idd9.3</i> interval in the NOD mouse strain:.....	63
3.2.3 Flow Cytometry:.....	64
3.2.4 Bone Marrow Chimera construction:	65
3.2.5 RT-PCR:.....	65
3.2.6 Proliferation Assay:.....	66
3.2.7 Treg Transwell Suppression Assay:	66
3.2.8 ELISA:	66
3.2.9 Treg culture:	67
3.3 RESULTS	67
3.3.1 Increased accumulation of CD137 ^{pos} Tregs with the B10 versus the NOD region <i>in vivo</i>	67
3.3.2 CD137 ^{neg} and CD137 ^{pos} Tregs express similar levels of intracellular Foxp3 in NOD and NOD.B10 <i>Idd9.3</i>	76
3.3.3 Increased accumulation of CD137 ^{pos} Tregs with the B10 versus the NOD <i>Idd9.3</i> region in mixed bone marrow chimeras <i>in vivo</i>	80
3.3.4 Enhanced proliferation of CD137 ^{pos} Tregs <i>ex vivo</i> and <i>in vitro</i> but no significant difference between NOD and NOD.B10 <i>Idd9.3</i> congenic mice.....	83
3.3.4 NOD and NOD.B10 <i>Idd9.3</i> CD137 ^{pos} Tregs do not differ in contact-dependent suppression..	90
3.3.5 CD137 ^{pos} Tregs are the major cellular source of alternately spliced soluble CD137 protein ...	93
3.3.6 Increased serum soluble CD137 in older NOD.B10 <i>Idd9.3</i> mice.....	98
3.4 DISCUSSION	100
3.5 Acknowledgements.....	105

4.0 THE SOLUBLE FORM OF CD137 IS SUPPRESSIVE AND PREVENTS DIABETES IN NOD MICE	106
4.1. INTRODUCTION	106
4.2 METHODS.....	108
4.2.1 Mice and reagents:	108
4.2.2 Anti-CD137 Treatment:.....	109
4.2.3 RT-PCR:.....	109
4.2.4 Treg Transwell Suppression Assay:	110
4.2.5 Proliferation Assay with thymidine:.....	110
4.2.6 Proliferation Assay with CFSE:.....	111
4.2.7 Cell death:	111
4.2.8 ELISA:	111
4.2.10 Purification of Soluble CD137:.....	113
4.2.11 Western Blot:.....	114
4.2.12 Analytical ultra-centrifugation (AUC):.....	115
4.2.13 Histology:.....	115
4.2.14 NOD treatment with soluble CD137:.....	116
4.3 RESULTS	117
4.3.1 CD4 ^{pos} CD25 ^{pos} T cells are essential for anti-CD137 mediated diabetes protection.....	117
4.3.2 Anti-CD137 treatment induces TRAF2 signaling response in CD137 ^{pos} Tregs <i>in vivo</i>	118
4.3.3 Anti-CD137 treatment enhances soluble CD137 production from CD137 ^{pos} Treg <i>in vitro</i> and <i>in vivo</i>	120
4.3.4 Soluble CD137 from CD137 ^{pos} Tregs suppresses CD4 ^{pos} T cells through CD137L.....	122
4.3.5 Soluble CD137-Fc suppresses CD4 T cells <i>in vitro</i>	124
4.3.6 Production of recombinant soluble CD137 <i>in vitro</i>	126
4.3.7 Recombinant Soluble CD137 exists predominantly as a dimer	128
4.3.8 Purified Soluble CD137 suppresses proliferation of CD4 T cells <i>in vitro</i>	131
4.3.9 Soluble CD137 reduces the incidence of diabetes in NOD mice.....	134
4.4 DISCUSSION	137

4.5 Acknowledgements.....	143
5. SUMMARY & SIGNIFICANCE.....	144
5.1 Proposed models.....	144
5.1.1 Proposed model for soluble CD137 function and B10 <i>Idd9.3</i> protection	144
5.1.2 Proposed model for anti-CD137 mediated NOD diabetes protection	150
5.2 Future directions and therapeutic implications.....	154
APPENDIX A	157
APPENDIX B	159
BIBLIOGRAPHY	160

LIST OF TABLES

Table 1.1. There are fifteen candidate genes within *Idd9.3* loci. 15

LIST OF FIGURES

Figure 1.1. Polymorphism in the <i>Idd9.3</i> region in NOD mice.	17
Figure 1.2. <i>Idd9.3</i> gene content and sequence polymorphisms.....	18
Figure 1.3. A schematic of membrane bound and soluble CD137.....	22
Figure 2.1. Anti-CD137 antibody prevents type 1 diabetes in NOD mice but not insulinitis.	35
Figure 2.2. CD4 T cells from anti-CD137 treated mice prevent diabetes in NOD- <i>scid</i> mice.....	37
Figure 2.3. Anti-CD137 treatment increases IL-4 and IL-10 production and the fraction of CD4 ^{pos} CD25 ^{pos} T cells.	39
Figure 2.4. Naïve CD4 ^{pos} CD25 ^{pos} T cells express CD137 and continue expressing Foxp3 after anti-CD137 treatment.	41
Figure 2.5. Anti-CD137 antibody specifically binds to CD4 ^{pos} CD25 ^{pos} T cells <i>in vivo</i>	42
Figure 2.6. Anti-CD137 treated CD4 ^{pos} CD25 ^{pos} T cells protect from diabetes.	44
Figure 2.7. CD137 ^{pos} Tregs have higher levels of <i>Il-10</i> and <i>Icos</i> mRNA compared to CD137 ^{neg} Tregs.	45
Figure 2.8. CD137 ^{pos} Tregs upregulate CD69 and ICOS higher than CD137 ^{neg} Tregs.	47
Figure 2.9. NOD CD137 ^{pos} Tregs are functionally superior to CD137 ^{neg} Tregs in contact-dependent mechanism. .	49
Figure 2.10. Suppression by CD137 ^{pos} Tregs is not abrogated by both IL-10 and TGF- β blocking <i>in vitro</i>	51
Figure 2.11. CD137 ^{pos} Tregs are functionally superior to CD137 ^{neg} Tregs in contact-independent suppression.....	53
Figure 3.1. CD137 ^{pos} Tregs are significantly lower in aged NOD versus NOD.B10 <i>Idd9.3</i> spleen.	69
Figure 3.2. NOD and NOD.B10 <i>Idd9.3</i> CD4 ^{pos} , CD4 ^{pos} CD25 ^{pos} , and splenic lymphocytes increase with age.....	71
Figure 3.3. Thymic CD4 ^{pos} CD25 ^{pos} CD137 ^{pos} T cells decline with age in NOD but not in NOD.B10 <i>Idd9.3</i> mice.....	73
Figure 3.4. Cellular CD137 increase in older NOD and younger NOD.B10 <i>Idd9.3</i> congenic than young NOD.....	75
Figure 3.5. NOD and NOD.B10 <i>Idd9.3</i> Treg subsets show no difference in intracellular Foxp3 levels.	77
Figure 3.6. CD137 ^{pos} Tregs from NOD and NOD.B10 <i>Idd9.3</i> Foxp3-GFP mice express high Foxp3.	79
Figure 3.7. CD137 ^{pos} Tregs expressing the B10 <i>Idd9.3</i> region demonstrate an intrinsic cell accumulation.	82
Figure 3.8. No proliferative differences between NOD and NOD.B10 <i>Idd9.3</i> CD137 ^{pos} Tregs <i>ex vivo</i> or <i>in vitro</i>	84
Figure 3.9. Peripheral NOD.B10 <i>Idd9.3</i> CD137 ^{pos} Tregs express higher levels of Bcl-xL mRNA than NOD.	87
Figure 3.10: <i>In vitro</i> cell death does not differ between NOD vs. NOD.B10 <i>Idd9.3</i> CD137 ^{pos} Tregs.....	89

Figure 3.11. NOD and NOD.B10 <i>Idd9.3</i> CD137 ^{pos} Tregs do not differ in suppression <i>in vitro</i>	91
Figure 3.12. NOD and NOD.B10 <i>Idd9.3</i> CD137 ^{pos} Tregs are the major cellular source of soluble CD137 <i>in vitro</i>	94
Figure 3.13. CD137 ^{pos} Tregs produce more soluble CD137 during suppression.....	97
Figure 3.14: NOD.B10 <i>Idd9.3</i> congenic mice have higher serum soluble CD137 levels than NOD.	99
Figure 4.1: CD4 ^{pos} CD25 ^{pos} T cells are essential for anti-CD137 mediated diabetes prevention.	117
Figure 4.2: CD137 ^{pos} Tregs from anti-CD137 treated NOD mice redistribute TRAF2 to the cell surface.....	119
Figure 4.3: Anti-CD137 treatment increases soluble CD137 production and serum soluble CD137.....	121
Figure 4.4: Blockade of CD137L decreases transwell, contact independent suppression mediated by CD137 ^{pos} Tregs.....	123
Figure 4.5: Soluble CD137-Fc directly suppresses T cells in an APC and Treg independent manner.	125
Figure 4.6. Lentivirally-transduced HEK293 cells produce recombinant soluble CD137 protein <i>in vitro</i>	127
Figure 4.7. Recombinant soluble CD137 protein exists primarily as dimers.	129
Figure 4.8. Purified soluble CD137 suppresses CD4 T cell proliferation <i>in vitro</i>	133
Figure 4.9. Purified soluble CD137 prevents diabetes <i>in vivo</i> and reduces pancreatic islet infiltration.....	136
Figure 5.1: Model for differences in CD137-CD137L bi-directional signaling.	146
Figure 5.2: Model for mechanism of autoimmunity prevention by anti-CD137 antibodies.....	152
Supplemental Figure 1. The CD62L ^{hi} or CD69 ^{hi} expression on CD137 ^{pos} Tregs are not entirely CD69 ^{low} or CD62L ^{low} respectively.	157
Supplemental Figure 2. NOD and NOD.B10 <i>Idd9.3</i> CD137 ^{neg} Tregs both equally upregulate CD137 <i>in vitro</i>	158

ACKNOWLEDGEMENTS

My graduate school journey began at a critical juncture in my life - just few months after I had lost my father. I remember feeling scattered but deep within I knew that my passion lied in research and that pursing this field would be worthwhile. In some ways, I was unprepared for where the ride was about to take me. Fittingly, from Pittsburgh to Cincinnati, through the course of academic pursuits and personal trials but it has been a fulfilling journey so far.

The years spent in the pursuit of this academic goal did not come without challenges - both outside and inside. These trials have helped me to introspect and redefine myself and my prescriptive towards life. Today I have gratitude for all the challenges, for they have made me strong but humble in acknowledging that life's plans are greater and grander than my own.

My years in graduate school would have been impossible without the unconditional love and support of my family. I would like to thank my mother and my father for teaching me to be a better person by instilling the importance of truth, righteousness, peace, non-violence and love. My mom has been my anchor in the times of turmoil; without her, I would not be here. She has taught me perseverance, sacrifice, love and faith. I am very fortunate to have a brother like Anuj, who has been my friend- an ever present helping hand in all my endeavors. I would not have been able to jump through many hoops without his love and support. I am also very thankful for my loving husband, Rajat, who has always supported me. I appreciate his understanding in letting our life revolve around schedules dictated by lab-work, while never letting go of important things in our life.

My journey so far would not have been possible without a tremendous guidance of my mentor Dr. Ridgway, who taught me how to do science and who personified the courage to “stir things up”. At times he nudged me out of my comfort zone to learn new things and appreciate seemingly small events. I thank him for challenging my boundaries and encouraging me so that I may grow. I will always admire his positive attitude. I have enjoyed our discussion in science and philosophy through which I have learned much. My heartfelt gratitude to Dr. Ridgway for listening to me through my challenges and giving me time and space to grow and learn. You have left an indelible impression in my mind for the rewards and rigors of science.

I would like to thank all my committee members for their supervision and support. My special thanks to Yuehong Wu and David Adams for their assistance and encouragement; to Kyle Bednar and Wenting Wu for their help in the lab. My years in graduate school would not have been the same without the support of my loving friend Cavita Chotoo.

Thank you everyone for your love, help and encouragement. My loving father and my mother, this work is dedicated to you.

1.0 INTRODUCTION

1.1 TYPE 1 DIABETES (T1D)

Human insulin-dependent diabetes mellitus or type 1 diabetes (T1D) is an inflammatory autoimmune disease characterized by the immunological destruction of insulin-producing pancreatic beta cells and the appearance of auto antibodies against self-proteins [1, 2]. In contrast to T1D, type 2 diabetes (T2D) is non-autoimmune-mediated and is characterized by insulin resistance and a lack of the pancreatic β -cells to compensate this insensitivity. The Juvenile Diabetes Research Foundation (JDRF) reports that estimated three million Americans have T1D. According to the Centers for Disease Control and Prevention (CDC) diabetes (both T1D and T2D) is the leading cause of heart disease and stroke and is the seventh leading cause of death in the United States. Studies have projected that the worldwide incidence of diabetes will rise to at least 366 million by 2030, qualifying as a “diabetes epidemic” [3]. There are two main stages of autoimmune diabetes in humans and mice: i) a silent insulinitis phase that occurs when autoreactive lymphocytes and other antigen presenting cells infiltrate the islets and ii) an overt diabetes phase after destruction of β -cells that leads to deficiency in insulin and resultant hyperglycemia [4]. Histological analysis of the pancreas shows that the immune infiltration consists of primarily CD8 T cells but has abnormalities in both T cells and antigen

presenting cells [5, 6]. The decrease in β -cell mass and the subsequent absence of endogenous insulin production requires patients to administer exogenous insulin to maintain their blood glucose levels. Patients with poor glycemic control have increased long-term risk of diabetes-related complications such as nephropathy, retinopathy and neuropathy and cardiovascular disease disorders which are the major causes of morbidity and mortality caused by the disease [7]. The disease pathogenesis is still unclear in humans but both genetic and environmental factors are important in disease progression and clinical onset [8]. Because of the nature of the disease, subjects are only diagnosed after the clinical onset of diabetes, making it hard to study the subsequent changes in immune mechanisms that lead to autoimmunity. Because of such practical constraints and other ethical issues in studying treatment mechanisms, animal models are indispensable to reveal the factors affecting development of T1D and its treatment. One of the most studied animal models for T1D is the nonobese diabetic (NOD) mouse model that spontaneously develops T1D.

The NOD mouse model was incidentally discovered in 1979 at Shionogi Research Laboratories in Japan while breeding mice that spontaneously developed cataracts [9]. Two lines exhibited fasting hyperglycemia and one of these lines developed diabetes; this established the NOD strain that now spontaneously develops insulin-dependent diabetes. In three to four week old NOD female mice, there is a progressive accumulation of autoreactive lymphocytes, dendritic cells and macrophages in the pancreatic islets of Langerhans (insulinitis) causing inflammation and destruction of insulin-producing islet β -cells. In males, insulinitis starts at 3 months of age [10]. The β cells are eliminated by various mechanisms such as Fas/FasL interactions and perforin- and cytokine-mediated cell killing, leading to diabetes in 80% of mice by 20 weeks of age [11-13].

The NOD mouse model has several similarities with T1D in human, such as presence of

autoantibodies, T cell-mediated insulinitis and various susceptibility genes. Both humans and mice have at least 50 T1D susceptibility genes [14, 15]. Both species have an early autoimmune response to insulin and beta cell proteins caused by partial failure in central and peripheral tolerance [16, 17]. In addition, in both species T1D susceptibility is associated with MHC class II molecules [18], genetic variations of CTLA-4, IL-2 [19] and CD25 [20] genes. The MHC region is a major genetic determinant for T1D in both humans and NOD mice [21, 22] and non-MHC genes also contribute to T1D susceptibility in both species. The variation in the *IL-2* allele reduces its signaling in T1D patients and NOD mice [23-25]. The resistant allele for *IL2* produces two fold increases in IL-2 compared to the diabetes susceptible allele [19]. Since IL-2 is essential for the function of tolerance inducing Foxp3+ regulatory T cells [26], the change in the number or function of Tregs affects the suppression of pathogenic effector cells. The NOD mouse model also recapitulates the dependence on both environmental factors (diet & infection) and genetic factors as indicated in humans [8]. However, there are some differences between human T1D and the NOD mouse model. Unlike humans, the incidence of diabetes is higher in female than in male NOD mice [27, 28]. In NOD mice peripheral lymphoid organs and the submandibular salivary glands also show leukocyte infiltration [29]. Although there are differences and limitations in comparing NOD with human T1D, the study of this mouse model has enhanced our understanding of the etiologic complexity of type 1 diabetes and helped to understand the mechanism of disease protection, which can ultimately help treat the human disease.

1.2 IMMUNITY IN NOD MICE

1.2.1 T cells in NOD diabetes

Diabetes is a T cell-mediated (involving both CD4 and CD8 T cells) disease that also involves innate immunity. The importance of T cells in diabetes is indicated by the reversal of diabetes with anti-CD3 antibody treatment in NOD mice [30]. Both CD4 and CD8 T cells are required to transfer diabetes to immunocompromised NOD-*scid* mice [31]. Although there has been debate regarding the requirement of TCR specificity for islet infiltration, a recent study comparing islet specific and non-specific TCR in mixed bone marrow chimera and retrogenic mice showed that TCR specificity is required for islet entry and accumulation of T cells [32]. As noninvasive insulinitis (“perinsulinitis”) progresses into invasive insulinitis, beta cell destruction and overt diabetes, there is expansion of diabetogenic T cell clones, autoimmune response to new antigens or epitopes (“epitope spreading”) and resistance of T effector cells to immune regulation. Beta cell death itself could release antigens that were either initially concealed (“clonal ignorance”) or modified such that they escape immune tolerance [33], resulting in new T cell clones that infiltrate the islets. As the disease progresses, T cells with high avidity are preferentially expanded in the islets [34]. Finally, it has been shown in both humans and mice that T effector cells become more resistant to suppression by regulatory T cells as the disease progresses [35, 36]. Thus there are multiple intrinsic and extrinsic factors that affect the pathogenicity of T cells during the progression of autoimmune diabetes.

1.2.2 Autoantigens in diabetes

There are at least eighteen proposed T cell auto-antigens that contribute to T1D pathogenesis including Heat-shock protein 60 (Hsp60), Glutamic acid decarboxylase 65 (GAD65), preproinsulin, Regenerating gene II (Reg II) and Pancreatic duodenal homeobox 1 (Pdx1) [37]. There is an unusually large repertoire of autoreactive T cells in NOD mice that is linked genetically to the MHC [38, 39]. MHC-linked and non-MHC-linked genes act together to cause a breakdown in tolerance. It has been shown that the diabetes-associated NOD MHC II molecule I-A^{g7} interacts with pathogenic T cell receptors and causes diabetes on NOD genetic background but not in B6.G7 mice with all non-NOD genes except for NOD MHC interval [38, 40]. This indicates that the NOD MHC II I-A^{g7} molecule is not sufficient to initiate autoimmunity and that non-MHC genes present in NOD background are crucial for the disease process [41].

1.2.3 Role of innate immunity and B cells in diabetes

Although CD4 and CD8 T cells are both essential for the transfer of diabetes, other antigen presenting cells such as B cells, dendritic cells and macrophages also play a crucial role in the pathogenesis of the disease [42-44]. Dendritic cells and macrophages are observed in the pancreatic islets before T cell infiltration, suggesting a critical role in the disease pathogenesis [45]. These innate cells produce pro-inflammatory cytokines that change the milieu in which antigen specific T cell are activated, enhancing subsequent destruction of β -cells. Dendritic cells capture self antigen released as a result of β -cell death between two to three weeks of age due to tissue remodeling or change in the metabolic rate at weaning [46]. These DCs then present self-antigen to T cells in the pancreatic lymph node and initiate priming that leads to generation of antigen specific T cells.

Macrophages and NK cells are also present in the pancreatic infiltrate and can contribute to beta cell destruction [47]. Blockade of adhesion promoting receptors in macrophages inhibits their homing into the pancreas and prevents diabetes [48]. In pancreatic islets the proinflammatory cytokines TNF and IL-1 β produced by macrophages stimulate β -cells to produce nitric oxide synthase (iNOS), which promotes tissue destruction [49]. Macrophages also produce IL-12 that promotes cytotoxic CD8 T cell differentiation [50]. Recent studies have shown that NK cell ligands are expressed by β -cells in the pancreatic islets in both NOD mice and humans and play a role in destruction of islets [51, 52]. The NK cells from the pancreatic islets are also known to express programmed cell death 1 (PD1) and killer cell lectin-like receptor group G member 1 (KLRG1) indicating cytotoxic function [53]. However, several studies have also reported a protective role for NK cells in NOD. Freund's adjuvant induced prevention of diabetes is dependent on NK cells [54]. Studies have also reported impaired NK cell function in diabetic patients and NOD mice, indicating a protective role in disease prevention [55, 56]. Invariant NKT cells (iNKT cells) are innate-like T cells that also play a role in diabetes protection. Adoptive transfer studies have shown that an increase in iNKT cells protects NOD mice from diabetes [57]. Activation of iNKT cells with a specific agonist (α -galactosylceramide or its analogues) inhibits diabetes in NOD mice by induction of Th2 cell responses to islet antigens [58, 59].

B cells also play a role in T1D pathogenesis. Earlier studies have identified numerous autoantibodies to islet antigens, including insulin, glutamic acid decarboxylase, tyrosine phosphatase IA-2 [60-62]. However it has been shown that serum from diabetic mice is not sufficient to transfer disease, suggesting that B cells may also contribute via antigen presentation rather than simply autoantibody production [63]. B cells also bind and present

antigens through cell surface immunoglobulin [64]. B cells constitutively express MHC molecules and can present sequestered antigens to CD4 T cells, hence diversifying the immune response [65]. T cells in B cell deficient NOD mice have an impaired ability to respond to islet antigen indicating the role of B cells in antigen presentation [66]. B cells infiltrating the pancreatic islets also produce TNF- α that may contribute to inflammation and recruitment of other inflammatory cells [67]. B cell depletion through gene targeting and antibody treatment protects from T1D [68, 69]. These studies show that most innate and adaptive immune cell types participate in T1D pathogenesis.

1.2.4 T regulatory cells in diabetes

T regulatory cells (Tregs) have been shown to suppress a wide range of immune cells through both cell contact dependent and independent mechanisms. Tregs can suppress T effector cells via production of “anti-inflammatory” cytokines (IL-10, TGF- β , IL-35, galectin-1), or via granzyme mediated cytotoxicity or IL-2 consumption [70]. Tregs can also indirectly block the activation of effector T cells by acting on APCs to decrease co-stimulation, maturation or antigen presentation of APC through CTLA-4, LAG-3, CD39 and Nrp-1 [70]. Many studies have highlighted the importance of T regulatory cells in controlling T1D. CD28 deficient NOD mice that lack Tregs, develop diabetes at an accelerated rate [71]. In humans, mutation in the Treg transcription factor, Foxp3 (immunodysregulation, polyendocrinopathy, enteropathy, X-linked [IPEX] syndrome) can cause T1D [72]. The NOD mouse does not have a decline in the number of Foxp3⁺ CD4 T cells with age in spleen, pancreatic lymph node or the pancreas [73]. Rather, NOD autoimmunity is associated with the decline of CD4^{pos}CD25^{pos} Treg function both *in vitro* and *in vivo* [73-76]. Gregori et al. has shown that CD4^{pos}CD25^{pos} T cells isolated from 8-week-old NOD are more suppressive than 16-week-old NOD against 16-week-old T responders in an

alloantigen-driven *in vitro* assay [75]. NOD Tregs also show loss of TGF- β surface expression with age [35, 76, 77]. Since T regulatory cells can suppress through surface TGF- β , the reduction in surface TGF- β could decrease suppression of pathogenic T cells [78]. Treg defects in NOD are associated with relative lack of IL-2 and IL-2R signaling [79, 80]. The impairment of Treg function and decreased IL-2 in NOD is linked with an IL-2 SNP (single nucleotide polymorphism) in the *Idd3* susceptibility locus [19].

Apart from thymus-derived naturally occurring CD4^{POS}CD25^{POS}Foxp3+ Tregs, there are other subsets of “adaptive” Tregs (Th2, Th3, Tr1 cells) that are generated *in vitro* and *in vivo* from CD4^{POS}CD25^{NEG} T cells. These precursor Foxp3 negative T cells under conditions such as specific antigenic stimulation, alter the nature of the APCs or cytokine milieu (IL-10 and TGF- β) to differentiate into adaptive regulatory T cells [81-83]. Studies show that NOD mice (and not C57BL/6 and BALB/C mice) have TGF- β dependent CD4^{POS}CD25^{NEG} FoxP3^{POS} adaptive Tregs that arise from peripheral CD4^{POS}CD25^{NEG} T lymphocytes to control ongoing autoimmunity [84]. These CD4^{POS}CD25^{NEG} adaptive Tregs are also induced during protective anti-CD3 immunotherapy in NOD mice [84]. In addition NOD mouse also have spontaneously arising IL-10-dependent Tr1 adaptive Tregs specific for an epitope in an important target antigen, glutamic acid decarboxylase (GAD) that can efficiently protect against diabetes development in an adoptive transfer study [85]. Therefore both natural and adaptive Tregs contribute towards immune tolerance, however their overall effect is not sufficient to prevent T1D in NOD mice.

1.3 ENVIRONMENTAL FACTORS IN DIABETES

Studies show a direct link between the composition of the gut microflora and diabetes development. Diabetes susceptibility is also linked to gut leakiness that allows trafficking of cells into the peritoneal cavity [86]. Since the pancreas, gastrointestinal tract and pancreatic lymph node have the same homing molecules, cells that leak into the peritoneum could traffic to the pancreatic lymph node [87]. Consequently, the intestinal microenvironment could drive activated APC to the pancreatic lymph node. As mentioned above, the initial islet infiltrates are activated macrophages and dendritic cells [33]. Consistent with these observations, the abrogation of signaling in Toll-like receptors (TLRs) through genetic deletion of MyD88, protects NOD mice from diabetes [88]. This suggests that intestinal microflora may trigger breakdown of tolerance and initiation of islet infiltration, which is an area of active research.

Autoimmune T cell response also results from cross-reactive immune responses due to similarity between infectious and self-antigen epitopes. Such “molecular mimicry” is one of the mechanisms responsible for the breakdown of self-tolerance. Viral or bacterial protein epitopes may have structural homology with β -cell autoantigens leading to activation of cross-reacting T or B cells that then cause destruction of β -cells. Similar epitopes are shared between β -cell antigens and viruses such as coxsackie virus B4, rotavirus, rubella and CMV [89-92]. Viruses are also proposed to modulate the expression of T1D through other mechanisms; direct cytolysis of virus infected pancreatic β -cells [93], induction of autoimmune responses to altered/sequestered self antigens as a result of increased β -cell antigenicity [94], viral super antigen-driven bystander activation of autoreactive T cells [95] and virus-induced imbalance

between autoreactive T cells and Tregs [96, 97]. Viral infections can therefore activate pathogenic T cells by cross-reactivity and cytokines produced by the innate cells during infection can further accelerate diabetes.

1.4 NOD CONGENICS

1.4.1 NOD genetics and linkage analysis

The initial genome scan of an NOD cross demonstrated disease associated regions called “insulin dependent diabetes” (*Idd*) loci that conferred genetic susceptibility or protection from the disease [98]. Linkage analysis was used to map the diabetic genes in the NOD mouse. For this, microsatellite genetic maps that showed the allelic differences between inbred strains were constructed [99, 100]. Backcrossing of (NOD X non-diabetic strain) F1 X NOD was performed and typed at each polymorphic locus for recombination events. The number of homozygotes and heterozygotes with disease was assessed and a bias different from equal numbers represented linkage of that locus with the disease; equal number of homozygotes and heterozygotes with disease was observed if there was no linkage of disease at a given marker. If linkage was detected in the analysis, new polymorphic markers that surround the original microsatellite marker were tested. The next step was to construct congenic mice using these *Idd* loci by introgressing resistant *Idd* loci (generally from B6 or B10) onto the NOD background to make congenic mice. The basic principle is to narrow the disease associated genetic interval while retaining the disease prevalence or protection phenotype. The resultant congenic mice

with resistant *Idd* loci showed variable protection from disease; resistance intervals were further reduced through recombination [4]. With smaller intervals, candidate gene investigations became possible. This approach has been successful in identifying a series of candidate genes in T1D, such as IL-2, CTLA-4, CD30 and CD137 [101-105]. CD137, a key focus of this thesis, is the major candidate gene in the *Idd9* region (see below).

1.4.2 Limitations in congenic mapping

NOD congenic mapping dissects critical genetic regions associated with T1D. However there are limits to congenic interval reduction. The development of smaller congenic interval depends upon recombination events near the gene of interest. As recombination events become small, larger colonies of mice are required to make congenic mice with even smaller intervals. This creates a practical difficulty in creating such congenic mouse. The reduction of interval is also limited by the fact that all recombination events are not random and that there are hot spots for recombination [106, 107]. Genetic manipulation in NOD congenics can produce a variety of autoimmune syndromes, such as production of anti-nuclear antibodies (ANAs) and anti-Smith (anti-Sm) antibodies or autoimmune liver disease [108, 109]. Thus the process of narrowing or intermixing *Idd* loci can alter the disease phenotype. Another drawback of the congenic model is that it becomes difficult to determine if the phenotype controlled by the genetic region is associated with the disease. For example, NOD.B10 *Idd9.3* congenic mice (1.2 Mb B10 region in NOD background) have increased protection against diabetes but produce anti-Smith auto-antibodies, [109] but the production of anti-Smith auto-antibodies is not known to be linked with the diabetes protection.

1.5 MAPPING *Idd9* AND ITS SMALLER INTERVALS

1.5.1 Mapping *Idd9*

Linkage mapping of the progeny of (NOD X B10.H2^{g7}) F1 X NOD BC1 led to identifying *Idd9* on chromosome 4 [110]. The increase in diabetes in mice with NOD homozygosity in the *Idd9* region suggested that the NOD alleles for these loci contained diabetes susceptibility genes. The first reciprocal backcross study using B10.H2^{g7} and NOD/Mrk strains showed weak linkage of chromosome 4 to diabetes [111]. The second outcross-backcross study was performed between the diabetes resistant strain B6.PL-*Thy1^a*/Cy and NOD/Mrk, followed by (B6.PL-*Thy1^a*/Cy and NOD/Mrk X)F1 X NOD/Mrk [110]. This cross showed significant linkage of the *D4Nds16* marker to diabetes, which indicated that *Idd9* locus was encoded in the distal region of chromosome 4. The *Idd9* locus also controlled the frequency of diabetes, but had no effect on insulinitis or cyclophosphamide-induced diabetes. Linda Wicker et al. next developed a congenic strain containing approximately 48 cM of B10 genetic region introgressed on the NOD background [104]. Resistance to diabetes confirmed the newly formed NOD.B10 *Idd9* congenic strain. The islet infiltrating cells from NOD.B10 *Idd9* mice primarily expressed IL-4 and CD30 (encoded within the *Idd9* genetic region) whereas NOD islet infiltrating cells expressed IFN- γ and TNF- α [104]. In a different study, CD4 T cells from *Idd9* mice prevented the loss of CD8 T cell tolerance to islet-specific glucose-6-phosphatase protein (IGRP) and indicated the potential role of *Idd9* regulatory T cells within the CD4 T cell compartment [112].

1.5.2 Mapping *Idd9* subcongenic strains

The NOD.B10 *Idd9* mouse, containing 48 cM of genetic interval (*Idd9*) from chromosome 4 of diabetes-resistant C57BL/10 mice has substantial resistance to diabetes, with 3-7% incidence in females [104, 113]. The Wicker group fine-mapped the *Idd9* region by deriving two subcongenic strains, *Idd9R28* and *IddR11* from the original NOD.B10 *Idd9* strain; both of these strains conferred significant protection from diabetes [104]. The *Idd9R28* strain offered significantly more protection than the *IddR11* strain and contained a 35.7 cM *Idd9.1* region. The *IddR11* strain was used to develop a second set of subcongenic strains: *Idd9R15*, *Idd9R38*, *Idd9R35* and *Idd9R73*. The *Idd9R15* and *Idd9R38* strains were significantly protected from diabetes similar to NOD.B10 *IddR11* strain. Subsequently the diabetes protection of NOD.B10 *IddR11* was identified to be within these two loci; a 5.6 cM *Idd9.2* and a 2 cM *Idd9.3* loci [104]. Thus the mechanism of diabetes protection in *Idd9* mice is attributed to three different loci within the region; *Idd9.1*, *Idd9.3* and *Idd9.3*.

1.5.3 NOD.B10 *Idd9.3* congenic strain

NOD.B10 *Idd9.3* congenic mice contain a 1.2 Mb B10 region on chromosome four on the NOD genetic background [114]. NOD.B10 *Idd9.3* congenic females have at least 50% protection from diabetes compared to 20% in NOD females [104]. Unlike NOD, the NOD.B10 *Idd9.3* congenic mice also have high penetrance of antinuclear and anti-Sm autoantibodies [109]. The *Idd9.3* region has 15 different candidate genes as listed in Table 1.1 [114]. CD137 is one of the candidate genes within the *Idd9.3* region [104].

Table 1.1**Genes in *Idd9.3* region**

Genes	Description	Protein function
<i>H6pd</i>	Hexose-6-phosphate dehydrogenase	Has H and G form. The H form dehydrogenates other hexose-6-phosphates. The G form is specific for glucose-6-phosphate [115].
<i>Gpr157</i>	G protein-coupled receptor 157	Transmembrane receptors that bind to the ligand and activate signal transduction pathways leading to cellular response [116].
<i>Slc2a5</i>	Solute carrier family 2, member 5	Absorption of fructose in the intestine and generation of fructose-induced hypertension [117].
<i>Slc2a7</i>	Solute carrier family 2, member 7	Intestinal absorption of glucose through diffusion [118].
<i>Ca6</i>	Carbonic anhydrase 6	Zinc metalloenzymes that catalyze the reversible hydration of carbon dioxide. Found in salivary glands and saliva [119].
<i>Eno1</i>	Enolase 1	Aids during glycolysis and downregulates the activity of c-myc protooncogene [120].
<i>Rere</i>	Arginine-glutamic acid dipeptide (RE) repeats.	Associates with histone deacetylase and functions as transcriptional co-repressor during embryonic development [121].
<i>Dnb-5</i>	Deleted in neuroblastoma 5	Localized to membrane to mediate the uptake of glucose along the pH gradient.
<i>Mig-6</i>	Mitogen-inducibile gene 6	Induces transcriptional activation of NF-kB gene. Overexpression leads to activation of SAPKs/JNKs

		pathways [122].
<i>Park7</i>	Parkinson protein 7	Positive regulator of androgen receptor-dependent transcription. functions as a sensor for oxidative stress, and it protects neurons against oxidative stress and cell death [123].
CD137	TNF receptor superfamily 9 (Tnfrsf9)	Co-stimulatory molecule expressed on activated CD4 and CD8 T cells. Constitutively expressed by Tregs and DC.
<i>Uts2</i>	Urotensin 2	An active cyclic heptapeptide that acts as a vasoconstrictor and expressed in the brain [124].
<i>Per3</i>	Period circadian protein homolog 3	Expressed in in a circadian pattern in suprachiasmatic nucleus of brain cells [125].
<i>Vamp3</i>	Vescicle-associated membrane protein 3	Localized in the secretory granules in pancreatic beta cells for insulin secretion and glucose uptake [126].
<i>Camta1</i>	Calmodulin binding transcription activator-1	Associated with memory performance [127].

Table 1.1. There are fifteen candidate genes within *ldd9.3* loci.

The table shows the list of candidate genes within the *ldd9.3* region and the function of the protein encoded by the gene. CD137 is one of the candidate genes within the *ldd9.3* congenic interval [114].

1.6 CD137 IN DIABTES

1.6.1 CD137 (4-1BB) costimulatory molecule

CD137 (also known as 4-1BB in mice and “induced by lymphocyte activation” [ILA] in humans) is an inducible type 1 transmembrane protein of the TNF receptor superfamily that functions as a co-stimulatory molecule [10, 128]. CD137 is a glycoprotein expressed as a 30 kDa monomer or a 55 kDa homodimer on T cells [129]. It is upregulated in T cells 48 hours after *in vitro* activation [130]. CD137 expression kinetics are similar on CD4 and CD8 T cells [131]. CD137 is also expressed on B cells [132], natural killer cells [133] and in both splenic and bone marrow derived dendritic cells [134-136]. We and others have confirmed that CD137 is constitutively expressed by a subset of CD4^{pos}CD25^{pos} T regulatory cells [136-140].

1.6.2 CD137 polymorphism

Sequencing has identified three CD137 sequence variants between NOD and B10 alleles; a valine to alanine at position 24, a leucine to proline at position 211 and an alanine insertion between amino acids 174 and 175 in NOD as shown by Figure 1.1 [104].

Figure1.1

***Mus musculus* CD137 clone in the B10 version**

Pos.	B10	NOD	Mutation Site	Comments
24	Val	Ala (T to C)	exon 1	extracellular domain
174/175	*	Ala (insert GCT)	exon 5	extracellular domain
211	Leu	Pro (T to C)	exon 6	cytoplasmic domain

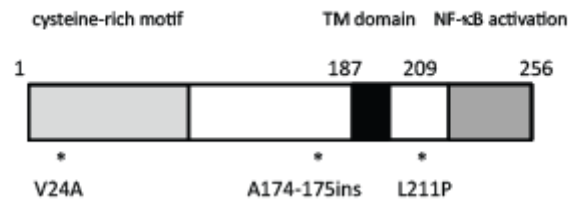


Figure1.1. Polymorphism in the *Idd9.3* region in NOD mice.

CD137 has three sequence variants between NOD and B10. The NOD *Cd137* allele has the following SNPs: i) a valine to alanine at position 24 in the extracellular domain, ii) a leucine to proline at position 211 in the extracellular domain and iii) an alanine insertion between amino acids 174 and 175 in the cytoplasmic domain [104].

Furthermore, the *Idd9.3* interval has been resequenced in the NOD and B6 strains to confirm these polymorphisms and assess other sequence variations throughout the 1.2 Mb *Idd9.3* interval, as shown in Figure 1.2.

Figure1.2

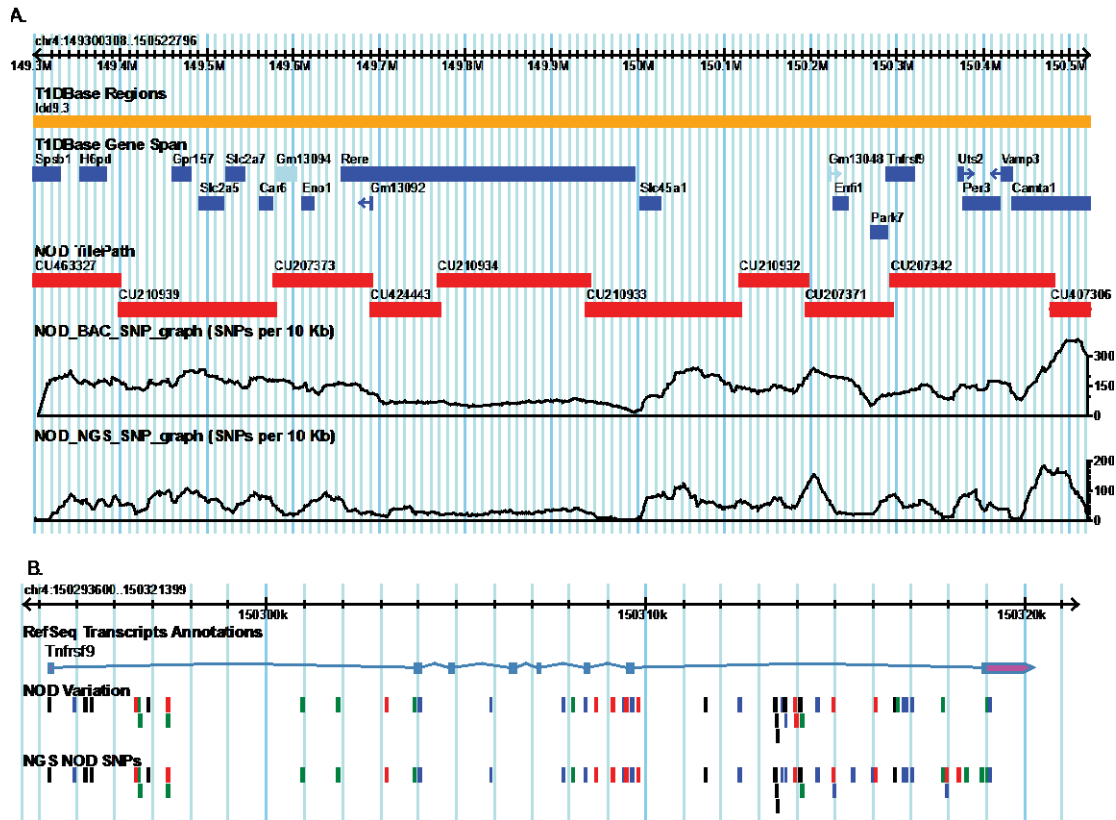


Figure1.2. *Idd9.3* gene content and sequence polymorphisms.

(a) The gene content of the *Idd9.3* interval is displayed in the T1DBase Gene Span track. The NOD tile path track shows the ten NOD/Tac BAC clones forming a minimal tile path spanning the *Idd9.3* region. The NOD BAC SNP graph displays the density of SNPs identified by comparing the NOD/Tac BAC clone sequence to the B6 reference (SNPs per 10 kb). The NOD/ShiLtJ strain has been next generation sequenced (NGS) by the Wellcome Trust Sanger Institute and the NOD NGS SNP graph displays the density of SNPs identified by comparing the NOD/ShiLtJ NGS sequence to the B6 reference. (b) Zoomed in view of *Tnfrsf9*. The NOD variation track represents the location of polymorphic NOD/B6 SNPs across *Tnfrsf9*, identified by comparing the NOD/Tac BAC clones to B6; black, red, blue, and green lines represent G, T, C, and A NOD alleles, respectively. The NGS NOD track shows the NOD/B6 SNPs

identified by comparing the NOD/ShiLtJ NGS sequence to the B6. Note that where multiple SNPs are located close together the lines in the B6/NOD SNPs tracks may represent more than one SNP [141].

Previously it has been shown that NOD and NOD.B10 *Idd9.3* congenic mice expressed CD137 similarly upon anti-CD3 activation *in vitro* [104]. However B10 allele for CD137 can provide greater signals for proliferation and IL-2 production compared to the NOD allele, when stimulated with CD137L [114]. Therefore the allelic polymorphism in CD137 affects the downstream signaling or cytokine production in T cells. However it is difficult to explain how the decreased signaling of the NOD CD137 allele could result in increased incidence of diabetes in NOD mice, and this is a major theme we have further explored in this thesis by focusing on the effects of the NOD and B6 alleles on Treg function.

1.6.3 CD137 stimulation of T cells

CD137 stimulation signals through TNF-receptor-associated factor 2 (TRAF2) which activates NF- κ B and apoptosis signal-regulating kinase-1 (ASK-1), that ultimately regulate genes for cytokine production, effector function and survival [10]. Stimulation of CD137 by agonistic anti-CD137 antibody, soluble CD137L or cell lines expressing CD137L in the presence of anti-TCR antibodies have shown T cell expansion, cytokine production and upregulation of anti-apoptotic genes that prevent activated-induced cell death [142, 143]. *In vitro* CD137 stimulation induces cell cycle progression, cytokine production and prevents activation-induced cell death by inducing anti-apoptotic genes [144]. CD137 signaling in T cells promotes survival and inhibition of apoptosis by induction of the anti-apoptotic molecule Bcl-xl [145, 146]. Viability studies of CD137 stimulated T cells have shown prevention of activation induced cell death (AICD) by repression of DNA fragmentation [147]. T cells with the B10 *Cd137* allele have enhanced

proliferation and IL-2 production compared to NOD T cells when stimulated with CD137L [114]. These studies indicate that CD137 stimulation on T cells results in proliferation, IL-2 production, reduction of AICD and expression of anti-apoptotic molecules, and that variation in NOD and B10 *cd137* allele affects these outcomes.

1.6.4 Agonist anti-CD137 treatment

Agonistic anti-CD137 (3H3) antibody has been shown to reduce the incidence and severity of different autoimmune diseases such as experimental autoimmune encephalomyelitis [148], collagen induced arthritis [149] and experimental allergic conjunctivitis in mice [150]. We have shown that anti-CD137 treatment prevents diabetes in NOD mice and is associated with IL-10 and IL-4 cytokine production and increasing numbers of CD4^{pos}CD25^{pos} T cells *in vivo* [137]. Since mouse CD137 is a dimer, crosslinking with bivalent high-affinity anti-CD137 antibody provides a supra-physiological stimulus that can form multimers on the surface [129]. The multimerized CD137 then recruits Traf2 and signals through nuclear factor NF- κ B and activator protein 1 (AP-1) and thereby can modify many genes at the transcriptional level. Anti-CD137 antibody, therefore, probably acts by enhancing CD137 signaling which, as we noted above, is decreased in the NOD allele. However this does not address which cell type is affected by enhanced CD137 signaling.

1.6.5 CD137 and human diabetes

Initial studies of CD137 did not find linkage with human T1D [151]. However, another recent study has found that the *Cd137* gene is differentially regulated in healthy first degree relatives of patients with type 1 diabetes compared to healthy controls [152]. Another study has shown that

an ubiquitin-editing enzyme TNFAIP3 (A20) was linked to human diabetes [153]. One function of A20 is to downregulate TRAF2 by transporting it to the lysosomal compartment, thus decreasing Traf2-mediated signaling [154]. Since CD137 signals via TRAF2, A20 might indirectly affect CD137 signaling [10]. A20 is also an important anti-apoptotic gene expressed by β cells in the pancreatic islets [155, 156] and loss of A20 expression renders β cells susceptible to apoptotic death [157]. However further studies need to be performed to understand the mechanistic connection between A20 and CD137 signaling in diabetes.

1.6.6 CD137 and T regulatory cells

We have shown that a subset of NOD CD4^{pos}CD25^{pos} T regulatory cells constitutively expresses CD137 (see chapter two below). Marson et al. showed that *Cd137* is one of a small set of genes directly upregulated by Foxp3 [158]. The Mathis group showed that Tregs isolated specifically from NOD pancreatic islets upregulated *Cd137* (*Tnfrsf9*) [159]. CD137L-Fc fusion protein was used to show that CD137 costimulation increases proliferation of Tregs both *in vitro* and *in vivo* [138]. Another *in vitro* study has shown that streptavidin-bound CD137L (CD137L-strep) causes proliferation of CD4^{pos}CD25^{pos} T cells in the presence of IL-2 [160]. Furthermore, this study also shows that proliferating CD4^{pos}CD25^{pos} Tregs express high levels of transcription factor Foxp3, confirming them as true Tregs. More importantly, T regulatory cells pre-treated with CD137L-Fc or CD137L-strep remained functionally suppressive *in vitro* [138, 160]. Therefore CD137 costimulation of Tregs may be important for proliferation both *in vitro* and *in vivo*. In particular, since a subset of Tregs constitutively express CD137 (unlike CD4 and CD8 T cells), they are natural targets for therapeutic effects of the anti-CD137 antibody, which we will explore further below.

1.6.7 Soluble form of CD137

PCR on 768 bp of CD137 coding sequence produced two PCR products; a full length band and another, 135 bp shorter, band [161]. Alternate splicing produces two isoforms of CD137: full length CD137 that is expressed on the surface and soluble CD137 in which transmembrane exon 8 is spliced out as shown in Figure 1.3 [161].

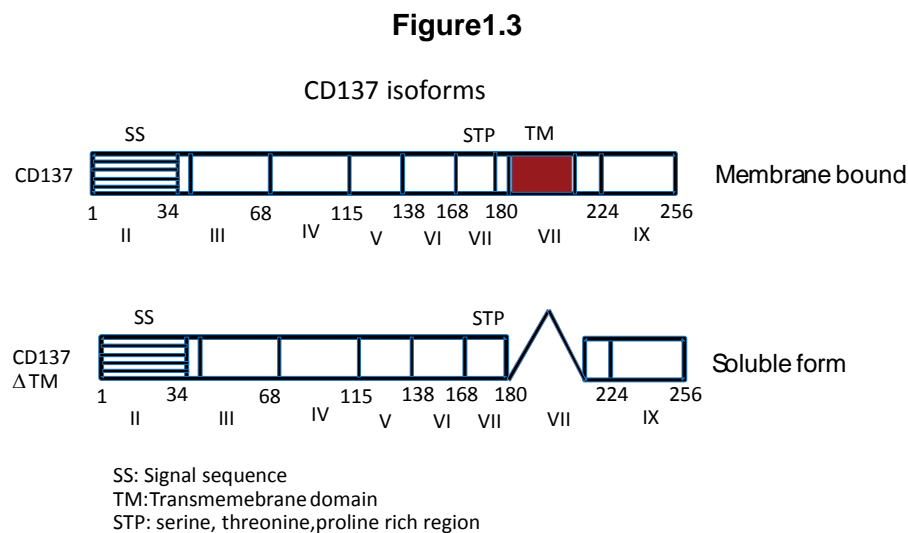


Figure 1.3. A schematic of membrane bound and soluble CD137.

The membrane bound CD137 contains the intracellular domain, the transmembrane domain (TM) and the extracellular domain. The soluble form of CD137 has exon 8 spliced out, which encodes the transmembrane domain [161].

The production of soluble CD137 has been associated with decreased proliferation and increased cell death and DNA fragmentation in human PBMC and mouse splenocytes [162, 163]. Soluble CD137 is increased in autoimmune diseases such as rheumatoid arthritis, multiple sclerosis and systemic lupus [162, 164] and, due to its anti-proliferative effects, its production has been hypothesized as a negative feedback mechanism to control autoimmunity or excess immune response [165]. However further studies are required to understand the function of

soluble CD137 *in vitro* and *in vivo*.

1.7 CD137L and its signaling

1.7.1 CD137 ligand (CD137L)

CD137 ligand (CD137L) is a type II transmembrane glycoprotein that contains TNF homology domains [166]. *In vivo*, the CD137 ligand is expressed on monocytes, DCs and B cells [166]. CD137 ligand is also expressed by activated CD8 T cell and T cell-lines [167, 168]. However CD137L expression must be tightly regulated, as its expression is mostly detectable via PCR detection of mRNA levels during chronic and inflammatory conditions [169, 170]. Similarly several studies have reported very low expression of CD137L protein on CD4 T cells [134, 169].

1.7.2 CD137L signaling on T cells.

As with other members of the TNF and TNFR family, CD137L mediates reverse signaling. CD137L signaling is important in the maintenance of CD8 T cells after viral clearance [169, 171]. The major effect of CD137L on CD8 T cell recall response is due to maintenance of T cell numbers at the end of the primary response and expansion of memory T cells during secondary response [172, 173]. Conversely, expression of CD137L on CD4 T cells has a minor effect on primary response and no effect in secondary response [174]. Notably, CD137L signaling may also be important for Treg survival as CD137 ligand knockout mice showed decreased frequency of Foxp3 expressing CD4^{pos}CD25^{pos} Tregs [175]. However this can also be due the lack of

CD137 stimulation. Soluble CD137-induced CD137L signaling reduced T cell proliferation and increased cell death [162, 176]. These studies indicate the variation and complexity of CD137L signaling in various cell types and that further studies are required to understand its role.

1.8 OUTLINE OF THE THESIS

Previous genetic studies have established that NOD.B10 *Idd9.3* mice are protected from diabetes compared to NOD mice and CD137 is the major candidate gene within the *Idd9.3* interval. Agonistic anti-CD137 treated mice are protected from different autoimmune diseases. Based on these observations, we hypothesized that anti-CD137 treatment might have a protective effect in NOD. Our study, discussed in **Chapter two**, showed that anti-CD137 treatment significantly reduced the incidence of diabetes in NOD mice. Anti-CD137 antibody specifically bound to a subset of CD4^{pos}CD25^{pos} T cells and increased the frequency of these Foxp3 expressing regulatory T cells. The importance of CD137 expressing CD4^{pos}CD25^{pos} Tregs became clear and hence we undertook a comprehensive study of the phenotypic and functional differences between CD4^{pos}CD25^{pos}CD137^{neg} and CD4^{pos}CD25^{pos}CD137^{pos} Treg subsets. These two Treg subsets produced equal amounts of Foxp3 but CD137^{pos} Tregs expressed high levels of CD69, IL-10 and ICOS. *In vitro* functional studies showed that CD137^{pos} Tregs are more suppressive than CD137^{neg} Tregs in contact-dependent and contact-independent system. We further used blocking antibodies against IL-10 or TGF- β or both to show that these factors did not play a significant role in suppressive differences between the two Treg subsets.

Next we tried to understand the role of the CD137 polymorphism in NOD and NOD.B10 *Idd9.3* congenic mice. Previous studies showed that the CD137 allelic differences result in increased proliferation and IL-2 production by T cells with B10 CD137 versus NOD CD137. However it is not clear how the hypo-functional allele results in increased incidence of diabetes in NOD compared to NOD.B10 *Idd9.3* mice. Since CD137 expressing CD4^{pos}CD25^{pos} Tregs are functionally superior, we hypothesized that the increased incidence of diabetes in NOD

compared to NOD.B10 *Idd9.3* mice is due to the differential effect of NOD and B10 CD137 alleles on T regulatory cells. In particular, CD137 allelic variation on Tregs could have an effect on the protein expression and subsequent downstream signaling through CD137, which in T cells is required for proliferation and survival signal. Furthermore, since CD137 signaling affects effector function, we tested if NOD and B10 CD137 allelic variation would alter suppressive function of Tregs. Our studies in **Chapter three** show that the total number and the percentage of CD4^{pos}CD25^{pos}CD137^{pos} T cells significantly declines with age in NOD spleen but not in NOD.B10 *Idd9.3* spleen, suggesting that the B10 allele acted to increase accumulation of CD137 expressing Tregs. To understand the increased accumulation of B10 CD137 Tregs with age, we studied proliferation, survival and cell death between CD137^{pos} Tregs from the two strains. We found that CD137^{pos} Tregs proliferate more than CD137^{neg} Tregs, but there was no difference between the two strains. Again, there was no difference in pro-survival molecules, Bcl-xl and Bcl2 protein levels and *in vitro* cell death between NOD and NOD.B10 *Idd9.3* CD137^{pos} Tregs.

In chapter 3, we also show that CD137^{pos}, but not CD137^{neg} Tregs, expressed higher levels of soluble CD137 mRNA *ex vivo*; in addition aged NOD.B10 *Idd9.3* congenic mice had significantly higher levels of serum soluble CD137 than NOD mice. This is consistent with the increased frequency of CD137^{pos} in aged NOD.B10 *Idd9.3* mice than NOD mice. Therefore CD137 polymorphism in NOD and NOD.B10 *Idd9.3* congenic results in accumulation of suppressive CD137^{pos} Tregs and increased soluble CD137 in NOD.B10 *Idd9.3* mice.

In **Chapter four**, we show studies on the mechanism of anti-CD137 mediated diabetes protection that integrate our prior findings on soluble CD137 and CD137^{pos} Tregs. We hypothesized that anti-CD137 antibody treatment mediates protection at least partially through soluble CD137 and that soluble CD137 can prevent diabetes in NOD mice. First, we used CD25

blocking antibodies to show the importance of CD4^{pos}CD25^{pos} in anti-CD137 mediated diabetes protection. We showed that anti-CD137 treatment specifically upregulates TRAF2 downstream signaling molecules in CD137^{pos} Tregs, but not in CD137^{neg} Tregs. The CD137^{pos} Tregs from treated mice produce significantly higher levels of soluble CD137 *in vitro* compared to untreated mice; in addition the treated NOD also produce high levels of serum soluble CD137. The blockade of CD137L abrogates the CD137^{pos} Treg mediated suppression indicating that Treg-produced soluble CD137 could suppress T cells. CD137-Fc fusion proteins also suppress CD4 T cell proliferation in culture suggesting a direct role of soluble CD137 suppression. In order to develop a more physiological form of soluble CD137, we produced recombinant soluble CD137 by transducing cell lines with lentiviral vectors containing soluble CD137 genome. The soluble CD137 thus obtained was purified and structurally characterized. *In vitro* the soluble CD137 is suppressive to CD4 T cells and further, also reduced the incidence of diabetes in NOD after treatment.

In summary, this thesis is focused on CD137 which is genetically associated with increased protection from diabetes in NOD.B10 *Idd9.3* mice. We have examined the role of CD137 in Tregs in an attempt to understand the genetic cause of disease protection in NOD.B10 *Idd9.3* congenic mice. The maintenance and long-term accumulation of peripheral B10 CD137^{pos} Tregs may play a critical role in disease protection. We generated novel data showing that CD137^{pos} Tregs are a major cellular source of soluble CD137, and that soluble CD137 directly suppresses CD4^{pos} T effector function in an APC independent manner. Systemic administration of soluble CD137 is effective in preventing diabetes in NOD mice. Overall our studies suggest that CD137^{pos} Tregs, and their production of soluble CD137, may play important homeostatic roles in immune regulation and could be used therapeutically to down regulate inflammation in autoimmune disease.

2.0 CD137 MODULATES PROTECTIVE CD4^{POS}CD25^{POS} T CELLS AND PATHOGENIC CD4 T CELLS IN NOD TYPE 1 DIABETES

Some portions of chapter 2 have been adapted from Irie J, Wu Y, Kachapati K, Mittler RS, Ridgway WM. 2007. *Diabetes*. 56:186-96 and some portions adapted from Kachapati K, Adams DE, Wu Y, Steward CA, Rainbow DB, Wicker LS, Mittler RS, Ridgway WM. *J Immunol*. 2012. 189:5001-15 while the remaining represents unpublished data. The use of data from published articles adheres to the copyright guidelines stated by Journal of Immunology and Diabetes. The initial antibody treatment, adoptive transfer study and *in vitro* results were generated by Junichiro Irie and Yuehong Wu. Kritika re-tested some earlier *in vitro* results and performed all studies with the T regulatory cell subsets.

2.1 INTRODUCTION

The NOD mouse spontaneously develops insulinitis (infiltration of the pancreatic islet cells) at 3 weeks of age and type 1 diabetes around 20 weeks [4]. The major histocompatibility complex (MHC) class II molecule, I-A^{g7} is necessary but not insufficient to mediate diabetes when placed on a non-autoimmune non-MHC background, suggesting that the disease is a complex multigenetic process [177]. NOD mice have multiple recessive loci, known as “insulin-dependent diabetes” (*Idd*) loci, which increase the susceptibility or resistance to diabetes [98]. There are at

least 20 known *Idd* loci [4]. B10 *Idd9* is one protective locus, which is further divided into *Idd9.1*, *Idd9.2* and *Idd9.3* [104]. *Idd9.3* has been mapped to a 1.2-mb interval with 15 genes, including *Cd137* [104, 114]. The NOD allele for *CD137* mediates decreased T cell signaling and interleukin (IL)-2 production when stimulated with *CD137L* compared with the B10 allele [114]. *CD137* is an costimulatory molecule of the TNF receptor superfamily, that is upregulated on T cells after *in vitro* activation [10]. The *CD137* ligand is expressed on activated antigen-presenting cells (APCs), especially at the sites of inflammation *in vivo* [134, 170]. Stimulation through *CD137* augments T cell proliferation and functions as a T cell costimulatory molecule in the absence of *CD28* [130, 178]. In *CD4* and *CD8* T cells, *CD137* costimulation causes expansion and survival [147, 179]. T cells from *CD137^{-/-}* or *CD137L^{-/-}* mice have decreased memory responses to antigen recall; *CD137L^{-/-}* mice adoptively transferred with antigen-specific *CD8* TCR TG cells showed decreased late-stage T cell survival, which suggests a costimulatory role of *CD137* later in T cell activation and in the preservation of memory T-cells [174]. Anti-*CD137* blocked development of collagen arthritis, accompanied by suppression of anti-collagen antibodies and decreased *CD4⁺* recall responses to type-2 collagen [149, 180]. Anti-*CD137* antibody treatment reverses or reduces the incidence of autoimmune diseases such as murine lupus and experimental autoimmune encephalomyelitis (EAE) [148, 181]. Overall, these results demonstrate a powerful effect of *CD137* on T cells and on the progression of autoimmune disease states. *CD4^{pos}CD25^{pos}* T regulatory cells are known to be essential in controlling autoimmunity in human and animal models [182]. In NOD diabetes, *CD4^{pos}CD25^{pos}* T regulatory cells have been shown to have quantitative and qualitative deficiencies, and transfer of these cells suppressed the onset of diabetes [71, 139, 183]. Two studies have shown that *CD137* was upregulated in *CD4^{pos}CD25^{pos}* Tregs [138, 139], although conflicting results on the role of *CD137* in Tregs have also been reported [140].

In this study, we demonstrate that treatment of NOD mice with anti-CD137 antibody prevents autoimmune diabetes but did not eliminate pancreatic insulinitis. Transfer studies show that pathogenic cells persisted despite protection from diabetes. Unfractionated anti-CD137 treated CD4 T cell populations reduce adoptive transfer of diabetes into NOD-*scid* mice, compared to untreated CD4 T cells. Anti-CD137 significantly increases the percent of CD4^{pos}CD25^{pos} T cells in treated mice. Transfer of anti-CD137 treated CD4^{pos}CD25^{pos} T cells completely prevents diabetes in NOD-*scid* recipients, whereas the CD4^{pos}CD25^{neg} T cells offer no significant protection. CD4^{pos}CD25^{pos}CD137^{neg} and CD4^{pos}CD25^{pos}CD137^{pos} T cells express similar levels of Foxp3, TGF- β and CTLA-4 but IL-10 and ICOS expression is higher in CD4^{pos}CD25^{pos}CD137^{pos} T cells. *In vitro* suppression assays show that CD137^{pos} Tregs are functionally superior to CD137^{neg} Tregs but blockade of IL-10, TGF- β or both do not alter the suppressive function of these Treg subsets. Our results show that CD137 expressing Tregs are functionally superior and play a significant role in diabetes protection.

2.2 METHODS

2.2.1 Mice and reagents:

NOD and NOD-*scid* colonies were maintained under specific pathogen-free conditions in the animal facility at University of Pittsburgh School of Medicine. Mice were handled in accordance with the institutional animal care guidelines. Urinary glucose analysis was performed using Tes-tape (Shionogi, Osaka, Japan) once a week. Plasma glucose levels were determined when

glycosuria was detected, and mice with a blood glucose level above 300 mg/dl were considered diabetic. Antibodies against mouse CD3, CD4, CD8, CD25, CD28, CD49b, and T-cell β -receptor were purchased from BD Bioscience. Anti-Foxp3 antibody was purchased from eBioscience. Anti-mouse CD137 antibody (3H3) was produced by R.S. Mittler as previously described [181].

2.2.2 Histology:

Pancreata were fixed in 10% formaldehyde and embedded in paraffin. Thin sections at six levels, 150 μ m apart, were cut for staining with hematoxylin-eosin to evaluate islet-infiltrating cells by light microscopy. At least 35 islets from each recipient mouse were observed and scored using the following criteria: grade 0, islets free of insulitis; grade 1, peri-insulitis; grade 2, intra-insulitis with mononuclear cell infiltration of <50% of the area of each islet; and grade 3, intra-insulitis with mononuclear cell infiltration of >50% of the area of each islet.

2.2.3 Cell purification and culture:

CD4^{pos}, CD4^{pos}CD25^{pos}, CD4^{pos}DX5^{neg}, or CD8^{pos} T cells were purified using magnetic beads (Miltenyi Biotec, Auburn, CA). The cells were >90% pure when tested by Flow cytometry. Purified CD4 populations were sorted using flow cytometry. CD4+ cells (1×10^6) in 2 ml culture medium were transferred to 24-well anti-CD3 antibody precoated plates with or without soluble anti-CD28 antibody (1 μ g/ml). The cells were cultured for 72 h at 37°C in a humidified 5% CO₂ incubator, and supernatant collected.

2.2.4 Suppression Assay:

For Treg suppression, 50,000 responder CD4 T cells or CD4^{pos}CD25^{pos} cells or both were plated in 96-well plates with soluble anti-CD3 antibodies and irradiated splenocytes as APCs. For the Treg subset suppression assay 50,000 CD4^{pos}CD25^{neg}CD137^{neg} T cells were cultured in U-

bottom 96 well plates with 1ug/well soluble anti-CD3, 50,000 irradiated splenocytes (1500 rads) and varying numbers of CD4^{pos}CD25^{pos}CD137^{neg} or CD4^{pos}CD25^{pos}CD137^{pos} Tregs. All cells were cultured and pulsed with 1 µCi [3H] thymidine on Day 3, 16 hours before harvest. On Day 4, thymidine incorporation was assessed using a beta scintillation counter.

2.2.5 Treg Transwell Suppression Assay:

100,000 sorted CD4^{pos}CD25^{neg}CD137^{neg} T cells were cultured with 100,000 irradiated splenocytes (1500 rads) and 1.25ug/ml soluble anti-CD3 in the bottom wells of a 96 well transwell plate (Corning). 25,000 or 50,000 CD4^{pos}CD25^{pos}CD137^{neg} or CD4^{pos}CD25^{pos}CD137^{pos} Tregs were cultured in the top wells with 100,000 irradiated (1500 rads) splenocytes and 1.25ug/ml soluble anti-CD3. In some assays the sorted CD4^{pos}CD25^{pos}CD137^{neg} or CD4^{pos}CD25^{pos}CD137^{pos} Tregs were also cultured in the bottom of the transwell along with the CD4^{pos}CD25^{neg}CD137^{neg} T effector cells (with no Tregs in the top transwell) to directly compare contact dependent and independent suppression by the same sorted cells. The cells were cultured at 37°C in 5% CO₂ and were pulsed with 1 µCi [3H] thymidine on Day 3. The cells in the bottom wells were harvested and counted using a beta scintillation counter.

2.2.6 Flow cytometry:

Cells were incubated with Fc blocker (Pharmingen) and stained with labeled antibodies for 25 min at 4°C. Samples were analyzed on a FACS Caliber (Becton Dickinson, Miami, FL). Intracellular cytokine staining of Foxp3 was performed according to the manufacturer's instructions. For FACS analysis, cells were stained with CD4-APC, CD25-FITC and stained for CD137 using IgG2a anti-CD137 or IgG2a isotype, then anti- IgG2a biotin and strepavidin-APC. For surface expression of CTLA-4 and ICOS, CD4 cells were purified from whole spleen using

CD4 magnetic beads (Miltenyl Biotech, California). The CD4 T cells were then stained with CD25-FITC, anti-CD137/APC (as above), and CTLA-4-PE or ICOS-PE (or their matched isotype control) and analyzed on a Facs Caliber (BD Biosciences). For CD69 and CD62L staining, splenocytes from female NOD mice were stained with CD4-APC, CD25-Percp-Cy5.5, CD137-PE, CD69-FITC and CD62L-APC-Cy7 and analyzed on FACS Cantos (BD Biosciences). All Facs data was analyzed using FlowJo (Treestar, Oregon).

2.2.7 RT-PCR:

CD4 T cells were extracted from splenocytes using CD4 magnetic beads (Miltenyl Biotech, California). The CD4 T cells were blocked with 2.4G2 and stained with CD4-APC, CD25-FITC, and anti-CD137-APC as above. The cells were sorted using a BD Facs Aria machine (BD bioscience) into CD4^{pos}CD25^{neg}CD137^{neg}, CD4^{pos}CD25^{pos}CD137^{neg} and CD4^{pos}CD25^{pos}CD137^{pos} cell subsets, RNA was extracted from the sorted cells using an RNeasy mini kit (Qiagen) and converted into cDNA (Promega Reverse Transcription System). Quantitative Real Time Polymerase Chain Reaction (RT-PCR) was performed on the cDNA using primers for *Gadph* or *B2m*, *Foxp3*, *Ctla4*, *Tgf-β*, *Girtr* and *Icos* using a StepOnePlus Real-Time PCR system (Applied Biosystems). The CT values of the gene of interest were subtracted from the CT of the housekeeping gene (*Gadph* or *B2m*) and the data graphed using GraphPad Prism 5 (Version 5.02).

2.2.8 ELISA:

Cytokines (IFN-γ, IL-4, and IL-10) were measured by enzyme-linked immunosorbent assay (ELISA) as previously described [184]. Briefly, flat-bottom 96-well plates were coated with anti-IFN-γ, anti-IL-4, or anti-IL-10 antibodies (Pharmingen), and supernatants were added. After incubation, biotinylated anti-cytokine antibodies and then europium-avidin solution (Perkin

Elmer, Turku, Finland) was added. After adding enhancement solution (Perkin Elmer), plates were measured with an ELISA reader (Perkin Elmer). Results are presented as means \pm SE. Differences between the two groups were analyzed using Mann-Whitney U test for nonparametric unpaired observations.

2.2.9 Adoptive transfer:

Log-rank tests were used to compare the incidence of diabetes between two groups using JMP IN software (SAS Institute) and Graph-pad (Graph-pad Software).

2.3 RESULTS

2.3.1 Anti-CD137 prevents diabetes but not insulinitis.

First we tested the effect of agonist anti-CD137 on the course of type 1 diabetes in NOD mice [104] by treating 6-week-old female NOD mice with a total of three 200- μ g doses of anti-CD137 antibody (clone 3H3) administered over a 9-week interval every 3rd week. Control mice received PBS alone. Mice were tested for glycosuria every week. The administration of anti-CD137 antibody significantly suppressed type 1 diabetes in NOD mice (Figure 2.1a; $P = 0.0005$).

Figure 2.1

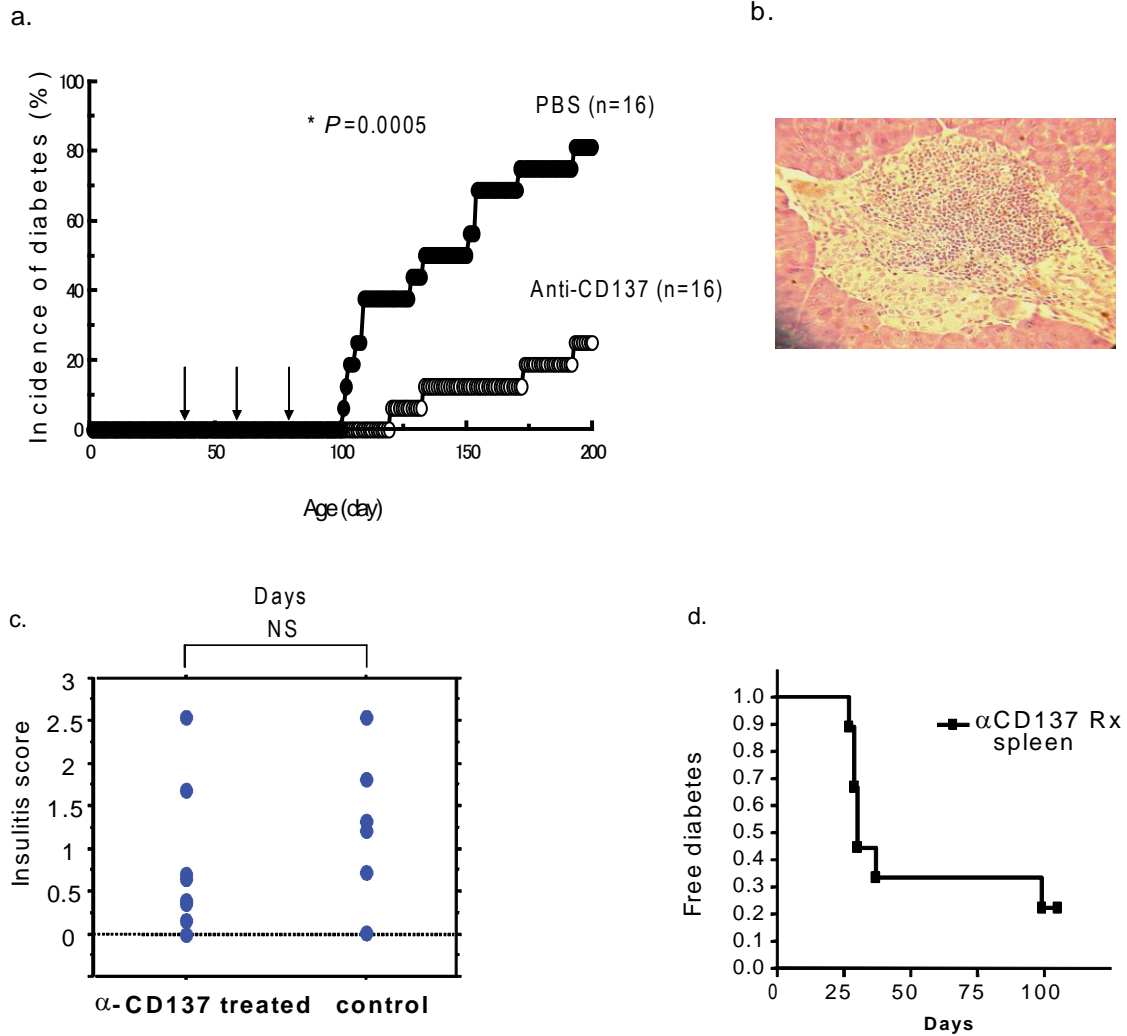


Figure 2.1. Anti-CD137 antibody prevents type 1 diabetes in NOD mice but not insulinitis.

(a) Female NOD mice aged 42–44 days were treated three times with 200 μ g anti-CD137 antibody (\circ ; n = 16) or 200 μ g PBS (\bullet ; n = 16) (see arrows). The onset of diabetes was detected by checking for glucosuria every week and confirmed when the blood glucose levels were >300 mg/dl. * $P = 0.0005$ vs. control by log-rank test. (b) The pancreases of anti-CD137–treated, diabetes-free female NOD mice aged 207–254 days were studied by hematoxylin-eosin staining. One representative of eight mice. (c) Female NOD mice aged 46–55 days were treated twice with 200 μ g anti-CD137 antibody (n = 8) or 200 μ g PBS (n = 6) and scored for insulinitis 1 week after the second injection. (d) Splenocytes were harvested from

anti-CD137–treated NOD mice aged over 200 days and transferred into a total of nine NOD-*scid* mice (n=3).

NOD.B10 *Idd9* mice that have decreased diabetes incidence show no reduction in insulinitis [104]. Consistent with this report, the histology of the pancreas showed that anti-CD137 did not suppress pancreatic islet infiltration (“insulinitis”) in mice protected from diabetes (Figure 2.1b). Next we scored pancreata for insulinitis in anti-CD137 antibody treated or PBS treated mice. The insulinitis score between treated and control NOD mice showed no difference (Figure 2.1c). Therefore anti-CD137 treatment prevents type 1 diabetes but not by preventing insulinitis. To test if the anti-CD137 treatment directly or indirectly altered or regulated the pathogenic effectors, we transferred 20×10^6 splenocytes from anti-CD137 treated non-diabetic NOD mice, aged over 200 days, into NOD-*scid* recipients. Although the donor mice were protected from diabetes, the NOD-*scid* recipients developed diabetes, indicating that the donors retained pathogenic T cells that were regulated in the donor mice (Figure 2.1d). The transfer of splenocytes into NOD-*scid* mice would also cause homeostatic expansion of autoreactive cells in the lymphopenic environment [185], which might overwhelm the remaining regulatory effect. These results showed that pathogenic T-cells were not destroyed or inactivated in anti-CD137–treated NOD mice.

2.3.2 CD4 T cells from anti-CD137 treated mice prevent adoptive transfer of diabetes.

Next we tested if unfractionated CD4 T cells from recently treated mice would ameliorate disease in a NOD-*scid* transfer model. To test this, we transferred CD4 T cells from anti-CD137 or PBS treated pre-diabetic NOD mice along with diabetic NOD CD8 into NOD-*scid* recipients. As a control we transferred diabetic NOD CD4 with diabetic NOD CD8 into NOD-*scid* recipients. The anti-CD137 treated CD4 T cells significantly reduced incidence of diabetes compared to

CD4 cells from the PBS-treated age-matched controls (Figure 2.2; $P = 0.0016$). The diabetic CD4 and CD8 caused a rapid onset of diabetes in the recipient mice (Figure 2.2). Therefore CD4 T cells from NOD mice recently treated with anti-CD137 counteract the disease process even in the NOD-*scid* transfer model. Notably, the protective effect of anti-CD137 antibody in the NOD-*scid* transfer model was less than in normal NOD mice (Figure 2.1a). This is likely due to rapid homeostatic effector expansion in NOD-*scid* mice.

Figure 2.2

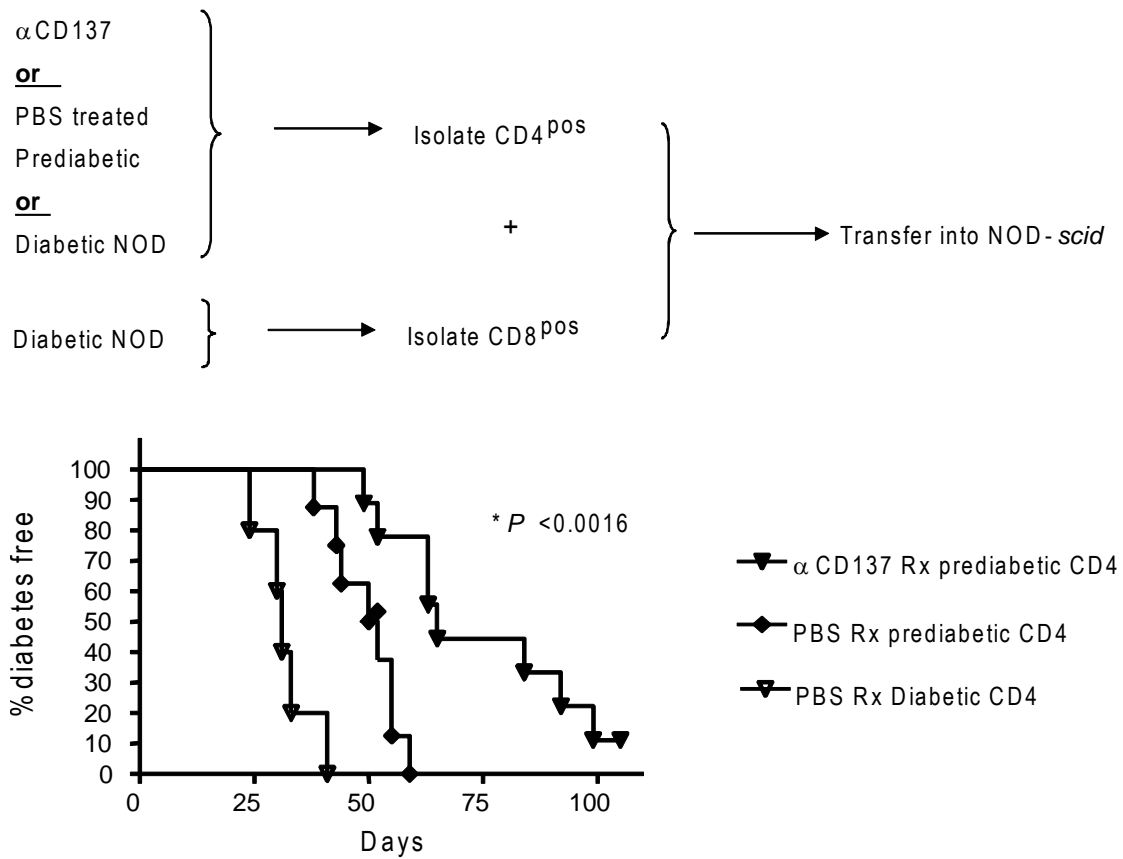


Figure 2.2. CD4 T cells from anti-CD137 treated mice prevent diabetes in NOD-*scid* mice.

Female NOD-*scid* mice received $(0.5-2) \times 10^6$ diabetic CD8 T cells with 2×10^6 CD4 T cells from pre-diabetic female NOD mice (74 days old), either treated with anti-CD137 or PBS as above (see transfer scheme). The sum of three independent experiments is shown (anti-CD137, \blacktriangle , $n = 9$; PBS, \blacklozenge , $n = 8$), $P =$

0.0016 by log-rank test. A group receiving CD4 and CD8 T cells from diabetic NOD donors is shown for comparison of diabetes onset between diabetic and pre-diabetic donors.

We also tested the protective role of CD8 T cells in a similar NOD-*scid* transfer model where we transferred diabetic CD4 T cells with CD8 T cells from either anti-CD137 treated or PBS treated NOD mice into NOD-*scid* recipients. The CD8 T cells from treated NOD mice showed no protection from diabetes, indicating that these cells are unlikely to participate in anti-CD137–induced diabetes protection (data not shown). Our results matched a previous study that showed that anti-CD137 mediated reversal of systemic lupus erythematosus (SLE) was independent of CD8 T cells [181]. Our results confirmed that anti-CD137 mediated protection is within the CD4 T cell population.

2.3.3 Anti-CD137 treatment alters the cytokine phenotype of CD4 T cells.

The CD4 T cell subset was clearly important in anti-CD137 antibody mediated diabetes protection. Next we tested the cytokine profile of the CD4 T cells from anti-CD137 treated versus untreated control. The CD4 T cells from anti-CD137 treated mice produced significantly more IL-4 and IL-10 and less IFN- γ than CD4 T cells from untreated mice (Figure 2.3).

Figure 2.3

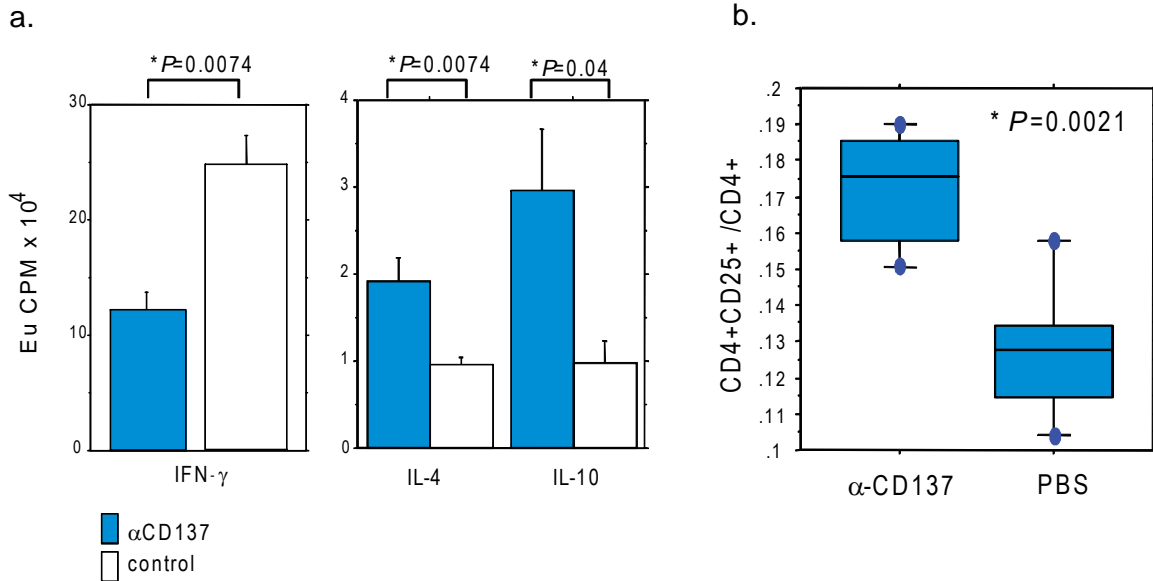


Figure 2.3. Anti-CD137 treatment increases IL-4 and IL-10 production and the fraction of CD4^{pos}CD25^{pos} T cells.

Female NOD mice aged 49–55 days were treated with 200 μ g anti-CD137 antibody (n = 7) or 200 μ g PBS (n = 5) every 3 weeks and studied 1 week after the second CD137 treatment. CD4 T cells were purified by magnetic beads and stimulated with plate-bound anti-CD3 antibody for 3 days. The supernatants were collected and IFN- γ (i), IL-4 (ii), and IL-10 (iii) concentrations were measured by ELISA. The europium counts for each sample are shown. P=0.0074; P=0.0074; and P=0.04 by Mann-Whitney U test. (b) Female NOD mice 5–8 weeks of age were treated with 200 μ g anti-CD137 antibodies twice at 3-week intervals, and splenocytes were tested for the ratio of number of CD4^{pos}CD25^{pos} T cells to CD4 T cells, one week after the second treatment.

Next, we asked to what extent the change in cytokine production in the CD4 population was due to Dx5+ cells. CD4+Dx5+ cells produced significantly high levels of IL-4 and IL-10 after treatment but these cells did not protect NOD-*scid* mice in an adoptive transfer model [137]. The

transfer of type 1 diabetes from splenocytes of anti-CD137–treated non-diabetic mice and the protective capability of anti-CD137–treated CD4 subsets indicated that anti-CD137 treatment did not destroy/inactivate pathogenic CD4 T cells but acted on regulatory cells. It has been well established that CD4⁺CD25⁺ T regulatory cells can modulate the development of type 1 diabetes in the presence of pathogenic T-cells. CD4^{pos}CD25^{pos} T regulatory cells are known to modulate the development of type 1 diabetes in the presence of pathogenic T cells. Quantitative and qualitative defects of CD4^{pos}CD25^{pos} Treg cells have been reported in NOD mice, and CD4^{pos}CD25^{pos} Tregs can prevent type 1 diabetes in NOD mice [71]. Therefore, we first investigated the quantitative phenotype of CD4^{pos}CD25^{pos} T cells in anti-CD137 treated NOD mice. Anti-CD137 antibody treatment increased the fraction of CD4^{pos}CD25^{pos} T cells in NOD mice (Figure 2.3b). This highlighted the importance of CD137 expressing CD4^{pos}CD25^{pos} T cells for treatment mediated diabetes protection.

2.3.4 Naive CD4^{pos}CD25^{pos} T cells express CD137 and continue expressing Foxp3 after treatment.

Since anti-CD137 treatment increased Treg frequency, we looked at the expression of CD137 within the CD4^{pos}CD25^{pos} T cell population. NOD CD4^{pos}CD25^{pos} T cells upregulate CD137 compared with CD4^{pos}CD25^{neg} T cells, consistent with previous reports (Figure 2.4a) [139]. To confirm that increased CD4^{pos}CD25^{pos} T cells were true regulatory cells and not polyclonally activated T cells upregulating CD25, we performed intracellular Foxp3 staining. The CD4^{pos}CD25^{pos} T cells in anti-CD137 treated mice predominantly expressed Foxp3 (Figure 2.4b). This indicated that the administration of anti-CD137 antibody induced CD4^{pos}CD25^{pos} T cells that are true Tregs with Foxp3 expression and could be associated with diabetes protection

Figure 2.4

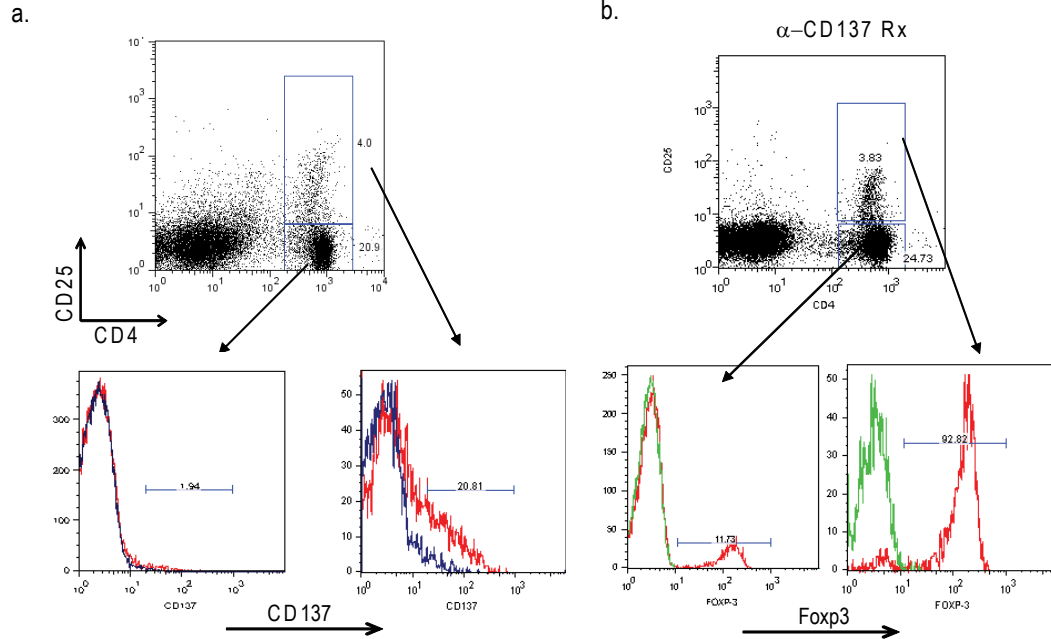


Figure 2.4. Naïve CD4^{pos}CD25^{pos} T cells express CD137 and continue expressing Foxp3 after anti-CD137 treatment.

(a) Splenocytes from 50- to 75-day-old NOD mice were analyzed for CD137 expression on CD4^{pos}CD25^{pos} and CD4^{pos}CD25^{neg} T cells. One representative of 11 NOD mice is shown. (b) Female NOD mice aged 43 days were treated with 200 μ g anti-CD137 antibody or PBS twice within 3-week intervals and studied at 1 week after the second treatment. Surface expression of CD4 and CD25 and intracellular staining for Foxp3 were analyzed.

2.3.5 Anti-CD137 antibody specifically binds to CD4^{pos}CD25^{pos} cells *in vivo*.

Next we tested whether anti-CD137 had a preferential cell target *in vivo*. We harvested splenocytes from NOD mice treated twice with anti-CD137 antibody and stained for CD4 and

CD25 or CD8 and C44 and used the second-step (anti-IgG2a-bio) antibody specific for anti-CD137, followed by streptavidin-PE.

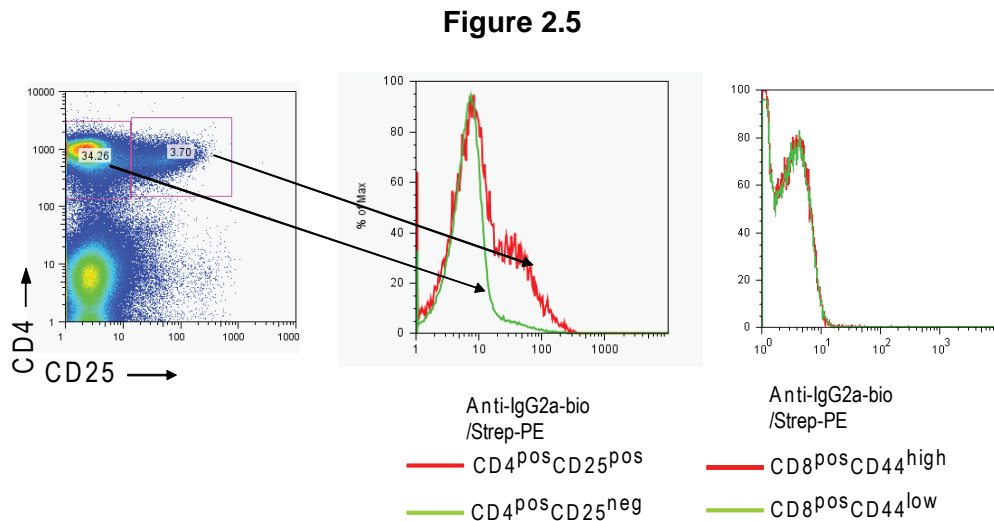


Figure 2.5. Anti-CD137 antibody specifically binds to CD4^{pos}CD25^{pos} T cells *in vivo*.

Female NOD mice were treated with 200 mg anti-CD137 antibody (3H3) or PBS twice at 3-week intervals and stained at 1 week after the second treatment. Splenocytes were stained with CD4 and CD25 or CD8 and CD44 in addition to anti-IgG2a-bio antibodies followed by streptavidin phycoerythrin or streptavidin APC. One representative of five experiments.

Anti-CD137 antibody bound only to CD4^{pos}CD25^{pos} T cells but not to CD4^{pos}CD25^{neg} T cells *in vivo* (Figure 2.5). The secondary antibody also did not bind to CD8^{pos}CD44^{pos} or CD8^{pos}CD44^{neg} T cells subsets (Figure 2.5). Therefore anti-CD137 antibody treatment specifically targeted CD4^{pos}CD25^{neg} T cells *in vivo* and studying these Treg subsets might be essential to understand the mechanism of anti-CD137 mediated protection.

2.3.6 Anti-CD137 treated CD4^{pos}CD25^{pos} T cells prevent adoptive transfer of diabetes

Next, in order to find the protective CD4 subset, we tested if anti-CD137 induced CD4^{pos}CD25^{pos} T cells were protective against diabetes. For this, we transferred CD4^{pos}CD25^{pos} or CD4^{pos}CD25^{neg} T cells from anti-CD137 treated mice, along with diabetic CD8 T cells, to NOD-*scid* recipients. The NOD-*scid* recipients transferred with CD4^{pos}CD25^{pos} cells were completely protected from diabetes compared with those that received CD4^{pos}CD25^{neg} T cells (Figure 2.6, $P < 0.0001$). Moreover, mice receiving anti-CD137 treated CD4^{pos}CD25^{neg} T cells showed no significant difference in disease onset compared with CD4 T cells from PBS treated NOD mice (Figure 2.6, $P = 0.91$). This explains the results shown in Figure 2.2 (above) and supports the hypothesis that anti-CD137 therapy acts on CD4^{pos}CD25^{pos} cells. We also found that some of the mice receiving CD4^{pos}CD25^{neg} T cells developed inflammatory bowel disease (IBD), manifested by wasting and rectal prolapse or neuropathy which was consistent with previous reports (data not shown) [186, 187]. Five of nine mice receiving CD4^{pos}CD25^{neg} T cells developed diabetes, whereas four of nine developed either IBD or neuropathy. The finding that diabetes and neuropathy/IBD were mutually exclusive is consistent with the report of Setoguchi et al. [186].

Figure 2.6

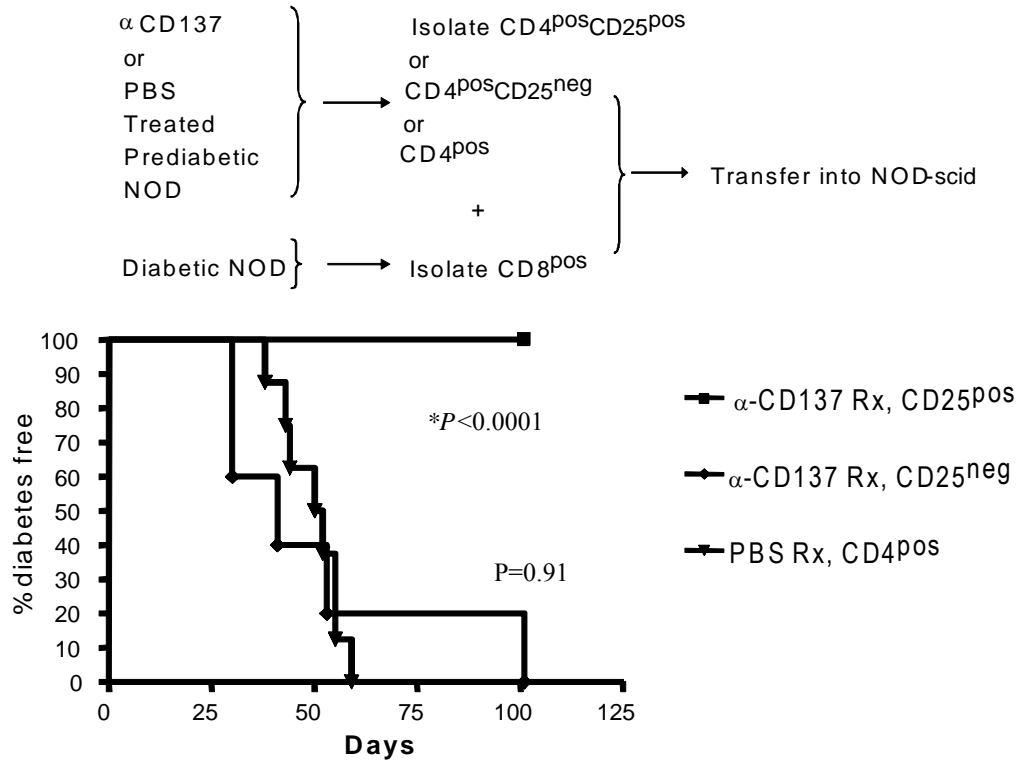


Figure 2.6. Anti-CD137 treated CD4^{pos}CD25^{pos} T cells protect from diabetes.

CD4^{pos}CD25^{pos} T cells from anti-CD137 treated mice protect against diabetes. Female NOD mice aged 38–49 days were treated with 200 µg anti-CD137 antibody (3H3) twice at 3-week intervals; at 10 weeks, CD25^{pos} and CD25^{neg} populations were sorted, and 4–6 × 10⁵ CD4^{pos}CD25^{pos} T cells or 4–6 × 10⁵ CD4^{pos}CD25^{neg} T cells were transferred to female NOD-*scid* mice with diabetic CD8 T cells. Results from two separate experiments are shown.

2.3.7 CD137 expressing CD4^{pos}CD25^{pos} T cells express high levels of IL-10 and ICOS.

Since anti-CD137 antibody preferentially binds to CD4^{pos}CD25^{pos}CD137^{pos} T cells *in vivo*, we studied the phenotypic characteristic of this Treg subset. Previously we have shown that anti-CD137 treated CD4^{pos}CD25^{pos} T cells express high levels of Foxp3 (Figure 2.5b).

Figure 2.7

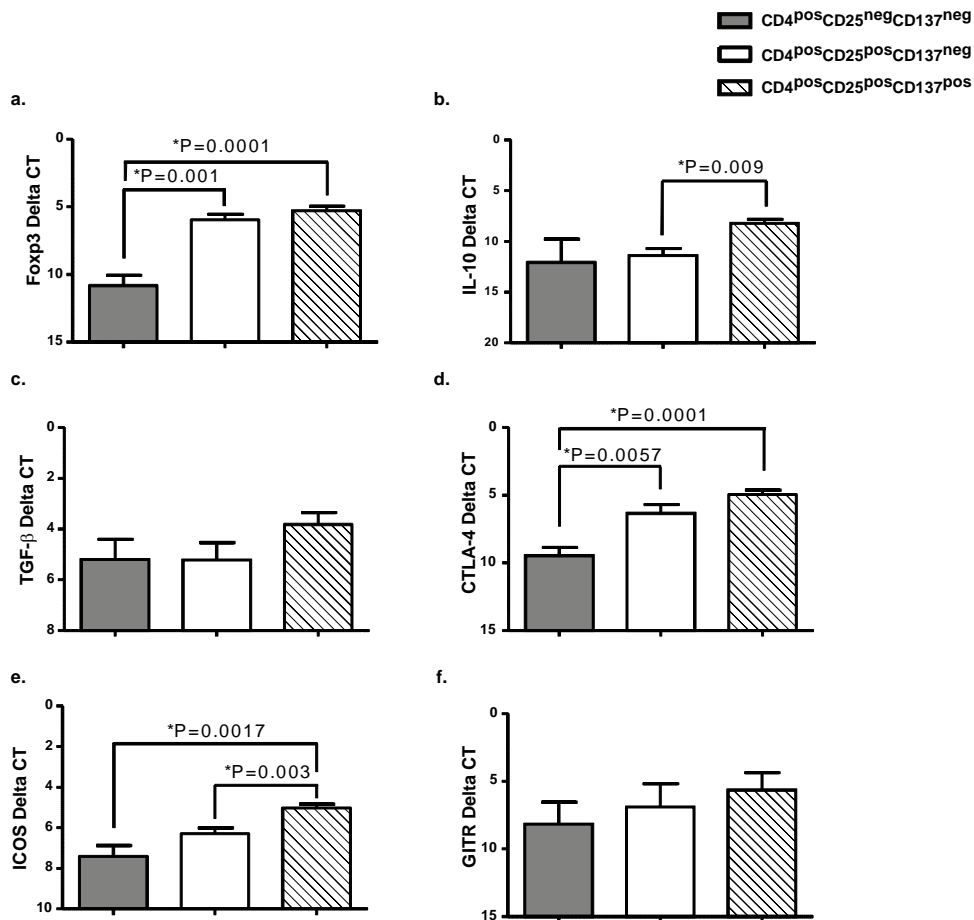


Figure 2.7. CD137^{pos} Tregs have higher levels of *Il-10* and *Icos* mRNA compared to CD137^{neg} Tregs.

Splenocytes from 4-12 week old NOD females were stained with CD4APC, CD25FITC, and anti-CD137APC as described above. 15,000 CD4^{pos}CD25^{neg}CD137^{neg}, CD4^{pos}CD25^{pos}CD137^{neg}, and CD4^{pos}CD25^{pos}CD137^{pos} T cells were FACS sorted. RNA was extracted from the sorted cells and

converted to cDNA as described in the methods. Quantitative Real Time Polymerase Chain Reaction (RT-PCR) was performed on the cDNA using GAPDH and (a) Foxp3 (n=8), (b) IL-10 (n=6), (c) TGF- β (n=6), (d) CTLA-4 (n=6), (e) ICOS (n=6) and (f) GITR (n=4) primers (Applied Bioscience). Statistical analysis was performed using the unpaired T test.

In order to further investigate the role of CD137, we sorted CD4^{pos}CD25^{pos} Tregs with or without CD137 from untreated mice and analyzed mRNA levels of various Tregs markers using RT-PCR. First we showed that both CD137^{neg} and CD137^{pos} Tregs express similar levels of Foxp3 mRNA, significantly greater than CD4^{pos}CD25^{neg}CD137^{neg} T cells (Figure 2.7a). Since Tregs are known to mediate some suppression through expression of TGF- β and IL-10 [78], we studied the expression of these molecules in the two subsets of CD4^{pos}CD25^{pos} T cell. CD137^{pos} cells produced significantly higher IL-10 mRNA than CD137^{neg} cells (Figure 2.7b). Previously we observed that anti-CD137 antibody treatment increased IL-10 production by CD4 T cells *in vitro* (Figure 2.3) and our results show that CD137 expressing CD4^{pos}CD25^{pos} T cell may contribute towards the increase in IL-10 production. Next we showed that both subsets of CD4^{pos}CD25^{pos} T cell have similar levels of TGF- β and GITR transcript (Figure 2.7c, f), although the CD137^{pos} subset showed an increased trend for CTLA-4 and ICOS mRNA expression (Figure 2.7d, e).

2.3.8 CD137^{pos} Tregs express high levels of CD69 and ICOS.

We further analyzed the surface expression of characteristic Treg proteins in the two subsets of CD4^{pos}CD25^{pos} T cell. Compared to CD137^{neg} Tregs, CD137^{pos} Tregs were CD69^{high} and CD62^{low}, indicating an activated phenotype (Figure 2.8a, b). In contrast virtually all CD137^{neg} Tregs were CD62L^{high} and CD69^{low} (Figure 2.8a, b).

Figure 2.8

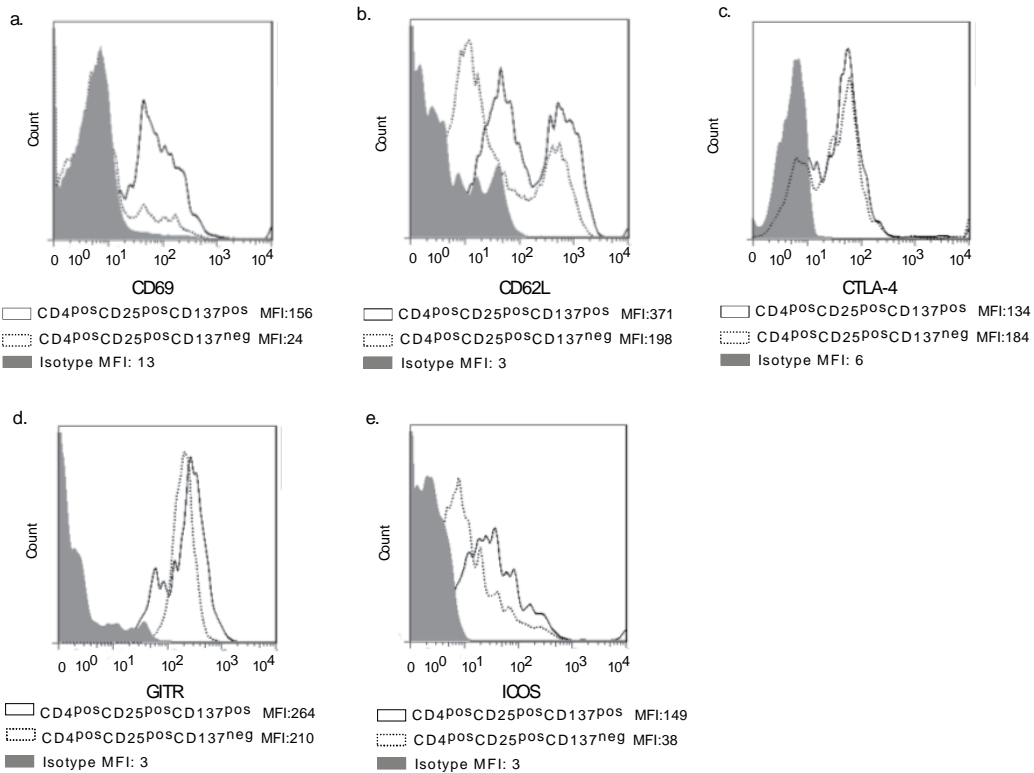


Figure 2.8. CD137^{pos} Tregs upregulate CD69 and ICOS higher than CD137^{neg} Tregs.

(a) 6-7 week old NOD splenocytes were mini-macs bead purified for CD4⁺ T cells. The CD4 T cells were stained with 2.4G2-Fc block followed by CD25FITC, three-step staining for CD137 using 3H3 (anti-CD137) followed by IgG2a biotin and strepavidin APC and CD69-PE (a) or CD62L-PE (b) or CTLA-4-PE (c) or GITR-PE (d) or ICOS-PE (e) and their matched isotype control. The surface expression of CD69, CD62L, CTLA-4, GITR and ICOS were analyzed by flow cytometry and analyzed by FlowJo. The isotype staining on CD4^{pos}CD25^{pos}CD137^{pos} T cells is marked as shaded histogram. Surface expression of the indicated marker on CD4^{pos}CD25^{pos}CD137^{neg} T (perforated line) and CD4^{pos}CD25^{pos}CD137^{pos} (solid line) are shown as indicated. One representative of three experiments each.

Notably CD137^{pos}CD62L^{low} Tregs were mostly CD69^{high}, and CD137^{pos}CD69^{low} Tregs were mostly CD62L^{high}, but CD137^{pos}CD62L^{high} Tregs consisted of both CD69^{high} and CD69^{low} T cells

and CD137^{pos}CD69^{high} Tregs were both CD62L^{low} and CD62L^{high} (Supplemental Figure 1). This is important because CD62L^{pos} Tregs can express CD69 as previously noted [188]. Both subsets of Tregs expressed similar levels of cell surface CTLA-4 and GITR, consistent with the RT-PCR results discussed above (Figure 2.8c, d). Previous studies have shown that costimulation through ICOS is effective in enhancing IL-10 production [189, 190]. Since we observed high IL-10 production in CD137^{pos} Tregs, we looked at ICOS levels. Consistent with our PCR results, CD137^{pos} Tregs produce significantly high levels of ICOS compared to CD137^{neg} Tregs (Figure 2.8e). Hence CD137^{pos} Tregs express an activated phenotype and produce high levels of the immunosuppressive cytokine IL-10 and activation induced co-stimulatory molecule ICOS, which could play a role in their suppressive function.

2.3.9 CD137 expressing CD4^{pos}CD25^{pos} T cells are highly suppressive *in vitro*

To further understand the role of CD137 expressing Tregs, we investigated functional differences between CD137^{neg} and CD137^{pos} Treg subsets. We performed an *in vitro* Treg contact dependent suppression assay using NOD CD4^{pos}CD25^{neg}CD137^{neg} T effector cells and titrated numbers of syngeneic NOD CD137^{pos} or CD137^{neg} Tregs (Figure 2.9). CD137^{pos} Tregs were significantly functionally superior to CD137^{neg} Tregs at every ratio (through 1:32, P=0.002) of Treg:T effector tested (Figure 2.9).

Figure 2.9

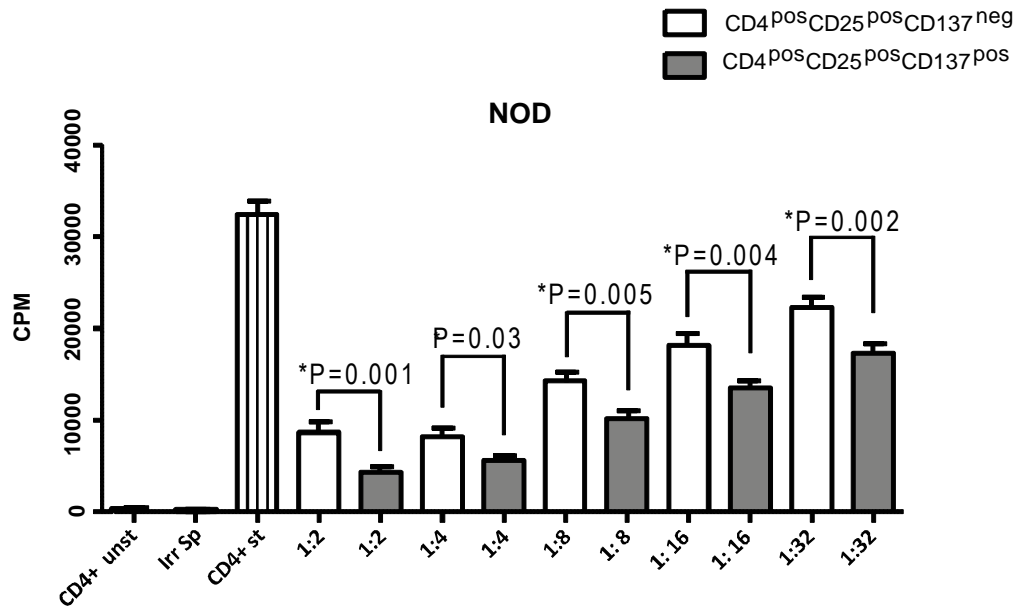


Figure 2.9. NOD CD137^{pos} Tregs are functionally superior to CD137^{neg} Tregs in contact-dependent mechanism.

(a, b) CD4^{pos}CD25^{neg}CD137^{neg} T cells and CD137^{neg} and CD137^{pos} Tregs were sorted from spleen of 4-12 week old NOD female mice as described in the methods. 50,000 CD4^{pos}CD25^{neg}CD137^{neg} T cells were plated in U-bottom 96 well plates with 1.25ug/well soluble anti-CD3, 50,000 irradiated (1500 rads) syngeneic splenocytes and titrated numbers of syngeneic CD137^{neg} or CD137^{pos} Tregs. Unstimulated CD4^{pos}CD25^{neg}CD137^{neg} T cells and irradiated splenocytes alone were used as negative controls. The cells were pulsed with ³H labeled thymidine on day 3 and harvested after 16 hours. The data was pooled from n=10 experiments for 1:2 (CD4 T cell:Treg ratio), n=7 experiments for 1:4, n=8 experiments for 1:8, n=8 experiments for 1:16 and n=7 experiments for 1:32.

CD137^{pos} Tregs are therefore functionally superior *in vitro* and thus anti-CD137 antibody treatment targeting these cells subsets might be important for diabetes protection.

2.3.10 IL-10 and TGF- β block do not abrogate CD137^{pos} Treg suppression.

Next we tried to understand the mechanisms for suppressive difference between CD137^{pos} and CD137^{neg} Tregs. We again showed that CD137^{pos} Tregs suppressed significantly better than CD137^{neg} Tregs (Figure 2.10a). Since we have seen high production of IL-10 by CD137^{pos} Tregs, we added IL-10R blocking antibodies to the culture. The addition of anti-IL-10R blocking antibodies did not alter the suppression of either CD137^{pos} or CD137^{neg} Tregs although the two subsets no longer differed significantly in suppression in the presence of IL-10R antibody (although this could simply be due to the small numbers of samples tested) (Figure 2.10a). As an additional control, we observed that IL-10R blocking antibody did not cause an effect on the proliferation of CD4 T cells without Tregs (Figure 2.10a).

Next, the addition of TGF- β neutralizing antibodies did not affect the suppressive function of either CD137^{pos} or CD137^{neg} Tregs (Figure 2.10b). Furthermore, the combination of both anti-IL-10R and TGF- β blocking antibodies did not alter the suppressive differences between CD137^{pos} and CD137^{neg} Tregs (Figure 2.10c). Our result is consistent with that seen by others where anti-IL-10R and/or TGF- β antibodies did not eliminate the *in vitro* suppression by Tregs although these cells are known to express IL-10 and TGF- β [191-194].

The ineffectiveness of the antibodies could reflect the multiple mechanisms of suppression that Tregs use to suppress such as CTLA-4, granzyme, perforin or by cytokine deprivation-mediated apoptosis [195-198]. These experiments do not rule out the possibility that these soluble immunosuppressive molecules could still be important for Treg function but it makes it difficult to interpret the role of IL-10 in CD137^{pos} Treg mediated suppression.

Figure 2.10

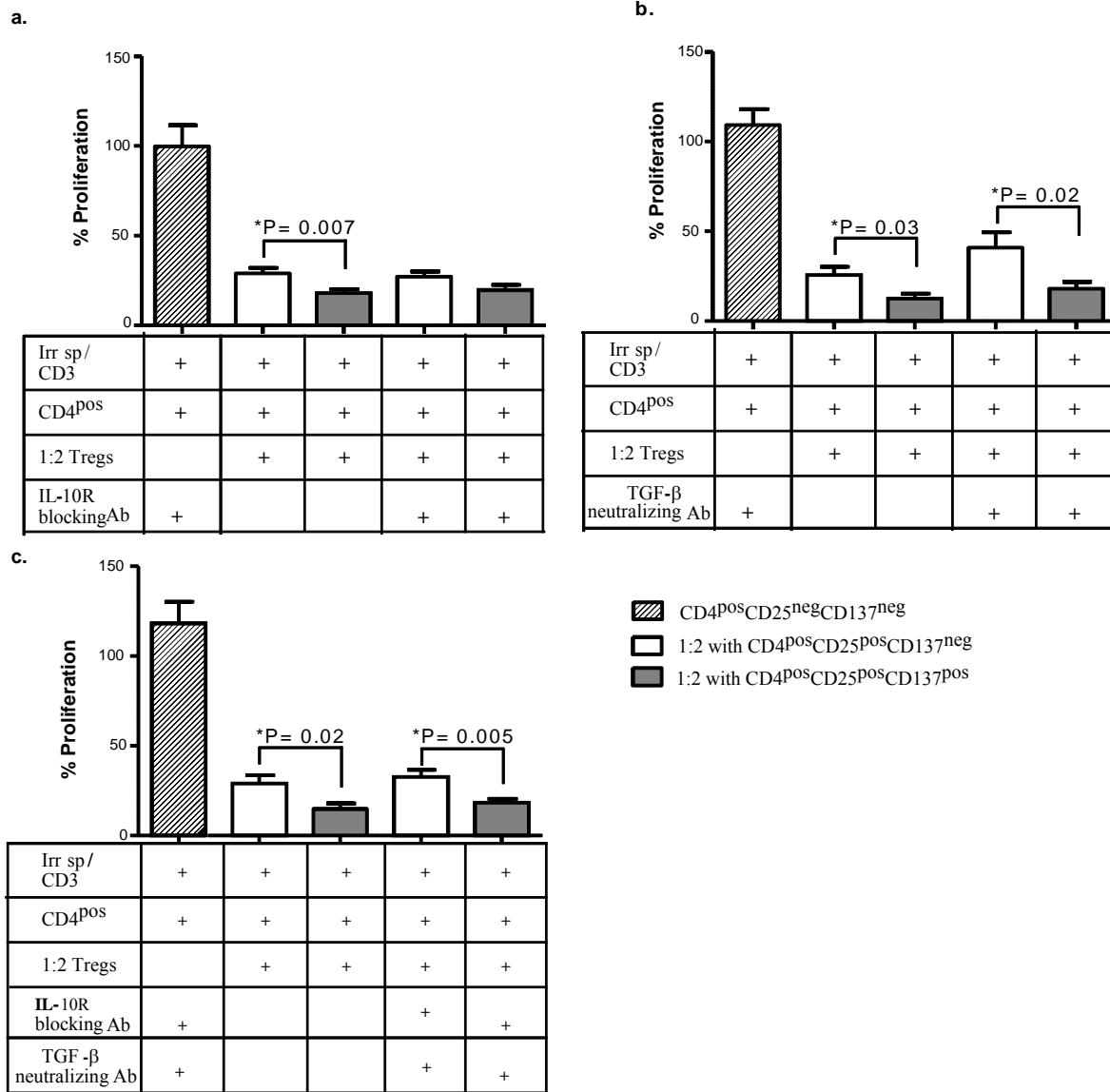


Figure 2.10. Suppression by CD137^{pos} Tregs is not abrogated by both IL-10 and TGF-β blocking *in vitro*.

NOD CD4^{pos}CD25^{neg}CD137^{neg} T cells and CD137^{neg} and CD137^{pos} Tregs were sorted from 5-9 week old NOD mice as mentioned above. 50,000 CD4^{pos}CD25^{neg}CD137^{neg} T cells were plated in 96 well plates with 1ug/ml well soluble anti-CD3 and 50,000 irradiated splenocytes (1500 Rads). 50,000 CD137^{neg} and

CD137^{pos} Tregs were added to the wells as indicated. (a) Some wells were left untreated (n=6 experiments) and 20ug/ml of IL-10R (n=3 experiments) blocking antibodies were added to some wells as indicated. (b) Under similar conditions, 20ug/ml of TGF- β (n=3 experiments) blocking antibodies or untreated wells (n=3 experiments) were tested simultaneously. (c) Some untreated wells (n=5 experiments) and combination of 20ug/ml of both IL-10R and TGF- β (n=3 experiments) blocking antibodies were added to another set of similar cultures. As a control, the blocking antibodies were also added to the proliferating CD4 T cells without Tregs in all types of cultures. The cells were pulsed with 3H labeled thymidine on Day 3 and harvested after 16 hours. The percentage proliferation was calculated by dividing the CPM counts of the wells with the mean CPM count of the wells containing only CD4^{pos}CD25^{neg}CD137^{neg} T cells (without blocking antibodies). Statistical analysis was performed using the unpaired T test.

2.3.11 CD137^{pos} Tregs are functionally superior to CD137^{neg} Tregs in contact-independent suppression.

Next we tested whether CD137^{pos} Tregs can mediate suppression in a contact-independent manner. Using transwell plates, we cultured CD4^{pos}CD25^{neg}CD137^{neg} T cells in the bottom well and Treg subsets in the upper well; both wells had irradiated splenocytes and anti-CD3 antibodies. At a 1:2 ratio, both CD137^{pos} and CD137^{neg} Tregs significantly suppressed the proliferation of T cells in a contact independent manner, but CD137^{pos} Tregs were significantly more suppressive than CD137^{neg} Tregs (P=0.008, Figure 2.11a). Next, we directly compared Tregs from the same donor in both contact dependent suppression (Tregs in the bottom well in contact with T effectors) and contact independent suppression (Tregs in the top well). Tregs were significantly more suppressive in the contact dependent assay than in the contact independent assay (Figure 2.11a, P=0.009 for CD137^{neg} Tregs and P=0.0001 for CD137^{pos}

Tregs). However, in both assays the CD137^{pos} subset mediated significantly more suppression than the CD137^{neg} subset.

Figure 2.11

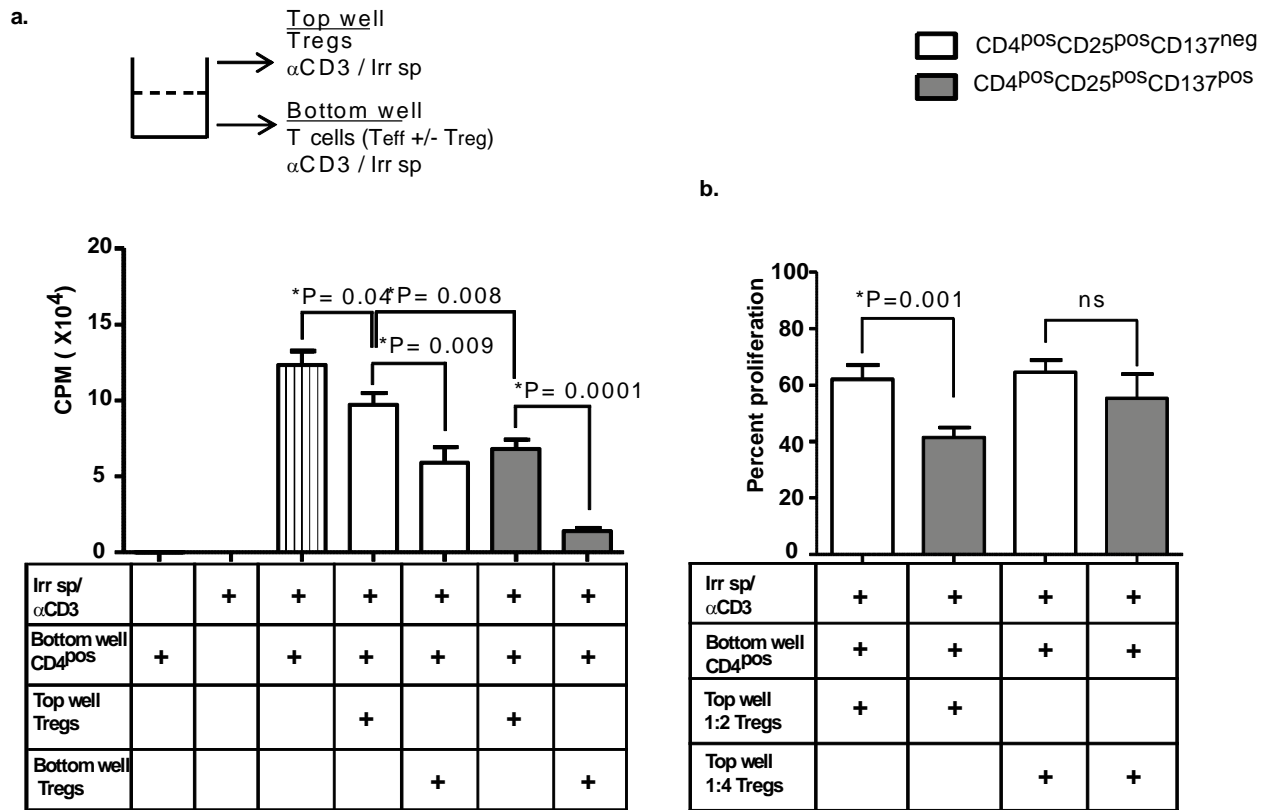


Figure 2.11. CD137^{pos} Tregs are functionally superior to CD137^{neg} Tregs in contact-independent suppression.

NOD CD4^{pos}CD25^{neg}CD137^{neg} T cells and CD137^{neg} and CD137^{pos} Tregs were sorted from 5-9 week old mice as described above. 100,000 CD4^{pos}CD25^{neg}CD137^{neg} T cells were plated in the bottom of 96 well transwell plates with 1ug/well soluble anti-CD3, and 50,000 CD137^{neg} or CD137^{pos} Tregs were cultured in either the top wells (columns four and six, testing for soluble suppression) or the bottom wells (columns five and seven, producing a standard contact dependent suppression as in Figure 7). 100,000 irradiated (1500 Rads) splenocytes were added to both the bottom and top transwells. The cells in the bottom well were pulsed with 3H-labeled thymidine on day 3 and harvested after 16 hours (n=3 experiments for all

conditions). Control wells contained either CD4^{pos} T cells alone (first column), irradiated splenocytes alone (second column) or no Tregs (third column). (b) Mean percent proliferation in transwell suppression assays performed at 1:2 (n=10) and 1:4 (n=3) ratios of Treg:T cell. The percentage proliferation was calculated by dividing the CPM counts of the wells containing Tregs by the mean CPM count of the wells with only CD4^{pos}CD25^{neg}CD137^{neg} T cells. Statistical analysis performed using the unpaired T test.

Finally, we assessed contact independent suppression via serial dilution assays. Ratios of Treg to effector below 1:2 did not show a significant difference in suppression between the CD137^{pos} vs. CD137^{neg} Tregs, consistent with a dilutional effect on a soluble factor (Figure 2.11b). This also shows that contact dependent mechanism is more important for suppression in both Treg subsets. These results suggest that in a contact independent system, both Treg subsets produce soluble suppressive factors when activated, but that CD137^{pos} Tregs can produce either quantitatively higher or different soluble factors that contribute to their functional superiority to CD137^{neg} Tregs.

2.4 DISCUSSION

Antibody treatment directed to the protein product of the *Idd9.3* candidate gene, CD137, prevented the onset of diabetes in NOD mice. In NOD mice, anti-CD137 preferentially bound to CD4^{pos}CD25^{pos} T cells and increased their number. Adoptive transfer models into NOD-*scid* mice showed that the antibody affected the regulatory function of CD4^{pos}CD25^{pos} T regulatory cells and enhanced their ability to control the pathogenicity of autoreactive T cells.

Previous studies have shown that anti-CD137 antibody treatment prevented murine SLE, EAE and collagen arthritis [148, 180, 181]. Here we have shown, for the first time, that anti-CD137 also prevents autoimmune diabetes. Paradoxically, transgenic expression of membrane-bound agonistic anti-4-1BB scFv in pancreatic islets increased the incidence of diabetes [199]. This may be explained by overstimulation of early autoreactive T cells that home the islets. For example, another member of TNF receptor superfamily, TNF- α has dual effects in type 1 diabetes: anti-TNF- α treatment at 9–10 weeks prevents diabetes, whereas TNF- α given to neonates increase diabetes severity [200-202]. Since CD137 is also a member of the TNF receptor superfamily, the dual effect of CD137 in diabetes is perhaps not unexpected. Our study has also shown this dual effect; anti-CD137 treatment at an early age prevented the onset of diabetes (Figure 2.1a), but does not prevent diabetes after adoptive transfer of diabetic cells into NOD-*scid* recipients, in fact it may worsen disease in this setting [137]. Anti-CD137 is most effective at preventing diabetes when given early in the disease process but once a cadre of autoreactive T cells is fully developed, anti-CD137 cannot prevent disease and may even worsen it. In this case, anti-CD137 antibody may target activated pathogenic CD4 T cells that upregulate CD137, thus expanding the autoimmune repertoire and opposing the protective

effect of CD4^{pos}CD25^{pos} Tregs. Furthermore, the splenocytes taken from aged anti-CD137 treated mice can transfer diabetes, suggesting a limit to the regulatory capacity of the anti-CD137 induced Treg cells.

Nevertheless, our results are important for several reasons. *Cd137* is a strong candidate gene for the *Idd9.3* locus, which reduced the incidence of diabetes in NOD genetic background [104]. However neither the genetic insertion of protective B10 *Idd9* nor treatment with anti-CD137 prevented insulinitis. Moreover, the insulitic lesions in the *Idd9* congenic upregulated IL-4, consistent with our results of IL-4 production in anti-CD137 treated CD4 T cells [104]. T cells from NOD.B10 *Idd9.3* congenic mice proliferated more vigorously to anti-CD3 plus anti-CD137 stimulation and produced more IL-2 compared to NOD T cells [114]. This suggested that NOD *Cd137* allele may have relatively defective signaling capability, presumably related to its three sequence polymorphisms compared to the B10 allele [114]. Cannons et. al speculated that decreased signaling through NOD CD137 could result in defective regulatory cell production. Our results are consistent with this hypothesis, because we showed that stimulation through CD137 prevented diabetes in NOD mice by the induction of a regulatory cell population. The specific binding of anti-CD137 to CD137^{pos} Tregs (Figure 2.5 above) supported the hypothesis that the agonist antibody boosts the “defective” NOD CD137 signal in Tregs and enhanced their regulatory function—which we will explore in more detail in later chapters. Although our results do not prove that *Cd137* is the *Idd9.3* gene, they are entirely consistent with this conclusion and supportive of prior studies defining the role of CD137 in type 1 diabetes.

Our study showed that anti-CD137 mediated protection from diabetes via effects on CD4^{pos}CD25^{pos} Tregs. We have seen that CD4^{pos}CD25^{pos} T cells expressed CD137 and more importantly, anti-CD137 antibody specifically bound to CD4^{pos}CD25^{pos} T cells *in vivo*. These findings are consistent with previous reports showing that a subset of CD4^{pos}CD25^{pos} T cells upregulate CD137 [138, 139]. Previous studies have reported qualitative defects of NOD

CD4^{pos}CD25^{pos} Tregs and that boosting NOD CD4^{pos}CD25^{pos} Tregs can prevent diabetes [71, 73]. Similarly, stimulation through CD137 ligand induced proliferation of CD4^{pos}CD25^{pos} T cells that maintain their suppressor function [140]. More importantly, we have seen that transfer of the CD4^{pos}CD25^{pos} T cells from treated mice completely prevented diabetes in an adoptive transfer model, whereas the CD4^{pos}CD25^{neg} T cell subset offered no significant protection. Our study here links NOD CD4^{pos}CD25^{pos} Treg function with the *Idd9.3* candidate gene, *Cd137* and indicates the protective role of these Tregs.

The effects of anti-CD137 antibody on CD4^{pos}CD25^{pos} Treg cells are still controversial (and we will further explore this topic in Chapter 4). Regulatory cells from CD137^{-/-} mice could control CD45RB^{high} T cell induced colitis, implying that CD4^{pos}CD25^{pos} Treg cells may exist independent of CD137 signaling [203]. Moreover, anti-CD137 antibody treatment in the setting of experimental autoimmune thyroiditis breaks tolerance and worsens the disease [204]. The double-edged effect of CD137 signaling likely depends on the balance of pathogenic and protective subsets at the time of treatment in any given model system. Nonetheless, the specific binding of anti-CD137 antibody to CD4^{pos}CD25^{pos} cells *in vivo* and the protective effect of anti-CD137 treated CD4^{pos}CD25^{pos} T cells strongly suggest that the CD4^{pos}CD25^{pos}CD137^{pos} Treg cell subset is a critical protective subset in type 1 diabetes.

Here we also confirmed the previous observation that CD25-depleted CD4 cells transfer several autoimmune diseases [186, 187]. In particular, we provided additional evidence for the observation that the transfer of diabetes versus another organ-specific autoimmune syndrome, such as IBD or peripheral neuropathy, is mutually exclusive in this system [186, 187]. The mechanism for this striking organ specificity and exclusivity of autoimmune attack remains unknown. However, a similar effect of genetic manipulation on disease outcome is also seen in a case where addition of B6/B10 *Idd9.3* loci onto the NOD background induces anti-Sm

antibodies, which are highly specific for SLE in humans [109]. The remarkable “switching” of the tissue focus of autoimmune attack via environmental (CD25 depletion) or genetic (introgression of congenic regions) mechanisms is incompletely explained but is clearly of great importance to understanding the pathogenesis of autoimmunity and type 1 diabetes.

Our results differentiate two sub-populations of CD4^{pos}CD25^{pos} Tregs; one that express CD137 and another that does not. The similar Foxp3 mRNA level in both CD4^{pos}CD25^{pos}CD137^{neg} and CD4^{pos}CD25^{pos}CD137^{pos} T cells is consistent with similar Foxp3 intracellular expression in the two Treg subsets. Also, CD137^{pos} Tregs are distinctly CD69^{pos}, which suggested that these cells have an activated phenotype. The activated phenotype of CD137^{pos} T regulatory cells may be important for efficient suppression at the site of autoimmunity. CD137^{pos}CD69^{pos} Tregs also included some CD62L, required for adhesion and homing [188] (Supplemental Figure 1). The high expression of IL-10 mRNA by CD137^{pos} Tregs suggested that it is important for suppression. IL-10, which is an anti-inflammatory and immunosuppressive TH2 cytokine, is important for preventing TH1 mediated diseases such as diabetes [205]. Microarray studies have demonstrated that there is a high expression of IL-10 and CD137 genes in pancreatic Tregs [159]. Induced Type 1 regulatory T cells (Tr1) are also known to produce high levels of IL-10 [191-193]. IL-10 produced by CD137^{pos} Tregs may prevent cytokine production and proliferation of antigen specific CD4 T effector cells by inhibiting the antigen-presenting cells (APCs) such as DCs, Langerhan’s cells and macrophages [206]. Furthermore we observed CD137^{pos} Tregs expressed significantly high levels of ICOS compared to the CD137^{neg} Tregs. Our results are consistent with other studies which have shown that costimulation through ICOS is effective in enhancing IL-10 production [189, 190, 207]. Previous studies showed that Tregs in the pancreatic lesions express high levels of ICOS and IL-10 in BDC2.5 mice [208]. Although we have not directly linked the ICOS expression with IL-10 production in CD137^{pos} Tregs, there is a strong literature supporting that hypothesis, although we have not proven an effect of IL-10

here. Finally, Treg subsets are not merely phenotypically differentiated by cell surface expression of CD137, but CD137^{pos} Tregs are also functionally superior to CD137^{neg} Tregs in contact mediated suppression.

We also explored the mechanism for suppressive function of CD137^{pos} Tregs compared to CD137^{neg} Tregs. The IL-10R and TGF- β blockade experiments showed that blockade could not abrogate the suppressive advantage of CD137^{pos} Tregs indicating that this subset suppresses through additional mechanism(s). We showed that CD137^{pos} Tregs are functionally superior to CD137^{neg} Tregs in contact independent suppression *in vitro*, indicating that soluble suppressive factors may contribute towards the superior suppression of CD137^{pos} Tregs. Treg mediated contact independent mechanisms include multiple short-range suppressive factors such as IL-10 [209] and TGF- β [210] galectin [211], and IL-35 [212]. While contact independent suppression is still not well understood, many papers have now demonstrated contact independent suppression mediated in transwell plate assays [188, 213-223]. While our study here has not identified the mechanism for functional superiority of CD137^{pos} Tregs, it shows that these Tregs are activated potent suppressors. In later chapters we will explore the finding that soluble CD137 is a source of soluble suppression mediated via CD137^{pos} Tregs. Moreover, the finding of soluble CD137 will show that this Treg subset is not simply an “activated” set of normal Tregs but has unique phenotypic and functional characteristics.

In conclusion, for the first time, we report that anti-CD137 antibody therapy suppressed diabetes in NOD mice and that this effect involved CD4^{pos}CD25^{pos} Tregs. The antibody treatment must be initiated before the development of a cadre of autoreactive T cells, indicating competing effects of anti-CD137 on protective and pathogenic cell subsets. These results implicate a role for the *Idd9.3* candidate gene, *Cd137*, in type 1 diabetes pathogenesis and identify CD4^{pos}CD25^{pos}CD137^{pos} Tregs as activated functionally superior subset that could be essential for preventing diabetes.

3.0 THE B10 *IDD9.3* LOCUS MEDIATES ACCUMULATION OF FUNCTIONALLY SUPERIOR CD137^{POS} T REGULATORY CELLS IN TYPE 1 DIABETES MODEL

Chapter 3 has been partially adapted from Kachapati K, Adams DE, Wu Y, Steward CA, Rainbow DB, Wicker LS, Mittler RS, Ridgway WM. J Immunol. 2012. 189:5001-15 but also includes unpublished data. The use of data from published articles adheres to the copyright guidelines stated by Journal of Immunology. Kritika Kachapati generated all the data presented in this chapter.

3.1 INTRODUCTION

In Non Obese Diabetic (NOD) Type I diabetes (T1D) several genetic elements likely mediate pathogenesis through their effects on disruption of immune tolerance [224]. NOD CD4^{POS}CD25^{POS}Foxp3^{POS} regulatory T cells are insufficient to control immune destruction of the beta cells in the pancreatic islets during progression to diabetes. NOD.B10 *Idd9.3* congenic mice have a 40% reduced incidence of diabetes compared to NOD mice [104, 225]. As

mentioned above, the *Idd9.3* region includes the *Tnfrsf9* gene, which encodes the CD137 co-stimulatory molecule [10] and there are three coding variants between the NOD and B10 *Tnfrsf9* gene, two non-synonymous SNPs and an alanine insertion in NOD [225]. T cells with the B10 *Tnfrsf9* allele have enhanced proliferation and IL-2 production when stimulated via CD137 compared to NOD T cells [225]. As shown by others and in chapter 2, CD137 is constitutively expressed by a subset of CD4^{pos}CD25^{pos} T regulatory cells [136-140]. CD137 signaling promotes proliferation and survival of natural Tregs *in vitro*, which is enhanced by IL-2 [138, 160]. Here we show, for the first time, that the B10 *Idd9.3* region mediates enhanced accumulation of peripheral CD137^{pos} Tregs *in vivo*. NOD.B10 *Idd9.3* congenic mice accumulate significantly more CD137^{pos} Tregs with age compared to NOD mice. Previously we showed that CD137^{pos} Tregs are functionally superior to CD137^{neg} Tregs in suppressing T cells *in vitro* by both contact dependent and independent suppression (Chapter 2). Alternate splicing produces two isoforms of CD137: full length CD137 that is expressed on the cell membrane and soluble CD137 in which transmembrane exon 8 is spliced out [161]. Soluble CD137 is increased in autoimmune diseases such as rheumatoid arthritis, multiple sclerosis and systemic lupus [162, 164]. It has been shown that soluble CD137 can inhibit T cell proliferation, and hypothesized that increased soluble CD137 functions as a negative feedback mechanism to control overactivation of pathogenic cells in autoimmunity [162, 165]. We present novel data showing that CD4^{pos}CD25^{pos}CD137^{pos} Tregs are the major cellular source of soluble CD137. We also show that older NOD.B10 *Idd9.3* congenic mice have significantly increased serum soluble CD137 compared to NOD mice. We suggest that the maintenance and long-term accumulation of functionally superior peripheral CD137^{pos} T regulatory cells (as we show in NOD.B10 *Idd9.3* congenic mice protected from T1D), and their production of soluble CD137, may play a critical role in protection from autoimmune diseases such as type one diabetes.

3.2 METHODS

3.2.1 Mice and reagents:

NOD/MrkTac mice were obtained from Taconic. NOD.B10 *Idd9.3* mice were developed as previously described [104, 225] and are available from The Jackson Laboratory as Stock No. 012311. The NOD.B6-*Ptprc* (hereafter referred to as “NOD.CD45.2”), which has a 1 Mb congenic interval, was developed as previously described [226] and is available from The Jackson Laboratory as Stock No. 014149). NOD.Foxp3-GFP knock-in mice (Hereafter “NOD.Foxp3-GFP mice”) were a kind gift from Vijay Kuchroo and Ana Anderson of Harvard University. The mice were generated by crossing the C57BL/6 Foxp3-GFP KI generated in Dr. Kuchroo's laboratory [227] to NOD Mrk/Tac for 12 generations and then intercrossed for hemi/homozygosity for Foxp3-GFP KI mutation. NOD.B10 *Idd9.3* Foxp3-GFP mice were produced by crossing the NOD.B10 *Idd9.3* to NOD.Foxp3-GFP mice, intercrossing and selecting mice positive for both the *Idd9.3* region and the Foxp3-GFP KI mutation. NOD.Foxp3-GFP mice have normal incidence of T1D in our Cincinnati LAMS facility while the NOD.B10 *Idd9.3* Foxp3-GFP mice show protection from T1D similar to NOD.B10 *Idd9.3* mice in our colony. Mice were maintained under specific pathogen-free conditions in our animal facilities. Mice were handled in accordance with the institutional animal care guidelines of University of Pittsburgh School of Medicine and University of Cincinnati School of Medicine. Anti-CD137 monoclonal antibody (clone 3H3) has been previously described [228]. Antibodies against mouse 2.4G2-Fc, CD4-APC, CD4-APC-Cy7, CD25-PerCP-Cy5.5, CD25-FITC, Streptavidin-PE and Streptavidin-APC were purchased from BD Biosciences. CD3/CD28 coated beads and recombinant mouse IL-2 were purchased from Invitrogen (California). Primers for mouse Gapdh (4352339E-0801016) and Beta-2 microglobulin (Mm00437762_m1) were purchased from

Applied Bioscience (California). We used custom designed primers for membrane bound and soluble CD137 (Applied Bioscience). For membrane bound CD137, the forward primer was CCCCCTGTGGTGAGCTTC and the reverse primer was AGGAGGGCACTCCTTGCA. For soluble CD137, the forward primer was CCCCCTGTGGTGAGCTTC and the reverse primer was GGGAGGACCAGCATTTAAGAAGA. The probe for both the primers is TCCCAGTACCACCATT.

3.2.2 Re-sequencing the *Idd9.3* interval in the NOD mouse strain:

The resequencing of *Idd9.3* in the NOD mouse strain involved aligning the bacterial artificial chromosome (BAC) clone end sequences of the NOD library against the B6 mouse genome sequence [229]. From this, ten NOD BAC clones that formed a minimal sequencing tile path spanning the 1.2 Mb *Idd9.3* interval were selected and sequenced at the Wellcome Trust Sanger Institute and deposited at the European Molecular Biology Laboratory <http://www.ebi.ac.uk/embl> (clone DN-135J18, accession number CU463327; DN-79L21, CU210939; DN-382D20, CU207373; DN-272K19, CU424443; DN-192H14, CU210934; DN-117C24, CU210933; DN-106G2, CU210932; DN-129I7, CU207371; DN-266N3, CU207342; DN-404A18, CU407306). As all the B6 and B10 SNPs were found to be identical by descent throughout the *Idd9.3* region (Mouse phenome database: <http://phenome.jax.org>), we identified polymorphisms between NOD and B6 in the *Idd9.3* interval. The NOD BAC clone sequences spanning the *Idd9.3* interval were aligned to the B6 mouse genome sequence (NCBI m37 mouse assembly) by using the sequence search and alignment by hashing algorithm program [230]. The polymorphisms were entered into T1DBase [231, 232] and displayed graphically using GBrowse [233] (Supplemental Figure 1). The SNP density plots were generated by counting the number of SNPs in 10-kb windows, sliding 2 kb at a time, and plotting the count at

the midpoint of each window (Supplemental Figure 1). The Wellcome Trust Sanger Institute has next generation sequenced 17 mouse strains, including NOD/ShiLtJ

(<http://www.sanger.ac.uk/resources/mouse/genomes/>). The SNP information was downloaded for the *Idd9.3* region and entered into T1DBase, and can be viewed at www.t1dbase.org.

3.2.3 Flow Cytometry:

For absolute cell counts, NOD and NOD.B10 *Idd9.3* splenocytes or thymocytes were extracted and counted using a hemocytometer. For staining membrane bound CD137, the cells were incubated with 2.4G2 Fc block. For FACS analysis, cells were stained with CD4-APC, CD25-FITC and stained for CD137 using IgG2a anti-CD137 or IgG2a isotype control antibody, then stained with anti-IgG2a biotin and streptavidin-PE and analyzed on a FacsCaliber (BD Biosciences). The cells were serially gated for total number of lymphocytes (by Fsc and Ssc), CD4, CD4^{pos}CD25^{pos}, CD4^{pos}CD25^{pos}CD137^{neg} and CD4^{pos}CD25^{pos}CD137^{pos} T cells. The percentage staining in each gate was multiplied by the absolute number of cells to calculate the total number of lymphocytes, CD4^{pos}, CD4^{pos}CD25^{pos} and CD4^{pos}CD25^{pos}CD137^{neg} and CD4^{pos}CD25^{pos}CD137^{pos} T cells. For intracellular staining, the splenocytes were stained with CD4-APC-Cy7, CD25-Percp-Cy5.5, CD137-PE and fixed with 2% formaldehyde (methanol free) and permeabilized with 0.3% saponin. Intracellular staining was performed with Foxp3-PE or IgG2a isotype-PE (eBioscience), Bclxl-Alexa-Fluor488 or IgG isotype-Alexa-Fluor488 (Cell Signaling), Bcl2-Alexa-Fluor488 or IgG1 isotype-Alexa-Fluor488 (BioLegend) and Ki-67-Alexa-Fluor488 or IgG isotype-Alexa-Fluor488 (Novus Biologicals). Anti-mouse Ki-67 or IgG isotype control antibody was labeled with APEX Alexa-Fluor488 Antibody Labeling Kit (Invitrogen). Foxp3 staining was performed using eBioscience Fixation/Permeabilization Kit. (NOD.CD45.2 X NOD.B10 *Idd9.3*) F1 bone marrow chimera spleen and pancreatic lymph nodes were stained with CD4-APC-Cy7, CD25-Percp-Cy5.5, CD45.1-FITC, CD45.2-APC and CD137-PE or IgG2a

isotype-PE and analyzed on a FACSCantos (BD Biosciences). All FACS data was analyzed using FlowJo (Treestar, Oregon).

3.2.4 Bone Marrow Chimera construction:

9-13 week old (NOD.CD45.2 X NOD.B10 *Idd9.3*) F1 mice were irradiated with 800 -1200 Rads (the dose was varied as we gained experience in this procedure, to optimize depletion of host cells). 15-25 million bone marrow cells from 5-12 week old NOD.B10 *Idd9.3* and NOD.CD45.2 mice were extracted without RBC lysis. Mature CD4, CD8 and CD90 cells were removed using magnetic beads (Miltenyi Biotech, California) and the bone marrow was then mixed at a 1:1 ratio and injected into the irradiated F1 mice. Recipient mice were given water treated with antibiotic (neomycin trisulfate salt hydrate) for two weeks after transfer. The recipient F1 mice were sacrificed 12-20 weeks post injection for analysis of peripheral T cell populations by FACS.

3.2.5 RT-PCR:

CD4 T cells were extracted from splenocytes using CD4 magnetic beads (Miltenyi Biotech, California). The CD4 T cells were blocked with 2.4G2 and stained with CD4-APC-Cy7, CD25-FITC, and anti-CD137-APC as above. The cells were sorted using a BD FACS Aria machine (BD Bioscience) into CD4^{pos}CD25^{neg}CD137^{neg}, CD4^{pos}CD25^{pos}CD137^{neg} and CD4^{pos}CD25^{pos}CD137^{pos} cell subsets, RNA was extracted from the sorted cells using an RNeasy mini kit (Qiagen) and converted into cDNA (Promega Reverse Transcription System). Quantitative Real Time Polymerase Chain Reaction (RT-PCR) was performed on the cDNA using primers for B2m, soluble CD137 and membrane bound CD137 using a StepOnePlus Real-Time PCR system (Applied Biosystems). The CT values of the gene of interest were subtracted from the CT of the housekeeping gene (Gadph or B2m) to produce the delta CT (designated “ Δ CT”) and the data graphed using GraphPad Prism 5 (Version 5.02).

3.2.6 Proliferation Assay:

The CD4^{pos}CD25^{neg}CD137^{neg}, CD4^{pos}CD25^{pos}CD137^{neg} and CD4^{pos}CD25^{pos}CD137^{pos} splenocytes were stained and sorted using BD Aria (BD Bioscience) with 90-95% purity. 50,000 sorted cells were cultured at 37°C with 5% CO₂ with (a) 25U/ml IL-2 or (b) 25U/ml/IL-2 and 1.25ug/ml anti-CD3 in triplicate wells. The cells were pulsed with 1 µCi ³H labeled thymidine on day 3 and harvested after 16 hours using a beta scintillation counter. For the suppression assay 50,000 CD4^{pos}CD25^{neg}CD137^{neg} T cells were cultured in U-bottom 96 well plate with 1ug/well soluble anti-CD3, 50,000 irradiated splenocytes (1500 rads) and varying numbers of CD4^{pos}CD25^{pos}CD137^{neg} or CD4^{pos}CD25^{pos}CD137^{pos} Tregs. All cells were cultured and pulsed with 1 µCi [³H] thymidine on Day 3, 16 hours before harvest. On Day 4, thymidine incorporation was assessed using a beta scintillation counter.

3.2.7 Treg Transwell Suppression Assay:

100,000 sorted CD4^{pos}CD25^{neg}CD137^{neg} T cells were cultured with 50,000 CD3/CD28-coated beads (Invitrogen) and 1.25ug/ml soluble anti-CD3 in the bottom wells of a 96 well transwell plate (Corning). 25,000 or 50,000 CD4^{pos}CD25^{pos}CD137^{neg} or CD4^{pos}CD25^{pos}CD137^{pos} Tregs were cultured in the top wells with 50,000 CD3/CD28-coated beads and 1.25ug/ml soluble anti-CD3. The cells were cultured at 37°C in 5% CO₂ and were pulsed with 1 µCi [³H] thymidine on Day 3. The cells in the bottom wells were harvested and counted using a beta scintillation counter.

3.2.8 ELISA:

Mouse 4-1BB DuoSet Elisa system (R&D Systems, California) was used to detect soluble CD137 from serum and culture supernatants. The kit uses rat anti-mouse 4-1BB capture

antibody and biotinylated goat anti-mouse 4-1BB detection antibody. Recombinant mouse 4-1BB, provided in the kit, was used as a standard. DeltaSoft software was used to calculate the amount of soluble CD137 in each well based on the standard for each experiment.

3.2.9 Treg culture:

50,000 CD4^{pos}CD25^{pos}CD137^{neg} or CD4^{pos}CD25^{pos}CD137^{pos} Tregs were cultured in 96 well U-bottom plate with no IL-2 (unstimulated), 25U/ml mouse recombinant IL-2 alone with or without 1.25ug/ml of anti-CD3 antibody for 4 days, and the supernatants were tested for soluble CD137 as above by ELISA. All statistical analysis was performed using either the unpaired T test or the Mann-Whitney test in GraphPad Prism 5 (Version 5.02).

3.3 RESULTS

3.3.1 Increased accumulation of CD137^{pos} Tregs with the B10 versus the NOD region *in vivo*

We previously demonstrated that agonist anti-CD137 treatment prevents diabetes in NOD mice, that a subset of Tregs constitutively expresses CD137, and that anti-CD137 binds to CD4^{pos}CD25^{pos}CD137^{pos} Tregs *in vitro* and *in vivo* [137]. Our results suggested that CD137^{pos} Tregs may be important in T1D pathogenesis. We quantified CD137 expression on CD4^{pos}CD25^{pos} T cells as previously published [137] and as in Figure 1a, which shows a well-defined CD137^{pos} population compared to isotype control; CD137^{pos} cells constitute 30% of all CD4^{pos}CD25^{pos} T cells in the representative example shown. Since it has been previously shown

that CD137 promotes CD4 and CD8 T cell survival [10, 145, 173], we investigated changes in the frequency and the number of CD137^{pos} T regulatory cells with age in non-diabetic NOD and NOD.B10 *Idd9.3* congenic mice. The percentage of CD137^{pos} cells within the CD4^{pos}CD25^{pos} T cell population significantly declines with age in NOD, but not in NOD.B10 *Idd9.3* spleen (P=0.006, Figure 3.1b). At both younger (3-9 weeks) and older (21-36 week) ages, the percentage of splenic CD137-expressing Tregs are significantly higher in NOD.B10 *Idd9.3* mice than in NOD mice (P=0.01 and P<0.0001 Figure 3.1b). The absolute number of CD137^{pos} Tregs significantly increased with age from 3-9 weeks to 21-36 weeks in NOD.B10 *Idd9.3* congenic mice (P=0.03, Figure 3.1c). In addition there was a significant increase in the absolute number of CD137^{pos} splenic Tregs in older NOD.B10 *Idd9.3* congenic mice compared to age matched NOD mice (P=0.03, Figure 3.1c). However the number of NOD CD137^{pos} Tregs did not change with age despite an age related decline in the percentage NOD CD137^{pos} Tregs. (We also looked at the percentage of CD137^{pos} Tregs at 10-20 weeks of age and observed no significant differences compared the other age groups of either strain - data not shown).

Figure 3.1

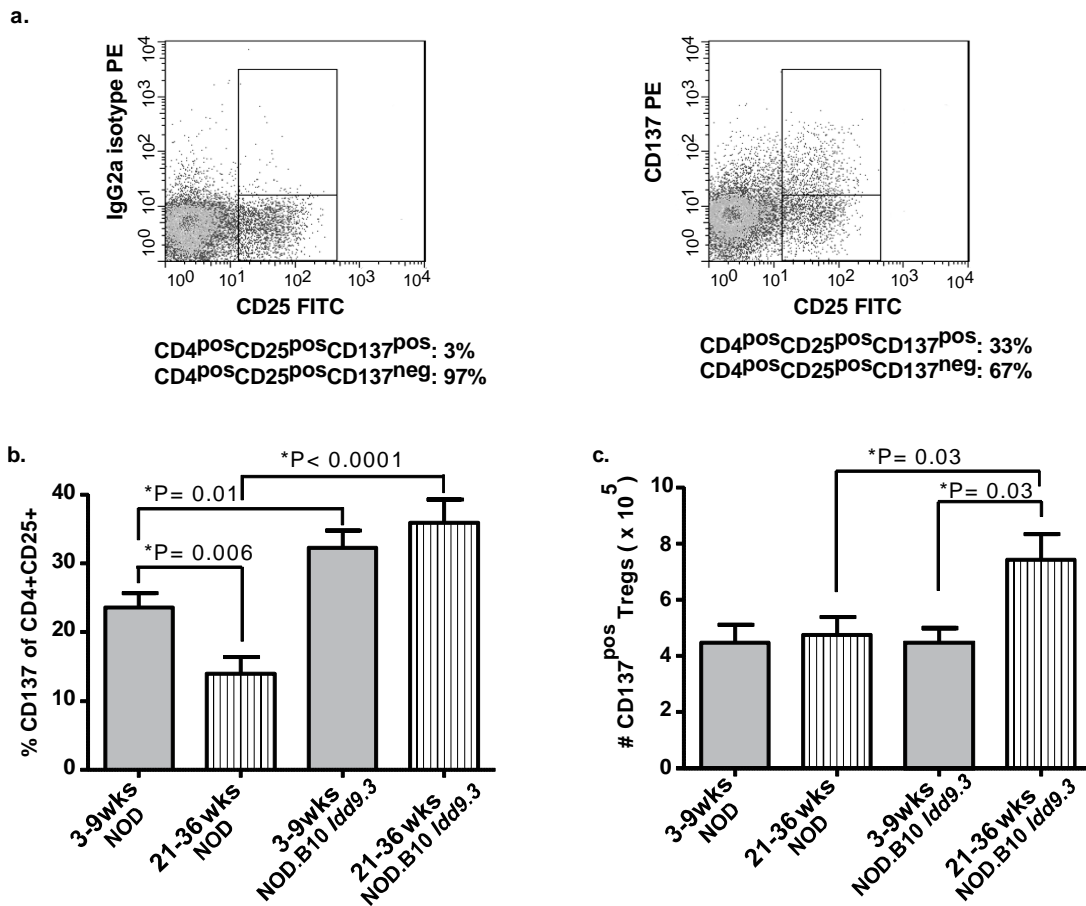


Figure 3.1. CD137^{pos} Tregs are significantly lower in aged NOD versus NOD.B10 *Idd9.3* spleen.

Splenocytes from six week old NOD mice were stained with CD4-APC, CD25-FITC and anti-CD137-PE or IgG2a isotype control, and analyzed by flow cytometry. The IgG2a isotype control staining was used to establish true CD137 staining. Percentages below the Figureshow the percent CD137^{pos} vs. CD137^{neg} in the CD4^{pos}CD25^{pos} gate. One representative of multiple experiments. (b, c, d) NOD and NOD.B10 *Idd9.3* splenocytes were isolated from younger (3-9 week) and older (21-36 week) non-diabetic females, stained with CD4-APC, CD25-FITC and anti-CD137-PE and analyzed by flow cytometry. (b) Isotype staining was used to gate for percentage of CD137^{pos} T cells in the CD4^{pos}CD25^{pos} T cell subset in NOD (n=18, 3-9 wk old and n=12, 21-36 wk old mice) and NOD.B10 *Idd9.3* (n=12, 3-9 wk old and n=16, 21-36 wk old)

spleen. (c) The number of CD4^{pos}CD25^{pos}CD137^{pos} T cells was counted in NOD (n=8, 3-9 wk old and n=7, 21-36 wk old) and NOD.B10 *Idd9.3* (n=5, 3-9 wk old and n=7, 21-36 wk old) spleen. (d) The mean fluorescence intensity of CD137 on CD137^{pos}CD4^{pos}CD25^{pos} T cells was analyzed on NOD (n=10, 3-9 wk old and n=5, 21-36 wk) and NOD.B10 *Idd9.3* (n=7, 3-9 wk old and n=9, 21-36 wk old mice) spleen.

Consistent with previously published observations [77], the number of splenic CD4^{pos}CD25^{pos} T cells increased significantly with age in both strains with no difference between the strains (Figure 3.2a). This explains the lack of decline of CD137^{pos} Treg number in NOD with age despite a significant drop in the percent of CD137^{pos} Tregs. Similarly, it also explains the significant increase in the total number of CD137^{pos} Tregs with age in NOD.B10 *Idd9.3* mice (P=0.03, Figure 3.1c), despite the finding that the percentage of CD137^{pos} Tregs did not increase with age (Figure 3.1b). Thus the increased number of NOD.B10 *Idd9.3* CD4^{pos}CD25^{pos}CD137^{pos} T cells with age is due to a combination of an increased percentage of CD137^{pos} T cells and an increased absolute number of CD4^{pos}CD25^{pos} T cells in older NOD.B10 *Idd9.3* mice. There was also no difference in the percentage of CD4^{pos}CD25^{pos} T cells with age in either strain (Figure 3.2b). Both NOD and NOD.B10 *Idd9.3* congenic mice showed significant increases in CD4^{pos} T cells and total numbers of splenic lymphocytes with age (Figure 3.2 c, d), but there was no difference between NOD.B10 *Idd9.3* and NOD mice in the corresponding age groups.

Figure 3.2

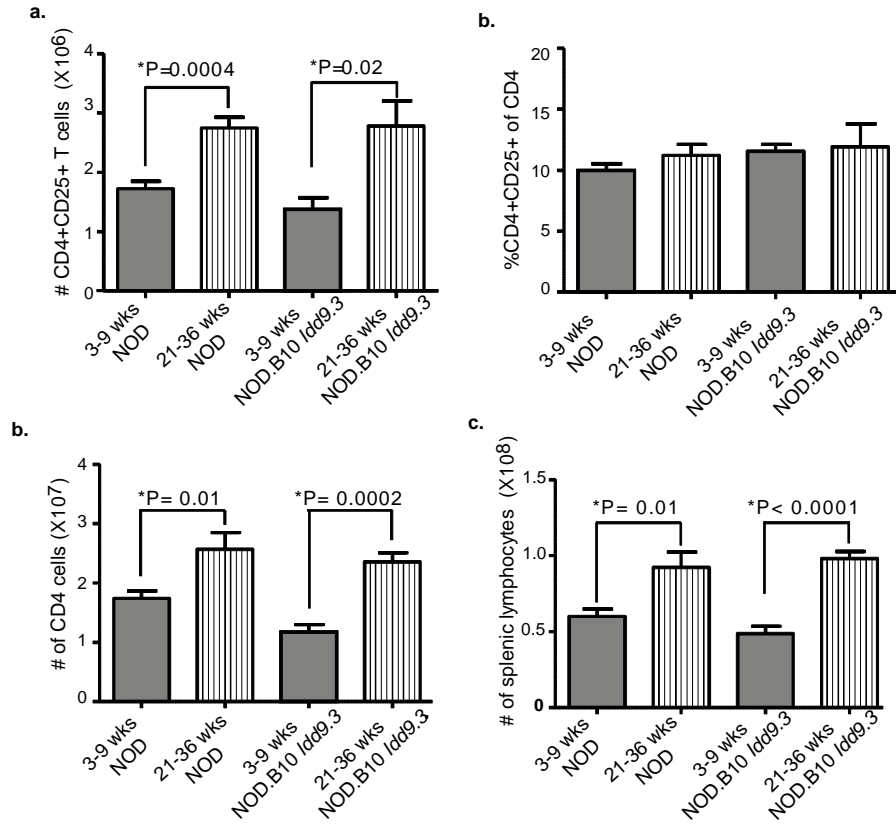


Figure 3.2. NOD and NOD.B10 *Idd9.3* CD4^{pos}, CD4^{pos}CD25^{pos}, and splenic lymphocytes increase with age.

NOD and NOD.B10 *Idd9.3* splenocytes were counted with a hemocytometer and stained with CD4-APC, CD25-FITC and anti-CD137-PE. The number of CD4^{pos}CD25^{pos} T cells (a), the number of CD4 cells (c), and the number of splenic lymphocytes (d) were calculated by multiplying the total number of splenocytes by the percentage of cells in each gate. (b) shows the percentage of CD4^{pos}CD25^{pos} T cells. (a-d) performed on NOD (n=8, 3-9 wk old and n=7, 21-36 wk old) and NOD.B10 *Idd9.3* (n=5, 3-9 wk old and n=7, 21-36 wk old) spleen using the staining protocol from Figure 1d.

We next studied the percentages and total number of thymic CD137^{pos} Tregs in NOD and NOD.B10 *Idd9.3* congenic mice and found that they were consistent with the peripheral population results. The percentage and absolute number of thymic CD137^{pos} Tregs was significantly higher in 21-36 week old NOD.B10 *Idd9.3* versus NOD mice (P=0.002, Figure 3.3a and P=0.02, Figure 3.3b). The total number of thymic CD4^{pos}CD25^{pos} T cells, however, remained approximately constant with age in both strains (Figure 3.3c). The percentage of NOD.B10 *Idd9.3* CD4^{pos}CD25^{pos} thymocytes rose significantly (P=0.02, Supp Figure 3d). The number of CD4^{pos} thymocytes significantly declined with age in both strains with no difference between the two strains (Figure 3.3e). The total number of thymocytes significantly decreased with age in NOD (P=0.007, Figure 3f); it decreased, but not significantly, in older NOD.B10 *Idd9.3* mice. In summary, it is clear that the decreased number of NOD thymic CD137^{pos} Tregs with age was due to a decreased percentage of these cells; in older NOD.B10 *Idd9.3* mice a significant increase in the percentage of CD137^{pos} Tregs caused a significant increase in the number of thymic CD137^{pos} Tregs. It is also possible that the increased accumulation of CD137^{pos} Tregs in the periphery is due to the increased thymic output but here we have not stained for thymic output markers to test this possibility.

Figure 3.3

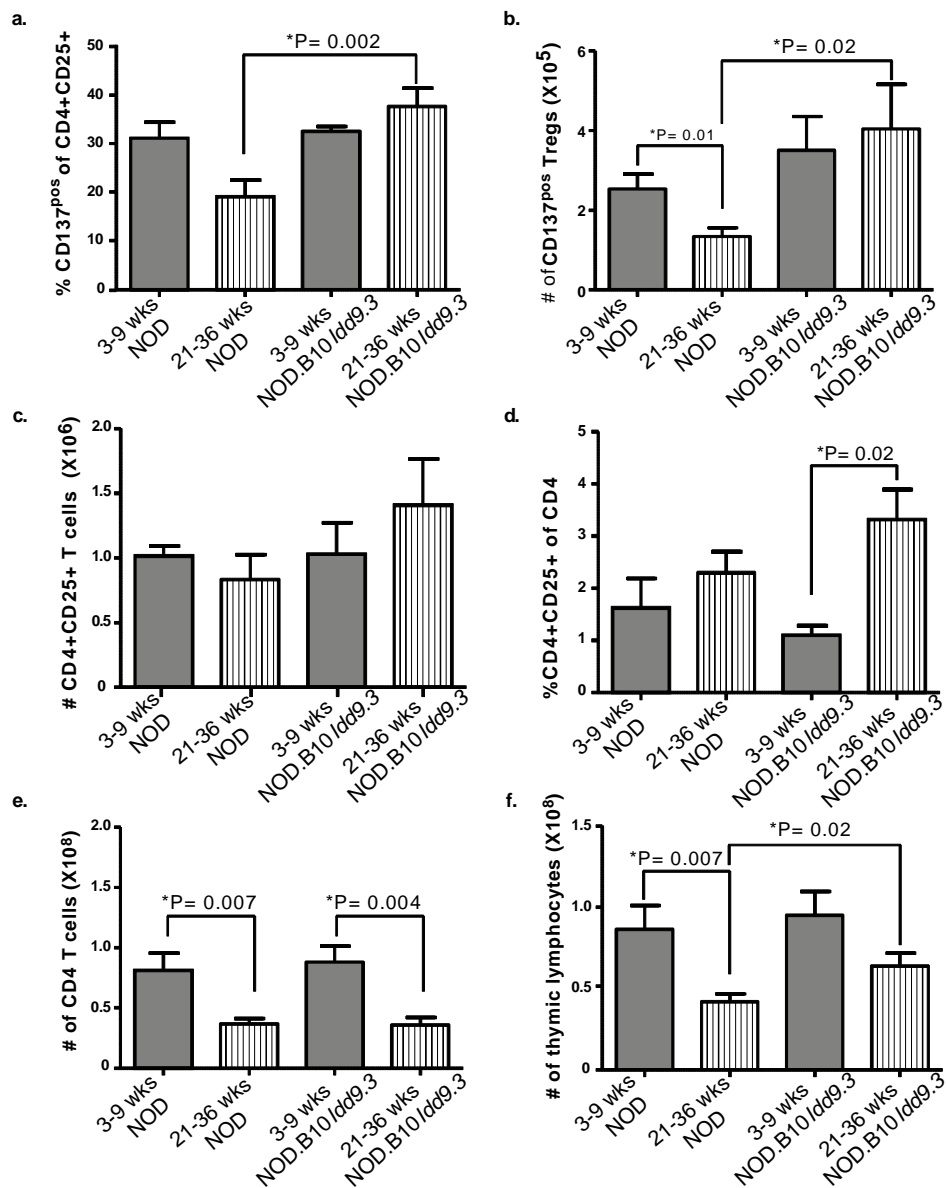


Figure 3.3. Thymic CD4^{pos}CD25^{pos}CD137^{pos} T cells decline with age in NOD but not in NOD.B10 *Idd9.3* mice.

NOD and NOD.B10 *Idd9.3* thymocytes were stained with CD4-APC, CD25-FITC and anti-CD137-PE. (a) The percentage CD4^{pos}CD25^{pos}CD137^{pos} T cells within the CD4^{pos}CD25^{pos} T cells stained in NOD (n=10, 3-9 wk old and n=11, 21-36 wk old mice) and NOD.B10 *Idd9.3* (n=13, 3-9 wk old and n=14, 21-36 wk old)

thymus. (b - f) The number of CD4^{pos}CD25^{pos}CD137^{pos} T cells (b), the total number of CD4^{pos}CD25^{pos} T cells (c), and the percentage of CD4^{pos}CD25^{pos} T cells within CD4 T cells (d), the total number of CD4^{pos} T cells (e), and the total number of thymic lymphocytes (f), were calculated from counting the absolute number of thymocytes in NOD (n=5, 3-9 wk old and n=7, 21-36 wk old) and NOD.B10 *Idd9.3* (n=4, 3-9 wk old and n=6, 21-36 wk old) and applying the indicated gates.

In order to begin to understand possible reasons for increased NOD.B10 *Idd9.3* CD137^{pos} Treg accumulation with age we examined the per cell surface expression of CD137 at the same time points. The mean fluorescence intensity of CD137 on CD4^{pos}CD25^{pos}CD137^{pos} T cells was significantly greater in young (3-9 week old) NOD.B10 *Idd9.3* versus age matched NOD (P=0.009, Figure 3.4a). Although the percentage of CD4^{pos}CD25^{pos}CD137^{pos} T cells declined markedly in 21-36 week old NOD spleen (P= 0.006, Figure 3.1b), the CD137^{pos} Tregs found in old NOD spleen expressed a significantly higher level of CD137 per cell compared to young NOD splenic Tregs (P=0.003, Figure 3.4a); not significantly different from old NOD.B10 *Idd9.3* cells (Figure 3.4a).

Figure 3.4

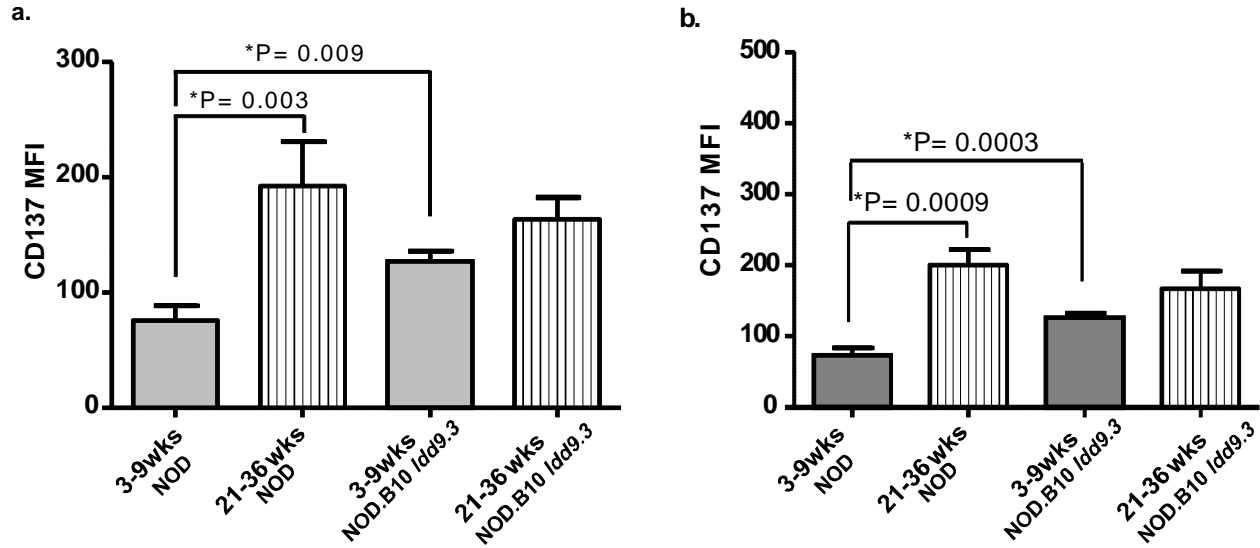


Figure 3.4. Cellular CD137 increase in older NOD and younger NOD.B10 *Idd9.3* congenic than young NOD

Splenocytes and thymocytes from NOD mice were stained with CD4-APC, CD25-FITC and anti-CD137-PE or IgG2a isotype control, and analyzed by flow cytometry. The mean fluorescence intensity of CD137 on CD137^{pos}CD4^{pos}CD25^{pos} T cells was analyzed in (a) NOD (n=10, 3-9 wk old and n=5, 21-36 wk) and NOD.B10 *Idd9.3* (n=7, 3-9 wk old and n=9, 21-36 wk old mice) spleen and thymus of (b) NOD (n=5, 3-9 wk old and n=4, 21-36 wk) and NOD.B10 *Idd9.3* (n=9, 3-9 wk old and n=8, 21-36 wk old mice) mice. Statistical analysis was performed using the unpaired t test.

Similar CD137 MFI was found in thymic CD4^{pos}CD25^{pos}CD137^{pos} T cells with age— old thymic NOD CD137^{pos} Tregs expressed more CD137 per cell than young NOD cells (P=0.0004, Figure 3.4b) and young thymic NOD.B10 *Idd9.3* CD137^{pos} Tregs were significantly higher than on young NOD cells (P=0.0003, Figure 3.4b). These findings suggest that early, increased expression of CD137 on Tregs might enhance long term accumulation of those cells, consistent with the previously published role of CD137 on CD8 and CD4 T cell survival *in vivo* and *in vitro* [145, 173, 234]. The increased expression of CD137 on a per cell basis in young NOD.B10 *Idd9.3* congenic spleen is associated with the increase in the number of

CD4^{pos}CD25^{pos}CD137^{pos} T cells with age. Overall, these studies show that the B10 *Idd9.3* region enhances accumulation of CD137^{pos} Tregs in the NOD.B10 *Idd9.3* congenic mice, and supports the hypothesis that CD137 is important for the long-term accumulation of CD137^{pos} Tregs.

3.3.2 CD137^{neg} and CD137^{pos} Tregs express similar levels of intracellular Foxp3 in NOD and NOD.B10 *Idd9.3*

The above results depended on identifying Tregs by CD25 expression. While this is a recognized Treg marker, it can also be a marker of T cell activation, as can CD137. It was important to evaluate the peripheral Treg subsets by intracellular Foxp3 expression to ensure that the increased number of NOD.B10 *Idd9.3* CD4^{pos}CD25^{pos}CD137^{pos} T cells with age were truly Tregs. To evaluate this, we first performed intracellular Foxp3 staining at all age points.

Figure 3.5

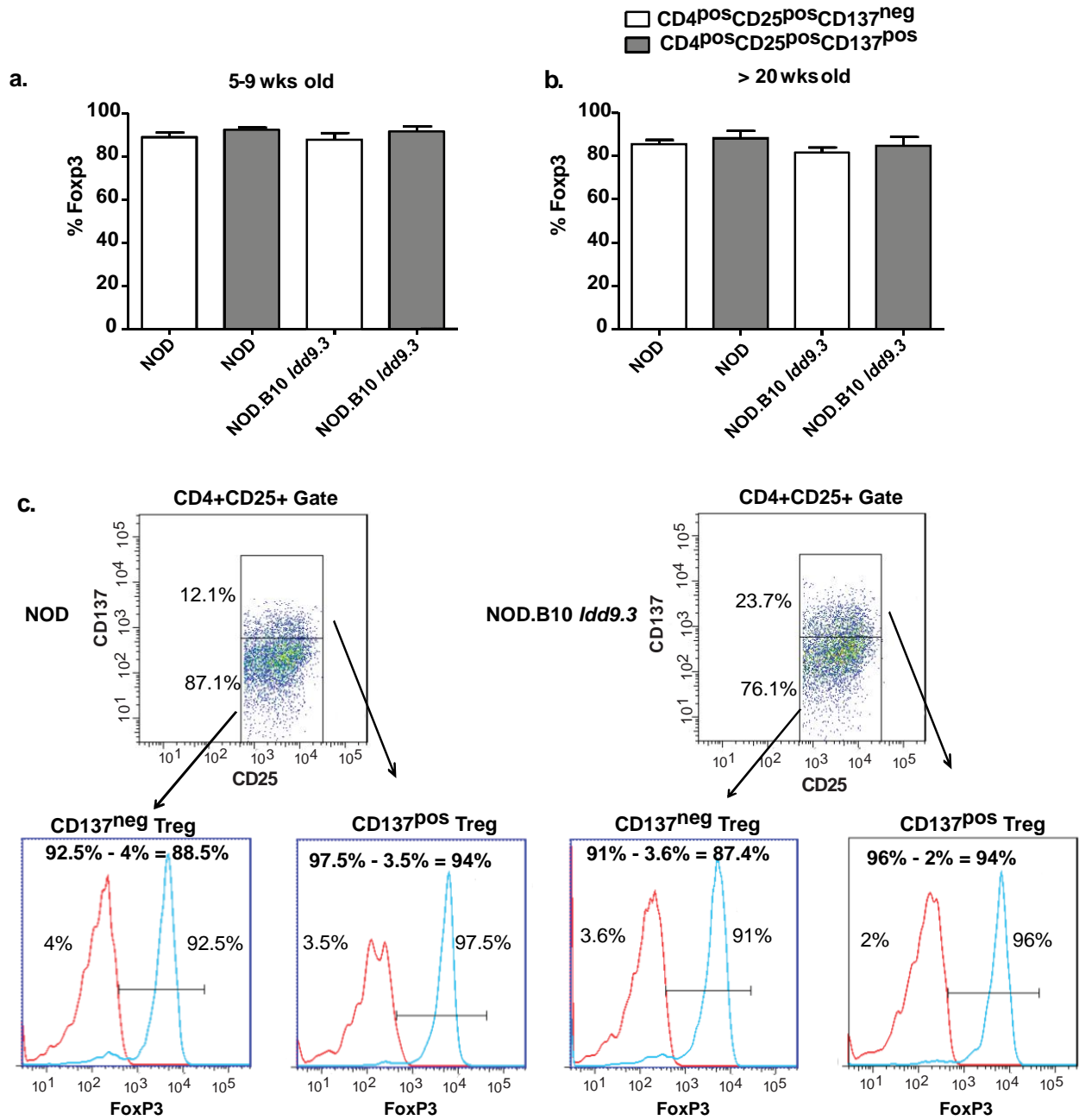


Figure 3.5. NOD and NOD.B10 *Idd9.3* Treg subsets show no difference in intracellular Foxp3 levels.

(a, b) Splenocytes from 5-9 week old NOD (n=3) and NOD.B10 *Idd9.3* (n=2) and 20-30 wk old NOD (n=4) and NOD.B10 *Idd9.3* (n=6) female mice were surface stained with CD4-APC.Cy7, CD25-Percep-Cy5.5

and anti-CD137APC, followed by intracellular staining for Foxp3-PE or IgG2a isotype control. (The CD137 gates are based on isotype staining for CD137, as shown in Figure 3.1a). (c) Representative dot plots of the FACS gating used to calculate the percent Foxp3 staining in parts (a) and (b) using seven week old NOD (left) and six week old NOD.B10 *Idd9.3* (right). Within the CD4^{pos}CD25^{pos} gate, the CD4^{pos}CD25^{pos}CD137^{neg} and CD4^{pos}CD25^{pos}CD137^{pos} Tregs were gated for Foxp3 or isotype histograms. The isotype histogram was used to establish gates for Foxp3 positive staining. The percent overlapping isotype staining in the gate was subtracted from the percent Foxp3+ in the gate (as noted on the top of each histogram) to calculate the true percent Foxp3.

We showed that the overwhelming majority of CD4^{pos}CD25^{pos}CD137^{pos} T cells are Foxp3 positive (Figure 3.5a, b) and that there is no significant difference in percentage of Foxp3 positive cells between CD4^{pos}CD25^{pos}CD137^{neg} and CD4^{pos}CD25^{pos}CD137^{pos} T cells in either 5-9 week old or 20-30 week old NOD or NOD.B10 *Idd9.3* congenic mice (Figure 3.5a, b). Our results match a previous study that showed similar percent Foxp3 expression in CD4^{pos}CD25^{pos} T cells in NOD with age [73], and shows that the increased number of NOD.B10 *Idd9.3* CD4^{pos}CD25^{pos}CD137^{pos} T cells is not due to an expansion of non-Tregs in this subset. We also found a slight increase in isotype staining with age (not shown), and since we subtracted the isotype staining (see Figure 3.5c for a representative example for gating) to calculate “true positive” Foxp3 cells, we may have underestimated the true Foxp3 expression.

After all the studies in this paper were performed, we obtained NOD.Foxp3-GFP mice, and used these mice to create NOD.B10 *Idd9.3* Foxp3-GFP mice. We aged these mice and used them to evaluate the percent of Foxp3-GFP positive cells in the CD4^{pos}CD25^{pos}CD137^{neg} and CD4^{pos}CD25^{pos}CD137^{pos} subsets in NOD and NOD.B10 *Idd9.3* at the same time points as we examined above (Figure 3.5a, b).

Figure 3.6

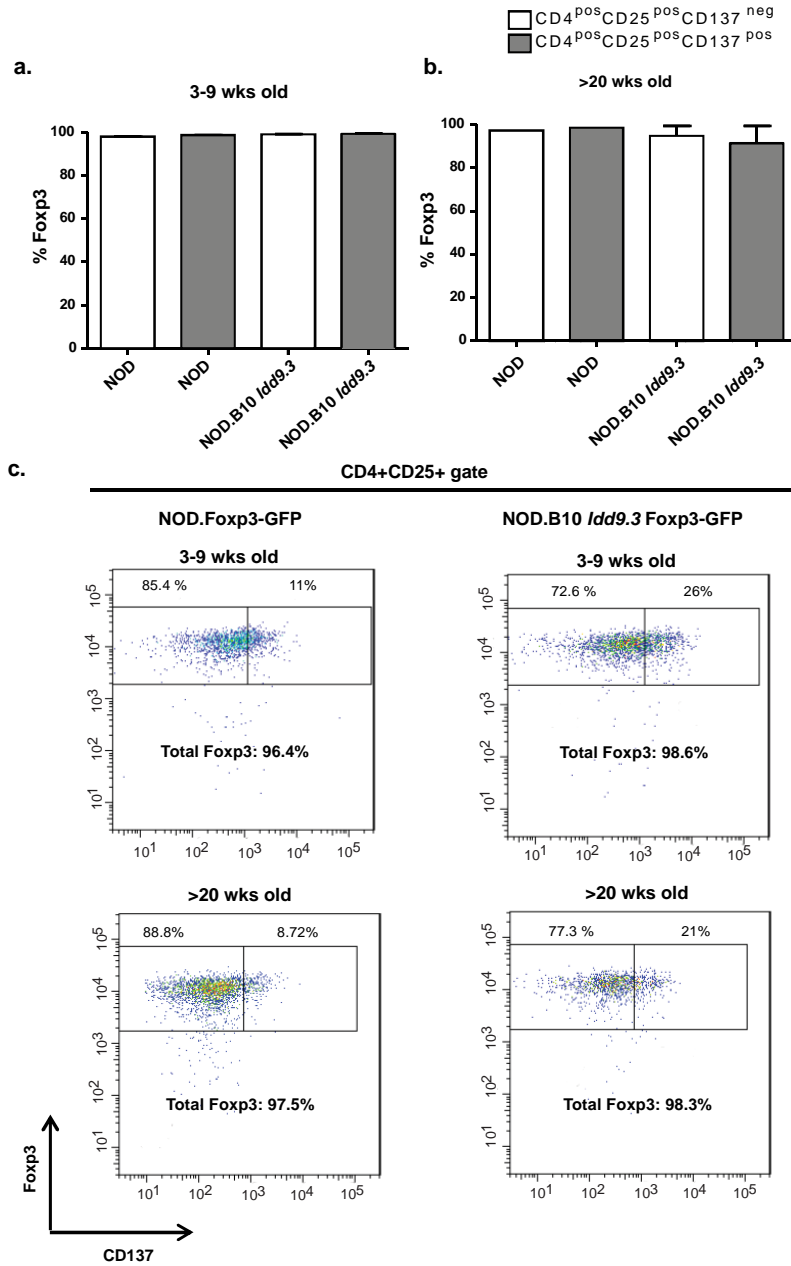


Figure 3.6. CD137^{pos} Tregs from NOD and NOD.B10 *Idd9.3* Foxp3-GFP mice express high Foxp3.

(a, b) Splenocytes from NOD.Foxp3-GFP (n=3, 3-9 wk old and n=2, 21-25 wk old) and NOD.B10 *Idd9.3*.Foxp3-GFP (n=3, 3-9 wk old and n=3, 21-25 wk old) were stained for CD4-APC-Cy7, CD25-Percep-Cy5.5 and CD137-APC or IgG2a isotype control. The cells were analyzed for Foxp3-GFP expression in CD137^{pos} and CD137^{neg} Tregs in (a) 3-9 week and (b) 21-25 week old mice. (c) Representative dot plots showing Foxp3/CD137 staining within the CD4^{pos}CD25^{pos} gate for each strain and age group shown in section a and b. FACS staining and gating were used to calculate the percent Foxp3 in the CD137^{neg} and CD137^{pos} subsets from young (top) and old (bottom) NOD.Foxp3-GFP (left) and NOD.B10 *Idd9.3*.Foxp3-GFP (right). (The CD137 gates are based on isotype staining for CD137, as shown in Figure 1a).

The Foxp3-GFP stainings (Figure 3.6) support the conclusions of Figures five above and show that well over 90% of CD4^{pos}CD25^{pos}CD137^{neg} and CD4^{pos}CD25^{pos}CD137^{pos} subsets in NOD and NOD.B10 *Idd9.3*, both young and old, were Foxp3-GFP positive, and that there were no significant differences between the strains (Figures 3.6a, b show the pooled result while Figure 3.6c shows representative FACS plots in NOD.Foxp3-GFP and NOD.B10 *Idd9.3* Foxp3-GFP mice). The combined results of Figures two and three very strongly show that the increase of CD4^{pos}CD25^{pos}CD137^{pos} cells in NOD.B10 *Idd9.3* mice with age truly represents a significant increase in Foxp3 expressing CD137^{pos} Tregs.

3.3.3 Increased accumulation of CD137^{pos} Tregs with the B10 versus the NOD *Idd9.3* region in mixed bone marrow chimeras *in vivo*

The finding of increased CD137^{pos} Tregs in NOD.B10 *Idd9.3* compared to NOD mice with age probably reflects multiple biological processes and complex intrinsic/extrinsic cellular effects in separate animals/strains. In order to confirm the finding of increased accumulation of Tregs

expressing the B10 *Idd9.3* region, we sought to demonstrate increased accumulation of these cells compared to cells with the NOD *Idd9.3* region, in the same animal. To do this, and to test whether the B10 *Idd9.3* region intrinsically mediated increased accumulation of CD137^{pos} Tregs, we constructed mixed bone marrow chimeras using NOD and NOD.B10 *Idd9.3* CD137^{pos} bone marrow transferred into irradiated (NOD.CD45.2 x NOD.B10 *Idd9.3* (CD45.1)) F1 mice. The resulting chimeric mice were analyzed for effective reconstitution and relative ratios of allotypically marked cells as shown in Figure 3.7.

Figure 3.7

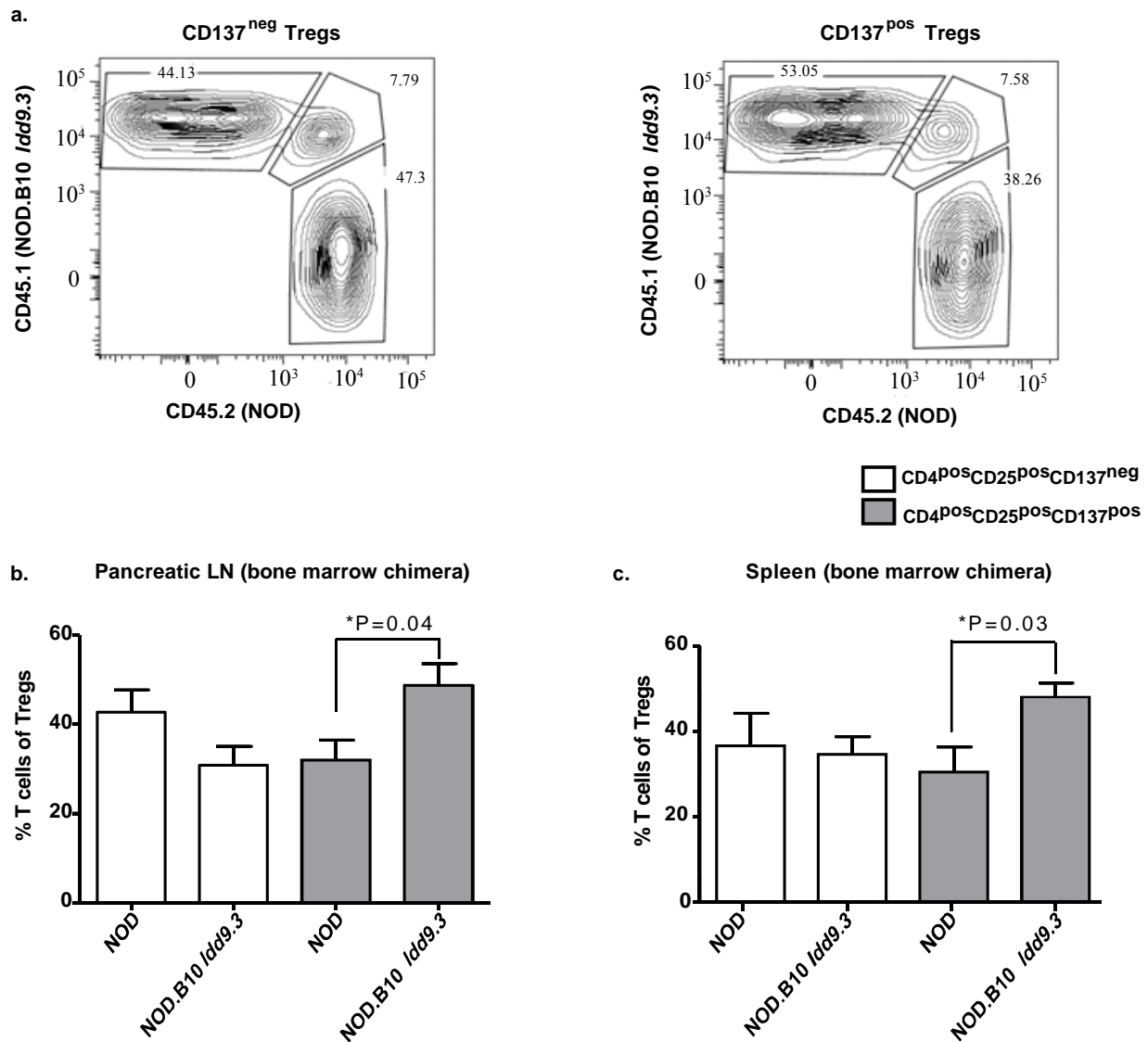


Figure 3.7. CD137^{pos} Tregs expressing the B10 *Idd9.3* region demonstrate an intrinsic cell accumulation.

15-25 million bone marrow cells from 5-12 week old NOD.B10 *Idd9.3* mice and NOD.CD45.2 mice were mixed at 1:1 ratio and injected into 9-13 week old irradiated (800 -1200 Rads in different experiments) (NOD.CD45.2 X NOD.B10 *Idd9.3*) F1 mice. Recipient non-diabetic mice were sacrificed 12-20 weeks after reconstitution. (a) One representative experiment showing the expression of the CD45.1 (NOD.B10 *Idd9.3*) vs. CD45.2 (NOD) allotype by CD137^{neg} (left) and CD137^{pos} (right) Tregs 12 weeks after reconstitution of the bone marrow chimera. (b) Spleen (n=5), and (c) pancreatic lymph nodes (n=4) were

harvested and stained with CD4-APC-Cy7, CD25-Percp-Cy5.5, CD45.1-APC, CD45.2-FITC and anti-CD137-PE and analyzed on a FACS Cantos cytometer. Percentage of each F1 (host) cells not shown. Statistical significance was calculated using the unpaired t test.

In the mixed bone marrow chimera mice, the percentage of peripheral (splenic or pancreatic lymph node) CD4^{pos}CD25^{pos}CD137^{pos} T cells expressing the B10 CD137 allotype was significantly increased compared to the NOD allotype (Figure 3.7b, c). CD4^{pos}CD25^{pos}CD137^{neg} Tregs from the same individual mice, in contrast, showed no significant CD45.1 vs. CD45.2 population differences (Figure 3.7a-c). Since the percentage of B10 and NOD allotype were from the CD137^{pos} Treg population in the same bone marrow chimeric mouse, the total number of splenocytes or lymph node cells were the same for each cell population; hence the total numbers of B10 or NOD allotype CD137^{pos} Tregs in the bone marrow chimeric mice were exactly proportional with these percentages. There was statistically no significant difference in thymic CD45.1 vs. CD45.2 proportions in CD4^{pos}CD25^{pos}CD137^{neg} and CD4^{pos}CD25^{pos}CD137^{pos} T cell populations (data not shown). These results, which are entirely consistent with the studies in Figure 4.1, strongly support the hypothesis that the B10 CD137 region intrinsically and selectively mediates enhanced accumulation of CD137^{pos} Tregs in the periphery.

3.3.4 Enhanced proliferation of CD137^{pos} Tregs *ex vivo* and *in vitro* but no significant difference between NOD and NOD.B10 *Idd9.3* congenic mice.

CD137 co-stimulation causes proliferation of Tregs *in vitro* [160, 228] and *in vivo* [179]. The increased frequency and accumulation of CD137^{pos} Tregs in NOD.B10 *Idd9.3* congenic mice could be due to intrinsic factors, such as greater proliferative capacity or enhanced cell survival mediated by the B10 CD137 allotype. To test proliferative capacity, we cultured NOD and

NOD.B10 *Idd9.3* CD137^{pos} and CD137^{neg} Tregs in the presence of IL-2 (Figure 3.8a) or IL-2 and CD3 (Figure 3.8b).

Figure 3.8

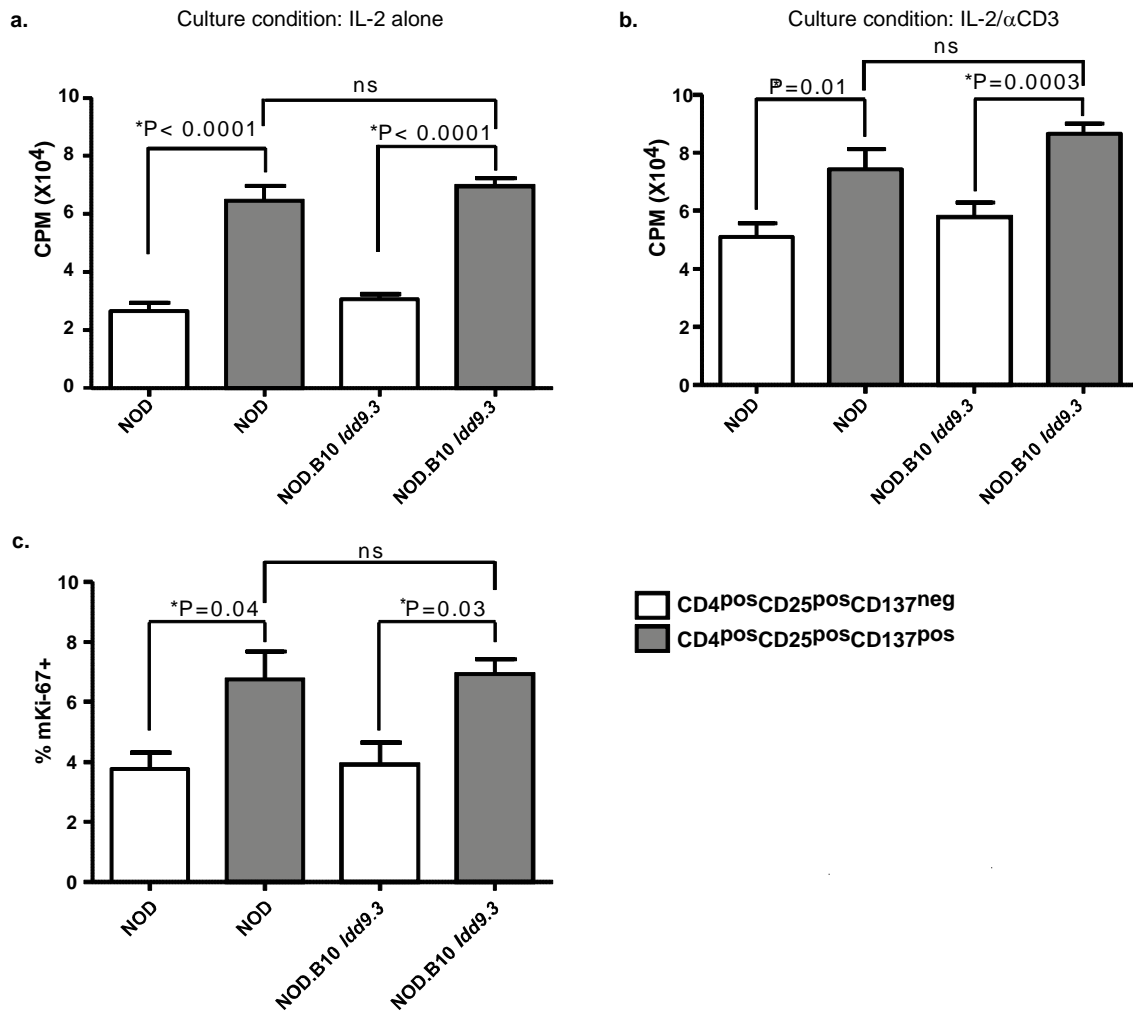


Figure 3.8. No proliferative differences between NOD and NOD.B10 *Idd9.3* CD137^{pos} Tregs *ex vivo* or *in vitro*.

(a, b) Splenocytes from 4-6 week old NOD and NOD.B10 *Idd9.3* females were stained with CD4-APC-Cy7, CD25-Percep-Cy5.5, and anti-CD137-APC, and FACS-sorted for CD4^{pos}CD25^{pos}CD137^{neg} and CD4^{pos}CD25^{pos}CD137^{pos} cells. 50,000 sorted cells were cultured with (a) 25U/ml IL-2 or (b) 25U/ml IL-2 and 1.25ug/ml anti-CD3 in triplicate wells. The cells were pulsed with ³H labeled thymidine on day 3 and

harvested after 16 hours and the data was pooled from n=3 experiments. (c) Splenocytes from 5-7 week old NOD (n=3) and NOD.B10 *Idd9.3* (n=3) females were surface stained with CD4-APC-Cy7, CD25-Percep-Cy5.5 and anti-CD137-APC, followed by intracellular staining for Ki-67-Alexa-488. The stained cells were analyzed by flow cytometry. Statistical significance was calculated with the unpaired t test.

The proliferation of CD137^{pos} Tregs was significantly greater than CD137^{neg} Tregs under both culture conditions and in both strains, but there was no difference in proliferation of CD137^{pos} Tregs between NOD and NOD.B10 *Idd9.3* mice (Figure 3.8a, b). Tregs cultured with no IL-2 showed virtually no proliferation (data not shown). Next, we quantified expression of the nuclear protein Ki-67, as a marker for proliferation *ex vivo*. Consistent with the *in vitro* results, a significantly higher percentage of CD137^{pos} Tregs were Ki-67 positive *ex vivo* compared to CD137^{neg} Tregs in both NOD and NOD.B10 *Idd9.3* mice (Figure 3.8c). Again, we found no difference in percentage of Ki-67 positive CD137^{pos} Tregs between NOD and NOD.B10 *Idd9.3* mice. These studies suggest that the increased numbers and frequency of CD137^{pos} Tregs in NOD.B10 *Idd9.3* congenic mice with age could not be explained by enhanced proliferation mediated by the B10 allotype.

Viability studies in CD137 stimulated and unstimulated T cells have shown that CD137 signaling prevents activation induced cell death (AICD) by repressing DNA fragmentation [147]. Since CD137 signaling can upregulate the pro-survival molecule Bcl-xL[145], we tested the expression of Bcl-xL in NOD and NOD.B10 *Idd9.3* Treg subsets. We found significantly increased Bcl-xL mRNA expression in NOD.B10 *Idd9.3* versus NOD CD137^{pos} Tregs (P=0.04, Figure 3.9a). We also found increased expression of Bcl-xL in NOD.B10 *Idd9.3* versus NOD CD137^{neg} Tregs (P=0.008), which suggests CD137 is not necessary for upregulation of Bcl-xL in these NOD.B10

Idd9.3 cells. We next tested Bcl-xL mRNA expression in the mixed bone marrow chimera cell subsets, stratified by allotype. In the mixed bone marrow chimera experiments, CD137^{pos}, but not CD137^{neg} Tregs with the B10 allotype expressed significantly increased Bcl-xL (P=0.008, Figure 3.9b). As a control, we tested levels of Bcl-2, a pro-survival molecule not known to be associated with CD137 signaling. There were no significant differences in expression of Bcl2 in NOD vs. NOD.B10 *Idd9.3* CD137^{pos} or CD137^{neg} Tregs, in contrast to Bcl-xL (Figure 3.9c). In the mixed bone marrow chimeric mice, the CD137^{pos} but not the CD137^{neg} Treg subset showed significantly increased Bcl2 mRNA in B10 allotype vs. NOD allotype cells (p=0.0003, Figure 3.9d). To summarize, the CD137^{pos} Treg subsets (in both normal NOD.B10 *Idd9.3* mice and in the B10 allotype cells of bone marrow chimera mice) showed significant increases of Bcl-xL mRNA. However in CD137^{neg} Tregs, NOD.B10 *Idd9.3* Tregs also show increased Bcl-xL mRNA compared to NOD, and B10 allotype CD137^{pos} Tregs in the bone marrow chimeras also showed upregulated Bcl2 message.

Figure 3.9

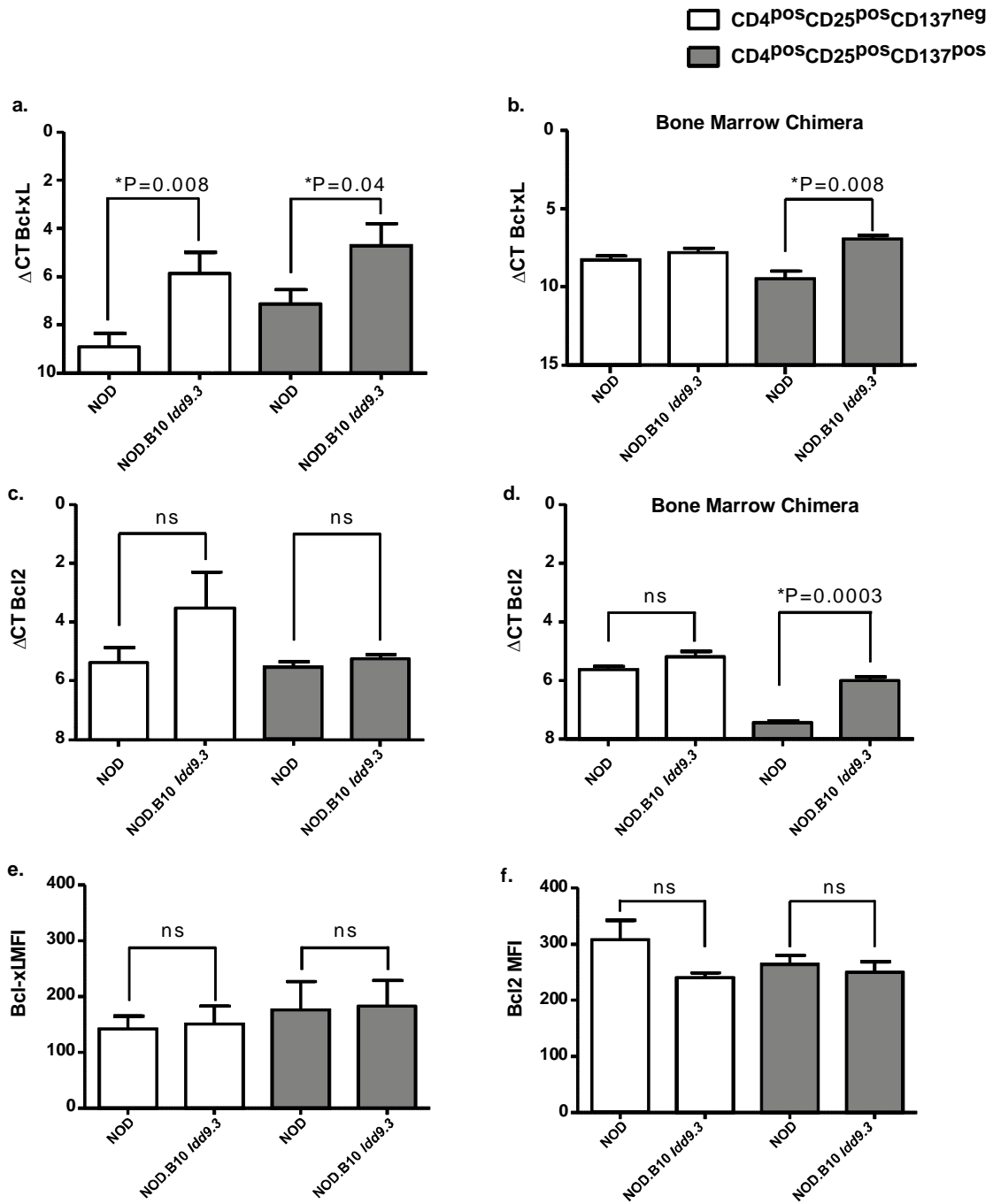


Figure 3.9. Peripheral NOD.B10 *Idd9.3* CD137^{pos} Tregs express higher levels of Bcl-xL mRNA than NOD.

(a) Splenocytes from 4-7 week old NOD (n=9) and NOD.B10 *Idd9.3* (n=6) females were used for sorting up-to 50,000 CD4^{pos}CD25^{neg}CD137^{neg}, CD4^{pos}CD25^{pos}CD137^{neg} and CD4^{pos}CD25^{pos}CD137^{pos} cells as

described above. RNA was extracted from the sorted cells and converted to cDNA as described in the methods. Quantitative Real Time Polymerase Chain Reaction (RT-PCR) was performed on the cDNA using either B2m or Gapdh and Bcl-xL primers. (b) NOD.B10 *Idd9.3* and NOD.CD45.2 mixed bone marrow chimeric mice were made as above. Recipient non-diabetic mice were sacrificed 9-10 week post injection. CD137^{neg} and CD137^{pos} Tregs were sorted according to their CD45.1 (NOD.B10 *Idd9.3*) and CD45.2 (NOD) allotype and used for RT-PCR with B2m and Bcl-xL primers. The mean of (n=3) separate experiments is shown. (c) 4-7 week old NOD (n=3) and NOD.B10 *Idd9.3* (n=3) female splenocytes were used for sorting 50,000 CD4^{pos}CD25^{neg}CD137^{neg}, CD4^{pos}CD25^{pos}CD137^{neg} and CD4^{pos}CD25^{pos}CD137^{pos} cells and used for RT-PCR with B2m and Bcl2 primers. (d) CD45.1 or CD45.2 expressing CD137^{neg} and CD137^{pos} Tregs were sorted from mixed bone marrow chimera as in (b) and used for RT-PCR with B2m and Bcl2 (n=3). (e, f) Splenocytes from 4-9 week old NOD (n=4) and NOD.B10 *Idd9.3* (n=3) females were surface stained with CD4APC.Cy7, CD25Percep-Cy5.5 and anti-CD137APC, followed by intracellular staining for Bcl-xL Alexa-Fluor 488 (e) or Bcl2 Alexa-Fluor 488 (f) and their matched isotype control. The stained cells were analyzed by flow cytometry for MFI for Bcl-xL or Bcl2 within CD4^{pos}CD25^{pos}CD137^{neg} and CD4^{pos}CD25^{pos}CD137^{pos} cells. All statistical calculations were performed using the unpaired t test.

To understand the significance of these findings, we examined protein levels of these survival molecules in both NOD and NOD.B10 *Idd9.3* Treg subsets. Contrary to the PCR results, the Bcl-xL expression per cell did not vary between the NOD.B10 *Idd9.3* versus NOD CD137^{pos} Tregs (Figure 3.9e). Similarly, CD137^{pos} Tregs showed no difference in Bcl2 MFI in between NOD.B10 *Idd9.3* and NOD (Figure 3.9f).

Figure 3.10

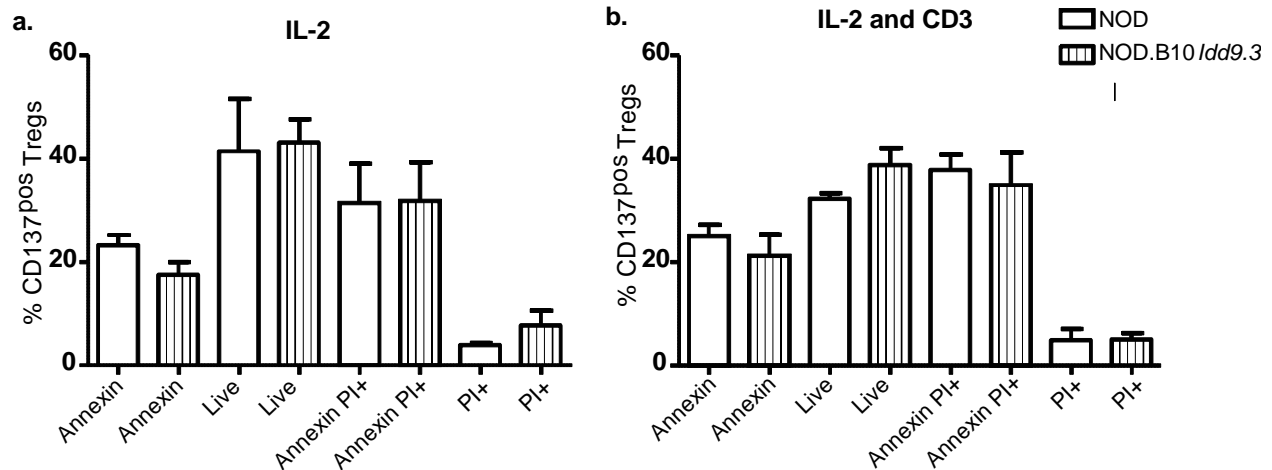


Figure 3.10: *In vitro* cell death does not differ between NOD vs. NOD.B10 *Idd9.3* CD137^{pos} Tregs.

(a, b, c, d) Splenocytes from 8-9 week old NOD and 6-7 week old NOD.B10 *Idd9.3* female mice were sorted for CD4^{pos}CD25^{pos}CD137^{pos} T cells as above. 50,000 sorted cells were cultured with (a,) 25U/ml IL-2 (NOD n=2, NOD.B10 *Idd9.3* n=4) or (b) 25U/ml/IL-2 and 1.25ug/ml anti-CD3 (NOD n=4, NOD.B10 *Idd9.3* n=5). On day 4, the cultured cells were stained with Annexin-FITC and PI staining and analyzed by flow cytometry. "Live" cells refer to the Annexin negative and PI negative gate.

The greater accumulation of NOD.B10 *Idd9.3* CD137^{pos} Tregs compared to NOD could be due to enhanced survival of cells expressing the B10 CD137 allele. We tested this *in vitro* by culturing NOD and NOD.B10 *Idd9.3* Tregs subsets in the presence of IL-2 or IL-2/CD3 as above. Under both conditions, the percentage of live, early apoptotic (Annexin positive), late apoptotic (Annexin /PI double positive) or dead (PI positive) cells do not differ between NOD and NOD.B10 *Idd9.3* in CD137^{pos} Tregs (Figure 3.10a, b). CD137^{neg} Tregs also showed no difference between culture condition and mouse strains (data not shown). Therefore while the

increased expression of Bcl-xL mRNA in Tregs expressing the B10 CD137 allele is intriguing, it is not definitive. In addition, since we have no evidence of increased survival *in vitro*, we cannot confirm or exclude the possibility that expression of the B10 CD137 allele causes survival advantage of Tregs without further studies.

3.3.4 NOD and NOD.B10 *Idd9.3* CD137^{pos} Tregs do not differ in contact-dependent suppression.

Our results show enhanced accumulation of CD137^{pos} Tregs in NOD.B10 *Idd9.3* mice. Previously we have seen that NOD CD137^{pos} Treg are functionally superior to CD137^{neg} Tregs (Chapter 2). To understand the possible significance of increased percentages and numbers of CD137^{pos} Tregs in the congenic mice with age, we compared the functional differences between NOD and NOD.B10 *Idd9.3* CD137^{neg} and CD137^{pos} Treg subsets. Previously, we performed an *in vitro* Treg contact dependent suppression assay using NOD CD4^{pos}CD25^{neg}CD137^{neg} T effector cells and titrated numbers of Tregs and showed that CD137^{pos} Tregs were significantly functionally superior to CD137^{neg} Tregs at every ratio (through 1:32, P=0.002) of Treg:T effector tested (Figure 2.9).

Figure 3.11

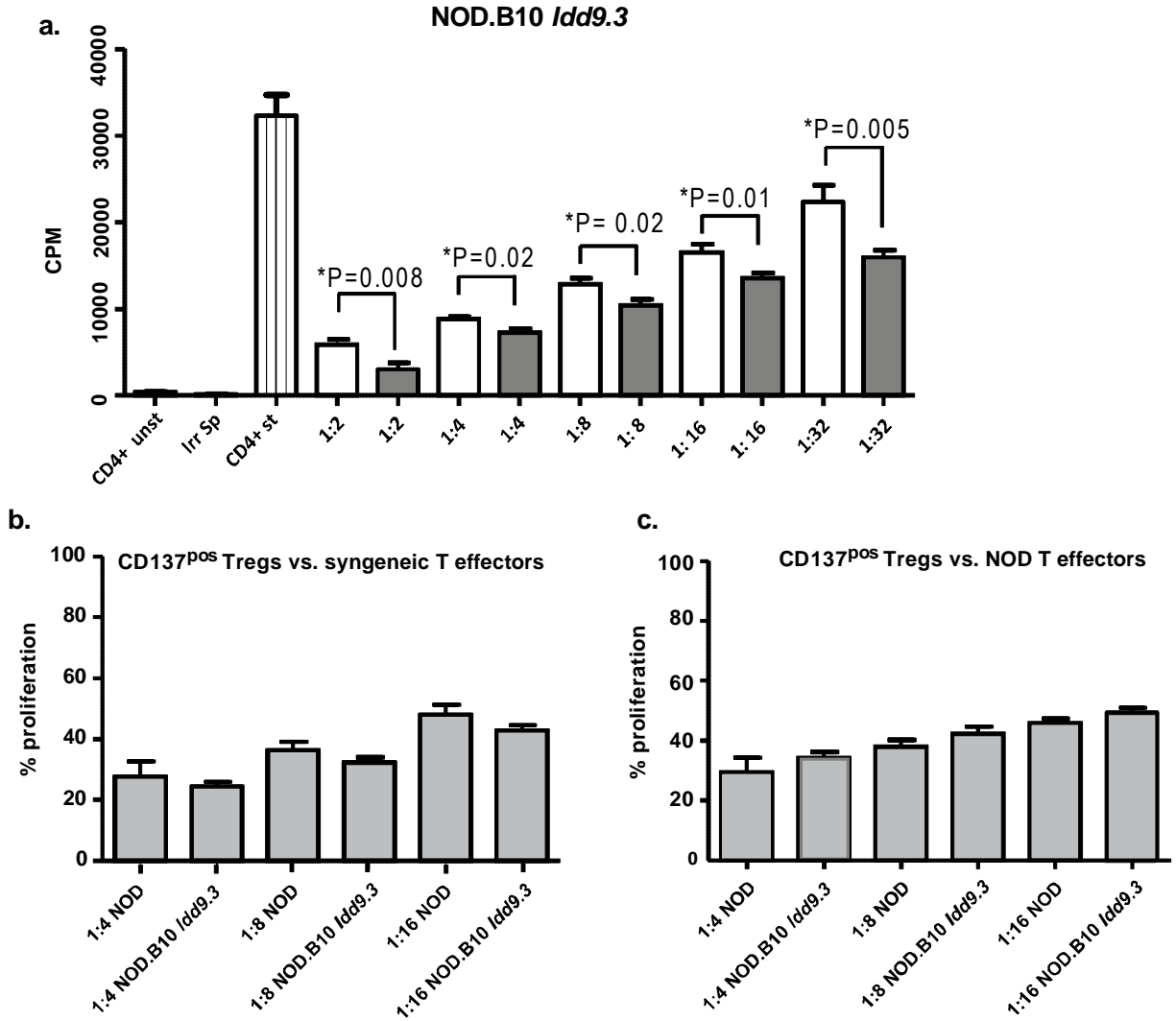


Figure 3.11. NOD and NOD.B10 *Idd9.3* CD137^{pos} Tregs do not differ in suppression *in vitro*.

(a) CD4^{pos}CD25^{neg}CD137^{neg} T cells and CD137^{neg} and CD137^{pos} Tregs were sorted from spleen of 4-12 week old NOD.B10 *Idd9.3* female mice as described in the methods. 50,000 CD4^{pos}CD25^{neg}CD137^{neg} T cells were plated in U-bottom 96 well plates with 1.25ug/well soluble anti-CD3, 50,000 irradiated (1500

rads) syngeneic splenocytes and titrated numbers of syngeneic CD137^{neg} or CD137^{pos} Tregs. Unstimulated CD4^{pos}CD25^{neg}CD137^{neg} T cells and irradiated splenocytes alone were used as negative controls. The cells were pulsed with ³H labeled thymidine on day 3 and harvested after 16 hours. The data was pooled from n=3 experiments for 1:2, n=2 experiments for 1:4, n=3 experiments for 1:8, n=4 experiments for 1:16 and n=5 experiments for 1:32. (b, c) CD4^{pos}CD25^{neg}CD137^{neg} T cells and CD137^{pos} Tregs were sorted from spleen of 5-8 week old NOD and NOD.B10 *Idd9.3* females as described above. (b) 50,000 NOD or NOD.B10 *Idd9.3* CD4^{pos}CD25^{neg}CD137^{neg} T cells were plated in U-bottom 96 well plates with 1.25ug/well soluble anti-CD3, 50,000 irradiated (1500 rads) syngeneic splenocytes and titrated numbers of syngeneic NOD or NOD.B10 *Idd9.3* CD137^{pos} Tregs. The data was pooled from n= experiments for 1:4 and n= experiments for 1:8 and 1:16 for both NOD and NOD.B10 *Idd9.3* mice. (c) 50,000 NOD CD4^{pos}CD25^{neg}CD137^{neg} T cells were plated in U-bottom 96 well plates with 1.25ug/well soluble anti-CD3, 50,000 irradiated (1500 rads) NOD splenocytes and titrated numbers of NOD or NOD.B10 *Idd9.3* CD137^{pos} Tregs. The data was pooled from n=2 experiments for 1:4 and n=5 experiments for 1:8 and 1:16 for both NOD and NOD.B10 *Idd9.3* mice. In both (b) and (c) sections, the cells were pulsed with ³H labeled thymidine on day 3 and harvested after 16 hours. The percentage proliferation was calculated by dividing the CPM counts in wells with Tregs by the mean CPM count of the wells containing only CD4^{pos}CD25^{neg}CD137^{neg} T cells. Statistical significance was calculated with the unpaired t test.

First we tested NOD.B10 *Idd9.3* Treg subsets in the same assay system and again found that NOD.B10 *Idd9.3* CD137^{pos} Tregs were functionally superior to CD137^{neg} Tregs when suppressing NOD.B10 *Idd9.3* CD4^{pos}CD25^{neg}CD137^{neg} T effector cells (Figure 3.11a). Next we compared the suppressive function of CD137^{pos} Tregs against their syngeneic responders. Our results showed that the amount of suppression by NOD CD137^{pos} and NOD.B10 *Idd9.3* CD137^{pos} Tregs is comparable against their syngeneic T responder cells (Figure 3.11b). Next we directly compared the suppressive capacity of NOD and NOD.B10 *Idd9.3* CD137^{pos} Tregs, in

the same experiment, against NOD CD4^{pos}CD25^{neg}CD137^{neg} T effector cells and found no significant difference in the suppressive capacity of the CD137^{pos} Tregs of these two strains (Figure 3.11c). These experiments show that NOD and NOD.B10 *Idd9.3* CD137^{pos} Tregs does not differ functionally *in vitro*.

3.3.5 CD137^{pos} Tregs are the major cellular source of alternately spliced soluble CD137 protein

Alternate splicing produces two isoforms of CD137: full length CD137 expressed on the cell membrane and soluble CD137 in which transmembrane exon 8 is spliced out [161]. Previously, however, production of soluble CD137 by Tregs has not been studied. We designed RT-PCR primers (see Methods) that discriminate soluble versus membrane bound CD137 and used them to detect soluble CD137 versus membrane bound CD137 from freshly sorted NOD and NOD.B10 *Idd9.3* subsets. CD137^{pos} Tregs expressed significantly higher levels of soluble and membrane CD137 mRNA compared to CD137^{neg} Tregs in NOD and NOD.B10 *Idd9.3* mice (Figure 3.12a, b); CD4^{pos}CD25^{neg}CD137^{neg} T cells produced negligible amounts of both isoforms of CD137 mRNA *ex vivo* (Figure 3.12a, b).

Figure 3.12

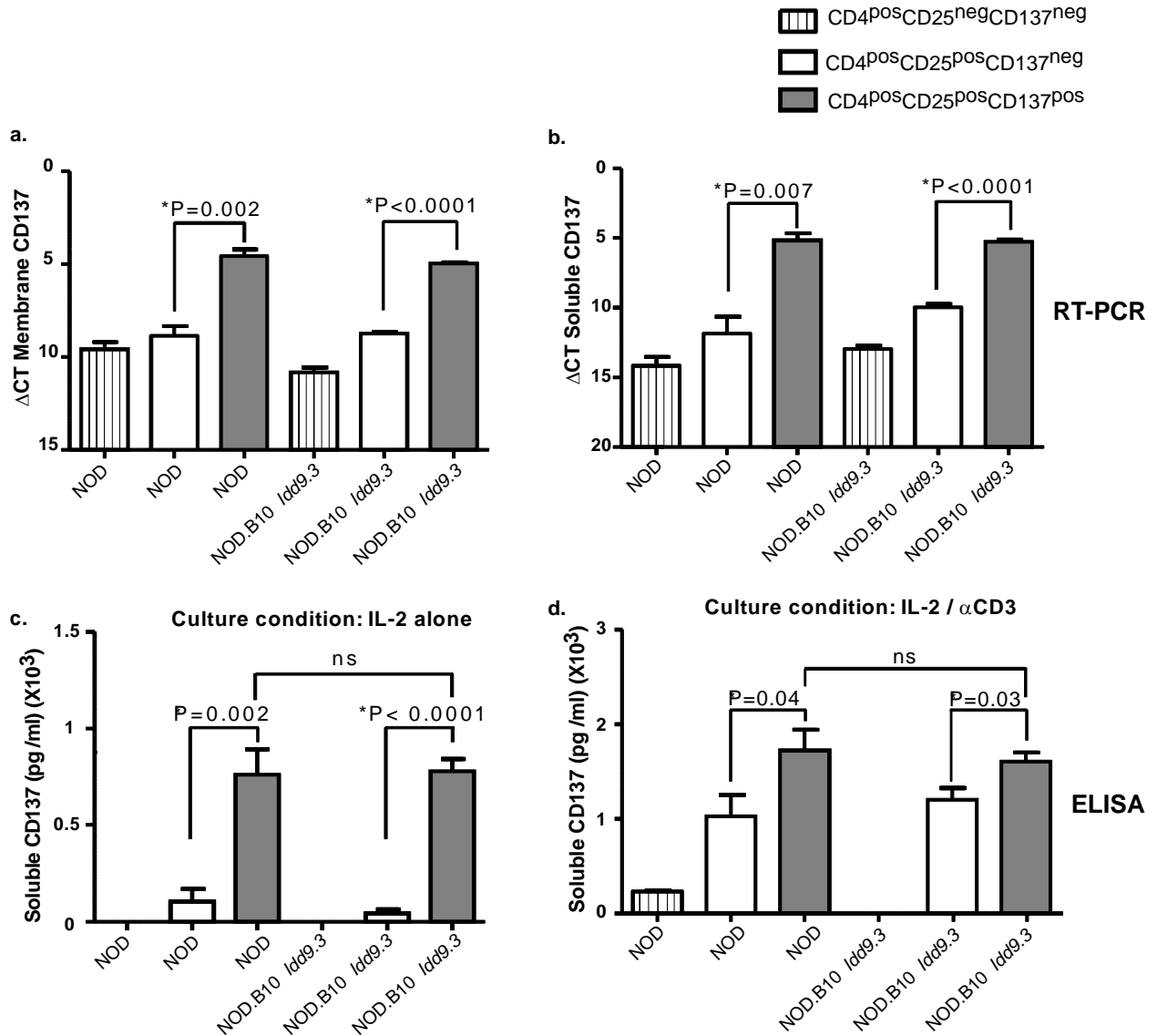


Figure 3.12. NOD and NOD.B10 *Idd9.3* CD137^{pos} Tregs are the major cellular source of soluble CD137 *in vitro*.

(a, b) RT-PCR for soluble and membrane CD137: NOD and NOD.B10 *Idd9.3* CD4^{pos}CD25^{neg}CD137^{neg}, CD4^{pos}CD25^{pos}CD137^{neg} and CD4^{pos}CD25^{pos}CD137^{pos} T cells were sorted from 4-8 week old females as above. RNA was immediately extracted and converted to cDNA. RT-PCR was performed with a set of custom designed primers used to detect either membrane (a) or soluble (b) CD137, (n=3 experiments for both (a) and (b)). B2m was used as an endogenous control. (c, d, e, f) ELISA for soluble CD137:

CD4^{pos}CD25^{neg}CD137^{neg}, CD4^{pos}CD25^{pos}CD137^{neg} and CD4^{pos}CD25^{pos}CD137^{pos} Tregs from 5-8 week NOD and NOD.B10 *Idd9.3* mice were sorted as above. 50,000 cells were cultured in 96-well U-bottom plate with (c) 25U/ml IL-2 (NOD n=2, NOD.B10 *Idd9.3* n=5) or (d) 1.25ug/ml of anti-CD3 and 25U/ml IL-2 (NOD n=4, NOD.B10 *Idd9.3* n=4) for 4 days. ELISA for soluble CD137 was performed on the supernatants. Statistical analysis was performed using the unpaired t test.

Next we sorted the CD137^{pos} and CD137^{neg} Tregs from NOD and NOD.B10 *Idd9.3* mice and cultured them (with IL-2 alone, to promote survival *in vitro* under non-activating conditions) to assess CD137 protein production. The cultured CD137^{pos} Tregs (from both NOD and NOD.B10 *Idd9.3* mice) produced significantly higher levels of soluble CD137 protein compared to CD137^{neg} Tregs; CD4 non-Treg cells did not produce significant amounts of soluble CD137 protein (Figure 3.12c). There was no significant difference in soluble CD137 protein production between NOD and NOD.B10 *Idd9.3* CD137^{pos} Tregs (Figure 3.12c, d). We did not detect significant soluble CD137 production from cell subset in the absence of IL-2 (data not shown). We have thus established, for the first time, that CD137^{pos} Tregs are the primary T cell source of soluble CD137.

Given that activated T cells express CD137, it was possible that our CD137^{neg} Tregs start producing soluble CD137 under activating conditions. To test this, we cultured CD137^{pos} and CD137^{neg} Tregs from NOD and NOD.B10 *Idd9.3* mice with IL-2 and anti-CD3, and tested culture supernatants on day 4 for soluble CD137. Under these activating conditions, CD137^{neg} Tregs produced some soluble CD137, although still significantly less than CD137^{pos} Tregs in both strains (Figure 3.12d). Again there was no significant difference in soluble CD137 production between the two strains. These results suggest that Treg activation causes CD137^{neg} Tregs to

increase alternate splicing of *Tnfrsf9* with subsequent production of soluble CD137 protein, although still significantly less than CD137^{pos} Tregs. Notably, non-Treg CD4^{pos} cells still did not produce significant amounts of soluble CD137 after stimulation under these activating conditions (Figure 3.12d).

We also tested CD137 membrane expression in CD137^{pos} and CD137^{neg} Tregs from both strains upon IL-2 and CD3 stimulation as above. As expected, the cells sorted as CD137^{neg} Tregs did not express any CD137 pre-culture (Supplemental Figure2). However after IL-2 and CD3 stimulation for 3 days, CD137^{neg} Tregs from both strains showed increased CD137 expression on a per cell basis, but the expression was still much lower than CD137^{pos} Tregs (Supplemental Figure2). Our data suggested that upon *in vitro* IL-2 and CD3 stimulation, CD137^{neg} Tregs start expressing membrane and soluble CD137 but the expression level is still much lower than Tregs that originally express CD137 pre-culture.

Next we tested if soluble CD137 is produced by NOD Tregs during *in vitro* suppression in the presence of CD4 T cells and CD3/CD28 beads, in the absence of APCs. Under these conditions, CD137^{neg} Tregs produced soluble CD137 protein but still significantly less (P=0.0001) than CD137^{pos} Tregs (Figure 3.13).

Figure 3.13

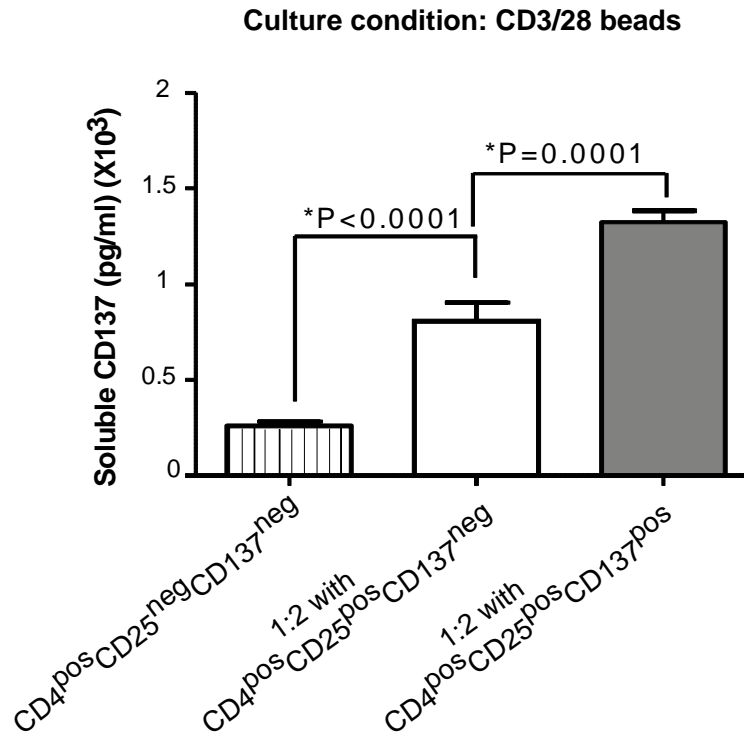


Figure 3.13. CD137^{pos} Tregs produce more soluble CD137 during suppression.

NOD CD4^{pos}CD25^{neg}CD137^{neg}, CD4^{pos}CD25^{pos}CD137^{neg} and CD4^{pos}CD25^{pos}CD137^{pos} T cells were sorted from 5-7 week old NOD mice as above. 50,000 CD4^{pos}CD25^{neg}CD137^{neg} T cells were plated in U-bottom 96 well plates with 50,000 CD3/CD28 beads and 25,000 (1:2, n=5 experiments) CD137^{neg} or CD137^{pos} Tregs. The supernatant was collected on day 4 and ELISA was performed on the supernatants for soluble CD137. The statistical analysis was performed using the unpaired t test. (f) 20-37 week old non-diabetic NOD (n=6) and NOD.B10 *Id9.3* (n=7) were sacrificed and their serum tested for soluble CD137 by ELISA. Statistical analysis was performed using the unpaired t test.

CD4 T cells cultured with CD3/CD28 beads (rather than irradiated APCs) also produced some soluble CD137 but significantly less than CD137^{neg} Tregs (P<0.0001). Our findings show that Tregs are the primary source of soluble CD137 *in vitro*. Our results also show that depending on

in vitro culture conditions CD137^{neg} Tregs can produce some soluble CD137 but significantly less than CD137^{pos} Tregs.

3.3.6 Increased serum soluble CD137 in older NOD.B10 *Idd9.3* mice

We have shown that NOD.B10 *Idd9.3* mice accumulate significantly increased numbers of CD137^{pos} Tregs with age (Figure 1c). We have also shown that CD137^{pos} Tregs are more suppressive (Figure 2.9) and express more soluble CD137 than CD137^{neg} Tregs (Figure 3.12). However, NOD and NOD.B10 *Idd9.3* CD137^{pos} Tregs do not differ in either direct contact mediated suppression (Figure 2.9) or soluble CD137 production on a per cell basis (Figure 3.12). We hypothesized that the increased numbers of CD137^{pos} Tregs with age in NOD.B10 *Idd9.3* mice might be reflected in increased soluble CD137 serum levels *in vivo*.

Figure 3.14

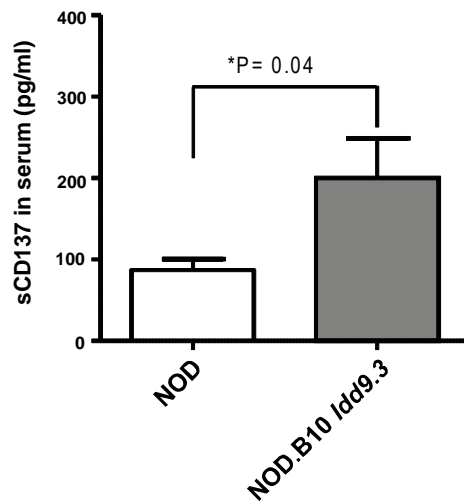


Figure 3.14: NOD.B10 *Idd9.3* congenic mice have higher serum soluble CD137 levels than NOD.

20-37 week old non-diabetic NOD (n=6) and NOD.B10 *Idd9.3* (n=7) were sacrificed and their serum tested for soluble CD137 by ELISA. Statistical analysis was performed using the unpaired t test.

In fact old NOD.B10 *Idd9.3* mice had significantly greater amount of serum soluble CD137 levels than age matched NOD mice (Figure 3.14). This result shows that the immunological effect of the B10 CD137 allotype could be quantitative, mediated by altering the accumulation of the affected cell subset (i.e., CD137^{pos} Tregs). Increased numbers of Tregs expressing the B10 allele thereby produce increased total amounts of soluble CD137 and also quantitatively expand the overall available contact mediated suppression.

In summary Tregs expressing the B10 *Idd9.3* region, compared to the NOD allotype, show increased peripheral accumulation of the functionally superior CD137^{pos} Tregs with age. We have also established that soluble CD137 may be one of the mechanisms of CD137^{pos} Tregs

suppression. NOD.B10 *Idd9.3* mice show a correlation between accumulation of CD137^{pos} Tregs with age and increased serum soluble CD137. The data presented here strongly support a critical role for CD137^{pos} Tregs in the regulation of T1D.

3.4 DISCUSSION

Our previous studies showed that anti-CD137 antibody treatment increased the number of CD4^{pos}CD25^{pos} T cells in NOD mice and that anti-CD137 antibodies bound specifically to CD4^{pos}CD25^{pos}CD137^{pos} Tregs *in vivo* while preventing diabetes (Chapter one) [137]. The B10 *Tnfrsf9* allele differs from the NOD allele by three coding variants [104, 225]. These sequence polymorphisms differences are likely responsible for the previously described decreased T cell signaling by the NOD allele when stimulated through CD137 [225], and it is known that CD137 signaling enhances Bcl-xL production and mediates cell survival [145]. It remained unclear how the decreased NOD allotype CD137 signaling could mediate increased T1D susceptibility [225]. We hypothesized that decreased signaling through the NOD CD137 allele, or increased signaling through the B10 CD137 allele, could influence T1D incidence by affecting Treg accumulation, and investigated this hypothesis using NOD and NOD.B10 *Idd9.3* mice. We found increased accumulation of Tregs expressing the B10 *Idd9.3* locus in two separate systems, i.e. *ex vivo* in NOD vs. NOD.B10 *Idd9.3* mice and in a mixed bone marrow chimera system. The absolute number of splenic lymphocytes, CD4 cells and CD4^{pos}CD25^{pos} T cells increased with age in both NOD and NOD.B10 *Idd9.3* mice; however the number of

CD4^{pos}CD25^{pos}CD137^{pos} Tregs increased only in NOD.B10 *Idd9.3* mice, reflecting a specific increase in their percentage in NOD.B10 *Idd9.3* and a decreased percentage in NOD. Conversely, in the thymus, the number of CD4^{pos}CD25^{pos}CD137^{pos} T cells decreased in NOD and increased in older NOD.B10 *Idd9.3* mice, reflecting a significantly increased percentage of thymic CD137^{pos} Tregs in older NOD.B10 *Idd9.3* mice. Our data suggests that increased thymic output of CD4^{pos}CD25^{pos}CD137^{pos} T cells in older NOD.B10 *Idd9.3* mice could contribute to the increased accumulation of these cells in the periphery. However we have not conclusively proven increased thymic output, and there could be additional mechanisms for peripheral accumulation of CD4^{pos}CD25^{pos}CD137^{pos} Tregs. Our data on cell numbers in spleen and thymus of NOD vs. NOD.B10 *Idd9.3* suggests a specific increase in CD137^{pos} Tregs in the NOD.B10 *Idd9.3* mice, but these results could be influenced by many intrinsic and extrinsic causes. To address this point and to show in a separate system that the B10 *Idd9.3* region supported increased accumulation of CD137^{pos} Tregs, we used a mixed bone marrow chimera approach, in which NOD and B10 *Idd9.3*-expressing Tregs could develop in the same mouse and hence have the same extrinsic cellular environment. The studies in bone marrow chimeras show that the increased accumulation of B10 *Idd9.3* expressing Tregs is a cell intrinsic feature in CD137^{pos} Tregs. This does not exclude the possibility that extrinsic factors, particularly IL-2 production from T cells, could also be contributing to expansion or survival of various cell types and protection from diabetes in NOD.B10 *Idd9.3* mice. Given that the B10 allele mediates enhanced IL-2 production in NOD.B10 *Idd9.3* CD4^{pos} T cells [225], this is a likely contributing factor that makes the system more complex and multifactorial.

We also explored possible mechanisms for accumulation of CD137^{pos} Tregs in old NOD.B10 *Idd9.3* mice. First we observed that the NOD.B10 *Idd9.3* CD137^{pos} Tregs do not proliferate more *in vitro* or *in vivo* than the same cell subset in NOD mice, suggesting that proliferation does not account for increased accumulation of CD137^{pos} Tregs in NOD.B10 *Idd9.3* mice. Next, we

showed that increased CD137^{pos} Treg accumulation is correlated with increased CD137^{pos} Treg Bcl-xL mRNA expression in both NOD.B10 *Idd9.3* mice and in the CD137^{pos} Tregs with the B10 allotype in the mixed bone marrow chimera mice. The lack of increased Bcl-xL protein expression and the increased Bcl-xL in CD137^{neg} Tregs in NOD.B10 *Idd9.3* mice, however, makes this correlation hard to interpret. Furthermore, we did not see any difference in cell death between NOD and NOD.B10 *Idd9.3* Treg subsets upon *in-vitro* stimulation. Hence further studies need to be performed to establish the mechanism of accumulation of CD137^{pos} Tregs in old NOD.B10 *Idd9.3* mice.

It has been reported that Foxp3^{pos}TGF- β ^{pos} T cells significantly decline with age in NOD mice and that the aged CD4^{pos}CD25^{pos} T cells are less suppressive against aged CD4^{pos}CD25^{neg} T cells [76, 77]. In addition, the increased protection from diabetes in the NOD BDC2.5 model is also associated with increased Foxp3+ T cells with age [235]. Therefore it is possible that the increased number of CD137^{pos} Tregs in NOD.B10 *Idd9.3* mice with age could result in increased peripheral immune regulation that could regulate the onset of T1D. We observed that the amount of CD137 (MFI) on the cell surface of CD4^{pos}CD25^{pos}CD137^{pos} Tregs is not decreased on aged NOD CD137^{pos} Tregs—the accumulating CD137^{pos} Tregs on aged NOD are all CD137-high expressers. The CD137 MFI is also higher in young NOD.B10 *Idd9.3* compared to young NOD CD137^{pos} Tregs. The decrease in cellular CD137 expression in young NOD vs. NOD.B10 *Idd9.3* CD137^{pos} Tregs might affect the accumulation of total number of surviving cells long term. Increased expression of an allele that in itself mediates increased signaling could combine to produce an intrinsically mediated signal that results in accumulation of these CD137^{pos} Tregs in NOD.B10 *Idd9.3* mice. This is entirely consistent with studies of the function of CD137 in CD137 knockout mice, which have decreased long term survival of antigen specific CD8 T cells [10]. Since we have shown that CD137^{pos} Tregs are functionally superior at regulation, an increase of this cell subset over time could result in increased peripheral regulation and

increased protection from T1D. Our study has not been able to link increased accumulation with increased cell proliferation, cell survival or cell death. Although further studies are needed to understand the link between CD137 and accumulation of Tregs, our results strongly suggest that CD137 co-stimulation is important for Treg mediated diabetes prevention.

Mouse CD4^{pos}CD25^{pos} Tregs have been differentiated into subsets based on their expression of cell surface molecules such as CD134 [236], integrin alpha E beta 7 [237] and CD62L [188, 238] that affect their suppressor activity, or by molecules such as CD45RA^{pos} [239] and P-selectin [240] that delineate Treg differentiation *in-vitro* or *in-vivo*. Our results differentiate two sub-populations of CD4^{pos}CD25^{pos} Tregs, CD137^{pos} and CD137^{neg}. These subsets are not merely phenotypically differentiated by cell surface expression of CD137, but by differences in functional cell mediated suppression, and by differences in the production of immunosuppressive soluble CD137.

Soluble CD137 has been reported in the sera of RA patients and in the CSF of MS patients, and MS patients have decreased expression of CD137 on their Tregs [164, 241-243]. It has been shown that soluble CD137 acts to inhibit T cell proliferation [162, 165]. Although the mechanism for soluble CD137 mediated suppression is not fully understood, it has been shown to bind with CD137L *in vitro* and likely mediates its effect through CD137L [162]. In addition, soluble CD137 has been reported to arise later in the immune response to counteract overactivation of the immune system [165]. These previous reports combined with the findings presented here suggest that production of soluble CD137 may act as a “brake” upon normal immune activation. In this scenario, activation of antigen specific CD137^{pos} Tregs could produce soluble CD137 which, in combination with contact dependent suppression, would down regulate the immune activation of both T cells and APCs expressing CD137L [244]. Insufficient production of soluble CD137 (for example, in our system, mediated by a decrease in frequency of NOD Tregs producing soluble CD137 with age) could lead to exaggerated immune activation; conversely

increased numbers of such Tregs could act to decrease immune activation in NOD.B10 *Idd9.3* mice. These considerations are strengthened by our observation of increased serum soluble CD137 in the protected NOD.B10 *Idd9.3* mice with age (Figure 3.14), correlating with the increased accumulation of CD137^{pos} Tregs in these mice, compared to NOD mice. We showed that there was no intrinsic cellular difference between NOD and NOD.B10 *Idd9.3* cells in either contact mediated suppression (Figure 3.11) or production of soluble CD137 (Figure 3.12). However, the accumulation of CD137^{pos} Tregs in the NOD.B10 *Idd9.3* mice was correlated with increased total amount of serum soluble CD137 (Figure 3.14) and thus increased overall immunosuppression. Similarly, while NOD and NOD.B10 *Idd9.3* CD137^{pos} Tregs do not differ in contact dependent suppression on a per cell basis (Figure 3.11), increased numbers of CD137^{pos} Tregs increases the total available contact mediated immunosuppression in NOD.B10 *Idd9.3* mice. Thus, the B10 *Idd9.3* allele acts primarily to enhance accumulation of CD137^{pos} cells, rather than by changing the immunosuppressive function on a per cell basis-- but the net overall effect is increased systemic immunosuppression. These conclusions are strongly supported by the evidence presented here but not directly proven, as will be done in future studies.

Our study explains how the hyporesponsive NOD CD137 allotype can contribute to increased T1D susceptibility in NOD mice, compared to the B10 allotype in the NOD.B10 *Idd9.3* mice. Thus, the NOD.B10 *Idd9.3* allele could lead to increased accumulation of functionally superior CD137^{pos} Tregs with age and thus downregulate autoimmunity; whereas NOD would have a quantitative deficiency of CD137^{pos} Tregs compared to NOD.B10 *Idd9.3*, contributing to enhanced NOD autoimmunity with age. A decreased number of CD137^{pos} Tregs results in decreased total cell mediated suppression as well as decreased production of counter-regulatory soluble CD137, which might be even more important at the site of inflammation (e.g. the pancreatic islet). These considerations lead us to suggest that enhancing site specific

expression of soluble CD137 could downregulate autoimmunity, and we will explore this hypothesis in future studies.

3.5 Acknowledgements

We are very grateful to Oliver Burren, and Mikkel Christensen, for BAC sequencing and annotation/display. NOD.Foxp3-GFP knock-in mice were a kind gift from Vijay Kuchroo and Ana Anderson of Harvard University.

4.0 THE SOLUBLE FORM OF CD137 IS SUPPRESSIVE AND PREVENTS DIABETES IN NOD MICE

This manuscript is being prepared for submission. The initial studies on CD137^{pos} Tregs and soluble CD137 production by Tregs were performed by Kritika Kachapati. David Adams developed the lentiviral vectors and transduced cell lines for soluble CD137 production. Soluble CD137 was purified and characterized by Kyle Bednar and tested *in vitro* by both Kyle and Kritika. NOD soluble CD137 treatment and histology was performed by Kyle.

4.1. INTRODUCTION

As discussed in Chapter 1, NOD mice serve as an excellent model for understanding genetic factors influencing disease, and genetic mapping studies performed over the last 25 years have identified multiple Insulin dependent diabetes (*Idd*) loci influencing disease in NOD mice. *Idd* loci have been incorporated into NOD congenic mice (containing the NOD background with protective *Idd* regions from B6 background). NOD.B10 *Idd9.3* congenic mice (strain 1106) offers a model for studying the candidate genes in *Idd9.3* loci, with CD137 being the strongest candidate gene in the region. In Chapters 2 and 3 we have shown several studies showing a

strong effect of CD137 on disease and on T-cell/Treg function. We showed that agonist anti-CD137 antibody treatment prevents diabetes in NOD mice, and increases the frequency of CD4^{pos}CD25^{pos} T cells *in vivo* (Figure 2.1 & 2.5). NOD.B10 *Idd9.3* mice have more CD137^{pos} Tregs with age compared to NOD mice, and that CD137^{pos} Tregs expressing the B10 allele accumulate specifically in NOD: NOD.B10 *Idd9.3* mixed bone marrow chimeras (Figure 3.2 & 3.7). The significance of this is found in our data showing functionally superior suppressive capacity of CD137^{pos} Tregs compared to CD137^{neg} Tregs (Figure 2.9 & 2.10). In addition, we showed that CD137^{pos} Tregs are the major cellular source of an alternately spliced CD137 product, soluble CD137 (Figure 3.12). Finally, NOD.B10 *Idd9.3* mice show increased serum soluble CD137 with age, correlated with increased accumulation of CD137^{pos} Tregs and protection from diabetes (Figure 3.14). Here we integrate our prior studies by showing the mechanistic connection of anti-CD137 antibody therapy with soluble CD137 production.

First, using a CD25 blocking antibody to deplete Treg cells *in vivo*, we show that CD4^{pos}CD25^{pos} Tregs are essential for anti-CD137 mediated diabetes protection. The anti-CD137 antibody treatment initiated a signaling response in CD137^{pos} Tregs, resulting in the redistribution of a downstream adaptor molecule, TRAF2 from the cytosol to the membrane, a response not seen in CD137^{neg} Tregs. Mouse CD137 is known to be alternately spliced in T cells to produce two different isoforms; full length CD137 protein that is bound to cell surface and a soluble CD137 isoform, in which the transmembrane-encoding exon 8 is spliced out [161]. Previously we have shown that CD137^{pos} Tregs produce high levels of soluble CD137, as well as the full length, membrane-bound protein (Figure 3.12). Here we show that soluble CD137 produced by CD137^{pos} Treg increases after anti-CD137 treatment and accumulates in the serum of the injected mice. Others have found that soluble CD137 is suppressive to T cells and that it can initiate activation induced cell death (AICD) [166]. We show here that blockade of CD137L abrogated CD137^{pos} Treg mediated transwell suppression of T cells in the absence of APC,

indicating an active role for soluble CD137 in proliferative suppression. Soluble CD137-Fc chimeric protein also suppressed CD4 T cell proliferation *in vitro*. To confirm the suppressive role of soluble CD137, we used a lentiviral construct to produce recombinant soluble CD137 *in vitro*. Virally-made soluble CD137 protein was purified from the culture supernatant using affinity chromatography and structurally characterized to exist predominantly as a dimer by western blot and analytical ultra-centrifugation (AUC). Purified soluble CD137 was found to be suppressive *in vitro* and greatly reduced the incidence of diabetes in female NOD mice. Taken together, these results show a strong association between anti-CD137 and soluble CD137 production *in vivo* and confirm that soluble CD137 is a novel immunosuppressive molecule able to reduce the incidence of diabetes in NOD mice.

4.2 METHODS

4.2.1 Mice and reagents:

NOD mice were maintained under specific pathogen-free conditions in our institution's animal facilities. Mice were handled in accordance with the animal care guidelines of University of Cincinnati School of Medicine. Urinary glucose analysis was performed once a week using Tes-tape (Shionogi, Osaka Japan) to assess diabetes progression. Agonist anti-CD137 monoclonal antibodies (clone 3H3) were previously described [11]. CD4-APC-Cy7, CD25-FITC, and anti-CD137-APC antibodies were purchased from BD pharmingen. Anti-mouse CD137L (clone TSK-1) blocking antibodies and IgG2a isotype control (clone RTK2758) antibodies were purchased from BioLegend (California). CD3/CD28 coated beads and recombinant mouse IL-2 were

purchased from Invitrogen. CD137-Fc conjugated recombinant protein was purchased from R&D Systems (Minnesota). Primers for GAPDH (4352339E-0801016), Beta-2 microglobulin (Mm00437762_m1), Foxp3 (Mm00475156_m1), IL-10 (Mm00439616_m1), TGF- β (Mm01178819_m1) and Bcl-xl (Mm00437783_m1) were purchased from Applied Bioscience. We used custom designed primers for membrane bound and soluble CD137 (Applied Bioscience). Anti-TRAF2 (clone C-20) antibodies and anti-CD137 (clone 6D295) were purchased from Santa Cruz Biotechnology. Polyclonal secondary antibodies to mouse IgG - H&L (AP) (clone ab6729) and goat anti-rabbit IgG (AP) were purchased from Invitrogen and Southern Biotech, respectively. AP-stained proteins were visualized using the BCIP/NBT Substrate Solution purchased from PerkinElmer Life Sciences.

4.2.2 Anti-CD137 Treatment:

NOD mice were treated with 330 μ g of anti-CD25 antibody or PBS twice at a one week interval. Starting one day after the second injection, the mice were either untreated or treated three times with 200 μ g of anti-CD137 at 3-week spaced intervals as described in chapter 1 (Figure 2.1). The mice were tested for glucosuria each week. Diabetes was confirmed when blood glucose levels reached >300 mg/dl. In experiments where Treg cells were analyzed after anti-CD137 treatment, the mice were treated with 100 μ g of anti-CD137 twice at a one week intervals and sacrificed for analysis one day after the last antibody treatment.

4.2.3 RT-PCR:

CD4 T cells were purified from splenocytes using CD4 magnetic beads (Miltenyl Biotech, California). The isolated CD4 T cells were blocked with 2.4G2 Ab and stained with CD4-APC-Cy7, CD25-FITC, and anti-CD137-APC Abs as described above. The cells were then sorted using a BD FACS Aria machine (BD Bioscience) into CD4^{pos}CD25^{neg}CD137^{neg} and

CD4^{pos}CD25^{pos}CD137^{pos} cell subsets. Whole cell mRNA was extracted from the purified cells using an RNeasy mini kit (Qiagen) and converted into cDNA (Promega Reverse Transcription System). Quantitative Real Time Polymerase Chain Reaction (RT-PCR) was performed on the amplified cDNAs using TaqMan primers for *Gadph* or *B2m* and *Bcl-xl* using a StepOnePlus Real-Time PCR system (Applied Biosystems). The experimental CT values for genes-of-interest were subtracted from the CT values for control housekeeping genes (either *Gadph* or *B2m*) and the data plotted using GraphPad Prism 5 (Version 5.02).

4.2.4 Treg Transwell Suppression Assay:

100,000 sorted CD4^{pos}CD25^{neg}CD137^{neg} T cells were cultured with 50,000 CD3/CD28-coated beads (Invitrogen) in the bottom wells of a 96 well transwell plate (Corning). 25,000 CD4^{pos}CD25^{pos}CD137^{pos} Tregs were cultured in the top wells with 50,000 CD3/CD28-coated beads. In some wells, 20µg/ml of CD137L (TKS-1) blocking antibodies were added to the bottom wells. The transwell plates were incubated at 37°C in 5% CO₂ and the cells pulsed with 1 µCi [³H] thymidine on Day 3. Cells in the bottom wells were later harvested and counted using a beta scintillation counter as indicated.

4.2.5 Proliferation Assay with thymidine:

CD4^{pos}CD25^{neg}CD137^{neg} cells were stained and sorted using BD Aria flow sorter (BD Bioscience) to 90-95% purity. 50,000 of the sorted CD4^{pos}CD25^{neg}CD137^{neg} T cells were cultured with 20,000 CD3/28 beads in triplicate wells in the presence or absence of 1µg/ml of soluble CD137-Fc. 20µg/ml of either CD137L blocking antibodies or IgG2a isotype control antibodies were added to select wells. All cells were subsequently pulsed-labelled with 1 µCi [³H] thymidine on Day 3, and 16 hours later, thymidine incorporation was assessed using a beta scintillation counter.

4.2.6 Proliferation Assay with CFSE:

Magnetically-sorted NOD CD4 T cells were stained with 0.5 μ M of carboxyfluorescein succinimidyl ester (CFSE) before being added to a 96-well u-bottom plate. 100,000 CD4 T cells per well were cultured under one of the following three conditions: Unstimulated (control), stimulated (20,000 CD3/CD28 beads), or stimulated with 15 μ g of purified recombinant soluble CD137. The CFSE-labeled cells were grown for 3 days at 37°C in 5% CO₂, and then on day 3, the labeled cells were harvested, blocked with 2.4G2 Ab and stained with a combination of CD4-PCP, propidium iodine, and Annexin V-APC.

4.2.7 Cell death:

NOD CD4 T cells were purified using magnetic column. 100,000 of CD4 T cells per well were left uncultured or stimulated with 20,000 CD3/CD28 beads. In some wells 15 μ g of purified recombinant soluble CD137 were added to the bead stimulated wells. The cells were then stained with CD4-FITC and PI on day 3. Percentage of dead cells was determined by gating on PI positive cells.

4.2.8 ELISA:

Mouse 4-1BB DuoSet Elisa system (R&D Systems, California) was used to detect soluble CD137 from serum and culture supernatants. The kit uses rat anti-mouse 4-1BB capture antibody and biotinylated goat anti-mouse 4-1BB detection antibody to detect soluble CD137 protein. Recombinant mouse 4-1BB, provided in the kit, was used as a standard.

4.2.9 Production of soluble CD137:

A sequence-verified, bacterial cDNA clone for *Mus musculus* soluble CD137 (B10 'wild type' allele) was obtained from Open Biosystems (Clone ID 1497753). This cDNA was originally ligated into the pT7T3-Pac vector, flanked by unique EcoRI and NotI sites; Using agarose gel electrophoretic analysis and ethidium bromide staining, we confirmed that the soluble CD137 clone releases the expected ~916 bp fragment after digestion with EcoR1 and NotI. We excised the soluble CD137 DNA band and inserted it into the multiple cloning site (MCS) of LeGO-iG2 using standard subcloning procedures. The soluble CD137 minigene was inserted immediately downstream from the strong Spleen Focus-Forming Virus (SFFV) promoter in the LeGO-iG2 lentiviral vector, (between the two unique restriction sites *EcoRI* and *NotI*) as previously described [245]. This location permits co-expression of sCD137 along with a downstream enhanced green fluorescent protein (EGFP) reporter gene, permitting green fluorescence to be used to monitor the efficiency of viral transduction and bicistronic protein expression. Immortalized mouse fibroblasts (NIH3T3) and human embryonic kidney (HEK293) cells were transduced with VSVg-enveloped lentiviral particles made with either the parent vector LeGO-iG2 or LeGO-iG2-sCD137. The resultant transduced cells were cultured in 10.0% CO₂ at 37° C and split as needed in antibiotic (pen strep) and L-glutamine supplemented DMEM media containing 10% FBS (Fetal Bovine Serum). The supernatant from confluent cultures was collected over several weeks and tested for the production of soluble CD137 by ELISA (see ELISA in methods). NIH3T3 and HEK293 cell lines exhibiting stable EGFP expression were subsequently sorted for high (top 10%) and medium (middle 40-70%) EGFP expression using a Beckman Coulter MoFlo XDP flow cytometry. The sorted cells were subsequently re-plated and cultured for an additional five days in IMDM with 10% FBS before checking soluble CD137 and EGFP expression by ELISA and flow cytometry, respectively. High CD137 expressors were later used for large-scale protein purification and for archiving producer stocks.

4.2.10 Purification of Soluble CD137:

To purify soluble CD137 protein from culture supernatants, we generated an anti-CD137 affinity chromatography column. For this, we first purified anti-CD137 antibodies using 3H3 antibody/hybridoma generously given to us by R. Mittler [131]. The antibody-producing cells were cultured in IgG-depleted Fetal Bovine Serum (FBS) at a cell density of 1×10^6 cells per flasks or in roller bottles, and split as required for 4 weeks. After this time period, the cells were serum-starved for two weeks to obtain optimal antibody production. The secreted antibody was subsequently coupled to GE Life Sciences CNBr-activated Sepharose™ 4B column, according to the manufacturer's instructions. This results in strong covalent bound between the antibody and CNBR-activated sepharose beads. Coupling efficiency was assessed by running the elution buffer, i.e., 3.5M MgCl₂, over the column and checking for release of the anti-CD137 antibody (3H3) from the CNBR-activated beads. A NanoDrop ND-1000 spectrophotometer was used to confirm that no CD137 antibody was lost from the column. Supernatant from HEK293:LeGO-iG2-sCD137 High cells was used for the purification due to their superior production of soluble CD137. The supernatant was 0.22μ filtered before being run over the column. The flowthrough supernatant was tested after each run by ELISA (see ELISA methods) to ensure the depletion of soluble CD137 due to binding to the column. After elution from the antibody column, soluble CD137 protein was dialyzed three times in Tris-Buffered Saline (TBS) and two times into phosphate buffered saline (PBS). The amount of purified soluble CD137 and degree of concentration was determined using a Ross Recorders spectrophotometer, ELISA, and NanoDrop ND-1000.

4.2.11 Western Blot:

For assaying the redistribution of TRAF2 in cells after anti-CD137 treatment, CD4^{pos}CD25^{neg}CD137^{neg}, CD4^{pos}CD25^{pos}CD137^{neg} and CD4^{pos}CD25^{pos}CD137^{pos} T cell subsets were sorted and lysed for 30 min on ice in the presence of broad specificity protease inhibitors (Sigma, cat no. P8340). The lysed cells were then briefly centrifuged for 30 sec at 6000 rpm to separate cellular proteins into either soluble (cytoplasmic) or insoluble (membrane-associated) fractions (Arch RH et al., 2000). After separation of recovered proteins on a 10% SDS-PAGE gel (Invitrogen) under +DTT reducing conditions, samples were transferred into a nitrocellulose membrane and immunostained. Low molecular weight, pre-stained protein markers (BioRad) were used as size controls. Primary anti-TRAF2 antibodies were added to the blots initially, followed by goat anti-Rabbit IgG Alkaline Phosphatase (AP) conjugate secondary antibodies. The AP-antibody-bound proteins were then stained using NBT (nitro-blue tetrazolium chloride) and BCIP (5-bromo-4-chloro-3'-indolyphosphate p-toluidine salt) as described above. The TRAF2 protein bands were imaged and analyzed using Alphamager hardware and AlphaView software supplied by the manufacturer (AlphaInnotech). For the soluble CD137 western blot, 15µl of soluble CD137 protein samples were mixed in either 15µL of reducing (10.0 ml 0.5 M Tris-HCl, 2.0 g SDS, 0.1 g Bromophenol Blue, 1.543 g of Dithiothreitol, 12.5 ml of 80% Glycerol, up to 50 ml with H₂O) or non-reducing (10.0 ml 0.5 M Tris-HCl, 2.0 g SDS, 0.1 g Bromophenol Blue, 12.5 ml 80% Glycerol, up to 50 ml with H₂O) sample buffer. The samples were then boiled for 5 minutes and cooled to RT. 25ul of each sample was loaded onto 12% Tris-glycine gels (Novex) and run at 125V for 105 minutes in a XCell II apparatus (Invitrogen). Low molecular weight pre-stained SDS-PAGE protein markers (BioRad, cat. no. 161-0305) were used as size markers. Next the protein was transferred onto nitrocellulose paper. Afterwards, the blots were blocked using 10% BSA (Bovine Serum Albumin) in TBS-T (Tris-Buffered Saline with 2.0% Tween 20) and. The primary anti-CD137 antibody (Millipore, rat anti-

mouse 4-1BB clone MAB3733) added to the blots. Afterwards, polyclonal secondary antibody to mouse IgG - H&L (AP) was added. The AP antibody-bound proteins were later stained using NBT and BCIP and their relative gel mobility and molecular size compared to the pre-stained protein markers, and recombinant CD137-Fc protein.

4.2.12 Analytical ultra-centrifugation (AUC):

Sedimentation velocity experiments were utilized to determine the size distribution of soluble CD137 at 20°C using a Beckman XL-I analytical ultracentrifuge. Soluble CD137 in PBS was spun at 48,000 rpm and successive scans were obtained at 280 nm using the absorbance optical system. Raw sedimentation data were deconvoluted to produce sedimentation coefficient distributions and molecular weight estimates using the c(s) analysis routine in the program SEDFIT [246].

4.2.13 Histology:

NOD female mice 4-6 weeks old were treated once a week for four weeks with either PBS or 200 µg of sCD137. After 225 days or at the first onset of disease the mouse was sacrificed. The pancreas was removed and stained using hematoxylin and eosin by The Pathology Research Core at Cincinnati Children's Hospital Medical Center. Pancreatic tissues were fixed for 24 h in 10% buffered formalin. Tissues were embedded in paraffin and stained with hematoxylin and eosin. To quantitatively assess pancreatic inflammation, the scoring system was adapted from previously described scoring systems validated in NOD mice [247, 248]. Based on that, the pancreatic inflammatory blinded scoring was performed where score ranged from 0 to 5 (score 0: normal islet, score 1: peri insulinitis, with a T cell depth of 5 or less and no penetration into the islet, score 2: full circumferential insulinitis or peri insulinitis with a T cell depth of 5 or greater, no penetration into the islet, score 3: full circumferential insulinitis or peri insulinitis with a T cell depth

of 5 or greater, less than 50% coverage of the islet by T-cell infiltrate, score 4: full circumferential insulinitis or peri insulinitis with a T cell depth of 5 or greater, more than 50% coverage of the islet by T-cell infiltrates, score 5: scar or complete absence of β -cells.) An overall pancreatic insulinitis score was obtained by adding the individual scores and dividing by the total number of islets counted per group (minimum of 36 islets were counted per group).

4.2.14 NOD treatment with soluble CD137:

Female NOD mice were treated with either PBS or 200ug of soluble CD137, once a week for four weeks. The blood glucose levels / diabetes progression was tested once a week using Tes-Tape for the duration of the experiment.

4.2.15 Data analysis:

All statistical analysis was performed using the unpaired T test or the Mann-Whitney test in GraphPad Prism 5 (Version 5.02). Survival analysis was performed using the log-rank test in GraphPad.

4.3 RESULTS

4.3.1 CD4^{pos}CD25^{pos} T cells are essential for anti-CD137 mediated diabetes protection.

Previously we demonstrated that agonistic anti-CD137 treatment prevents diabetes in NOD mice, and that anti-CD137 binds to CD4^{pos}CD25^{pos}CD137^{pos} Tregs *in vivo* (Figure 2.1 & 2.5). To test whether CD4^{pos}CD25^{pos} Tregs are essential for anti-CD137 mediated disease protection, we pretreated NOD mice with anti-CD25 antibody to deplete CD4^{pos}CD25^{pos} T cells (as confirmed by FACS). We have previously published that ~95% of peripheral CD25^{pos} cells are FoxP3^{pos} at this age (Figure 3.5). CD25 depletion was followed by three doses of anti-CD137 Ab injection at one-week intervals as described previously (Figure 2.1). Control mice were treated with anti-CD25 alone or PBS.

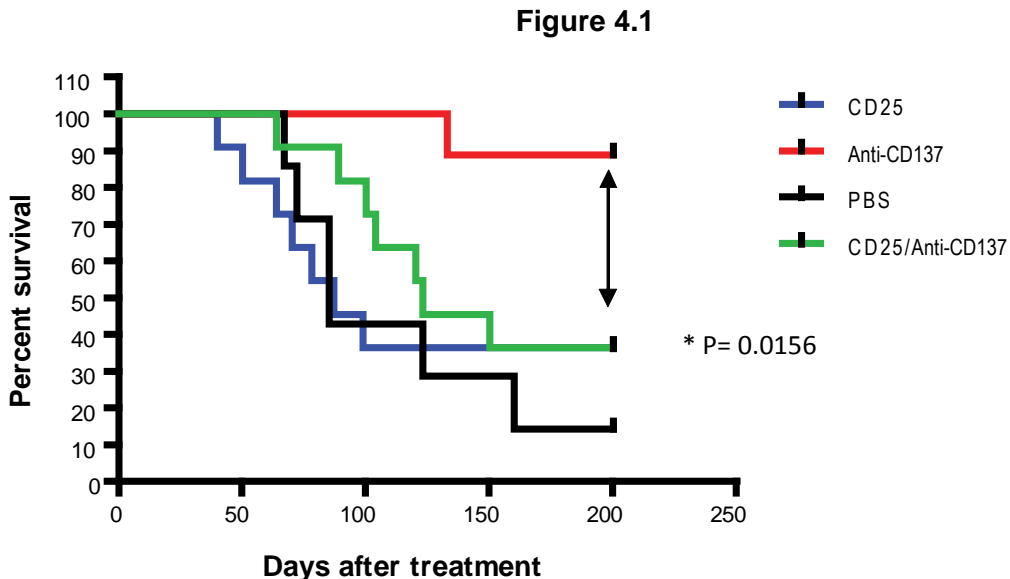


Figure 4.1: CD4^{pos}CD25^{pos} T cells are essential for anti-CD137 mediated diabetes prevention.

Seven week old NOD female mice were treated with 330µg of anti-CD25 antibody or PBS twice at a one week interval. One day after the second injection, the mice were either mock treated or treated three times with 200µg of anti-CD137 (clone 3H3, provided by Dr. R. Mittler, Emory University, Atlanta, GA) at 3-week intervals. The groups consist of: CD25 alone (n=11), 3H3 alone (n=9), PBS alone (n=7), and both CD25 and 3H3 (n=11). The mice were tested for glucosuria weekly thereafter. The P value was calculated using the logrank statistic in GraphPad.

Mice treated with anti-CD137 antibody were significantly protected from diabetes consistent with our result previously described in chapter 2 (Figure 4.1). Mice that were pre-treated with anti-CD25 antibody prior to anti-CD137 treatment, however, showed no protection from diabetes (Figure 4.1), demonstrating that the presence of CD25^{pos} Tregs at the time of anti-CD137 treatment was necessary for the observed protective effect. Anti-CD25/anti-CD137 combined treatment, anti-CD25 alone and PBS treated mice all succumbed to diabetes within 50-150 days with no statistically significant differences in outcome; notably treatment with anti-CD25 alone did not hasten the onset of diabetes (Figure 4.1). These results confirm that CD4^{pos}CD25^{pos} T cells are indispensable for preventing diabetes with anti-CD137 therapy in NOD mice. The combined data suggest that CD137^{pos} Tregs, targeted by anti-CD137 antibody treatment, are important for the preventing of diabetes progression.

4.3.2 Anti-CD137 treatment induces TRAF2 signaling response in CD137^{pos} Tregs *in vivo*

CD137 belongs to TNFR superfamily of receptors that bind to TNFR-associated factors (TRAFs) intracellularly when stimulated [175]. Since TRAF1/2 has been shown to be upregulated by CD137 stimulation in T cells [10], we next tested whether anti-CD137 antibody treatment could cause downstream signaling of CD137 in Tregs. We treated NOD mice with anti-CD137

antibody *in vivo* and after 24 hours isolated CD4^{pos}CD25^{neg}CD137^{neg}, CD4^{pos}CD25^{pos}CD137^{neg} and CD4^{pos}CD25^{pos}CD137^{pos} T cells by cell sorting.

Figure 4.2

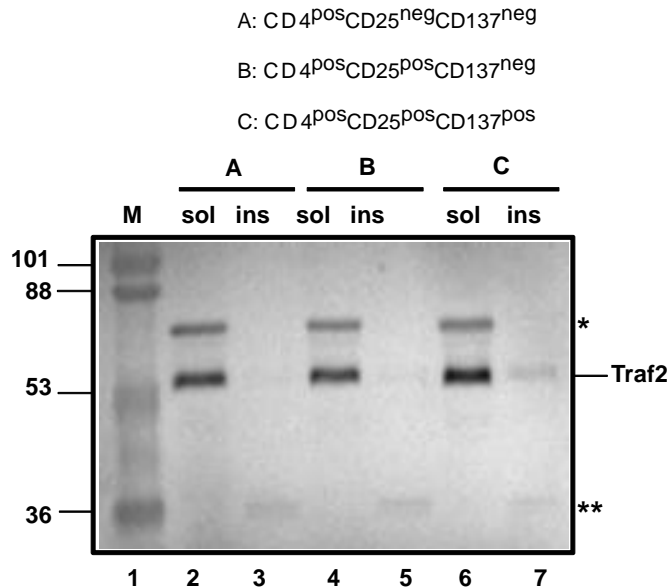


Figure 4.2: CD137^{pos} Tregs from anti-CD137 treated NOD mice redistribute TRAF2 to the cell surface.

NOD mice (n = 2) were treated with 200µg of anti-CD137 once and CD4^{pos}CD25^{neg}CD137^{neg}, CD4^{pos}CD25^{pos}CD137^{neg} and CD4^{pos}CD25^{pos}CD137^{pos} T cells were isolated by sorting 24 hrs later. Western blot of lysate proteins (after separation of proteins by centrifugation and 10% SDS-PAGE) show redistribution of 55 kDa TRAF2 protein from soluble (i.e., cytoplasm) to insoluble (i.e., membrane-bound) fractions only in the CD137^{pos} Tregs, not in T cells or CD137^{neg} Tregs, following stimulation with antibody *in vivo*. Starred bands represent either residual fetal bovine serum (*) from the media or an unidentified, membrane-bound mouse phosphatase (**), which reacts with the BCIP/NBT substrate. Lane 1 contains pre-stained, low range protein size markers (kDa).

TRAF2 western blot analysis performed under reducing conditions was used to look for the redistribution of the TRAF2 protein from the cytoplasm (i.e., soluble) to membrane-associated (i.e., insoluble) cell-fractions. 55 kDa TRAF2 is recruited to the cell surface only in

CD4^{pos}CD25^{pos}CD137^{pos} T cells following binding to CD137 antibody *in vivo* (after treatment) but not in CD4^{pos}CD25^{neg}CD137^{neg} or CD4^{pos}CD25^{pos}CD137^{neg} T cells (Figure 4.2). These data indicate that anti-CD137 antibody treatment specifically targets CD137^{pos} Tregs *in vivo* and initiates the CD137 mediated TRAF2 downstream signaling pathway in these in these cells.

4.3.3 Anti-CD137 treatment enhances soluble CD137 production from CD137^{pos} Treg *in vitro* and *in vivo*

We have previously shown that NOD CD137^{pos} Tregs produce high levels of soluble CD137 when cultured *in vitro* with IL-2 alone (Figure 3.12). Here we tested if anti-CD137 treatment alters soluble CD137 production from CD137^{pos} Tregs *in vitro*. We isolated CD137^{pos} Tregs from anti-CD137 antibody treated (which binds to anti-CD137 *in vivo*) or untreated mice. Untreated CD4^{pos}CD25^{neg} T cells were used as a control. We then assayed soluble CD137 production in CD137^{pos} Tregs sorted from the respective mice. CD137^{pos} Tregs from anti-CD137 treated mice produced significantly higher levels of soluble CD137 than untreated Tregs (Figure 4.3a). These data indicated that Tregs stimulated by anti-CD137 antibody *in vivo* produced high levels of soluble CD137. As seen before, CD4^{pos}CD25^{neg} T cells from untreated NOD did not produce any soluble CD137 in our *in vitro* conditions (Figure 3.12).

Figure 4.3

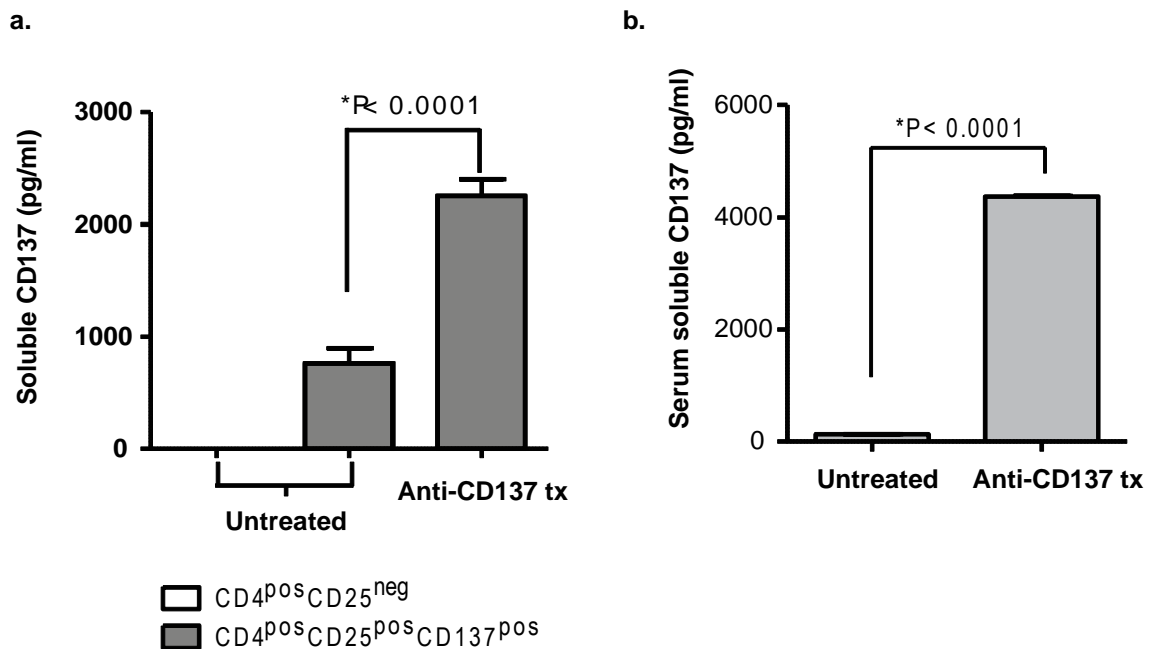


Figure 4.3: Anti-CD137 treatment increases soluble CD137 production and serum soluble CD137.

(a) NOD mice (n=2) were treated with 100 μ g of anti-CD137 antibody or left untreated (n=2). Sorted CD4^{pos}CD25^{neg}CD137^{neg} and CD4^{pos}CD25^{pos}CD137^{pos} T cells were cultured in 96-well U-bottom plate with 25U/ml IL-2 for 5 days. ELISA was performed on their supernatants for soluble CD137 (n=2). (b) NOD mice (n=3) were treated with 100 μ g of anti-CD137 antibody or left untreated (n=8). The mice were sacrificed after 24 hrs and their serum tested for soluble CD137 with ELISA as described in the methods section. Statistical analysis was performed using GraphPad Prism (unpaired t-test.)

Since CD137^{pos} Tregs produce high levels of soluble CD137 *in vitro* after anti-CD137 treatment *in vivo*, we assessed whether anti-CD137 antibody treatment *in vivo* alters the amount of serum soluble CD137. NOD mice were treated with either anti-CD137 antibody or PBS, and serum tested for soluble CD137 levels using ELISA. Anti-CD137 treatment caused a dramatic increase in the amount of soluble CD137 in NOD serum compared to untreated control (Figure 4.3b).

These results show that the increased production of soluble CD137 by CD137^{pos} Tregs could result in increased expression of serum soluble CD137 after anti-CD137 treatment.

4.3.4 Soluble CD137 from CD137^{pos} Tregs suppresses CD4^{pos} T cells through CD137L

The production of soluble CD137 *in vivo* has been associated with decreased T cell proliferation, and increased activated induce cell death and DNA fragmentation [165]. Our lab has previously shown that in untreated NOD mice, CD137^{pos} Tregs are the primary cellular source of soluble CD137 (Figure 3.12). Hence we tested here whether soluble CD137 produced from CD137^{pos} Tregs can suppress CD4^{pos} effector cells in a contact independent manner *in vitro*. We have previously shown that NOD CD137^{pos} Tregs can suppress effector T cells at 1:2 Treg to T effectors ratio in a contact independent transwell system (Figure 2.11). Others have shown that soluble CD137 binds to CD137L *in vitro* [162]. Thus we used a CD137L blocking antibody (TKS1.1) to test if we could block soluble CD137 mediated suppression of CD4^{pos} effector T cells in a transwell assay. To eliminate any confounding effects due to expression of CD137L on splenic macrophages or dendritic cells [249], we used anti-CD3/CD28 coated beads for stimulation instead of APC.

Figure 4.4

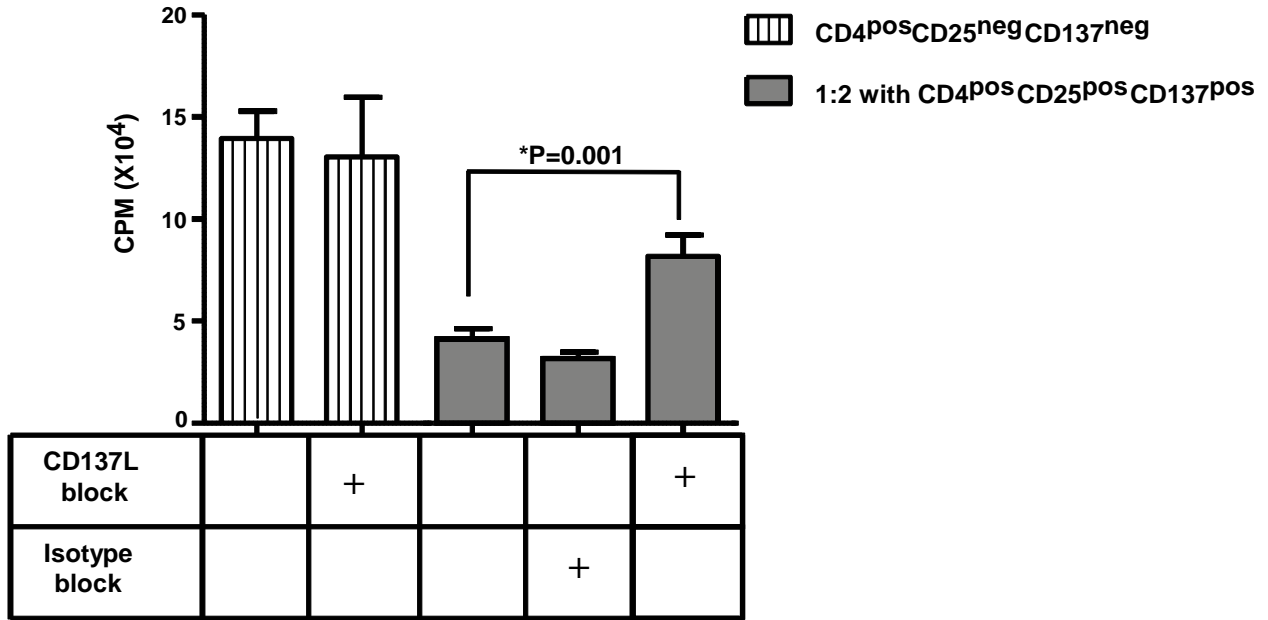


Figure 4.4: Blockade of CD137L decreases transwell, contact independent suppression mediated by CD137^{pos} Tregs.

NOD CD4^{pos}CD25^{neg}CD137^{neg} and CD4^{pos}CD25^{pos}CD137^{pos} T cells were sorted from 5-7 week old NOD mice as above. 100,000 CD4^{pos}CD25^{neg}CD137^{neg} T cells were plated in the bottom of a 96 well transwell plate with 50,000 CD4^{pos}CD25^{pos}CD137^{pos} T cells in the top well. 50,000 CD3/CD28 beads were added to the bottom and to the top of the plate. 20µg/ml of CD137 ligand blocking antibody (n=4 experiments) or IgG2a isotype antibody (n=3 experiments) were added to the bottom wells. The cells were pulsed with 3H labeled thymidine on day 3 and harvested after 16 hours. Statistical analysis was performed using GraphPad (unpaired t-test.)

First we used CD137L blocking on CD4^{pos}CD25^{neg}CD137^{neg} T cells to assess the role, if any, of the anti-CD137L antibody on the proliferation of CD4 T cells. Blockade of CD137L did not alter the proliferation of CD4^{pos}CD25^{neg}CD137^{neg} T cells, suggesting that CD137L blocking antibody does not decrease proliferation (by interrupting any CD137-CD137L interactions between CD4^{pos} effector T cells) (Figure 4.4). However, the presence of CD137L blocking antibody

significantly decreased transwell suppression mediated by CD137^{pos} Tregs (P=0.001), while isotype antibody had no effect on suppression (Figure 4.4). These observations suggested that soluble factors produced by CD137^{pos} Tregs including soluble CD137 suppressed the proliferation of CD4^{pos} effector T cells through CD137L. This conclusion is consistent with our previous observation that CD137^{pos} Tregs produce high levels of soluble CD137 in a contact-dependent APC-independent suppression assay (Figure 3.13).

4.3.5 Soluble CD137-Fc suppresses CD4 T cells *in vitro*

Our previous data suggested that soluble CD137 from CD137^{pos} Tregs directly suppresses CD3/CD28 stimulated CD4^{pos} T effector cells *in vitro*, and does not act simply by passively blocking CD137: CD137L interactions between T cells. To more directly explore the mechanism of soluble CD137-dependent suppression, we used a recombinant mouse CD137-Fc chimeric protein in a Treg-free assay. We cultured CD4^{pos}CD25^{neg}CD137^{neg} T cells with CD3/28 beads in the presence of soluble CD137-Fc (Figure 4.5). The addition of soluble CD137-Fc significantly reduced the proliferation of CD3/CD28 stimulated CD4 T cells (P=0.0001), showing that soluble CD137-Fc protein can directly suppress CD4^{pos}CD25^{neg}CD137^{neg} T cells *in vitro*, consistent with prior results [244].

Figure4.5

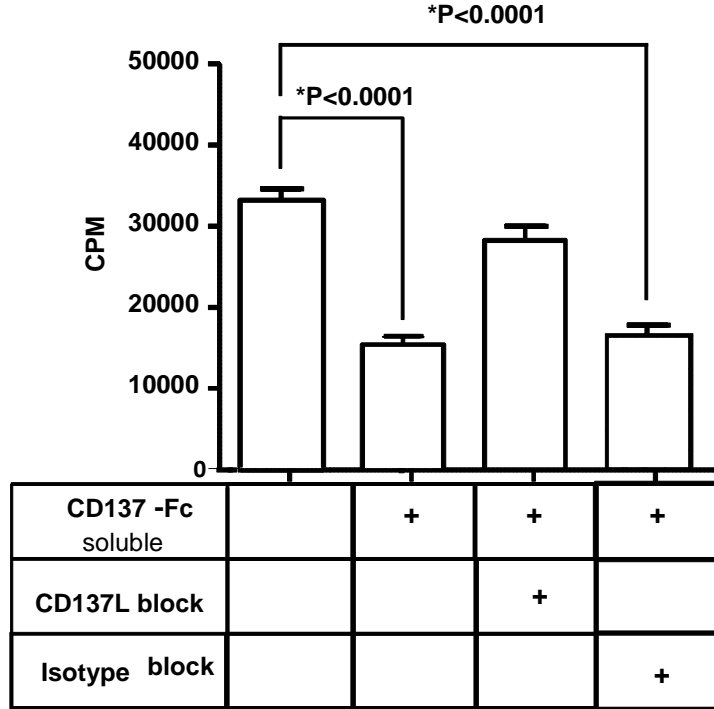


Figure 4.5: Soluble CD137-Fc directly suppresses T cells in an APC and Treg independent manner.

NOD CD4^{pos}CD25^{neg}CD137^{neg} T cells were sorted from 6-9 week old NOD female mice as above. 50,000 CD4^{pos}CD25^{neg}CD137^{neg} T cells were cultured with 20,000 CD3/28 beads and 1 µg/ml of soluble CD137-Fc (n=6) in a 96 well U-bottom well. In the wells containing soluble CD137-Fc, 20 µg/ml of either CD137L blocking antibodies or isotype control antibodies (n=4) were added to the wells as indicated. All cells were plated in triplicates and pulsed with 1 uCi ³H/well on day 3 and harvested after 16 hours. Statistical analysis was performed using GraphPad prism (unpaired t-test).

To test whether soluble CD137 mediated suppression of proliferation is mediated through CD137L, we added CD137L blocking or isotype control antibodies to the culture along with CD137-Fc (Figure 4.5). The addition of CD137L blocking antibody, but not the isotype control,

abrogated the suppression mediated by CD137-Fc, confirming that CD137L is essential for suppression of CD4^{pos} effector T cells by soluble CD137. Our results demonstrate that the interaction of soluble CD137 directly with CD137L negatively regulates CD4^{pos} effector T cells as hypothesized previously [162, 165].

4.3.6 Production of recombinant soluble CD137 *in vitro*

It was possible that the Fc-portion of the soluble CD137-Fc molecule had an effect on its action or mechanism, so we sought to develop a pure form of soluble CD137 as it is expressed *in vivo* to test for suppression and effects on disease *in vivo*. To produce soluble CD137 we first subcloned a soluble CD137 minigene into the lentiviral expression vector, LeGO-iG2 (Figure 4.6a). The LeGO-iG2 vector is bicistronic and has an EGFP reporter gene immediately downstream from the CD137 insert, which allows for co-expression of the two transgenes from the highly active, spleen focus forming viral (SFFV) promoter. The LeGO-iG2 construct is also self-inactivating [250, 251], which allows for the viral production of soluble CD137 protein without contamination from viral particles. VSVg-enveloped LeGO-iG2-sCD137 viral particles were made in separate producer cells and then used to transduce two different eukaryote cell lines, NIH3T3 and HEK293 cells (see methods). Stably transduced cell lines were sorted for medium and high EGFP expression (Figure 4.6b) and the sorted cells were subsequently checked for soluble CD137 production by ELISA.

Figure 4.6

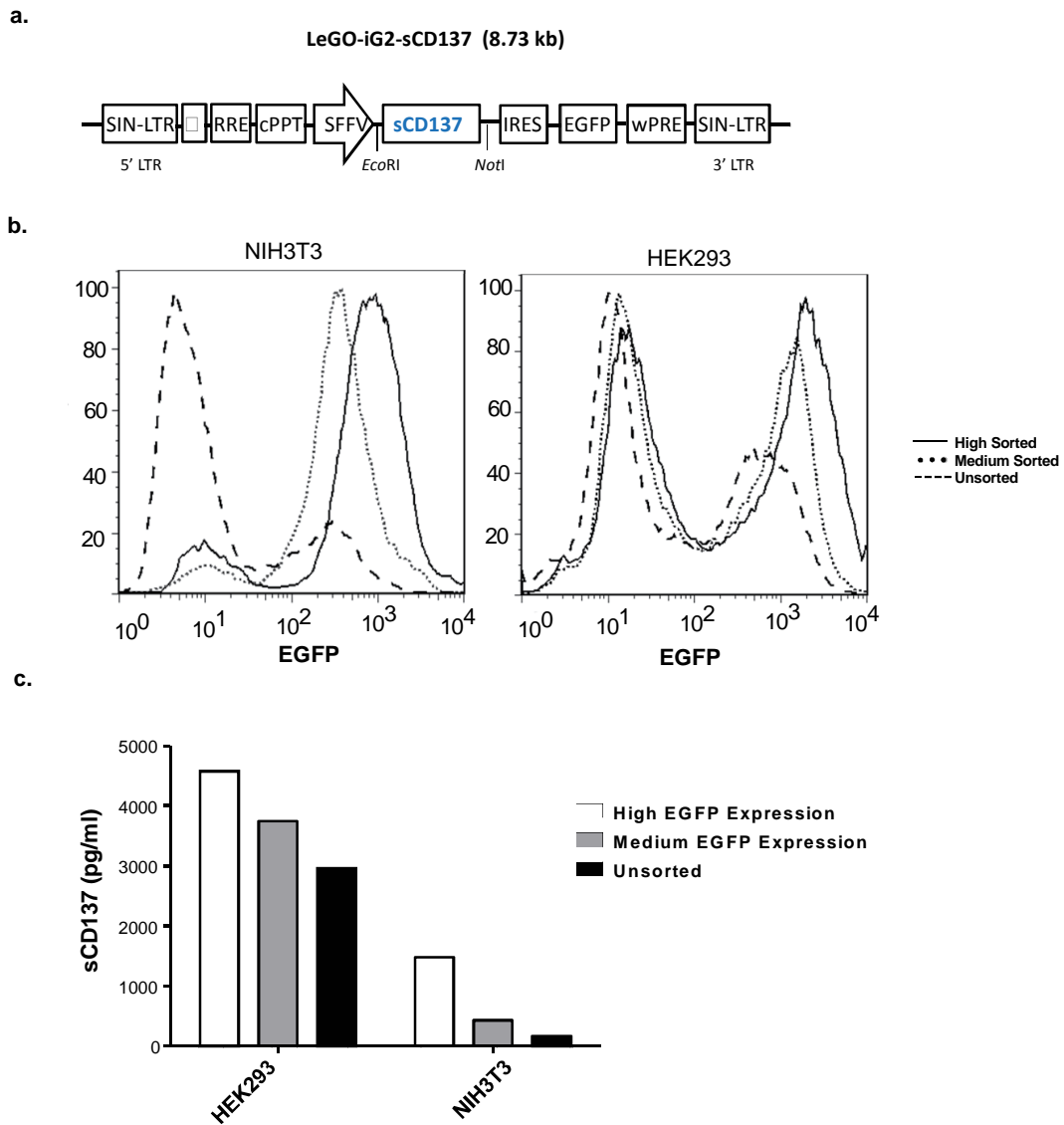


Figure 4.6. Lentivirally-transduced HEK293 cells produce recombinant soluble CD137 protein in vitro.

(a) Schematic of the lentiviral vector, LeGO-iG2-sCD137, used to express soluble protein. The wild type (B10) mouse sCD137 cDNA was inserted between the unique restriction sites *EcoRI* and *NotI*. The soluble CD137 minigene is expressed from the strong SFFV promoter with a downstream EGFP reporter used to mark cells with integrated vector. (b) Transduced 0.5×10^6 NIH3T3 (left) or HEK293 (right) cells were sorted based on medium or high EGFP expression. The transduced cells were initially cultured in

DMEM for three weeks and stable EGFP expression was later assessed by FACs using a FACSCalibur flow cytometer. (c) Mouse NIH3T3 fibroblasts and human embryonic kidney (HEK293) cells were transduced with LeGO-iG2-sCD137 lentiviral particles. The sorted cell lines were checked for soluble CD137 expression by ELISA. One representative example of multiple transductions.

HEK293-EGFP high expressers produced the greatest amount of soluble CD137 protein (Figure 4.6c). Hence we used this cell line for large scale purification and characterization of the soluble protein. Lentivirally-produced soluble CD137 protein, made in either mouse NIH3T3 or human HEK293 cell lines, exhibited similar gel mobility and other physical characteristics (multimeric size, number of glycoprotein isoforms), indicating that the proteins produced from the mouse and human cell lines are comparable to each other (data not shown).

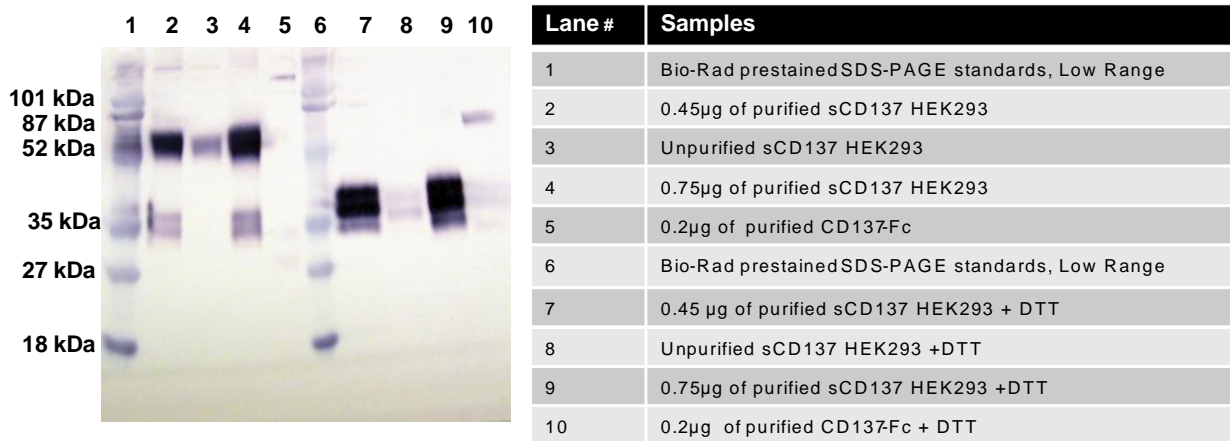
4.3.7 Recombinant Soluble CD137 exists predominantly as a dimer

Next we characterized the structure of the soluble CD137 protein isolated from HEK293 high EGFP producer cells. Western blotting was performed comparing purified and unpurified HEK293-made proteins on an SDS-PAGE-gel under both reducing (with DTT) and non-reducing (without DTT) conditions. Soluble CD137 protein isolated without purification from the medium is mainly a ~55 kDa homodimer under non-reducing conditions and a ~35 kDa monomer under reducing conditions (Figure 4.7a, lane 3 & 8). These observations are consistent with previous studies, which reported that soluble CD137 exists as both a 30kDa monomer and a 55kDa homodimer [162, 252]. Affinity chromatography was used to purify soluble CD137 from the supernatant of the HEK-293 high-EGFP producing cell line (see methods). Since ethylene glycol (EG) and magnesium chloride ($MgCl_2$) help to avoid the degradation or alteration of proteins during disassociation from affinity columns [253], we used these solvents during elution. After elution (under non-reducing buffer conditions), we performed western blot analysis on purified

protein using two different amounts of protein (0.45 μ g and 0.75 μ g). The observed sizes of the purified protein were equivalent to our previous observations with unpurified protein and again yielded a homodimer migrating at ~55kDa and a monomer at ~35kDa (Figure 4.7a, lane 2 & 4), indicating that neither binding nor elution from the affinity column affected the apparent physical structure of the protein.

Figure4.7

a.



b.

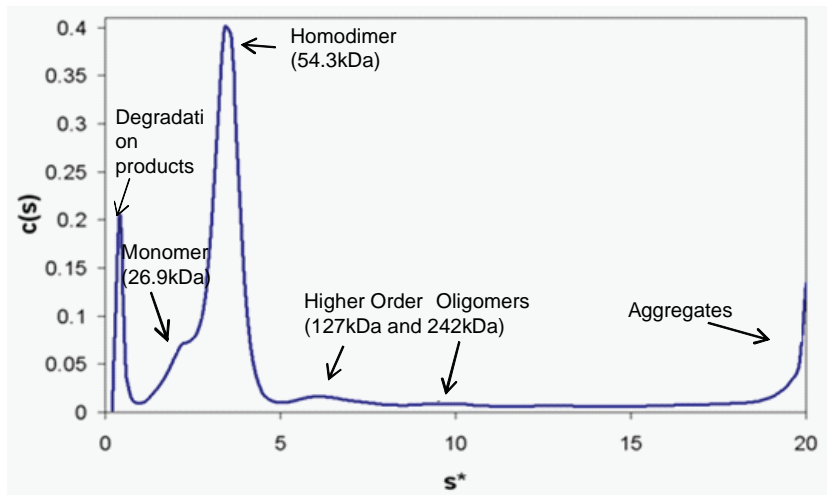


Figure 4.7. Recombinant soluble CD137 protein exists primarily as dimers.

(a) Western blot was performed on purified and unpurified soluble CD137 protein secreted into the media of transduced HEK293 high-EGFP sorted cells and separated on a 12% Tris-Glycine SDS-page gel under non-reducing (-DTT, lanes 1-6) or reducing (+DTT, lanes 7-10) conditions. Purified soluble CD137 of

different concentration (0.45 μ g, 0.75 μ g), or an unpurified aliquot of equal volume was loaded in each lane at 15 μ L per lane. Low molecular weight protein standards served as size markers (lanes 1 and 6). 0.2 μ g of CD137-Fc fusion protein served as an antibody specificity control (lanes 5 and 10). (b) Analytical ultra-centrifugation (AUC) was performed on purified soluble CD137 from HEK293 high-EGFP cells. 1 OD of protein in PBS was used as the starting concentration. 500 μ L of soluble CD137 was separated by AUC for 24 hours. The sCD137 multimers were characterized by sedimentation velocity and their molecular sizes estimated by curve fitting data analysis.

It is important to note that soluble CD137 exists predominantly as a dimer under non-reducing conditions, but as a monomer under reducing conditions, strongly suggesting that the dimer is linked by a disulfide bond (Figure 4.7a, lane 2 & 4 vs. lane 7 & 9). This is in accordance with sequence homology data indicating the existence of homodimerization domains in the CD137 structure (Pubmed – Protein search / NCBI Conserved Protein Domains). Other TNFR family members (e.g. CD27 and CD40) are also known to exist as dimers through intermolecular disulfide bonds [254]. Three distinct monomer bands were also seen on the reduced western blot, suggesting that the purified protein is differentially glycosylated (0, 1, or 2 modifications; Figure 4.7a, lane 7 & 9). This is consistent with the predicted protein sequence that suggests soluble CD137 protein harbors two canonical N-linked glycosylation sites (Pubmed – Protein search / NCBI Conserved Protein Domains). To further confirm the structure of purified protein, we used sedimentation velocity analytical ultra-centrifugation (AUC), the gold standard for analyzing protein structure. Consistent with the western blot results, AUC showed that the bulk of soluble CD137 is present as a 54.3kDa dimer, with a small amount of monomer appearing as a shoulder at 26.9kDa (Figure 4.7b). Interestingly 12% of the total soluble CD137 formed higher order oligomers and/or aggregates at elevated concentrations (Figure 4.7b). There are two possible explanations for this. First at non-physiologically high concentration of the protein we used for AUC, it may interact through non-specific interactions. The other possibility is that

soluble CD137 contains uncharacterized protein-protein association domains which allow for different multimeric forms.

4.3.8 Purified Soluble CD137 suppresses proliferation of CD4 T cells *in vitro*

Having produced a more physiologic soluble CD137 protein, we next tested the ability of our recombinant purified soluble CD137 to suppress T cell proliferation *in vitro*. We cultured CFSE-labeled CD4 T cells with CD3/CD28 beads with or without purified soluble CD137.

Figure 4.8

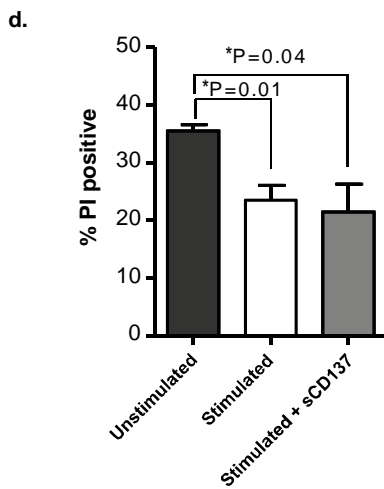
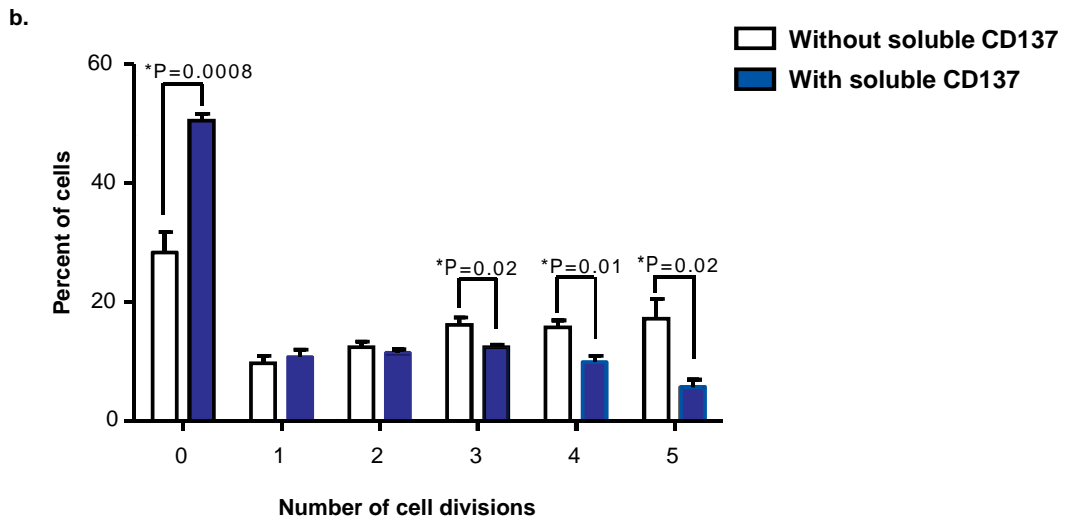
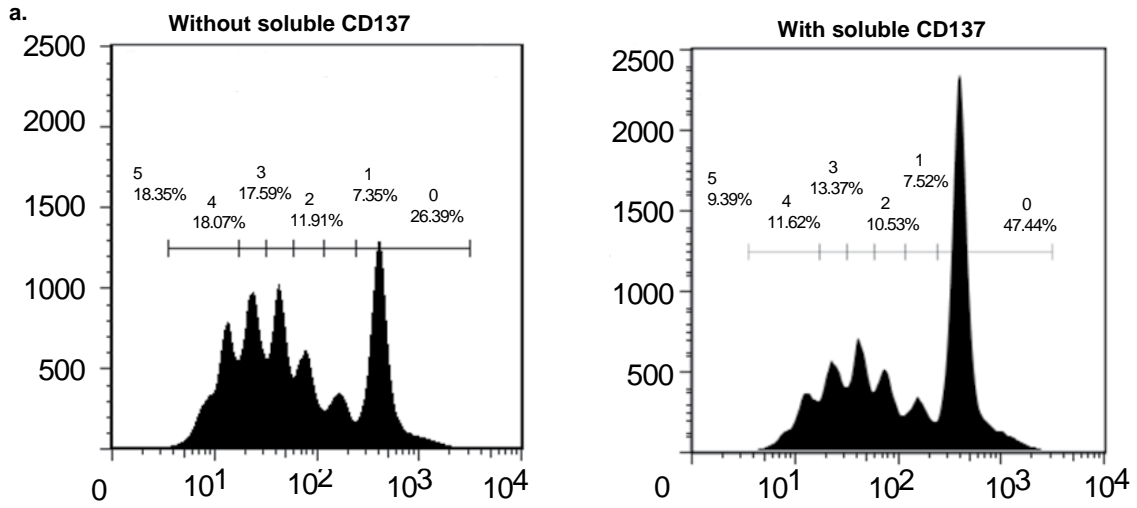


Figure 4.8. Purified soluble CD137 suppresses CD4 T cell proliferation *in vitro*.

(a, b) CD4 T cells were CD4 magnetic bead purified from 6-8 week old NOD mice and labeled with carboxyfluorescein succinimidyl ester (CFSE) *in vitro*. 1×10^5 CD4 T cells, stimulated with 20,000 CD3/CD28 beads, were cultured in a U-bottom 96-well plate for 3 days with or without 15 μ g of purified soluble CD137. After three days in culture, the cells were harvested and stained with CD4. The amount of proliferation was assessed by CFSE FACS. (a) One representative of four independent experiments for CFSE dilution without soluble CD137 (left) and with soluble CD137 (right) are shown. (b) The percent of cells within each cell subset was calculated and graphed as histograms (n=4). (c) The cells were cultured as mentioned before. After three days in culture, the cells were harvested and stained with CD4 (FITC) and amount of cells that were stained with propidium iodide (PI) staining (n=3). Statistical analysis was performed using the GraphPad Prism (unpaired t-test).

Addition of soluble CD137 significantly reduced the CFSE dilution of CD4 T cells, with a reduction in the number of cells entering the later cell cycles and an increased number of cells that did not enter the cell cycle at all (Figure 4.8a, b). The percent of cells dividing multiple times is significantly reduced in the presence of soluble CD137. This is especially evident in the percent of cells in the third, fourth and fifth cell divisions with the addition of soluble CD137 (Figure 4.8b, c). These data show that our purified protein is biologically active and functionally suppressive. We also observed that the culture treated with soluble CD137 did not have increased cell death compared to untreated bead stimulated cells (Figure 4.8c). Hence purified soluble CD137 is functionally suppressive but not physiologically harmful to cells under the conditions examined.

4.3.9 Soluble CD137 reduces the incidence of diabetes in NOD mice

Next we tested if purified recombinant soluble CD137 when injected *in vivo* can prevent diabetes in NOD mice. We treated seven week old female NOD mice with 200 µg of purified soluble CD137 or PBS control, once weekly for four weeks. Urinary glucose was monitored for diabetes. PBS treated NOD mice showed the typical incidence of diabetes by 178 days of age (Figure 4.9a). In contrast, soluble CD137 treated NOD mice showed protection from diabetes (Figure 4.9a). These results convincingly demonstrate that our recombinant soluble CD137 is functional *in vivo* and can prevent the onset of T1D in NOD mice. These *in vivo* results confirm that soluble CD137 can have a positive biological effect *in vivo* to downregulate immunity. Pancreatic histology with Hematoxylin and Eosin staining (H&E) of the control versus soluble CD137 treated mice showed that soluble CD137 treatment did not completely eliminate recruitment of pathogenic cells to the islets but reduced the number of islet infiltrates, suggesting a regulatory effect of soluble CD137 (Figure 4.9b). Blinded scoring of the pancreatic sections for histological insulinitis confirmed that soluble CD137 treatment reduced insulinitis in pancreatic islets (Figure 9c).

Figure 4.9

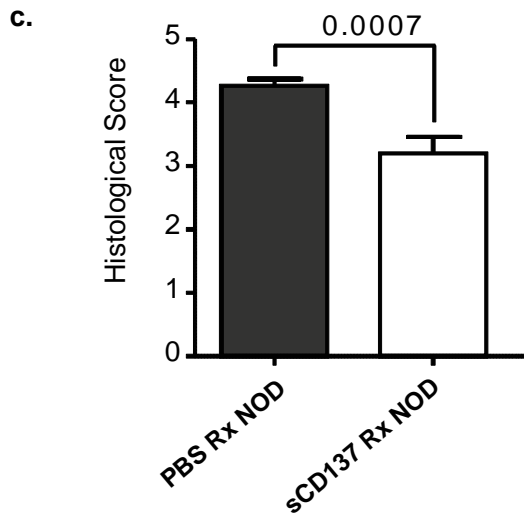
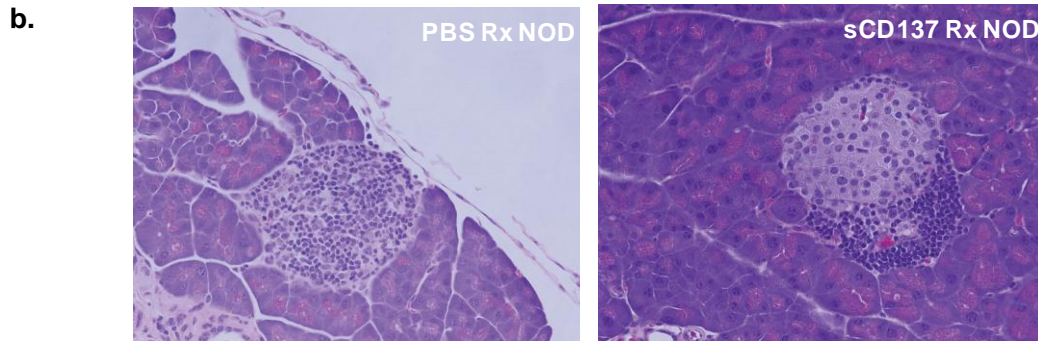
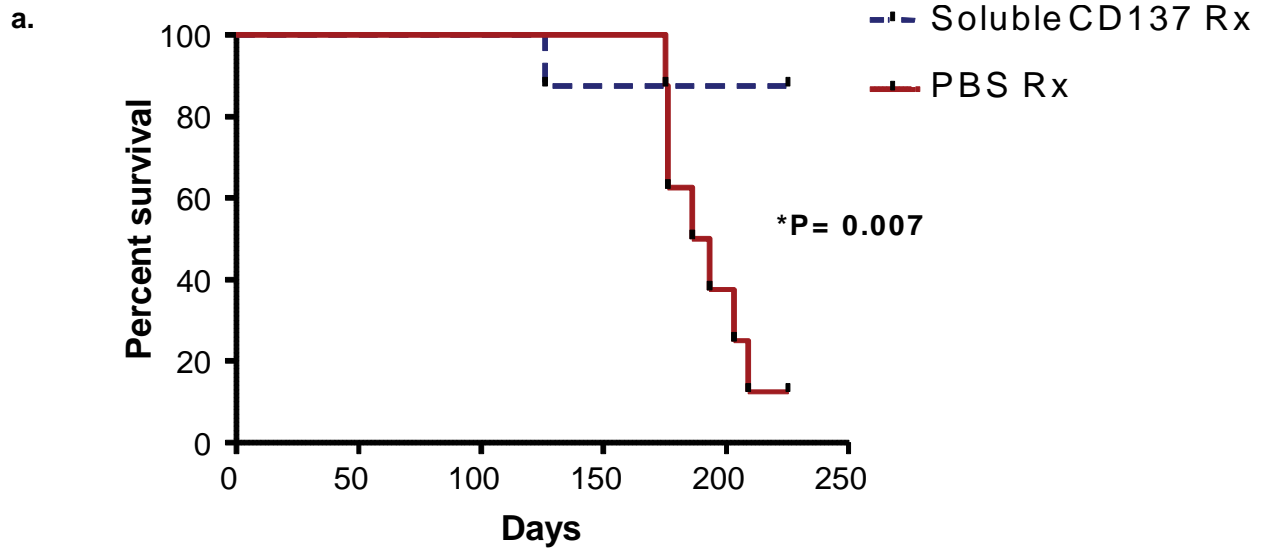


Figure 4.9. Purified soluble CD137 prevents diabetes *in vivo* and reduces pancreatic islet infiltration.

a) Seven week old female NOD mice were treated with either PBS or with 200 µg of soluble CD137, once a week for four weeks (n=8 per group). The blood glucose level of the treated animals was tested for diabetes over time. H&E staining of the pancreas from treated vs. control mice. b, c) NOD female mice 4-6 weeks old were treated once a week for four weeks with either PBS (n=9), 200ug of soluble CD137 (n=7). Incidence of diabetes was measured once a week using urine glucose levels tested by tes-tape (Japan). After 225 days or at the first onset of disease the mouse was sacrificed. The pancreas was removed and stained using hematoxylin and eosin (H&E). b) One representative pancreatic section for PBS treated NOD and soluble CD137 treated NOD under 40x magnification. c) The slides were blindly scored as mentioned in the methods section and graphed as histograms. The P value was calculated using the logrank statistic (a) or unpaired t-test (c) in GraphPad Prism.

In summary, we have established that CD4^{pos}CD25^{pos} T cells are essential for anti-CD137 antibody mediated diabetes protection and that the Tregs treated with anti-CD137 produce high levels of soluble CD137 *in vitro* and *in vivo*. We have also shown that purified soluble CD137 is functionally suppressive to CD4 T cells *in vitro*. Recombinant purified soluble CD137 prevented the development of diabetes and significantly reduced the number of islet infiltrates in NOD mice. The data presented here strongly supports a role for soluble CD137 in both anti-CD137 antibody mediated diabetes protection and antibody-independent diabetes protection in NOD mice.

4.4 DISCUSSION

Our previous studies in chapter 2 showed that anti-CD137 antibody treatment increased the number of CD4^{pos}CD25^{pos} T cells in NOD mice and that anti-CD137 antibodies bound specifically to a subset of CD4^{pos}CD25^{pos} Tregs *in vivo* while preventing diabetes. The anti-CD137 treated CD4^{pos}CD25^{pos} T regulatory cells were also protective against diabetes in adoptive cell transfer experiments (Figure 2.6). Here we have confirmed that CD4^{pos}CD25^{pos} T cells are essential for anti-CD137 mediated diabetes prevention since elimination of CD4^{pos}CD25^{pos} T cells by anti-CD25 antibody before anti-CD137 treatment abrogates disease protection (Figure 4.1). We conclude therefore that anti-CD137 antibody mediated diabetes protection via these CD4^{pos}CD25^{pos}CD137^{pos} T cells (i.e., anti-CD137 antibody-bound CD4^{pos}CD25^{pos} T cells).

The pro-survival members of the TNFR family such as CD137 are known to signal through a set of signaling adapter proteins known as TRAFs [255]. Upon receptor ligation, the TRAF1 and TRAF2 molecules are recruited to the TRAF-binding motifs in the cytoplasmic tails of CD137 [255]. The association of TRAF2, in particular, with the cell membrane (insoluble fraction) in anti-CD137 treated CD137^{pos} Tregs confirmed that the antibody signals intracellularly through CD137 (Figure 4.2a). Importantly, TRAF2 was not found to be redistributed in CD4 T cells, which did not contain CD137 on their cell surface (Figure 4.2a). These observations are consistent with the previous observation that CD137 co-stimulation promotes the survival of T cells by signaling through TRAF1 and TRAF2 with the eventual phosphorylation and activation

of NF-KB and AP-1 [10, 179, 256]. Previous studies have shown that CD137 costimulation led to upregulation of pro-survival molecule Bcl-xl, which promoted the expression of several survival and effector genes in T cells [10, 145]. Overall, our findings confirmed and supported the idea that anti-CD137 antibody treatment specially targeted CD137 expressing CD4^{pos}CD25^{pos} Tregs and resulted in a downstream signaling cascade arising from CD137 signaling.

Cultured CD137^{pos} Tregs produced significantly higher levels of soluble CD137 from anti-CD137 treated mice compared to untreated mice (Figure 4.3a). It is possible that CD137^{pos} Tregs from the treated mice proliferate to a greater extent than the untreated mice and hence produce higher levels of soluble CD137, although we have not tested that possibility here. Previously, we showed that CD137^{pos} Tregs from untreated mice proliferated upon IL-2 culture *in vitro* (Figure 3.12). Importantly, we also observed that soluble CD137 increased significantly in the serum of NOD mice after anti-CD137 treatment (Figure 4.3b). Previously, we showed that anti-CD137 antibody treatment increased the frequency of CD4^{pos}CD25^{pos} Tregs *in vivo* (Figure 2.3). Hence the observed increased serum soluble CD137 after treatment could result from both the increase in Tregs and the increased production of soluble CD137 from these same CD137^{pos} Tregs after treatment. The increased levels of detected soluble CD137 *in vivo* after antibody treatment could also result from accumulation of soluble CD137 and anti-CD137 antibody complexes, which would be expected to stabilize the soluble CD137 protein. However, the increased soluble CD137 production by CD137^{pos} Tregs after antibody treatment *in vitro* suggested that the increase in serum soluble CD137 is not due wholly to an increase in the half-life of soluble CD137. It is also possible that other cell types express soluble CD137 following antibody treatment but we have not explored that possibility here. Elevated soluble CD137 serum levels have also been seen in other autoimmune disease models [241, 257]. The increased production of soluble CD137 may be a common response following over-activation of

the immune system in such cases and may be an essential mechanism for the protective effect seen anti-CD137 antibody treatment.

To investigate a possible role for soluble CD137 in diabetes protection, we first tested its functions *in vitro*. Previously we have seen that NOD CD137^{pos} Tregs suppressed T cell proliferation *in vitro* in a contact independent system (Figure 2.11). Transwell CD137L blockade experiments described here showed that CD137^{pos} Tregs suppressed CD4 effector T cell proliferation in a contact independent manner, likely through secretion of soluble CD137 (Figure 4.3). Notably, CD137L blockade alone had no effect on the proliferation of CD4^{pos}CD25^{neg}CD137^{neg} T cells, suggesting that the suppressive signal does not arise from competition for CD137L binding (Figure 4.4) (i.e. that the effect is not simply a passive effect of soluble CD137 blocking the CD137L receptor). Indeed soluble CD137 has been shown previously to bind to CD137L *in vitro* [162]. The protein expression of CD137L in CD4 T cells by FACS was very low, (data not shown), similar to the results published by another group [168]. Despite these negative observations, it is clear that soluble CD137, in our *in vitro* culture conditions, actively suppressed the proliferation of CD4^{pos}CD25^{neg}CD137^{neg} T cells and does not simply act by passively blocking interactions between membrane-bound CD137 and CD137L molecules expressed on separate, but otherwise similar, T cells. We also showed that soluble CD137-Fc fusion protein resulted in suppression through CD137L on CD4 effector T cells, further confirming the effect of soluble CD137 on suppression of CD4 T cells (Figure 4.5).

To test directly the hypothesis that soluble CD137 can act in an endocrine-type manner, we set up an *in vitro* system for the production and purification of soluble CD137. Analysis of our recombinant protein showed that soluble CD137 is primarily a 54.3kDa dimer, with a smaller

fraction existing as 26.9kDa monomer. The dimeric form of soluble CD137 is likely linked by an intermolecular disulfide bond, which can be reduced to monomer protein in the presence of DTT. Our results are consistent with previous findings indicating that soluble CD137 exists as both homodimers and monomers [162, 252]. They also agree with *in silico* sequence analysis of the soluble CD137 protein (Pubmed – Protein search / NCBI Conserved Protein Domains). Analytical ultra-centrifugation also showed that less than 12% of the purified soluble CD137 protein forms higher-order multimeric forms, which is consistent with another report which has also shown multimeric forms of soluble CD137 [162]. Thus, we produced, purified and characterized for the first time, to our knowledge, a recombinant soluble CD137 protein, which can be used for functionally studies both *in vitro* and *in vivo*.

More importantly, we found that the purified soluble CD137 protein is functionally suppressive *in vitro* during T cell proliferation experiments (Figure 4.8). The purified soluble CD137 protein reduced the number of T cells entering cell division in purified CD4 T cells *in vitro* using a CFSE dilution assay (Figure 4.8a) but did not increase cell death (Figure 4.8b). It is possible that soluble CD137 induces cell cycle arrest or anergy in activated CD4 T cells, although we have not studied that here. Our new results supported our previous observations that blockade of CD137L abrogated the suppression of CD4 T cells (most likely) due to the secreted soluble CD137 produced by Tregs (Figure 4.3). We also tested and verified that our soluble CD137 is non-toxic to T cells and that it does not cause cell death (Figure 4.8b). It has been shown previously that expression of soluble CD137 correlates with T cell suppression and cell death and that soluble CD137 arises late in the immune response to prevent excessive immune activation [165]. Our present results confirmed CD4 T cell suppression but did not show increased cell death as observed before. However our results are consistent with our previous observations that indicated that soluble CD137-Fc is suppressive to CD4 T cells *in vitro* (Figure

4.6) and also matches another observation from another group that showed suppression with soluble CD137-Fc [244].

As suggested previously, soluble CD137 suppression was found to be mediated through CD137L. Like other members of TNF ligand super family, CD137L also mediates “reverse” signaling and causes activation of APCs (macrophages, B cells, monocytes) [249, 258, 259]. However its role in T cells is not well established. The question as to how soluble CD137 inhibited proliferation is interesting. Prior studies have shown that soluble CD137-Fc does not induce activation of monocytes, B cells and DC through CD137L [249, 260, 261]. In these studies, CD137L cross-linking with immobilized CD137-Fc was essential for activation of APC. Similarly, cross-linking at least two trimeric CD137L was required to elicit significant costimulatory activity [262]. The three dimensional molecular modeling of CD137L showed that a single extracellular cysteine residue in the tail (Cys-51) could form a disulfide bond under physiological condition and that cross-linking CD137L *in vitro* formed dimers of trimers [262, 263]. By contrast, we hypothesized that soluble CD137 (predominantly dimers) binds to CD137L on T cells without cross-linking it, and thus initiates inhibitory signals, consistent with our results. Other well-known immune signaling molecules differ in their stimulatory effects according to whether they are plate bound or soluble—the most notable being anti-CD3 antibody, which can stimulate Treg-mediated suppression in soluble form but not when plate bound. Similarly, soluble CD137L cannot induce proliferation in CD3 stimulated T cells, while cross-linked CD137L can stimulate these cells [262]. These studies indicated that in the absence of cross-linking, an inhibitory signal can be generated by soluble CD137, but further biochemical studies will be needed to verify this hypothesis.

Most significantly of all, we found that soluble CD137 treatment significantly reduced the incidence of diabetes in NOD mice, indicating that our purified protein is functional and immunosuppressive *in vivo* (Figure 4.10a). The histology from the soluble CD137 treated mice

suggested that the pathogenic NOD immune cells are not completely deleted, but their entry into the islet is regulated (Figure 4.1b, c). Since anti-CD137 treatment increased serum soluble CD137 (Figure 4.4b), the antibody-mediated diabetes protection likely acts at least partly through the same pathway, that is, through the production and suppressive function of soluble CD137. Since anti-CD137 treatment increased the fraction of Tregs in NOD (Figure 2.3), it is possible that the diabetes protection is rendered by other mechanisms of Treg suppression, along with soluble CD137. Our results strongly suggested that after injection, anti-CD137 antibody targeted Tregs *in vivo*, which initiated an internal signaling event that caused an increase in TRAF2 in the Treg cells. These cells could then produce higher levels of soluble CD137. The increase in secreted soluble CD137 after treatment caused an increase in total suppressive capacity against pathogenic effector cells. This downregulation of autoimmune activation is likely sufficient to prevent the further progression of diabetes. Treatment with anti-CD137 antibody also likely activated a positive feedback loop that increases the expression of soluble CD137. This, in-turn, may be important for suppressing pathogenic effector cells during diabetes progression. Since CD137L blocking antibody alone *in vitro* did not affect the proliferation of CD4 T cells (in an APC-free assay), indirect suppression through CD137-CD137L blockade between T cells does not appear to play as much of a role as direct suppressive effect of soluble CD137 via CD137L. However we do not know whether there would be an effect of CD137L blockade in an *in vitro* system containing APC. Furthermore, in an *in vivo* situation, soluble CD137 can bind to both CD137L expressing APC and activated T cells and further prevent CD137 costimulation of pathogenic cells. Thus soluble CD137 may suppress pathogenic T cells *in vivo* by directly initiating negative signaling through CD137L or by blocking T:APC CD137-CD137L interactions or both. The production and secretion of soluble CD137 by T regulatory cells appears to be a novel mechanism by which they can suppress, and more importantly, immunoregulate pathogenic effector cells, to avert the incidence of diabetes.

Our experiments with soluble CD137 have opened new opportunities for the development of potent immunosuppressive therapies that make use of soluble immune molecules, which are implicated in the pathology of various autoimmune diseases. While we do not yet fully understand the mechanisms by which soluble CD137 exerts its immunosuppressive effects, and we have only begun to explore its possible uses in systemic and site specific immunotherapy, it serves as a compelling candidate and prototype for further investigation. The adaptation and use of naturally-occurring, soluble isoforms of immune signaling molecules for the purpose of immunosuppression, is a promising alternative to current immunosuppressive therapies, which utilize artificial or man-made molecules, which can have unintended and/or uncontrolled side effects.

4.5 Acknowledgements

We are very grateful to Dr. Andrew Herr and Dr. Michael Jordan for providing us with equipment and guiding us for soluble CD137 purification and characterization.

5. SUMMARY & SIGNIFICANCE

5.1 Proposed models

5.1.1 Proposed model for soluble CD137 function and B10 *Idd9.3* protection

We have shown that while CD137^{pos} and CD137^{neg} Tregs expressed equal levels of Foxp3, CD137^{pos} Tregs are functionally superior to CD137^{neg} Tregs *in vitro*. The functional superiority of CD137^{pos} Tregs is associated with diabetes protection in NOD.B10 *Idd9.3* mice that accumulate significantly increased numbers of CD137^{pos} Tregs with age compared to NOD mice. The functional superiority of CD137^{pos} Tregs is not explained by effects of IL-10 or TGF- β expression. Rather, we showed that CD137^{pos} Tregs are the primary cellular source of high levels of soluble CD137 *ex vivo* and *in vitro*. Further studies showed that CD137L blockade decreased the suppression mediated by CD137^{pos} Tregs in a contact-independent APC-free assay, indicating that soluble CD137 produced by CD137^{pos} Tregs could suppress through interaction with CD137L. Soluble CD137-Fc chimeric protein and recombinant soluble CD137 suppressed CD4 T cells *in vitro*, via interaction with CD137L (in a Treg-free, APC-free assay), directly proving a role of soluble CD137 in T cell regulation. The potential importance of soluble CD137 in diabetes was indicated by increased levels of serum soluble CD137 in NOD.B10 *Idd9.3* congenic compared to NOD mice, likely explained by our finding of increased accumulation of CD137^{pos} Tregs in NOD.B10 *Idd9.3* compared to NOD mice. We directly showed a possible effect of soluble CD137 on diabetes by treating NOD mice with recombinant

soluble CD137, which prevented disease. Thus the long-term accumulation of peripheral B10 *Idd9.3* expressing CD137^{pos} Tregs and increased production of soluble CD137 may both play a critical role in disease protection in NOD.B10 *Idd9.3* congenic mice. In addition, the disease protection afforded by anti-CD137 antibody treatment is also associated with increased soluble CD137. All of these lines of evidence point to a key role for the subset of CD137^{pos} Tregs in immune regulation, as well as for a critical role for soluble CD137 in regulating the effector T cell response. Both factors may play a role in diabetes pathogenesis and explain the protective effect of the B10 *Idd9.3* allele against Type one diabetes.

The mechanism for soluble CD137 mediated suppression is not yet known in detail. We showed that recombinant soluble CD137 directly suppressed proliferation of CD4^{pos} effector T cells. It has been shown that soluble CD137 binds to CD137L *in vitro* [162]. It is conceivable that soluble CD137 simply blocked the interaction between membrane bound CD137 and CD137L, thus preventing T cell costimulation. However, we showed that soluble CD137 downregulates T cell proliferation directly in an APC-free setting. Moreover, this soluble CD137-mediated downregulation is unlikely to be due to interrupting T:T CD137:CD137L interaction, because in our APC-free system, adding CD137L blocking antibody did not affect anti-CD3/CD28 mediated proliferation of CD4 T cells. However in the presence of APC *in vivo*, soluble CD137 may block CD137-CD137L costimulation and thereby also indirectly downregulate pathogenic T cell activation although we have not tested that here.

Figure 5.1

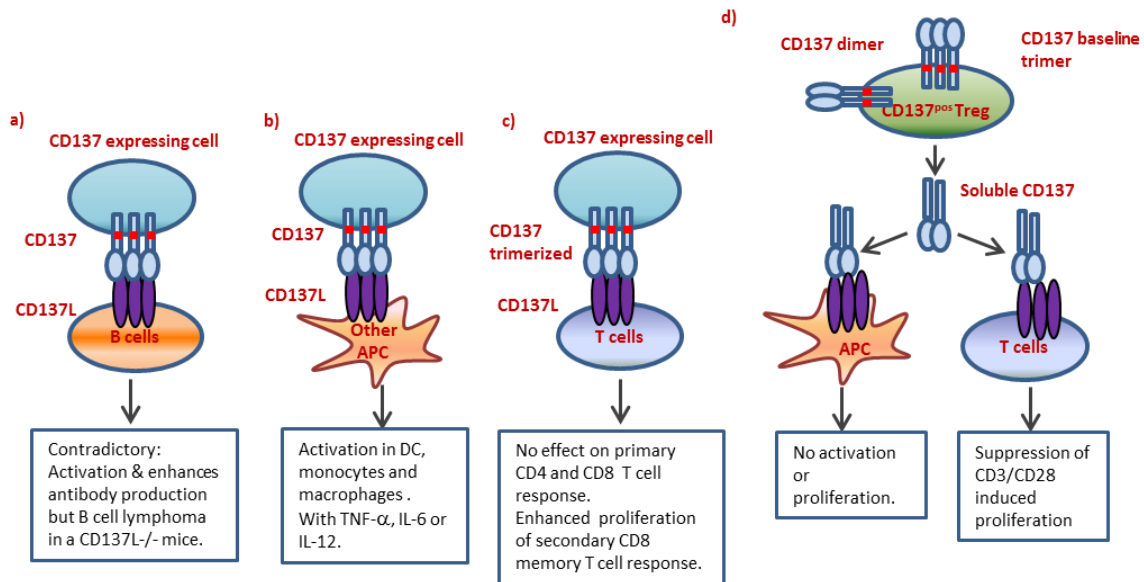


Figure 5.1: Model for differences in CD137-CD137L bi-directional signaling.

a) CD137L signaling in B cells has produced activation and enhanced antibody production, but CD137L knockout mice can develop B cell lymphoma (i.e. unregulated proliferation) . b) CD137L signaling in APCs (monocytes, dendritic cells & macrophages) has produced maturation, activation and differentiation with IL-12 and TNF- α production. c) CD137L signaling is required for maintenance and proliferation of CD8 T cells after secondary response but has no known effect on CD4 T cell primary and secondary response d) Soluble CD137 produced by CD137^{pos} Tregs binds to CD137L on APC without trimerization and does not induce activation or proliferation. Soluble CD137 interaction with CD137L on T cells suppressed proliferation and prevented diabetes in NOD mice.

Understanding the effects of soluble CD137 requires an appreciation that the CD137:CD137L system shows bi-directional signaling, as seen in other members of the TNF and TNFR family. Hence while we showed that direct stimulation of CD137 via an agonist antibody prevents diabetes by mediating signaling in the TRAF2 pathway in CD137^{pos} Tregs (Chapters 2 and 4), the effect of soluble CD137 (produced after CD137 stimulation on Tregs) is mediated via CD137L. Moreover, while we investigated the effect of soluble CD137 on T cell activation, the

effect could be different on other cell types, and in fact the literature is contradictory in this regard. Previous studies showed various effects of CD137L signaling on various cell types. CD137L stimulation on B cells showed contradictory results as indicated in Figure 5.1a. Crosslinking of CD137L in activated B cells by plate bound rCD137 protein produced enhanced proliferation and Ig secretion [261]. However overexpression of CD137L caused B cell deficiency in mice after 3 weeks of age and could be due to prolonged suppression of growth signals [47]. Similarly, CD137 ligand signaling is essential to suppress B cell lymphoma development indicating negative regulation via CD137L on B cells [264]. Supporting this, microarray analysis showed that lack of CD137L in B cells causes overexpression of molecules associated with cell growth (Stat-1, Elf-1, CIITA, AID, Bcl-10 and Rad21) and plasma cell differentiation (Bach-2, Spi-B and Bcl-6) [264].

In dendritic cells, CD137L signaling induced IL-12 production, maturation, activation and differentiation [176, 258]. The expression of CD137L on a macrophage cell line produced increased expression of ICAM-1, TNF, MCP-1, IL-6, IL-1b, IL-1R antagonist and M-CSF resulting in increased survival [260]. Another study showed that CD137L signaling induced the expression of IL-6, IL-8, and TNF- α and resulted in monocyte activation [249]. These studies showed that CD137L signaling in dendritic cells, macrophages and monocytes is stimulatory resulting in activation and effector function (Figure 5.1b). However, most of these studies used plate bound CD137, which could have very different effects than soluble CD137. In particular, plate bound CD137 might be better able to cross link CD137L, and cannot result in receptor internalization (compared to soluble CD137).

The effect of CD137L reverse signaling in T cells has mostly been studied in viral infection. Absence of CD137L had no obvious effect on the primary CD8 T cell response but reduced secondary CD8 T response during viral infection, with no effect on CD4 T cells [172, 173].

CD137L signaling is important in the maintenance of CD8 T cell after viral clearance but not for initial priming or programming of memory [169, 171]. CD137L knockout on transgenic OTII CD4 T cells has a minor effect on primary response and no effect in secondary response [174]. These studies showed that CD137L signaling in CD4 and CD8 T cells has different effects during viral infection and that CD137L reverse signaling is important for secondary memory CD8 T cell response (Figure 5.1c).

The proliferative effect of membrane bound or plate bound CD137 signaling on different cell types differed from our observation that showed a suppressive effect of soluble CD137 on CD4 T cells. This disparity of CD137L signaling could be due to the differences in membrane bound versus soluble form of CD137 receptor. The question as to how a soluble form of a molecule can be biologically different from a fixed (membrane or plate bound CD137) form is interesting. It is not known if soluble CD137 versus membrane-bound CD137 bind to CD137L with variable affinity and subsequently elicit differential signaling. Membrane bound and soluble form of CD30, another member of TNF receptor superfamily, bind to its ligand, CD153 with different affinity [265]. Hence it is possible that membrane and soluble CD137 binds to the ligand with different affinity which could affect ligand signaling as also seen in the Epidermal Growth Factor Receptor (EGFR) [266]. Site-directed mutagenesis of human CD137L to map the receptor binding sites of the CD137-CD137L trimer showed that mutation of residues Lys127 and Gln227 to alanine caused 170 and 80 fold decrease in binding affinity, respectively [267]. The authors predicted that since these mutations are on exposed sites of CD137L, they can have a direct effect on receptor binding. Similarly the absence of exon 8 in soluble CD137 could alter the binding affinity with CD137L compared to full-length CD137 or even destabilize the trimer structure. Upon receptor binding, the cytoplasmic domains of the CD137 ligand become fixed in a specific conformation, resulting in recruitment of adaptor proteins and molecules for downstream signaling. The affinity of the binding will thus affect the structure of the ligand and

affect downstream signaling. Similar observations have been made in a study where different IFN variants signal through the same cell surface receptors, IFNAR1 and IFNAR2 but cause different physiological effects based on their binding affinities and receptor recognition chemistries [268]. Although the binding affinity of soluble versus full-length CD137 has not been studied yet, it is essential to recognize that exon deletion could impact the signaling response.

This disparity of CD137L signaling in APC versus T cells could result from the effect of CD137L cross-linking on signaling. Prior studies have shown that cross-linking of CD137L with immobilized CD137 (membrane or plate bound CD137) is essential for monocyte, B cell and DC survival/activation [249, 260, 261] and that soluble CD137 is not sufficient to induce activation of APC (Figure 5.1d). Cross-linking CD137L with immobilized CD137 is essential for activation signaling in APC [263]. As with other members of TNF superfamily, surface CD137L likely aggregates to form trimers [269, 270]. It has been shown that human CD137L exists as homotrimers [262, 267]. In other TNF-TNFR complexes, a trimeric form of the ligand binds to a trimeric form of the receptor [270-272]. Similarly, CD137-CD137L may also bind with this stoichiometry although it has not been confirmed by a crystal structure of the CD137-CD137L complex. A study has shown that the trimeric form of CD137L only costimulates via CD137 when cross-linked [262]. Since we show in Chapter four that soluble CD137 is predominantly dimeric, it might not be able to cross-link CD137L as do trimers of two membrane-bound CD137 molecules, and therefore could signal differently. Treating macrophages with soluble CD137-Fc does not induce TNF production, suggesting that soluble CD137 cannot cross-link CD137L, and furthermore soluble CD137-Fc could only mediate TNF production when anti-Fc was added (thus allowing crosslinking) [259]. Since soluble CD137 exists predominantly as dimers, it could bind differently to CD137L on T cells, and thus could send inhibitory signals, consistent with our T cell proliferation results (Figure 4.1d). Other well-known immune signaling molecules differ in their effect according to whether they are plate bound or soluble—the most notable anti-CD3

antibody, which can stimulate Treg mediated suppression in soluble form but not when plate bound. Similarly, soluble CD137L cannot induce proliferation in CD3 stimulated T cells, while cross-linked CD137L can stimulate these cells [262]. Cross-linking is essential to its T cell co-stimulation activity. The absence of cross-linking may explain the inhibitory signaling observed with soluble CD137, compared to membrane bound CD137. These studies indicate the variation and complexity of CD137L signaling in various cell types and different state of the receptor and further biochemical studies of soluble CD137 will be needed to verify this hypothesis.

5.1.2 Proposed model for anti-CD137 mediated NOD diabetes protection

Immune modulation by agonist CD137 antibody previously showed diverse effect on various diseases; on viral clearance [273], tumor regression [274, 275] and prevention of asthma [276] and autoimmunity [137, 180, 277, 278]. Based on the disease model, the immune response to anti-CD137 antibody has also shown contradictory results. For example, anti-CD137 treatment increased IFN- γ production by CD8 T cells in autoimmune uveoretinitis [277], allergic asthma [276], experimental autoimmune encephalomyelitis (EAE) mouse models [278] but reduced IFN- γ production in autoimmune diabetes in NOD mice [137]. It is unclear how stimulation through CD137 can trigger enhanced immune responses to viruses and tumors but at the same time suppress autoimmune responses. It is possible that the immune microenvironment and the proportion of activated T cells, APCs, or T regulatory cells play a crucial role in such differences. Since the effect of anti-CD137 antibody is broad depending on the disease model, we have focused on the effect of anti-CD137 antibody on autoimmunity.

Studies have shown that anti-CD137 treatment inhibits autoimmunity by various mechanisms. Initial studies with anti-CD137 treatment in the EAE model showed that it increased IFN- γ production, promoted initial proliferation of antigen specific CD4 T cell and ultimately caused

activation induced cell death, nine days after immunization [148]. In collagen type II–induced arthritis (CIA) anti-CD137 treatment suppressed CD4 T cell recall response to antigen and caused expansion of CD11c+CD8+ cells which produced IFN- γ and subsequently induced production of indoleamine 2,3-dioxygenase (IDO) in macrophages and DCs [180]. IDO is known to suppress adaptive T-cell immunity by catabolizing the essential amino acid tryptophan from the cellular microenvironment and by inhibiting IL-2 expression [279, 280]. Another study of anti-CD137 treatment on experimental autoimmune uveoretinitis (EAU) model, consistent with the CIA model, also showed that antibody treatment expanded CD11c+CD8+ T cells that produced IFN- γ , which increased the levels of IDO in CD11c+ dendritic cells and decreased the proliferation and absolute number of CD4 T cells by inducing CD4 T cell death. [277]. These studies have associated anti-CD137 mediated inhibition of autoimmunity to CD8 T cell mediated IFN- γ production which leads to production of IDO by DC and macrophages that suppresses CD4 T cells proliferation (Figure 5.2a). As shown in Figure 5.2b CD137-primed CD8 T cells suppressed CD4 T cells in a TGF- β dependent manner [281, 282]

Figure 5.2

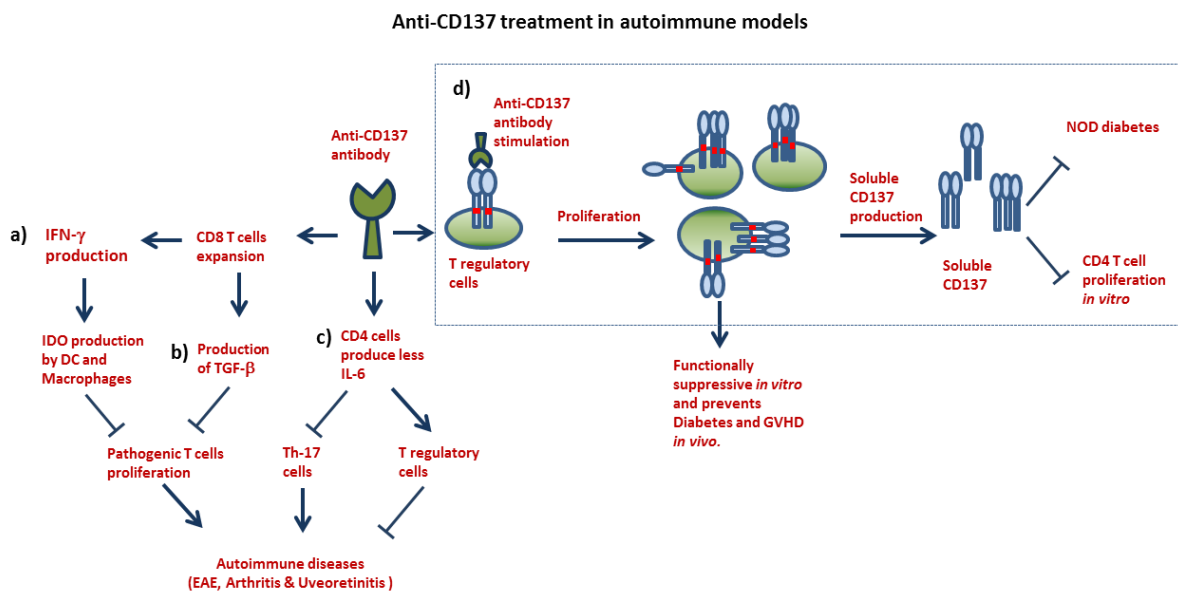


Figure 5.2: Model for mechanism of autoimmunity prevention by anti-CD137 antibodies.

The mechanism applicable to anti-CD137 mediated diabetes prevention is shown within the boxed area.

a) In NOD mice, the anti-CD137 antibodies bind to CD4^{pos}CD25^{pos}CD137^{pos} Tregs and increase their number. These CD4^{pos}CD25^{pos} Tregs from anti-CD137 treated mice can act directly on effector cells to prevent diabetes in NOD (and Graft Versus Host Disease (GVHD)). The expanded Treg population produces high levels of soluble CD137 that downregulates CD4 T cell proliferation *in vitro* and contributes to decreased diabetes in NOD mice. b) In other autoimmune models, anti-CD137 treatment has been shown to expand CD8 T cells that produce IFN- γ which induces the production of indoleamine 2,3-dioxygenase (IDO) from DC and macrophages. The production of IDO suppresses pathogenic CD4 T cell function and prevents autoimmunity. c) Alternatively, the expanded CD8 T cells also produce TGF- β and suppress pathogenic T cells to prevent autoimmunity. d) In the absence of IFN- γ , anti-CD137 treatment can induce IL-6 production that inhibits Th-17 differentiation and favors Treg differentiation. The expansion of the Treg compartment again prevents autoimmunity in various immune models.

Subsequent studies on the effect of anti-CD137 treatment on EAE showed that the disease could also be suppressed independent of CD8 T cells (after CD8 depletion) and IFN- γ production (using IFN- γ knockout mice) [278]. In IFN- γ knockout mice, CD137 treatment reduced IL-6 expression from CD4 T cells, which inhibits Th-17 and favors Treg differentiation [278] (Figure 5.2c). Furthermore, the anti-CD137 treated IFN- γ knockout mice increased expression of Foxp3 in CD4 T cells and increased the total number of Foxp3^{pos}CD4^{pos} Tregs [278]. This increase in Treg was independent of IL-2 levels. Thus in several models, anti-CD137 mediated prevention of autoimmunity is thus associated with increase in T regulatory cells that are potent suppressors of pathogenic effector cells.

We have demonstrated that anti-CD137 antibody prevented the onset of diabetes in NOD mice (Figure 2.1). The antibody preferentially bound to CD4^{pos}CD25^{pos}CD137^{pos} Tregs and increased

their fraction *in vivo* (Figure 2.3). As shown in Figure 5.2d, our result is consistent with the study in EAE which also showed that anti-CD137 treatment increased the percentage of Foxp3 expressing CD4 T cells [278]. Other groups have also shown the *in vitro* and *in vivo* expansion of CD4^{pos}CD25^{pos} T cells by CD137L-Fc and CD137L-streptavidin [138, 160]. CD137-induced Treg expansion *in vivo* is dependent on IL-2 levels [283]. Adoptive transfer models into NOD-*scid* mice showed that the antibody treated CD4^{pos}CD25^{pos} T cells were suppressive and protective against diabetes (Figure 2.6). Our results are consistent with another study that has also shown adoptive transfer of anti-CD137-primed Tregs prevented Graft versus host disease (GVHD) [283]. These CD137L-Fc or CD137L-strep stimulated Tregs remained functionally suppressive *in vitro* and *in vivo* [138, 160]. Apart from the quantitative increase in Treg numbers that aid in suppression, we have also identified a new mechanism for Treg suppression. We showed that soluble CD137 is functionally suppressive *in vitro* and reduces the incidence of diabetes *in vivo* (Figure 4.9a). Anti-CD137 treatment increases soluble CD137 production by CD137^{pos} Tregs *in vitro*, in addition to the increase in the level of serum soluble CD137 (Figure 4.4). The recombinant soluble CD137 does not cause cell death in CD4 T cells *in vitro* (Figure 4.8b). CD137L blockade abrogated Treg mediated suppression that probably acts through soluble CD137 but we have not clearly identified the mechanism for suppression. The suppression of CD4 T cells after anti-CD137 treatment in various disease models [140, 277] is consistent with our result of increased soluble CD137 mediated suppression. Although the mechanism of suppression is not clear, our results suggests that anti-CD137 mediated diabetes prevention in NOD mice is through expansion of T regulatory cells that are functionally superior in contact dependent suppression and also produce the immunosuppressive soluble CD137 molecule.

5.2 Future directions and therapeutic implications

Diabetes in NOD mice is a complex, multigenic, and immunologically “delicate” disease. The whole immune system acts in an orchestrated manner to mediate disease; DCs present auto-antigens for initiating an immune response, CD4 and CD8 T cells are necessary for disease progression, and B cells play an important role in autoantibody production and as APCs. The many interventions that prevent diabetes in NOD may therefore act at various time points and on different cell subsets to disrupt the development of disease. We have seen that anti-CD137 treatment prevents diabetes in NOD mice [137]. Anti-CD137 treatment has been shown to reverse a number of autoimmune diseases [149, 181, 277] but antibody treatment after the diabetogenic T cells transfer into a NOD-*scid* mice worsened diabetes in the recipient mice [137]. It is important to understand these discrepancies and what they imply for productive research using the NOD model. While systemic administration of soluble CD137 is effective in preventing diabetes in NOD mice, we do not know at this point if soluble CD137 will be effective in reversing T1D. To understand the role of soluble CD137 during various stage of the disease, it is important to understand the effect of soluble CD137 on various immune cells types (CD8 T cells, DCs, B cells etc) during culture *in vitro* and after treatment *in vivo*.

To further understand the mechanism of soluble CD137 suppression, it is necessary to test the direct role of soluble CD137 in suppression. For this we plan to use soluble CD137 for suppression of CD137 deficient CD4 T cells (hence lacking CD137-CD137L costimulation). CD4 T cells from CD137 deficient mice have shown enhanced proliferation [284, 285] and soluble CD137 mediated suppression of CD137 deficient CD4 T cells would indicate the direct role of CD137 in suppression. We can also use T cells from CD137L knockout mice to test the importance of CD137L in soluble CD137 mediated suppression. The absence of CD4 T cell

suppression in CD137L knockout mice in the presence of soluble CD137 would further indicate that soluble CD137 mediates its suppression through CD137L.

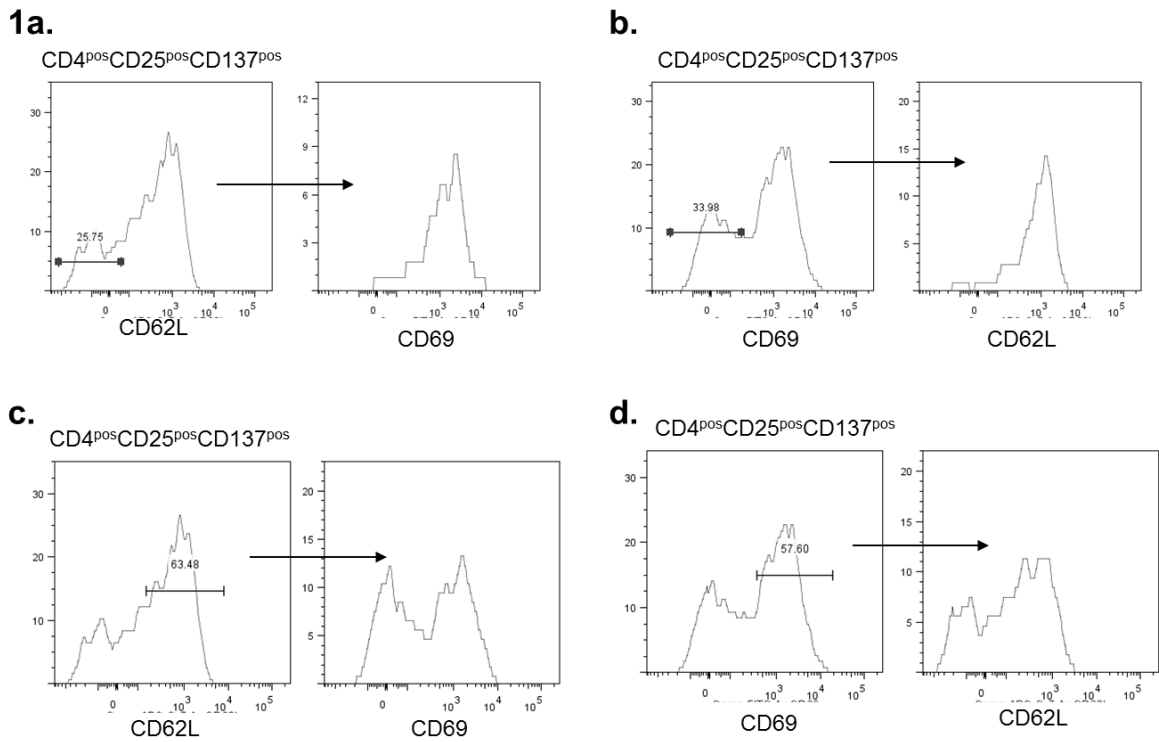
We can also test the variation between soluble versus membrane-bound CD137 in CD137L signaling in T cells. As with other members of TNF superfamily, membrane bound CD137 binds to CD137L as a trimer and cross-links it. On the other hand, soluble CD137 dimer could cross-link CD137L differently than membrane bound CD137 and initiate signaling that causes suppression of CD4 T cell proliferation. It is important to test if cross-linking CD137L by surface CD137 (or by surface bound CD137-Fc or anti-Fc bound CD137-Fc) on T cells would signal differently compared to cross-linking CD137L by soluble CD137 or soluble CD137-Fc. Suppression with soluble CD137 but not with plate bound CD137-Fc or anti-Fc bound CD137-Fc on CD4 T cells would indicate that different degrees of cross-linking CD137L on CD4 T cells are important for suppression. Similar studies on different cell types will help us understand the proliferative versus suppressive effect in CD137L signaling in various immune cells. Our current understanding of the CD137 ligand signaling pathway on T cells is limited and a systematic and comprehensive analysis of the signaling pathway is required to further understand the mechanism of suppression.

Ideally we would like to use tissue-specific cellular therapy to deliver soluble CD137 to the pancreatic islets, where it could bind to and downregulate CD137L in ligand-expressing islet cells. Given the recent demonstration that T cell accumulation in the islets is largely driven by antigen specificity [32], we plan to use a lentiviral approach with transduced BDC2.5 T cells (specific for an islet autoantigen) to deliver the therapeutic agent. An alternate approach is to use retrogenically modified Tregs to deliver soluble CD137 locally. As others have shown we plan to use the retrogenic approach to over-express the soluble B10 CD137 minigene, [286]. Retrogenic mice (potentially useful as sources of soluble CD137 expressing cell subsets for use

in cellular therapy) will be made by reconstitution of LeGOiG2-solubleCD137-transduced bone marrow cells or empty vector into a lethally irradiated NOD recipient. Preliminary studies with CD137-modified lentivirus, LeGOiG2-solubleCD137, effectively transduced both T cells for BDC2.5 site-specific delivery and bone marrow cells for making retrogenic mice. The lentiviral system described above is also highly modular, and will allow us to rapidly splice in and out different candidate genes, as well as test different cell types for gene delivery and therapeutic effectiveness. Hence these dual approaches will be very useful when used in conjunction with genetic studies oriented towards identifying potential candidate genes and their function. CD137 is the major candidate gene in the NOD *Idd9.3* genetic interval. Our studies showed that NOD.B10 *Idd9.3* congenic mice have increased accumulation of CD137^{pos} Tregs compared to NOD mice supporting the hypothesis that CD137 is the *Idd9.3* candidate gene. This hypothesis is further strengthened by the mixed bone marrow chimera results which also showed increased fraction of *Idd9.3* CD137^{pos} Tregs compared to NOD CD137^{pos} Tregs. These studies would further support detailed genetic studies to demonstrate whether CD137 is the *Idd9.3* gene. A knockout of CD37 in NOD.B10 *Idd9.3* Tregs could worsen diabetes in NOD.B10 *Idd9.3* mice which would probably represent the strongest evidence, in addition to the many findings we have produced, supporting Cd137 as the *Idd9.3* candidate gene. The NOD model has been very successful in identifying common immunogenetic pathways shared between mouse and human T1D [287, 288] and further understanding of mouse genetic control of diabetes has great potential for insights in human T1D. By focusing on genes implicated in immunopathogenesis of T1D, and by delivering variants of these genes to the islets in T1D, we hope to study the effect of immune molecules that are genetically associated with the disease.

APPENDIX A

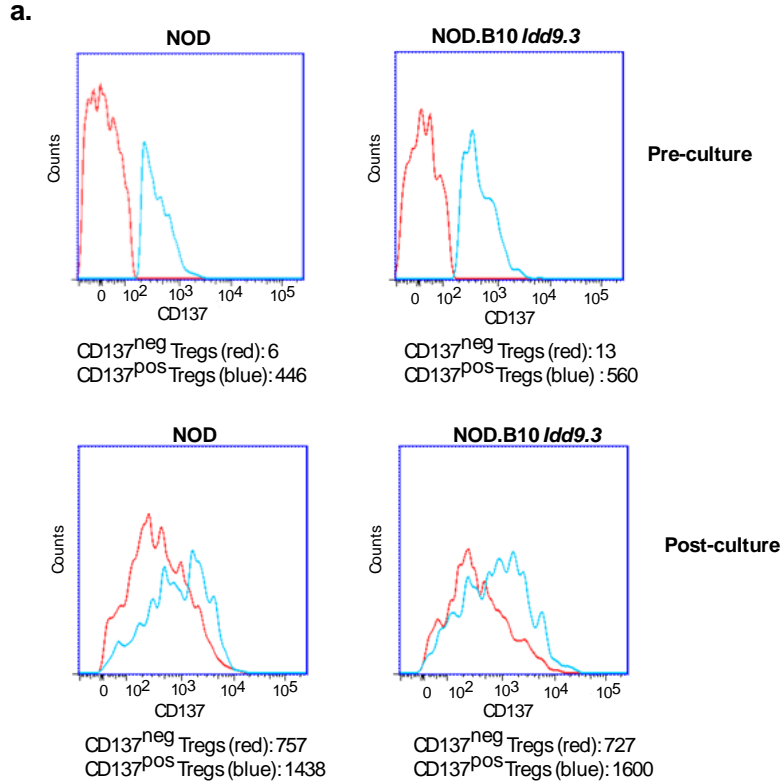
Supplemental Figure 1



Supplemental Figure 1. The CD62L^{hi} or CD69^{hi} expression on CD137^{pos} Tregs are not entirely CD69^{low} or CD62L^{low} respectively.

NOD female splenocytes, 4-8 weeks old were stained with CD4APC, CD25Perpcy5.5, CD137PE, CD69FITC and CD62LAPCCy7 and processed through FACS Cantos. The CD69 and CD62L staining was analysed on CD137^{pos} Tregs using FlowJo.

Supplemental Figure2



Supplemental Figure 2. NOD and NOD.B10 *l*dd9.3 CD137^{neg} Tregs both equally upregulate CD137 *in vitro*.

Splenocytes from 4-7 week old NOD and NOD.B10 *l*dd9.3 females were sorted for CD4^{pos}CD25^{neg}CD137^{neg} T cells and CD137^{neg} and CD137^{pos} Tregs as described above. 25,000 sorted cells were cultured with 25U/ml IL-2 and 1.25ug/ml anti-CD3 for three days. The cultured cells were stained for CD4, CD25 and CD137 and analyzed by flow cytometry; CD137 MFI for each subset is shown beneath each FACS plot. One representative of three experiments.

APPENDIX B

Kachapati, K., D. E. Adams, Y. Wu, C. A. Steward, D. B. Rainbow, L. S. Wicker, R. S. Mittler, and W. M. Ridgway. "The B10 Idd9.3 Locus Mediates Accumulation of Functionally Superior Cd137+ Regulatory T Cells in the Nonobese Diabetic Type 1 Diabetes Model." *J Immunol* 189, no. 10 (2012): 5001-15.

Kachapati, K., D. Adams, K. Bednar, and W. M. Ridgway. "The Non-Obese Diabetic (Nod) Mouse as a Model of Human Type 1 Diabetes." *Methods Mol Biol* 933, (2012): 3-16.

Irie, J., Y. Wu, K. Kachapati, R. S. Mittler, and W. M. Ridgway. "Modulating Protective and Pathogenic Cd4+ Subsets Via Cd137 in Type 1 Diabetes." *Diabetes* 56, no. 1 (2007): 186-96.

O'Brien, T. R., K. Kachapati, M. Zhang, J. Bergeron, B. R. Edlin, and M. Dean. "Hcv Infection Clearance with Functional or Non-Functional Caspase-12." *Scand J Gastroenterol* 42, no. 3 (2007): 416-7.

Kachapati, K., T. R. O'Brien, J. Bergeron, M. Zhang, and M. Dean. "Population Distribution of the Functional Caspase-12 Allele." *Hum Mutat* 27, no. 9 (2006): 975.

Sachdeva, G., J. D'Costa, J. E. Cho, K. Kachapati, V. Choudhry, and S. K. Arya. "Chimeric Hiv-1 and Hiv-2 Lentiviral Vectors with Added Safety Insurance." *J Med Virol* 79, no. 2 (2007): 118-26.

BIBLIOGRAPHY

1. Daneman, D., *Type 1 diabetes*. Lancet, 2006. **367**(9513): p. 847-58.
2. Bach, J.F., *Insulin-dependent diabetes mellitus as an autoimmune disease*. Endocr Rev, 1994. **15**(4): p. 516-42.
3. Wild, S., et al., *Global prevalence of diabetes: estimates for the year 2000 and projections for 2030*. Diabetes Care, 2004. **27**(5): p. 1047-53.
4. Wicker, L.S., J.A. Todd, and L.B. Peterson, *Genetic control of autoimmune diabetes in the NOD mouse*. Annu Rev Immunol, 1995. **13**: p. 179-200.
5. Imagawa, A., et al., *Pancreatic biopsy as a procedure for detecting in situ autoimmune phenomena in type 1 diabetes: close correlation between serological markers and histological evidence of cellular autoimmunity*. Diabetes, 2001. **50**(6): p. 1269-73.
6. Todd, J.A. and L.S. Wicker, *Genetic protection from the inflammatory disease type 1 diabetes in humans and animal models*. Immunity, 2001. **15**(3): p. 387-95.
7. Eiselein, L., H.J. Schwartz, and J.C. Rutledge, *The challenge of type 1 diabetes mellitus*. ILAR J, 2004. **45**(3): p. 231-6.
8. Gale, E.A., *Spring harvest? Reflections on the rise of type 1 diabetes*. Diabetologia, 2005. **48**(12): p. 2445-50.
9. Makino, S., et al., *Breeding of a non-obese, diabetic strain of mice*. Jikken Dobutsu, 1980. **29**(1): p. 1-13.
10. Watts, T.H., *TNF/TNFR family members in costimulation of T cell responses*. Annu Rev Immunol, 2005. **23**: p. 23-68.
11. Kang, S.M., et al., *Fas ligand expression in islets of Langerhans does not confer immune privilege and instead targets them for rapid destruction*. Nat Med, 1997. **3**(7): p. 738-43.
12. Estella, E., et al., *Granzyme B-mediated death of pancreatic beta-cells requires the proapoptotic BH3-only molecule bid*. Diabetes, 2006. **55**(8): p. 2212-9.
13. McKenzie, M.D., et al., *Perforin and Fas induced by IFN γ and TNF α mediate beta cell death by OT-I CTL*. Int Immunol, 2006. **18**(6): p. 837-46.
14. Todd, J.A., et al., *Robust associations of four new chromosome regions from genome-wide analyses of type 1 diabetes*. Nat Genet, 2007. **39**(7): p. 857-64.
15. Rainbow, D.B., et al., *Commonality in the genetic control of Type 1 diabetes in humans and NOD mice: variants of genes in the IL-2 pathway are associated with autoimmune diabetes in both species*. Biochem Soc Trans, 2008. **36**(Pt 3): p. 312-5.
16. Jasinski, J.M. and G.S. Eisenbarth, *Insulin as a primary autoantigen for type 1A diabetes*. Clin Dev Immunol, 2005. **12**(3): p. 181-6.
17. Mathis, D. and C. Benoist, *A decade of AIRE*. Nat Rev Immunol, 2007. **7**(8): p. 645-50.
18. Cucca, F., et al., *A correlation between the relative predisposition of MHC class II alleles to type 1 diabetes and the structure of their proteins*. Hum Mol Genet, 2001. **10**(19): p. 2025-37.

19. Yamanouchi, J., et al., *Interleukin-2 gene variation impairs regulatory T cell function and causes autoimmunity*. Nat Genet, 2007. **39**(3): p. 329-37.
20. Lowe, C.E., et al., *Large-scale genetic fine mapping and genotype-phenotype associations implicate polymorphism in the IL2RA region in type 1 diabetes*. Nat Genet, 2007. **39**(9): p. 1074-82.
21. Erlich, H., et al., *HLA DR-DQ haplotypes and genotypes and type 1 diabetes risk: analysis of the type 1 diabetes genetics consortium families*. Diabetes, 2008. **57**(4): p. 1084-92.
22. Nejentsev, S., et al., *Localization of type 1 diabetes susceptibility to the MHC class I genes HLA-B and HLA-A*. Nature, 2007. **450**(7171): p. 887-92.
23. Brusko, T.M., et al., *Functional defects and the influence of age on the frequency of CD4+ CD25+ T-cells in type 1 diabetes*. Diabetes, 2005. **54**(5): p. 1407-14.
24. Lindley, S., et al., *Defective suppressor function in CD4(+)CD25(+) T-cells from patients with type 1 diabetes*. Diabetes, 2005. **54**(1): p. 92-9.
25. Tritt, M., et al., *Functional waning of naturally occurring CD4+ regulatory T-cells contributes to the onset of autoimmune diabetes*. Diabetes, 2008. **57**(1): p. 113-23.
26. Yu, S., et al., *B cell-deficient NOD.H-2h4 mice have CD4+CD25+ T regulatory cells that inhibit the development of spontaneous autoimmune thyroiditis*. J Exp Med, 2006. **203**(2): p. 349-58.
27. Leiter, E.H. and M. von Herrath, *Animal models have little to teach us about type 1 diabetes: 2. In opposition to this proposal*. Diabetologia, 2004. **47**(10): p. 1657-60.
28. Mordes, J.P., et al., *Rat models of type 1 diabetes: genetics, environment, and autoimmunity*. ILAR J, 2004. **45**(3): p. 278-91.
29. Atkinson, M.A. and E.H. Leiter, *The NOD mouse model of type 1 diabetes: as good as it gets?* Nat Med, 1999. **5**(6): p. 601-4.
30. Chatenoud, L., et al., *Anti-CD3 antibody induces long-term remission of overt autoimmunity in nonobese diabetic mice*. Proc Natl Acad Sci U S A, 1994. **91**(1): p. 123-7.
31. Phillips, J.M., et al., *Type 1 diabetes development requires both CD4+ and CD8+ T cells and can be reversed by non-depleting antibodies targeting both T cell populations*. Rev Diabet Stud, 2009. **6**(2): p. 97-103.
32. Lennon, G.P., et al., *T cell islet accumulation in type 1 diabetes is a tightly regulated, cell-autonomous event*. Immunity, 2009. **31**(4): p. 643-53.
33. Stadinski, B., J. Kappler, and G.S. Eisenbarth, *Molecular targeting of islet autoantigens*. Immunity, 2010. **32**(4): p. 446-56.
34. Han, B., et al., *Developmental control of CD8 T cell-avidity maturation in autoimmune diabetes*. J Clin Invest, 2005. **115**(7): p. 1879-87.
35. You, S., et al., *Autoimmune diabetes onset results from qualitative rather than quantitative age-dependent changes in pathogenic T-cells*. Diabetes, 2005. **54**(5): p. 1415-22.
36. Schneider, A., et al., *The effector T cells of diabetic subjects are resistant to regulation via CD4+ FOXP3+ regulatory T cells*. J Immunol, 2008. **181**(10): p. 7350-5.

37. Babad, J., A. Geliebter, and T.P. DiLorenzo, *T-cell autoantigens in the non-obese diabetic mouse model of autoimmune diabetes*. Immunology, 2010. **131**(4): p. 459-65.
38. Wicker, L.S., et al., *Genetic control of diabetes and insulinitis in the nonobese diabetic mouse. Pedigree analysis of a diabetic H-2nod/b heterozygote*. J Immunol, 1989. **142**(3): p. 781-4.
39. Kanagawa, O., et al., *Autoreactivity of T cells from nonobese diabetic mice: an I-Ag7-dependent reaction*. Proc Natl Acad Sci U S A, 1998. **95**(4): p. 1721-4.
40. Wicker, L.S., *Major histocompatibility complex-linked control of autoimmunity*. J Exp Med, 1997. **186**(7): p. 973-5.
41. Ridgway, W.M., M. Fasso, and C.G. Fathman, *A new look at MHC and autoimmune disease*. Science, 1999. **284**(5415): p. 749, 751.
42. Miller, B.J., et al., *Both the Lyt-2+ and L3T4+ T cell subsets are required for the transfer of diabetes in nonobese diabetic mice*. J Immunol, 1988. **140**(1): p. 52-8.
43. Bendelac, A., et al., *Syngeneic transfer of autoimmune diabetes from diabetic NOD mice to healthy neonates. Requirement for both L3T4+ and Lyt-2+ T cells*. J Exp Med, 1987. **166**(4): p. 823-32.
44. Christianson, S.W., L.D. Shultz, and E.H. Leiter, *Adoptive transfer of diabetes into immunodeficient NOD-scid/scid mice. Relative contributions of CD4+ and CD8+ T-cells from diabetic versus prediabetic NOD.NON-Thy-1a donors*. Diabetes, 1993. **42**(1): p. 44-55.
45. Dahlen, E., et al., *Dendritic cells and macrophages are the first and major producers of TNF-alpha in pancreatic islets in the nonobese diabetic mouse*. J Immunol, 1998. **160**(7): p. 3585-93.
46. Turley, S., et al., *Physiological beta cell death triggers priming of self-reactive T cells by dendritic cells in a type-1 diabetes model*. J Exp Med, 2003. **198**(10): p. 1527-37.
47. Zhu, G., et al., *Progressive depletion of peripheral B lymphocytes in 4-1BB (CD137) ligand/I-Ealpha-transgenic mice*. J Immunol, 2001. **167**(5): p. 2671-6.
48. Hutchings, P., et al., *Transfer of diabetes in mice prevented by blockade of adhesion-promoting receptor on macrophages*. Nature, 1990. **348**(6302): p. 639-42.
49. Arnush, M., et al., *Potential role of resident islet macrophage activation in the initiation of autoimmune diabetes*. J Immunol, 1998. **160**(6): p. 2684-91.
50. Jun, H.S., et al., *The role of macrophages in T cell-mediated autoimmune diabetes in nonobese diabetic mice*. J Exp Med, 1999. **189**(2): p. 347-58.
51. Gur, C., et al., *The activating receptor NKp46 is essential for the development of type 1 diabetes*. Nat Immunol, 2010. **11**(2): p. 121-8.
52. Ogasawara, K., et al., *Impairment of NK cell function by NKG2D modulation in NOD mice*. Immunity, 2003. **18**(1): p. 41-51.
53. Brauner, H., et al., *Distinct phenotype and function of NK cells in the pancreas of nonobese diabetic mice*. J Immunol, 2010. **184**(5): p. 2272-80.
54. Lee, I.F., et al., *Regulation of autoimmune diabetes by complete Freund's adjuvant is mediated by NK cells*. J Immunol, 2004. **172**(2): p. 937-42.
55. Rodacki, M., et al., *Altered natural killer cells in type 1 diabetic patients*. Diabetes, 2007. **56**(1): p. 177-85.

56. Carnaud, C., et al., *Protection against diabetes and improved NK/NKT cell performance in NOD.NK1.1 mice congenic at the NK complex*. J Immunol, 2001. **166**(4): p. 2404-11.
57. Hammond, K.J., et al., *alpha/beta-T cell receptor (TCR)+CD4-CD8- (NKT) thymocytes prevent insulin-dependent diabetes mellitus in nonobese diabetic (NOD)/Lt mice by the influence of interleukin (IL)-4 and/or IL-10*. J Exp Med, 1998. **187**(7): p. 1047-56.
58. Hong, S., et al., *The natural killer T-cell ligand alpha-galactosylceramide prevents autoimmune diabetes in non-obese diabetic mice*. Nat Med, 2001. **7**(9): p. 1052-6.
59. Sharif, S., et al., *Activation of natural killer T cells by alpha-galactosylceramide treatment prevents the onset and recurrence of autoimmune Type 1 diabetes*. Nat Med, 2001. **7**(9): p. 1057-62.
60. Palmer, J.P., et al., *Insulin antibodies in insulin-dependent diabetics before insulin treatment*. Science, 1983. **222**(4630): p. 1337-9.
61. Rabin, D.U., et al., *Islet cell antigen 512 is a diabetes-specific islet autoantigen related to protein tyrosine phosphatases*. J Immunol, 1994. **152**(6): p. 3183-8.
62. Baekkeskov, S., et al., *Identification of the 64K autoantigen in insulin-dependent diabetes as the GABA-synthesizing enzyme glutamic acid decarboxylase*. Nature, 1990. **347**(6289): p. 151-6.
63. Wong, F.S., et al., *To B or not to B--pathogenic and regulatory B cells in autoimmune diabetes*. Curr Opin Immunol, 2010. **22**(6): p. 723-31.
64. Watts, C., et al., *Processing of immunoglobulin-associated antigen in B lymphocytes*. Cold Spring Harb Symp Quant Biol, 1989. **54 Pt 1**: p. 345-52.
65. Mamula, M.J. and C.A. Janeway, Jr., *Do B cells drive the diversification of immune responses?* Immunol Today, 1993. **14**(4): p. 151-2; discussion 153-4.
66. Falcone, M., et al., *B lymphocytes are crucial antigen-presenting cells in the pathogenic autoimmune response to GAD65 antigen in nonobese diabetic mice*. J Immunol, 1998. **161**(3): p. 1163-8.
67. Hussain, S. and T.L. Delovitch, *Dysregulated B7-1 and B7-2 expression on nonobese diabetic mouse B cells is associated with increased T cell costimulation and the development of insulinitis*. J Immunol, 2005. **174**(2): p. 680-7.
68. Hu, C.Y., et al., *Treatment with CD20-specific antibody prevents and reverses autoimmune diabetes in mice*. J Clin Invest, 2007. **117**(12): p. 3857-67.
69. Serreze, D.V., et al., *B lymphocytes are essential for the initiation of T cell-mediated autoimmune diabetes: analysis of a new "speed congenic" stock of NOD.Ig mu null mice*. J Exp Med, 1996. **184**(5): p. 2049-53.
70. Shevach, E.M., *Mechanisms of foxp3+ T regulatory cell-mediated suppression*. Immunity, 2009. **30**(5): p. 636-45.
71. Salomon, B., et al., *B7/CD28 costimulation is essential for the homeostasis of the CD4+CD25+ immunoregulatory T cells that control autoimmune diabetes*. Immunity, 2000. **12**(4): p. 431-40.
72. Wildin, R.S. and A. Freitas, *IPEX and FOXP3: clinical and research perspectives*. J Autoimmun, 2005. **25 Suppl**: p. 56-62.

73. Mellanby, R.J., et al., *Diabetes in non-obese diabetic mice is not associated with quantitative changes in CD4+ CD25+ Foxp3+ regulatory T cells*. Immunology, 2007. **121**(1): p. 15-28.
74. Bettini, M. and D.A. Vignali, *Regulatory T cells and inhibitory cytokines in autoimmunity*. Curr Opin Immunol, 2009. **21**(6): p. 612-8.
75. Gregori, S., et al., *Dynamics of pathogenic and suppressor T cells in autoimmune diabetes development*. J Immunol, 2003. **171**(8): p. 4040-7.
76. Gregg, R.K., et al., *A sudden decline in active membrane-bound TGF-beta impairs both T regulatory cell function and protection against autoimmune diabetes*. J Immunol, 2004. **173**(12): p. 7308-16.
77. Pop, S.M., et al., *Single cell analysis shows decreasing FoxP3 and TGFbeta1 coexpressing CD4+CD25+ regulatory T cells during autoimmune diabetes*. J Exp Med, 2005. **201**(8): p. 1333-46.
78. Nakamura, K., A. Kitani, and W. Strober, *Cell contact-dependent immunosuppression by CD4(+)/CD25(+) regulatory T cells is mediated by cell surface-bound transforming growth factor beta*. J Exp Med, 2001. **194**(5): p. 629-44.
79. Tang, Q., et al., *Central role of defective interleukin-2 production in the triggering of islet autoimmune destruction*. Immunity, 2008. **28**(5): p. 687-97.
80. Long, S.A., et al., *Defects in IL-2R signaling contribute to diminished maintenance of FOXP3 expression in CD4(+)/CD25(+) regulatory T-cells of type 1 diabetic subjects*. Diabetes, 2010. **59**(2): p. 407-15.
81. Zheng, S.G., et al., *TGF-beta requires CTLA-4 early after T cell activation to induce FoxP3 and generate adaptive CD4+CD25+ regulatory cells*. J Immunol, 2006. **176**(6): p. 3321-9.
82. Karim, M., et al., *Alloantigen-induced CD25+CD4+ regulatory T cells can develop in vivo from CD25-CD4+ precursors in a thymus-independent process*. J Immunol, 2004. **172**(2): p. 923-8.
83. Chen, W., et al., *Conversion of peripheral CD4+CD25- naive T cells to CD4+CD25+ regulatory T cells by TGF-beta induction of transcription factor Foxp3*. J Exp Med, 2003. **198**(12): p. 1875-86.
84. You, S., et al., *Adaptive TGF-beta-dependent regulatory T cells control autoimmune diabetes and are a privileged target of anti-CD3 antibody treatment*. Proc Natl Acad Sci U S A, 2007. **104**(15): p. 6335-40.
85. You, S., et al., *Presence of diabetes-inhibiting, glutamic acid decarboxylase-specific, IL-10-dependent, regulatory T cells in naive nonobese diabetic mice*. J Immunol, 2004. **173**(11): p. 6777-85.
86. Sapone, A., et al., *Zonulin upregulation is associated with increased gut permeability in subjects with type 1 diabetes and their relatives*. Diabetes, 2006. **55**(5): p. 1443-9.
87. Vaarala, O., *The role of the gut in beta-cell autoimmunity and type 1 diabetes: a hypothesis*. Pediatr Diabetes, 2000. **1**(4): p. 217-25.
88. Wen, L., et al., *Innate immunity and intestinal microbiota in the development of Type 1 diabetes*. Nature, 2008. **455**(7216): p. 1109-13.

89. Atkinson, M.A., et al., *Cellular immunity to a determinant common to glutamate decarboxylase and coxsackie virus in insulin-dependent diabetes*. J Clin Invest, 1994. **94**(5): p. 2125-9.
90. Honeyman, M.C., et al., *Evidence for molecular mimicry between human T cell epitopes in rotavirus and pancreatic islet autoantigens*. J Immunol, 2010. **184**(4): p. 2204-10.
91. Ou, D., et al., *Cross-reactive rubella virus and glutamic acid decarboxylase (65 and 67) protein determinants recognised by T cells of patients with type 1 diabetes mellitus*. Diabetologia, 2000. **43**(6): p. 750-62.
92. Pak, C.Y., et al., *Human pancreatic islet cell specific 38 kilodalton autoantigen identified by cytomegalovirus-induced monoclonal islet cell autoantibody*. Diabetologia, 1990. **33**(9): p. 569-72.
93. Coulson, B.S., et al., *Growth of rotaviruses in primary pancreatic cells*. J Virol, 2002. **76**(18): p. 9537-44.
94. Horwitz, M.S., et al., *Diabetes induced by Coxsackie virus: initiation by bystander damage and not molecular mimicry*. Nat Med, 1998. **4**(7): p. 781-5.
95. Conrad, B., et al., *A human endogenous retroviral superantigen as candidate autoimmune gene in type 1 diabetes*. Cell, 1997. **90**(2): p. 303-13.
96. Chung, Y.H., et al., *Cellular and molecular mechanism for Kilham rat virus-induced autoimmune diabetes in DR-BB rats*. J Immunol, 2000. **165**(5): p. 2866-76.
97. Zipris, D., et al., *Infections that induce autoimmune diabetes in BBDR rats modulate CD4+CD25+ T cell populations*. J Immunol, 2003. **170**(7): p. 3592-602.
98. Todd, J.A., et al., *Genetic analysis of autoimmune type 1 diabetes mellitus in mice*. Nature, 1991. **351**(6327): p. 542-7.
99. Love, J.M., et al., *Towards construction of a high resolution map of the mouse genome using PCR-analysed microsatellites*. Nucleic Acids Res, 1990. **18**(14): p. 4123-30.
100. Copeland, N.G., et al., *A genetic linkage map of the mouse: current applications and future prospects*. Science, 1993. **262**(5130): p. 57-66.
101. Hill, N.J., et al., *NOD Idd5 locus controls insulinitis and diabetes and overlaps the orthologous CTLA4/IDDM12 and NRAMP1 loci in humans*. Diabetes, 2000. **49**(10): p. 1744-7.
102. Wicker, L.S., et al., *Fine mapping, gene content, comparative sequencing, and expression analyses support Ctla4 and Nramp1 as candidates for Idd5.1 and Idd5.2 in the nonobese diabetic mouse*. J Immunol, 2004. **173**(1): p. 164-73.
103. Lyons, P.A., et al., *Congenic mapping of the type 1 diabetes locus, Idd3, to a 780-kb region of mouse chromosome 3: identification of a candidate segment of ancestral DNA by haplotype mapping*. Genome Res, 2000. **10**(4): p. 446-53.
104. Lyons, P.A., et al., *The NOD Idd9 genetic interval influences the pathogenicity of insulinitis and contains molecular variants of Cd30, Tnfr2, and Cd137*. Immunity, 2000. **13**(1): p. 107-15.
105. Ueda, H., et al., *Association of the T-cell regulatory gene CTLA4 with susceptibility to autoimmune disease*. Nature, 2003. **423**(6939): p. 506-11.
106. Ridgway, W.M., et al., *New tools for defining the 'genetic background' of inbred mouse strains*. Nat Immunol, 2007. **8**(7): p. 669-73.

107. Petes, T.D., *Meiotic recombination hot spots and cold spots*. Nat Rev Genet, 2001. **2**(5): p. 360-9.
108. Koarada, S., et al., *Genetic control of autoimmunity: protection from diabetes, but spontaneous autoimmune biliary disease in a nonobese diabetic congenic strain*. J Immunol, 2004. **173**(4): p. 2315-23.
109. Irie, J., et al., *Genetic control of anti-Sm autoantibody production in NOD congenic mice narrowed to the Idd9.3 region*. Immunogenetics, 2006. **58**(1): p. 9-14.
110. Rodrigues, N.R., et al., *Mapping of an insulin-dependent diabetes locus, Idd9, in NOD mice to chromosome 4*. Mamm Genome, 1994. **5**(3): p. 167-70.
111. Ghosh, S., et al., *Polygenic control of autoimmune diabetes in nonobese diabetic mice*. Nat Genet, 1993. **4**(4): p. 404-9.
112. Hamilton-Williams, E.E., et al., *Idd9.2 and Idd9.3 protective alleles function in CD4+ T-cells and nonlymphoid cells to prevent expansion of pathogenic islet-specific CD8+ T-cells*. Diabetes, 2010. **59**(6): p. 1478-86.
113. Wicker, L.S., et al., *Resistance alleles at two non-major histocompatibility complex-linked insulin-dependent diabetes loci on chromosome 3, Idd3 and Idd10, protect nonobese diabetic mice from diabetes*. J Exp Med, 1994. **180**(5): p. 1705-13.
114. Cannons, J.L., et al., *Genetic and functional association of the immune signaling molecule 4-1BB (CD137/TNFRSF9) with type 1 diabetes*. J Autoimmun, 2005. **25**(1): p. 13-20.
115. Tan, S.G. and G.C. Ashton, *An autosomal glucose-6-phosphate dehydrogenase (hexose-6-phosphate dehydrogenase) polymorphism in human saliva*. Hum Hered, 1976. **26**(2): p. 113-23.
116. Gilman, A.G., *G proteins: transducers of receptor-generated signals*. Annu Rev Biochem, 1987. **56**: p. 615-49.
117. Uldry, M. and B. Thorens, *The SLC2 family of facilitated hexose and polyol transporters*. Pflugers Arch, 2004. **447**(5): p. 480-9.
118. Li, Q., et al., *Cloning and functional characterization of the human GLUT7 isoform SLC2A7 from the small intestine*. Am J Physiol Gastrointest Liver Physiol, 2004. **287**(1): p. G236-42.
119. Kivela, J., et al., *Salivary carbonic anhydrase isoenzyme VI*. J Physiol, 1999. **520 Pt 2**: p. 315-20.
120. Subramanian, A. and D.M. Miller, *Structural analysis of alpha-enolase. Mapping the functional domains involved in down-regulation of the c-myc protooncogene*. J Biol Chem, 2000. **275**(8): p. 5958-65.
121. Yanagisawa, H., et al., *Protein binding of a DRPLA family through arginine-glutamic acid dipeptide repeats is enhanced by extended polyglutamine*. Hum Mol Genet, 2000. **9**(9): p. 1433-42.
122. Makkinje, A., et al., *Gene 33/Mig-6, a transcriptionally inducible adapter protein that binds GTP-Cdc42 and activates SAPK/JNK. A potential marker transcript for chronic pathologic conditions, such as diabetic nephropathy. Possible role in the response to persistent stress*. J Biol Chem, 2000. **275**(23): p. 17838-47.
123. Bonifati, V., et al., *Mutations in the DJ-1 gene associated with autosomal recessive early-onset parkinsonism*. Science, 2003. **299**(5604): p. 256-9.

124. Ames, R.S., et al., *Human urotensin-II is a potent vasoconstrictor and agonist for the orphan receptor GPR14*. *Nature*, 1999. **401**(6750): p. 282-6.
125. Chellappa, S.L., et al., *Human melatonin and alerting response to blue-enriched light depend on a polymorphism in the clock gene PER3*. *J Clin Endocrinol Metab*, 2012. **97**(3): p. E433-7.
126. Jewell, J.L., E. Oh, and D.C. Thurmond, *Exocytosis mechanisms underlying insulin release and glucose uptake: conserved roles for Munc18c and syntaxin 4*. *Am J Physiol Regul Integr Comp Physiol*, 2010. **298**(3): p. R517-31.
127. Bouche, N., et al., *A novel family of calmodulin-binding transcription activators in multicellular organisms*. *J Biol Chem*, 2002. **277**(24): p. 21851-61.
128. Schwarz, H., J. Tuckwell, and M. Lotz, *A receptor induced by lymphocyte activation (ILA): a new member of the human nerve-growth-factor/tumor-necrosis-factor receptor family*. *Gene*, 1993. **134**(2): p. 295-8.
129. Pollok, K.E., et al., *Inducible T cell antigen 4-1BB. Analysis of expression and function*. *J Immunol*, 1993. **150**(3): p. 771-81.
130. Vinay, D.S. and B.S. Kwon, *Role of 4-1BB in immune responses*. *Semin Immunol*, 1998. **10**(6): p. 481-9.
131. Shuford, W.W., et al., *4-1BB costimulatory signals preferentially induce CD8+ T cell proliferation and lead to the amplification in vivo of cytotoxic T cell responses*. *J Exp Med*, 1997. **186**(1): p. 47-55.
132. Zhang, X., et al., *CD137 promotes proliferation and survival of human B cells*. *J Immunol*, 2010. **184**(2): p. 787-95.
133. Melero, I., et al., *NK1.1 cells express 4-1BB (CDw137) costimulatory molecule and are required for tumor immunity elicited by anti-4-1BB monoclonal antibodies*. *Cell Immunol*, 1998. **190**(2): p. 167-72.
134. Futagawa, T., et al., *Expression and function of 4-1BB and 4-1BB ligand on murine dendritic cells*. *Int Immunol*, 2002. **14**(3): p. 275-86.
135. Wilcox, R.A., et al., *Cutting edge: Expression of functional CD137 receptor by dendritic cells*. *J Immunol*, 2002. **168**(9): p. 4262-7.
136. McHugh, R.S., et al., *CD4(+)CD25(+) immunoregulatory T cells: gene expression analysis reveals a functional role for the glucocorticoid-induced TNF receptor*. *Immunity*, 2002. **16**(2): p. 311-23.
137. Irie, J., et al., *Modulating protective and pathogenic CD4+ subsets via CD137 in type 1 diabetes*. *Diabetes*, 2007. **56**(1): p. 186-96.
138. Zheng, G., B. Wang, and A. Chen, *The 4-1BB costimulation augments the proliferation of CD4+CD25+ regulatory T cells*. *J Immunol*, 2004. **173**(4): p. 2428-34.
139. Gavin, M.A., et al., *Homeostasis and anergy of CD4(+)CD25(+) suppressor T cells in vivo*. *Nat Immunol*, 2002. **3**(1): p. 33-41.
140. Choi, B.K., et al., *4-1BB-dependent inhibition of immunosuppression by activated CD4+CD25+ T cells*. *J Leukoc Biol*, 2004. **75**(5): p. 785-91.
141. Kachapati, K., et al., *The B10 Idd9.3 Locus Mediates Accumulation of Functionally Superior CD137+ Regulatory T Cells in the Nonobese Diabetic Type 1 Diabetes Model*. *J Immunol*, 2012. **189**(10): p. 5001-15.
142. Croft, M., *Costimulation of T cells by OX40, 4-1BB, and CD27*. *Cytokine Growth Factor Rev*, 2003. **14**(3-4): p. 265-73.

143. Croft, M., *Co-stimulatory members of the TNFR family: keys to effective T-cell immunity?* Nat Rev Immunol, 2003. **3**(8): p. 609-20.
144. Vinay, D.S., K. Cha, and B.S. Kwon, *Dual immunoregulatory pathways of 4-1BB signaling.* J Mol Med, 2006. **84**(9): p. 726-36.
145. Lee, H.W., et al., *4-1BB promotes the survival of CD8+ T lymphocytes by increasing expression of Bcl-xL and Bfl-1.* J Immunol, 2002. **169**(9): p. 4882-8.
146. Starck, L., et al., *Costimulation by CD137/4-1BB inhibits T cell apoptosis and induces Bcl-xL and c-FLIP(short) via phosphatidylinositol 3-kinase and AKT/protein kinase B.* Eur J Immunol, 2005. **35**(4): p. 1257-66.
147. Hurtado, J.C., Y.J. Kim, and B.S. Kwon, *Signals through 4-1BB are costimulatory to previously activated splenic T cells and inhibit activation-induced cell death.* J Immunol, 1997. **158**(6): p. 2600-9.
148. Sun, Y., et al., *Administration of agonistic anti-4-1BB monoclonal antibody leads to the amelioration of experimental autoimmune encephalomyelitis.* J Immunol, 2002. **168**(3): p. 1457-65.
149. Foell, J.L., et al., *Engagement of the CD137 (4-1BB) costimulatory molecule inhibits and reverses the autoimmune process in collagen-induced arthritis and establishes lasting disease resistance.* Immunology, 2004. **113**(1): p. 89-98.
150. Fukushima, A., et al., *Engagement of 4-1BB inhibits the development of experimental allergic conjunctivitis in mice.* J Immunol, 2005. **175**(8): p. 4897-903.
151. Maier, L.M., et al., *Construction and analysis of tag single nucleotide polymorphism maps for six human-mouse orthologous candidate genes in type 1 diabetes.* BMC Genet, 2005. **6**: p. 9.
152. Stechova, K., et al., *Healthy first degree relatives of patients with type 1 diabetes exhibit significant differences in basal gene expression pattern of immunocompetent cells compared to controls: expression pattern as predeterminant of autoimmune diabetes.* Scand J Immunol, 2011.
153. Fung, E.Y., et al., *Analysis of 17 autoimmune disease-associated variants in type 1 diabetes identifies 6q23/TNFAIP3 as a susceptibility locus.* Genes Immun, 2009. **10**(2): p. 188-91.
154. Li, L., et al., *The zinc finger protein A20 targets TRAF2 to the lysosomes for degradation.* Biochim Biophys Acta, 2009. **1793**(2): p. 346-53.
155. Grey, S.T., et al., *Genetic engineering of a suboptimal islet graft with A20 preserves beta cell mass and function.* J Immunol, 2003. **170**(12): p. 6250-6.
156. Grey, S.T., et al., *A20 inhibits cytokine-induced apoptosis and nuclear factor kappaB-dependent gene activation in islets.* J Exp Med, 1999. **190**(8): p. 1135-46.
157. Liuwantara, D., et al., *Nuclear factor-kappaB regulates beta-cell death: a critical role for A20 in beta-cell protection.* Diabetes, 2006. **55**(9): p. 2491-501.
158. Marson, A., et al., *Foxp3 occupancy and regulation of key target genes during T-cell stimulation.* Nature, 2007. **445**(7130): p. 931-5.
159. Chen, Z., et al., *Where CD4+CD25+ T reg cells impinge on autoimmune diabetes.* J Exp Med, 2005. **202**(10): p. 1387-97.

160. Elpek, K.G., et al., *Ex vivo expansion of CD4+CD25+FoxP3+ T regulatory cells based on synergy between IL-2 and 4-1BB signaling*. J Immunol, 2007. **179**(11): p. 7295-304.
161. Setareh, M., H. Schwarz, and M. Lotz, *A mRNA variant encoding a soluble form of 4-1BB, a member of the murine NGF/TNF receptor family*. Gene, 1995. **164**(2): p. 311-5.
162. Shao, Z., et al., *Characterisation of soluble murine CD137 and its association with systemic lupus*. Mol Immunol, 2008. **45**(15): p. 3990-9.
163. Schwarz, H., et al., *ILA, a member of the human nerve growth factor/tumor necrosis factor receptor family, regulates T-lymphocyte proliferation and survival*. Blood, 1996. **87**(7): p. 2839-45.
164. Jung, H.W., et al., *Serum concentrations of soluble 4-1BB and 4-1BB ligand correlated with the disease severity in rheumatoid arthritis*. Exp Mol Med, 2004. **36**(1): p. 13-22.
165. Michel, J. and H. Schwarz, *Expression of soluble CD137 correlates with activation-induced cell death of lymphocytes*. Cytokine, 2000. **12**(6): p. 742-6.
166. Shao, Z. and H. Schwarz, *CD137 ligand, a member of the tumor necrosis factor family, regulates immune responses via reverse signal transduction*. J Leukoc Biol, 2011. **89**(1): p. 21-9.
167. Palma, C., et al., *CD137 and CD137 ligand constitutively coexpressed on human T and B leukemia cells signal proliferation and survival*. Int J Cancer, 2004. **108**(3): p. 390-8.
168. Polte, T., et al., *CD137 ligand prevents the development of T-helper type 2 cell-mediated allergic asthma by interferon-gamma-producing CD8+ T cells*. Clin Exp Allergy, 2007. **37**(9): p. 1374-85.
169. Lin, G.H., et al., *Endogenous 4-1BB ligand plays a critical role in protection from influenza-induced disease*. J Immunol, 2009. **182**(2): p. 934-47.
170. Seko, Y., et al., *Expression of tumour necrosis factor (TNF) ligand superfamily co-stimulatory molecules CD30L, CD27L, OX40L, and 4-1BBL in murine hearts with acute myocarditis caused by Coxsackievirus B3*. J Pathol, 2001. **195**(5): p. 593-603.
171. Pulle, G., M. Vidric, and T.H. Watts, *IL-15-dependent induction of 4-1BB promotes antigen-independent CD8 memory T cell survival*. J Immunol, 2006. **176**(5): p. 2739-48.
172. Bertram, E.M., et al., *A switch in costimulation from CD28 to 4-1BB during primary versus secondary CD8 T cell response to influenza in vivo*. J Immunol, 2004. **172**(2): p. 981-8.
173. Bertram, E.M., P. Lau, and T.H. Watts, *Temporal segregation of 4-1BB versus CD28-mediated costimulation: 4-1BB ligand influences T cell numbers late in the primary response and regulates the size of the T cell memory response following influenza infection*. J Immunol, 2002. **168**(8): p. 3777-85.
174. Dawicki, W. and T.H. Watts, *Expression and function of 4-1BB during CD4 versus CD8 T cell responses in vivo*. Eur J Immunol, 2004. **34**(3): p. 743-51.
175. Wang, C., et al., *Immune regulation by 4-1BB and 4-1BBL: complexities and challenges*. Immunol Rev, 2009. **229**(1): p. 192-215.

176. Kwajah, M.M.S. and H. Schwarz, *CD137 ligand signaling induces human monocyte to dendritic cell differentiation*. Eur J Immunol, 2010. **40**(7): p. 1938-49.
177. Yui, M.A., et al., *Production of congenic mouse strains carrying NOD-derived diabetogenic genetic intervals: an approach for the genetic dissection of complex traits*. Mamm Genome, 1996. **7**(5): p. 331-4.
178. Saoulli, K., et al., *CD28-independent, TRAF2-dependent costimulation of resting T cells by 4-1BB ligand*. J Exp Med, 1998. **187**(11): p. 1849-62.
179. Cannons, J.L., et al., *4-1BB ligand induces cell division, sustains survival, and enhances effector function of CD4 and CD8 T cells with similar efficacy*. J Immunol, 2001. **167**(3): p. 1313-24.
180. Seo, S.K., et al., *4-1BB-mediated immunotherapy of rheumatoid arthritis*. Nat Med, 2004. **10**(10): p. 1088-94.
181. Foell, J., et al., *CD137 costimulatory T cell receptor engagement reverses acute disease in lupus-prone NZB x NZW F1 mice*. J Clin Invest, 2003. **111**(10): p. 1505-18.
182. Sakaguchi, S., *Naturally arising CD4+ regulatory t cells for immunologic self-tolerance and negative control of immune responses*. Annu Rev Immunol, 2004. **22**: p. 531-62.
183. Wu, A.J., et al., *Tumor necrosis factor-alpha regulation of CD4+CD25+ T cell levels in NOD mice*. Proc Natl Acad Sci U S A, 2002. **99**(19): p. 12287-92.
184. Koarada, S., et al., *Increased nonobese diabetic Th1:Th2 (IFN-gamma:IL-4) ratio is CD4+ T cell intrinsic and independent of APC genetic background*. J Immunol, 2002. **169**(11): p. 6580-7.
185. King, C., et al., *Homeostatic expansion of T cells during immune insufficiency generates autoimmunity*. Cell, 2004. **117**(2): p. 265-77.
186. Setoguchi, R., et al., *Homeostatic maintenance of natural Foxp3(+) CD25(+) CD4(+) regulatory T cells by interleukin (IL)-2 and induction of autoimmune disease by IL-2 neutralization*. J Exp Med, 2005. **201**(5): p. 723-35.
187. Ono, M., et al., *Control of autoimmune myocarditis and multiorgan inflammation by glucocorticoid-induced TNF receptor family-related protein(high), Foxp3-expressing CD25+ and CD25- regulatory T cells*. J Immunol, 2006. **176**(8): p. 4748-56.
188. Fu, S., et al., *CD4+ CD25+ CD62+ T-regulatory cell subset has optimal suppressive and proliferative potential*. Am J Transplant, 2004. **4**(1): p. 65-78.
189. Carreno, B.M. and M. Collins, *The B7 family of ligands and its receptors: new pathways for costimulation and inhibition of immune responses*. Annu Rev Immunol, 2002. **20**: p. 29-53.
190. Witsch, E.J., et al., *ICOS and CD28 reversely regulate IL-10 on re-activation of human effector T cells with mature dendritic cells*. Eur J Immunol, 2002. **32**(9): p. 2680-6.
191. Sundstedt, A., et al., *Role for IL-10 in suppression mediated by peptide-induced regulatory T cells in vivo*. J Immunol, 2003. **170**(3): p. 1240-8.
192. Vieira, P.L., et al., *IL-10-secreting regulatory T cells do not express Foxp3 but have comparable regulatory function to naturally occurring CD4+CD25+ regulatory T cells*. J Immunol, 2004. **172**(10): p. 5986-93.

193. Maynard, C.L., et al., *Regulatory T cells expressing interleukin 10 develop from Foxp3+ and Foxp3- precursor cells in the absence of interleukin 10*. Nat Immunol, 2007. **8**(9): p. 931-41.
194. Thornton, A.M. and E.M. Shevach, *CD4+CD25+ immunoregulatory T cells suppress polyclonal T cell activation in vitro by inhibiting interleukin 2 production*. J Exp Med, 1998. **188**(2): p. 287-96.
195. Takahashi, T., et al., *Immunologic self-tolerance maintained by CD25(+)CD4(+) regulatory T cells constitutively expressing cytotoxic T lymphocyte-associated antigen 4*. J Exp Med, 2000. **192**(2): p. 303-10.
196. Luhder, F., et al., *Cytotoxic T lymphocyte-associated antigen 4 (CTLA-4) regulates the unfolding of autoimmune diabetes*. J Exp Med, 1998. **187**(3): p. 427-32.
197. Cao, X., et al., *Granzyme B and perforin are important for regulatory T cell-mediated suppression of tumor clearance*. Immunity, 2007. **27**(4): p. 635-46.
198. Pandiyan, P., et al., *CD4+CD25+Foxp3+ regulatory T cells induce cytokine deprivation-mediated apoptosis of effector CD4+ T cells*. Nat Immunol, 2007. **8**(12): p. 1353-62.
199. Sytwu, H.K., et al., *Anti-4-1BB-based immunotherapy for autoimmune diabetes: lessons from a transgenic non-obese diabetic (NOD) model*. J Autoimmun, 2003. **21**(3): p. 247-54.
200. Jacob, C.O., et al., *Prevention of diabetes in nonobese diabetic mice by tumor necrosis factor (TNF): similarities between TNF-alpha and interleukin 1*. Proc Natl Acad Sci U S A, 1990. **87**(3): p. 968-72.
201. Cope, A., R. Ettinger, and H. McDevitt, *The role of TNF alpha and related cytokines in the development and function of the autoreactive T-cell repertoire*. Res Immunol, 1997. **148**(5): p. 307-12.
202. Green, E.A., E.E. Eynon, and R.A. Flavell, *Local expression of TNFalpha in neonatal NOD mice promotes diabetes by enhancing presentation of islet antigens*. Immunity, 1998. **9**(5): p. 733-43.
203. Maerten, P., et al., *Involvement of 4-1BB (CD137)-4-1BBligand interaction in the modulation of CD4 T cell-mediated inflammatory colitis*. Clin Exp Immunol, 2006. **143**(2): p. 228-36.
204. Morris, G.P., L. Chen, and Y.C. Kong, *CD137 signaling interferes with activation and function of CD4+CD25+ regulatory T cells in induced tolerance to experimental autoimmune thyroiditis*. Cell Immunol, 2003. **226**(1): p. 20-9.
205. Rabinovitch, A., *Immunoregulatory and cytokine imbalances in the pathogenesis of IDDM. Therapeutic intervention by immunostimulation?* Diabetes, 1994. **43**(5): p. 613-21.
206. Akdis, C.A. and K. Blaser, *Mechanisms of interleukin-10-mediated immune suppression*. Immunology, 2001. **103**(2): p. 131-6.
207. Kohyama, M., et al., *Inducible costimulator-dependent IL-10 production by regulatory T cells specific for self-antigen*. Proc Natl Acad Sci U S A, 2004. **101**(12): p. 4192-7.
208. Herman, A.E., et al., *CD4+CD25+ T regulatory cells dependent on ICOS promote regulation of effector cells in the prediabetic lesion*. J Exp Med, 2004. **199**(11): p. 1479-89.

209. Asseman, C., et al., *An essential role for interleukin 10 in the function of regulatory T cells that inhibit intestinal inflammation*. J Exp Med, 1999. **190**(7): p. 995-1004.
210. Mamura, M., et al., *CD28 disruption exacerbates inflammation in Tgf-beta1-/- mice: in vivo suppression by CD4+CD25+ regulatory T cells independent of autocrine TGF-beta1*. Blood, 2004. **103**(12): p. 4594-601.
211. Garin, M.I., et al., *Galectin-1: a key effector of regulation mediated by CD4+CD25+ T cells*. Blood, 2007. **109**(5): p. 2058-65.
212. Collison, L.W., et al., *The inhibitory cytokine IL-35 contributes to regulatory T-cell function*. Nature, 2007. **450**(7169): p. 566-9.
213. Baratelli, F., et al., *Prostaglandin E2 induces FOXP3 gene expression and T regulatory cell function in human CD4+ T cells*. J Immunol, 2005. **175**(3): p. 1483-90.
214. Chaturvedi, V., et al., *Cutting edge: Human regulatory T cells require IL-35 to mediate suppression and infectious tolerance*. J Immunol, 2011. **186**(12): p. 6661-6.
215. Chauhan, S.K., et al., *Levels of Foxp3 in regulatory T cells reflect their functional status in transplantation*. J Immunol, 2009. **182**(1): p. 148-53.
216. Chen, M.L., et al., *Latency-associated peptide identifies a novel CD4+CD25+ regulatory T cell subset with TGFbeta-mediated function and enhanced suppression of experimental autoimmune encephalomyelitis*. J Immunol, 2008. **180**(11): p. 7327-37.
217. Collison, L.W., et al., *Regulatory T cell suppression is potentiated by target T cells in a cell contact, IL-35- and IL-10-dependent manner*. J Immunol, 2009. **182**(10): p. 6121-8.
218. Jonuleit, H., et al., *Infectious tolerance: human CD25(+) regulatory T cells convey suppressor activity to conventional CD4(+) T helper cells*. J Exp Med, 2002. **196**(2): p. 255-60.
219. Kim, Y.G., et al., *Human CD4+CD25+ regulatory T cells inhibit the differentiation of osteoclasts from peripheral blood mononuclear cells*. Biochem Biophys Res Commun, 2007. **357**(4): p. 1046-52.
220. Lin, J., et al., *The role of CD4+CD25+ regulatory T cells in macrophage-derived foam-cell formation*. J Lipid Res, 2010. **51**(5): p. 1208-17.
221. Strauss, L., et al., *Expression of ICOS on human melanoma-infiltrating CD4+CD25highFoxp3+ T regulatory cells: implications and impact on tumor-mediated immune suppression*. J Immunol, 2008. **180**(5): p. 2967-80.
222. Sun, L., S. Yi, and P.J. O'Connell, *Foxp3 regulates human natural CD4+CD25+ regulatory T-cell-mediated suppression of xenogeneic response*. Xenotransplantation, 2010. **17**(2): p. 121-30.
223. Szczepanski, M.J., et al., *Increased frequency and suppression by regulatory T cells in patients with acute myelogenous leukemia*. Clin Cancer Res, 2009. **15**(10): p. 3325-32.
224. Bluestone, J.A., K. Herold, and G. Eisenbarth, *Genetics, pathogenesis and clinical interventions in type 1 diabetes*. Nature, 2010. **464**(7293): p. 1293-300.
225. Cannons, J.L., et al., *Genetic and functional association of the immune signaling molecule 4-1BB (CD137/TNFRSF9) with type 1 diabetes*. J Autoimmun, 2005.

226. Hamilton-Williams, E.E., et al., *Expression of diabetes-associated genes by dendritic cells and CD4 T cells drives the loss of tolerance in nonobese diabetic mice*. J Immunol, 2009. **183**(3): p. 1533-41.
227. Bettelli, E., et al., *Reciprocal developmental pathways for the generation of pathogenic effector TH17 and regulatory T cells*. Nature, 2006. **441**(7090): p. 235-8.
228. Foell, J., et al., *CD137-mediated T cell co-stimulation terminates existing autoimmune disease in SLE-prone NZB/NZW F1 mice*. Ann N Y Acad Sci, 2003. **987**: p. 230-5.
229. Steward, C.A., et al., *Genome-wide end-sequenced BAC resources for the NOD/MrkTac() and NOD/ShiLtJ() mouse genomes*. Genomics, 2010. **95**(2): p. 105-10.
230. Ning, Z., A.J. Cox, and J.C. Mullikin, *SSAHA: a fast search method for large DNA databases*. Genome Res, 2001. **11**(10): p. 1725-9.
231. Hulbert, E.M., et al., *T1DBase: integration and presentation of complex data for type 1 diabetes research*. Nucleic Acids Res, 2007. **35**(Database issue): p. D742-6.
232. Smink, L.J., et al., *T1DBase, a community web-based resource for type 1 diabetes research*. Nucleic Acids Res, 2005. **33**(Database issue): p. D544-9.
233. Stein, L.D., et al., *The generic genome browser: a building block for a model organism system database*. Genome Res, 2002. **12**(10): p. 1599-610.
234. Kim, J., et al., *Constitutive expression of 4-1BB on T cells enhances CD4+ T cell responses*. Exp Mol Med, 2003. **35**(6): p. 509-17.
235. Thomas, D.C., et al., *An early age-related increase in the frequency of CD4+ Foxp3+ cells in BDC2.5NOD mice*. Immunology, 2007. **121**(4): p. 565-76.
236. Nolte-'t Hoen, E.N., et al., *Identification of a CD4+CD25+ T cell subset committed in vivo to suppress antigen-specific T cell responses without additional stimulation*. Eur J Immunol, 2004. **34**(11): p. 3016-27.
237. Lehmann, J., et al., *Expression of the integrin alpha Ebeta 7 identifies unique subsets of CD25+ as well as CD25- regulatory T cells*. Proc Natl Acad Sci U S A, 2002. **99**(20): p. 13031-6.
238. Szanya, V., et al., *The subpopulation of CD4+CD25+ splenocytes that delays adoptive transfer of diabetes expresses L-selectin and high levels of CCR7*. J Immunol, 2002. **169**(5): p. 2461-5.
239. Hoffmann, P., et al., *Only the CD45RA+ subpopulation of CD4+CD25high T cells gives rise to homogeneous regulatory T-cell lines upon in vitro expansion*. Blood, 2006. **108**(13): p. 4260-7.
240. Kohm, A.P. and S.D. Miller, *Role of ICAM-1 and P-selectin expression in the development and effector function of CD4+CD25+regulatory T cells*. J Autoimmun, 2003. **21**(3): p. 261-71.
241. Liu, G.Z., et al., *Decreased 4-1BB expression on CD4+CD25 high regulatory T cells in peripheral blood of patients with multiple sclerosis*. Clin Exp Immunol, 2008. **154**(1): p. 22-9.
242. Liu, G.Z., et al., *Increased soluble 4-1BB ligand (4-1BBL) levels in peripheral blood of patients with multiple sclerosis*. Scand J Immunol, 2006. **64**(4): p. 412-9.

243. Sharief, M.K., *Heightened intrathecal release of soluble CD137 in patients with multiple sclerosis*. Eur J Neurol, 2002. **9**(1): p. 49-54.
244. Hurtado, J.C., et al., *Potential role of 4-1BB in T cell activation. Comparison with the costimulatory molecule CD28*. J Immunol, 1995. **155**(7): p. 3360-7.
245. Kachapati, K., et al., *The Non-Obese Diabetic (NOD) Mouse as a Model of Human Type 1 Diabetes*. Methods Mol Biol, 2012. **933**: p. 3-16.
246. Schuck, P., *Size-distribution analysis of macromolecules by sedimentation velocity ultracentrifugation and lamm equation modeling*. Biophys J, 2000. **78**(3): p. 1606-19.
247. Melanitou, E., et al., *Evidence for the presence of insulin-dependent diabetes-associated alleles on the distal part of mouse chromosome 6*. Genome Res, 1998. **8**(6): p. 608-20.
248. Jimeno, R., et al., *New insights into the role of VIP on the ratio of T-cell subsets during the development of autoimmune diabetes*. Immunol Cell Biol, 2010. **88**(7): p. 734-45.
249. Langstein, J., et al., *CD137 (ILA/4-1BB), a member of the TNF receptor family, induces monocyte activation via bidirectional signaling*. J Immunol, 1998. **160**(5): p. 2488-94.
250. Weber, K., et al., *A multicolor panel of novel lentiviral "gene ontology" (LeGO) vectors for functional gene analysis*. Mol Ther, 2008. **16**(4): p. 698-706.
251. Weber, K., et al., *Lentiviral gene ontology (LeGO) vectors equipped with novel drug-selectable fluorescent proteins: new building blocks for cell marking and multi-gene analysis*. Gene Ther, 2010. **17**(4): p. 511-20.
252. Kwon, B.S., et al., *Genomic organization and chromosomal localization of the T-cell antigen 4-1BB*. J Immunol, 1994. **152**(5): p. 2256-62.
253. Ohtake Satoshi, K.T., Masao Tokunaga, Yoshiko Kita, Tsutomu Arakawa, *The mechanism of elution by MgCl₂, ethylene glycol and arginine in affinity chromatography* Global Journal of Biochemistry., 2010. **2**(1): p. 1-27.
254. Chan, F.K., *Three is better than one: pre-ligand receptor assembly in the regulation of TNF receptor signaling*. Cytokine, 2007. **37**(2): p. 101-7.
255. Aggarwal, B.B., *Signalling pathways of the TNF superfamily: a double-edged sword*. Nat Rev Immunol, 2003. **3**(9): p. 745-56.
256. Cannons, J.L., Y. Choi, and T.H. Watts, *Role of TNF receptor-associated factor 2 and p38 mitogen-activated protein kinase activation during 4-1BB-dependent immune response*. J Immunol, 2000. **165**(11): p. 6193-204.
257. Michel, J., et al., *A soluble form of CD137 (ILA/4-1BB), a member of the TNF receptor family, is released by activated lymphocytes and is detectable in sera of patients with rheumatoid arthritis*. Eur J Immunol, 1998. **28**(1): p. 290-5.
258. Lippert, U., et al., *CD137 ligand reverse signaling has multiple functions in human dendritic cells during an adaptive immune response*. Eur J Immunol, 2008. **38**(4): p. 1024-32.
259. Kang, Y.J., et al., *Cell surface 4-1BBL mediates sequential signaling pathways 'downstream' of TLR and is required for sustained TNF production in macrophages*. Nat Immunol, 2007. **8**(6): p. 601-9.
260. Kim, D.K., S.C. Lee, and H.W. Lee, *CD137 ligand-mediated reverse signals increase cell viability and cytokine expression in murine myeloid cells:*

- involvement of mTOR/p70S6 kinase and Akt.* Eur J Immunol, 2009. **39**(9): p. 2617-28.
261. Pauly, S., et al., *CD137 is expressed by follicular dendritic cells and costimulates B lymphocyte activation in germinal centers.* J Leukoc Biol, 2002. **72**(1): p. 35-42.
262. Rabu, C., et al., *Production of recombinant human trimeric CD137L (4-1BBL). Cross-linking is essential to its T cell co-stimulation activity.* J Biol Chem, 2005. **280**(50): p. 41472-81.
263. Lynch, D.H., *The promise of 4-1BB (CD137)-mediated immunomodulation and the immunotherapy of cancer.* Immunol Rev, 2008. **222**: p. 277-86.
264. Middendorp, S., et al., *Mice deficient for CD137 ligand are predisposed to develop germinal center-derived B-cell lymphoma.* Blood, 2009. **114**(11): p. 2280-9.
265. Hargreaves, P.G. and A. Al-Shamkhani, *Soluble CD30 binds to CD153 with high affinity and blocks transmembrane signaling by CD30.* Eur J Immunol, 2002. **32**(1): p. 163-73.
266. Krall, J.A., E.M. Beyer, and G. MacBeath, *High- and low-affinity epidermal growth factor receptor-ligand interactions activate distinct signaling pathways.* PLoS One, 2011. **6**(1): p. e15945.
267. Won, E.Y., et al., *The structure of the trimer of human 4-1BB ligand is unique among members of the tumor necrosis factor superfamily.* J Biol Chem, 2010. **285**(12): p. 9202-10.
268. Thomas, C., et al., *Structural linkage between ligand discrimination and receptor activation by type I interferons.* Cell, 2011. **146**(4): p. 621-32.
269. Vassalli, P., *The pathophysiology of tumor necrosis factors.* Annu Rev Immunol, 1992. **10**: p. 411-52.
270. Locksley, R.M., N. Killeen, and M.J. Lenardo, *The TNF and TNF receptor superfamilies: integrating mammalian biology.* Cell, 2001. **104**(4): p. 487-501.
271. Bodmer, J.L., P. Schneider, and J. Tschopp, *The molecular architecture of the TNF superfamily.* Trends Biochem Sci, 2002. **27**(1): p. 19-26.
272. Banner, D.W., et al., *Crystal structure of the soluble human 55 kd TNF receptor-human TNF beta complex: implications for TNF receptor activation.* Cell, 1993. **73**(3): p. 431-45.
273. Choi, B.K., et al., *Unified immune modulation by 4-1BB triggering leads to diverse effects on disease progression in vivo.* Cytokine, 2011. **55**(3): p. 420-8.
274. Melero, I., et al., *Monoclonal antibodies against the 4-1BB T-cell activation molecule eradicate established tumors.* Nat Med, 1997. **3**(6): p. 682-5.
275. Ye, Z., et al., *Gene therapy for cancer using single-chain Fv fragments specific for 4-1BB.* Nat Med, 2002. **8**(4): p. 343-8.
276. Polte, T., et al., *CD137-mediated immunotherapy for allergic asthma.* J Clin Invest, 2006. **116**(4): p. 1025-36.
277. Choi, B.K., et al., *4-1BB-mediated amelioration of experimental autoimmune uveoretinitis is caused by indoleamine 2,3-dioxygenase-dependent mechanisms.* Cytokine, 2006. **34**(5-6): p. 233-42.
278. Kim, Y.H., et al., *4-1BB triggering ameliorates experimental autoimmune encephalomyelitis by modulating the balance between Th17 and regulatory T cells.* J Immunol, 2011. **187**(3): p. 1120-8.

279. Mellor, A., *Indoleamine 2,3 dioxygenase and regulation of T cell immunity*. Biochem Biophys Res Commun, 2005. **338**(1): p. 20-4.
280. Li, R., et al., *IDO inhibits T-cell function through suppressing Vav1 expression and activation*. Cancer Biol Ther, 2009. **8**(14): p. 1402-8.
281. Myers, L., et al., *Peptide-specific CD8 T regulatory cells use IFN-gamma to elaborate TGF-beta-based suppression*. J Immunol, 2005. **174**(12): p. 7625-32.
282. Myers, L., et al., *Effector CD8 T cells possess suppressor function after 4-1BB and Toll-like receptor triggering*. Proc Natl Acad Sci U S A, 2003. **100**(9): p. 5348-53.
283. Kim, J., et al., *Host CD25+CD4+Foxp3+ regulatory T cells primed by anti-CD137 mAbs inhibit graft-versus-host disease*. Biol Blood Marrow Transplant, 2012. **18**(1): p. 44-54.
284. Kwon, B.S., et al., *Immune responses in 4-1BB (CD137)-deficient mice*. J Immunol, 2002. **168**(11): p. 5483-90.
285. Lee, S.W., et al., *Enhanced CD4 T cell responsiveness in the absence of 4-1BB*. J Immunol, 2005. **174**(11): p. 6803-8.
286. Szymczak, A.L., et al., *Correction of multi-gene deficiency in vivo using a single 'self-cleaving' 2A peptide-based retroviral vector*. Nat Biotechnol, 2004. **22**(5): p. 589-94.
287. Wicker, L.S., et al., *Type 1 diabetes genes and pathways shared by humans and NOD mice*. J Autoimmun, 2005. **25 Suppl**: p. 29-33.
288. Ridgway, W.M., et al., *Gene-gene interactions in the NOD mouse model of type 1 diabetes*. Adv Immunol, 2008. **100**: p. 151-75.